

Berichte

zur Polar-
und Meeresforschung

517
2005

Reports
on Polar and Marine Research



Scientific Cruise Report of the
Arctic Expedition ARK-XX/3 of RV „Polarstern“ in 2004:
Fram Strait, Yermak Plateau and East Greenland
Continental Margin

Wissenschaftlicher Fahrtbericht über die
Arktis-Expedition ARK-XX/3 von 2004
mit FS „Polarstern“: Framstraße, Yermak-Plateau
und ostgrönländischer Kontinentalrand

Edited by
Ruediger Stein
with contributions of the participants

ALFRED-WEGENER-INSTITUT FÜR POLAR- UND MEERESFORSCHUNG
Alfred Wegener Institute for Polar and Marine Research
D-27568 BREMERHAVEN
Bundesrepublik Deutschland – Federal Republic of Germany

**Scientific Cruise Report of the
Arctic Expedition ARK-XX/3 of RV "Polarstern" in 2004:
Fram Strait, Yermak Plateau and East Greenland
Continental Margin**

**Wissenschaftlicher Fahrtbericht über die
Arktis-Expedition ARK-XX/3 von 2004
mit FS "Polarstern":
Framstraße, Yermak-Plateau und ostgrönländischer
Kontinentalrand**

**Edited by
Ruediger Stein
with contributions of the participants**

**Ber. Polarforsch. Meeresforsch. 517 (2005)
ISSN 1618 - 3193**

Table of contents

1. Objectives and Summary	1
R. Stein	
2. Itinerary	4
R. Stein	
3. Meteorological Conditions	8
M. Gebauer, K. Buldt	
4. Sea-ice Observations	12
V. Shevchenko	
5. Sea-ice Sedimentology and Snow Chemistry	15
V. Shevchenko, N. Kukina	
5.1 Ice-rafted Sediments	15
V. Shevchenko, N. Kukina	
5.2 Snow Chemistry	21
V. Shevchenko	
6. Secchi Depth Measurements	22
V. Shevchenko	
7. Bathymetric Investigations	23
B. Platen, R. Rathlau, A. Winkler	
8. Marine Geophysics	27
W. Jokat, M. Schmidt-Aursch, M. Schroeder, Y. Behr, H. Birnstiel, A. Gebauer, C. Gebhardt, K. Goeßling, D. Guenther, N. Lensch, H. Martens, W. Raabe, T. Spengler	
9. Marine Geology	41
R. Stein, F. Niessen, F. Schoster, B. Bahr, C. Gebhardt, N. Kukina, N. Lensch, S. Nam, H. Noffke, D. Penschorn, A. Puhr, R. Saraswat, Chr. Schäfer, J. Schneider, J. Thiele, D. Winkelmann, Y. Yanina	
9.1 Introduction	41
9.2 Marine Sediment Echosounding using PARASOUND	42
F. Niessen, J. Rogenhagen, F. Schoster	
9.3 Physical Properties and Core Logging	54
F. Niessen, J. Rogenhagen, C. Gebhardt, D. Penschorn, J. Schneider, D. Winkelmann	
9.3.1 Multi-sensor Core Logging	54
J. Rogenhagen, F. Niessen, D. Penschorn, J. Schneider	
9.3.2 Colour Scan Logging	56
C. Gebhardt, F. Niessen, D. Penschorn, J. Schneider	
9.3.3 Shear Strength	58
D. Winkelmann, D. Penschorn	

9.4 Geological Sampling, Description, and Methods Applied	60
F. Schoster, B. Bahr, C. Gebhardt, N. Kukina, N. Lensch, S. Nam, H. Noffke, D. Penschorn, A. Pühr, R. Saraswat, Chr. Schäfer, J. Schneider, R. Stein, J. Thiele, D. Winkelmann, Y. Yanina	
9.5 Characteristics of ARK-XX/3 Surface Sediments	64
S. Nam, N. Kukina, R. Saraswat, J. Thiele, Y. Yanina	
9.6 Characteristics of ARK-XX/3 Sediment Cores	68
R. Stein, N. Kukina, H. Noffke, A. Pühr, Chr. Schäfer, D. Winkelmann, Y. Yanina	
9.6.1 X-Ray photographs: Sediment Structure and IRD Content.....	68
D. Winkelmann, H. Noffke, A. Pühr, Chr. Schäfer	
9.6.2 Results of Smear-slide Analysis	70
N. Kukina	
9.6.3 Results of coarse fraction analysis	80
J. Thiele, R. Saraswat	
9.6.4 Main Lithologies and Preliminary Interpretation of	82
ARK-XX/3 Sediment Cores R. Stein	
10. The Lost Deutsche Arktische Expedition 1912:	95
A Pilot Study in the North East Land of Spitsbergen N. Fricke, I. Mende	
11. References	99
12. Annex	103
12.1 Station List	103
12.2 Sea-ice Conditions	106
12.3 Graphical Core Descriptions	114
12.4 Geological Data Tables Smear-slide Data	151
12.5 Summary Plots of Logging Data for Selected Sediments Cores	157
12.6 Parasound Profiles at Coring Stations	181
12.7 List of Participants	186



1. Objectives and Summary

R. Stein

The scientific program of the "Polarstern" ARK-XX/3 expedition, which started in Tromsø on August 31 and ended in Bremerhaven on October 03, 2004, was concentrating on geophysical and geological aspects in the Yermak Plateau, Fram Strait and East Greenland continental margin areas (Fig. 1.1). Major part of these geoscientific studies has to be seen in the context of a drilling proposal submitted to the Integrated Ocean Drilling Program (IODP) (Jokat, Stein et al., 2004).

In addition, a pilot study devoted to the lost „Deutsche Arktische Expedition 1912“ was included in the expedition program. As undone work taken-over from the preceding ARK-XX/2 oceanography program, three PIES (Pressure Inverted Echo Sounder) were deployed west of Spitsbergen.

The seismic network concentrated on the Yermak Plateau area and additional site survey boxes along the East Greenland margin. In total, 2920 km of new seismic data were acquired. These data will allow determining in the optimum way the locations of IODP drill sites for our IODP proposal. Parallel to the seismic profiling across the Yermak Plateau an intensive aeromagnetic survey was performed by helicopter, and more than 7250 km were flown.

Overall goal of the geophysics program was to enlarge the geophysical database in the Fram Strait/Yermak Plateau area to provide further constraints on the deeper structure and the tectonic evolution of this region. In detail the following problems should be addressed:

- Seismic investigations across the northern Yermak Plateau to identify the continent-ocean transition.
- Deep seismic investigations to identify the deeper structure of the Yermak Plateau. With the wide-angle reflection data it should be possible to make estimates on the magmatic underplating, if any is present, of the Yermak Plateau.
- Try to sample basement rocks in order to date and constrain the evolution of the plateau.

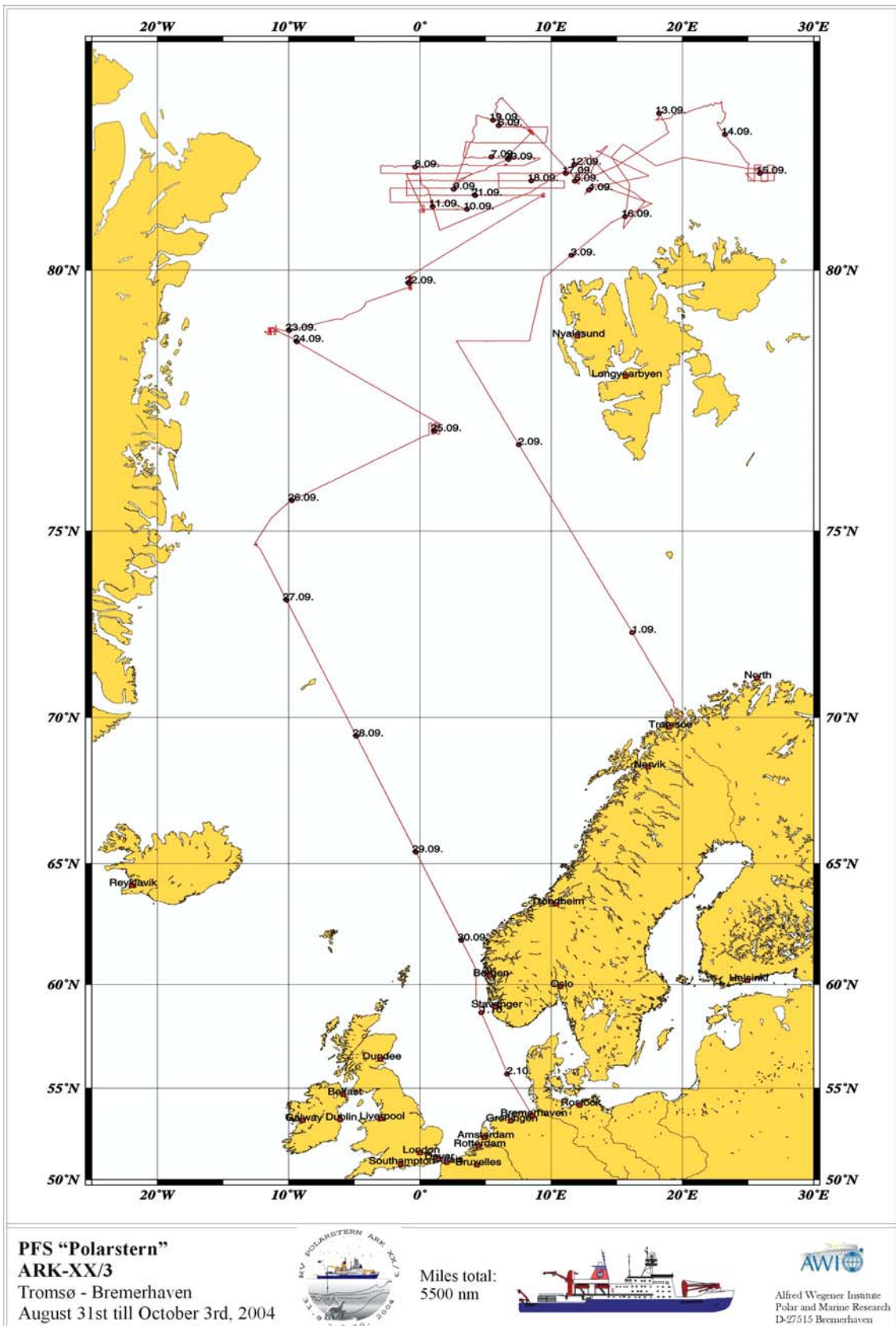


Fig. 1.1: Cruise track of RV "Polarstern" during ARK-XX/3.

One of the key marine-geology objectives was the study of sediment dynamics of megaslides along the Svalbard continental margin (as part of the ESF Program „EUROMARGINS“), using Hydrosweep (bathymetry) and PARASOUND profiling data, multi-sensor-core-logging data, and long sediment cores. In this context, the characterization of sediment facies within debris flow and turbidite sequences as well as undisturbed pelagic sequences, the dating of sediment mass flows and estimates of sedimentary budgets are of interest. Furthermore, detailed multidisciplinary (i.e., sedimentological, mineralogical, micropaleontological, and geochemical) studies will be performed on the sediment cores for high-resolution reconstructions of paleoclimate, paleoceanic circulation patterns, paleosea-ice cover, and paleoproductivity and their variability during late Quaternary times. In order to reach these goals, an intensive sampling program was performed using large-volume box corer, multicorer, gravity corer, and kastenlot corer. In addition, gravity cores were taken from the central part of the Yermak Plateau as well as the East Greenland continental margin as part of the IODP Site survey work. During the entire period of working within the study area, a Hydrosweep and PARASOUND survey was performed. In total, 7800 km of new Hydrosweep and PARASOUND profiles were obtained.

Along the ice-edge area in the Yermak-Plateau area, a sea-ice sampling program was carried-out. In total, 9 stations were sampled for snow, sea ice, and sea-ice sediments.

A pilot study was devoted to the lost Deutsche Arktische Expedition (DAE) 1912, also known as Schroeder Stranz Expedition, a trial expedition to the North East Land of Spitsbergen thought to be a forerunner of the ambitious plan to cross the North East Passage. During “Polarstern” cruise ARK-XX/3 two reported places of historical interest were visited by helicopter to locate and to document: (a) the landing place of the DAE in the Duvefjord and (b) the landing place of the Lerner relief expedition 1913 in search for Schroeder Stranz. The expedition vessel of Lerner got entrapped in the pack ice and sunk off the Beverlysund near the North Cape. With the help of historical stereo-photographs and ARK-XX/3 field observations, the wreck site could be identified more accurately. The wreck is the most northern wreck of the world, and it is planned to investigate it for various research purposes during a submersible expedition in 2006.

In summary, a huge amount of new geoscientific data could be selected. These data will be an important basis for the more concrete planning of our IODP drilling proposal.

Acknowledgement

The Scientific Party of "Polarstern" Cruise ARK-XX/3 gratefully thank captain Udo Domke and his crew, as the success of our expedition was substantially supported by their excellent cooperation and efforts.

2. Itinerary

R. Stein

RV „Polarstern“ left the port of Tromsø/Norway on August 31, 2004.

After a 52h transit we reached the area of PIES deployment west of Spitsbergen along 78°50'N (Fig. 2.1, Area A) on September 02, 22.00 UTC. As undone work taken-over from the preceding ARK-XX/2 oceanography program, three PIES (Pressure Inverted Echo Sounder) were deployed within a 6h work program:

PIES 71	78°50.25'N, 02°48.20'E	2496 m water depth
PIES 141	78°49.87'N, 05°00.93'E	2708 m water depth
PIES 62	78°50.03'N, 08°19.91'E	793 m water depth

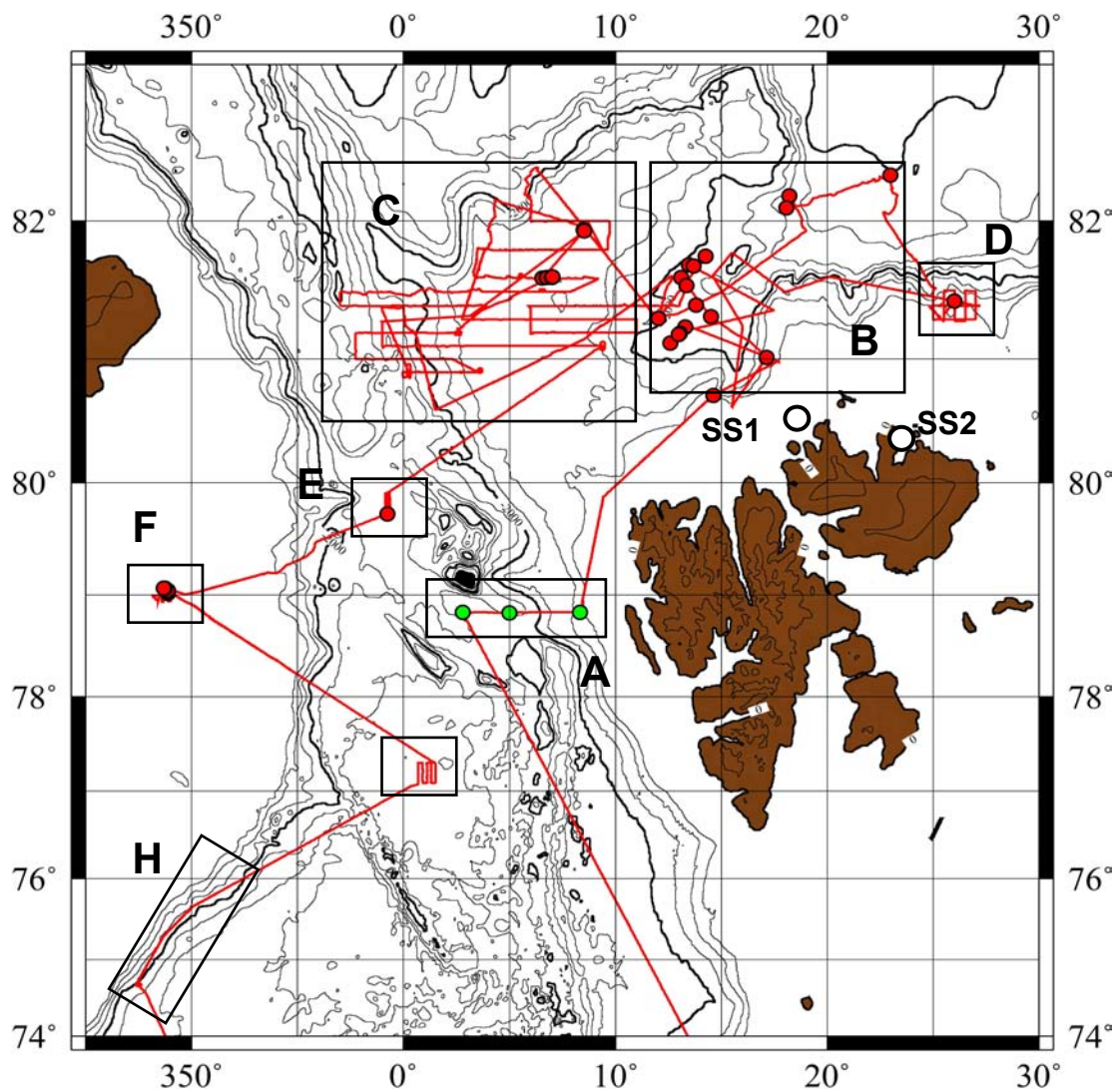


Fig. 2.1: Working areas (A to H) of Cruise ARK-XX/3. Cruise track and stations are shown. In addition, the two locations on North East Land of Spitsbergen, devoted to the Schroeder Stranz Expedition 1912, are marked (SS1 and SS2).

On September 03, 15.00h UTC, we arrived at the first geological station (PS66/304; 80°43.36'N, 14°39.39'E) and started with our own research program in the area north of Spitsbergen (Fig. 2.1, Area B) under optimum ice-free conditions. The ice edge was retreated as far north as 82°N (Fig. 2.2). An intense sampling of near-surface sediments and sediment cores was carried out between September 03 and 05, using giant box corer (GKG), multicorer (MUC), gravity corer (SL), and kastenlot corer (KAL). On September 03 a first helicopter flight, devoted to the Schroeder-Strantz program, was performed to Cape Rubin (Fig. 2.1, area around location SS1).

The seismic profiling program on Yermak Plateau started in the morning of September 05 (Fig.2.1, eastern part of Area C). On September 06, 05.20 UTC, we had to stop seismic profiling near 82°25'N, 06°E (our northernmost location of this expedition) due to too strong ice conditions (Fig. 2.2). We steamed towards 82°N, 06°E where seismic profiling was continued until the afternoon of September 12. In the following two days, the eastern flank of the Yermak Plateau (Fig. 2.1, Area B) was sampled by means of GKG, MUC, SL, and KAL coring systems. Due to strong pack ice, we were proceeding slowly to our northeasternmost station (PS66/323; 82°03.52'N, 22°38.30'E). After having finished the station work at that site, we were steaming towards the SE.

In the early afternoon of September 14, we reached the continental slope north of North East Land at about 81°30'N, 25°E (Fig. 2.1, Area D) where a detailed seismic site survey for a proposed IODP drilling location was carried out. Parallel to the seismic profiling, a helicopter flight was performed to the Duvefjord area where remains of the Schroeder-Strantz Expedition were found in 1937 (Fig. 2.1, area around SS2). We finished the work in Area D with a geological sampling at site PS66/325 (81°26.18'N, 25°59.86'E) in the afternoon of September 15. Until the early morning of September 17, we completed our geological sampling program in Area B at further four stations.

We continued our work program with a seismic profiling on Yermak Plateau (Area C) during the following two days. On top of the central Yermak Plateau where it is assumed that older sediments are cropping out, a geological sampling was carried out by means of GKG, SL and the sediment dredge on September 20 (Fig. 2.1, Area C). We finished our working program on Yermak Plateau Area C with a seismic profiling lasting until September 21, 20.00 UTC.

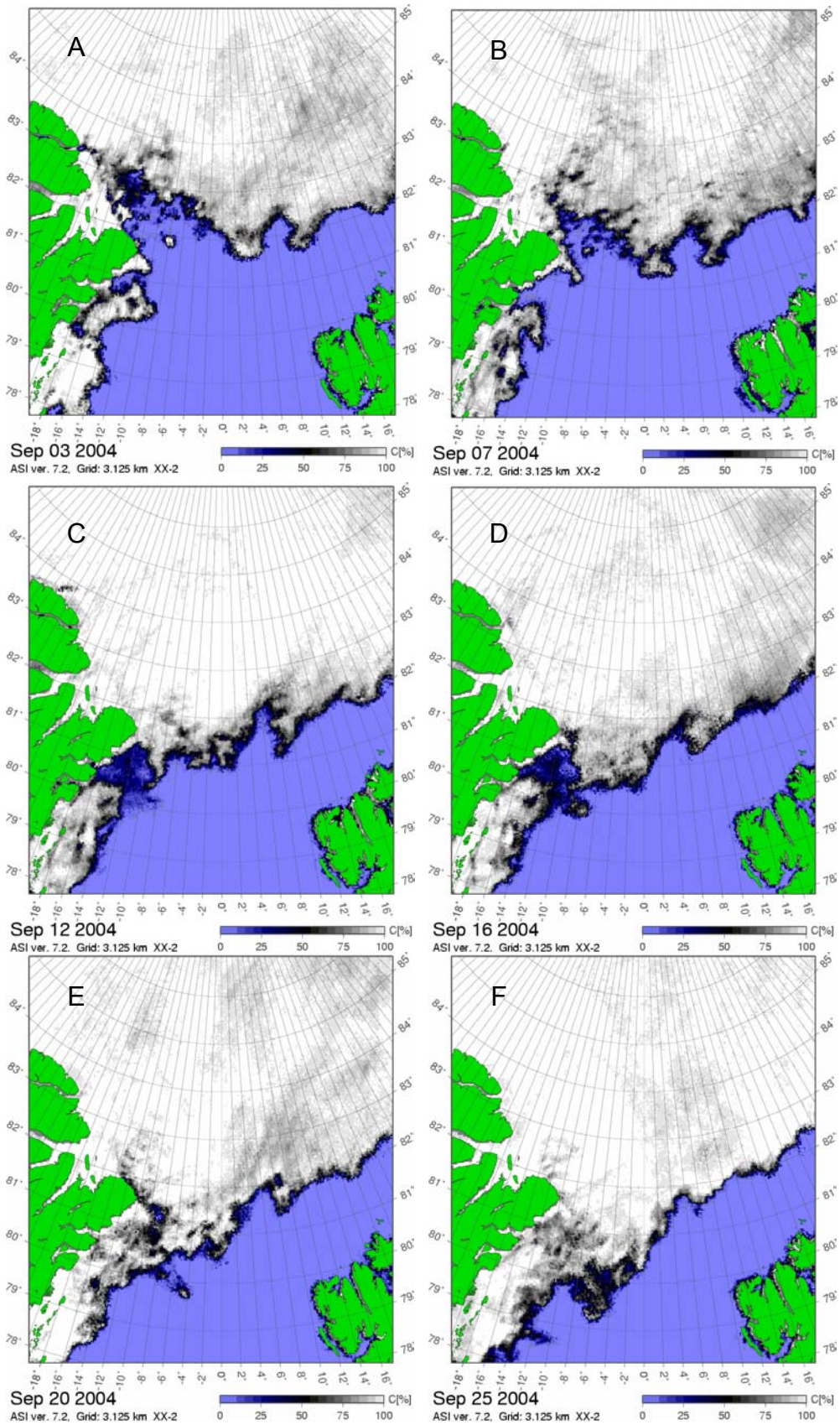


Fig. 2.2: Sea-ice condition during ARK-XX/3
<http://iup.physik.uni-bremen.de:8084/amsr/amsre.html>

Parallel to the seismic profiling and geological sampling across the Yermak Plateau and the Svalbard continental margin, an aeromagnetic survey was performed by helicopter. Within nine days and 20 flights most of the survey area was successfully completed and more than 7250 km were flown.

Furthermore, a sea-ice sampling program was carried out along the ice-edge area in the Yermak-Plateau area (see Fig. 2.2) between September 07 and 19, using the helicopter. In total, 9 stations were sampled for snow, sea ice, and sea-ice sediments. These samples will be investigated for mineralogy, grain size, organic carbon content and composition, and/or major and minor element composition.

On September 21, 22.00 UTC, we steamed towards the south and reached Area E on September 22 (Fig. 2.1) where a seismic site survey for a proposed IODP drilling location was carried-out. In addition, near-surface sediments were sampled by means of gravity corer (Station PS66/341; 79°44.07'N, 00°45'W).

In the early morning of September 23, we arrived on the East Greenland continental shelf (Fig. 2.1, Area F). Several big icebergs were observed here, some of them contained large amount of sediment (see Chapter 4). In Area F, seismic profiling work was done. In this area, seismic data reveal the presence of a prominent salt province and suggest that Mesozoic strata are cropping-out at the surface (Schmitz and Jokat, 2005). In order to sample these old strata, 10 short gravity cores were taken. In one of the gravity cores (PS66/345-2), a large crystal of gypsum was found in the core catcher, which may be related to Permian salt deposits (see Chapter 9.6.4).

After having finished this station work, we steamed towards the SW. During the last two days of our working program (September 25 and 26), seismic site survey profiling was continued in the central southern Fram Strait (Boreas Basin) (Fig. 2.1, Area G) and along the East Greenland continental slope between about 76°N and 74°30'N (Fig. 2.1., Area H).

On September 27, 05.30h UTC, we started our way back to Bremerhaven. „Polarstern“ arrived in Bremerhaven on October 03 early in the morning, bringing to an end a scientifically very successful cruise.

3. Meteorological Conditions

M. Gebauer, K. Buldt

During departure on 31 August 2004 the weather was fine. An anticyclone was centered near the Greenland Sea, only a shallow low moved from Svalbard in direction of Novaja Semlja. The following days the high pressure influence presented moderate easterly winds until we reached Fram Strait. During arrival in this area the wind changed to a southerly direction and its force increased a little bit. Due to warm air advection in front of a cyclone that had developed near Iceland, there was occasional drizzle und poor visibility.

On September 03, "Polarstern" passed the eastern coast of Svalbard and arrived at the exploration area near Yermak Plateau during the next day. The wind speed increased up to 6 Bft (Fig.3.1), but there were some fog patches due to southerly winds that brought moist and rather mild air over the under-cooled water near ice fields. Flight weather was problematic with some restrictions of visibility and ceiling conditions (Figs. 3.2 and 3.3). In the meantime the Iceland low moved across the Greenland Sea to the Svalbard area (Fig. 3.4).

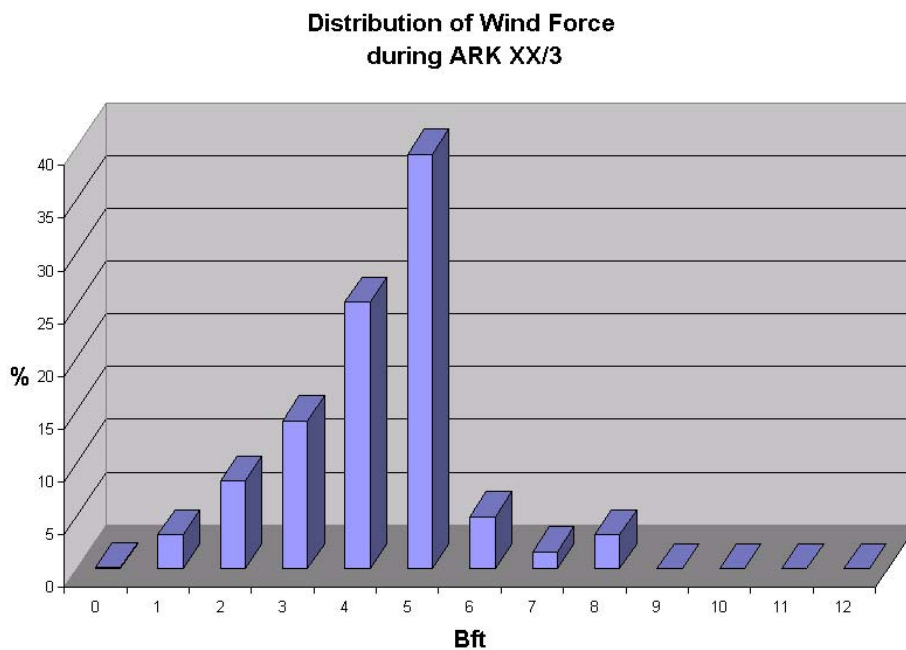


Fig. 3.1: Distribution of wind speed according to normal climatic conditions in September

Ceiling during ARK XX/3

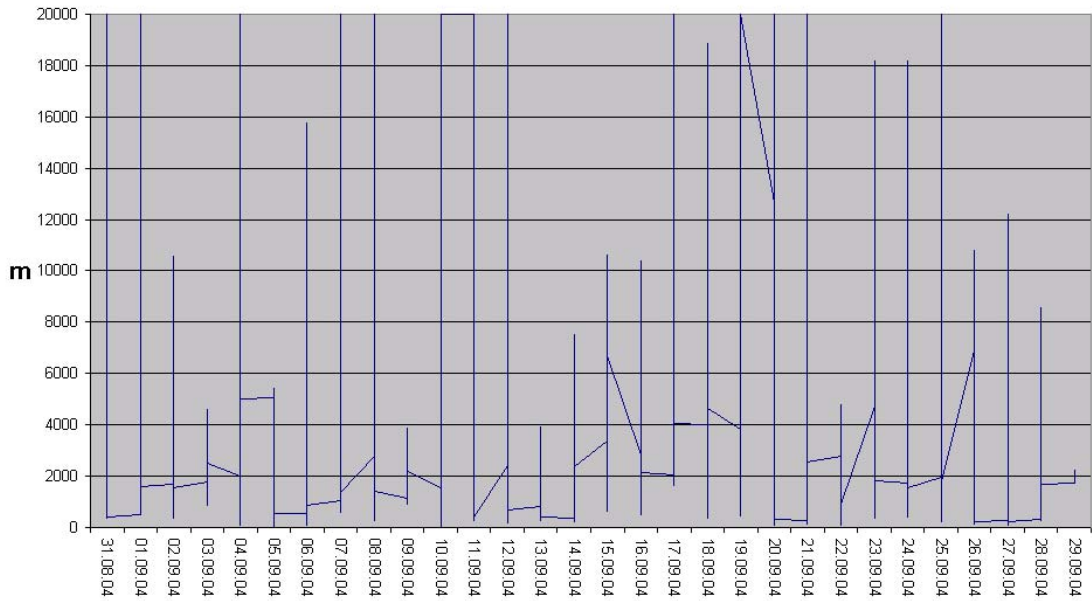


Fig. 3.2: Ceiling: Measurements per 10 minutes; cloud conditions changed very fast.

Visibility during ARK XX/3

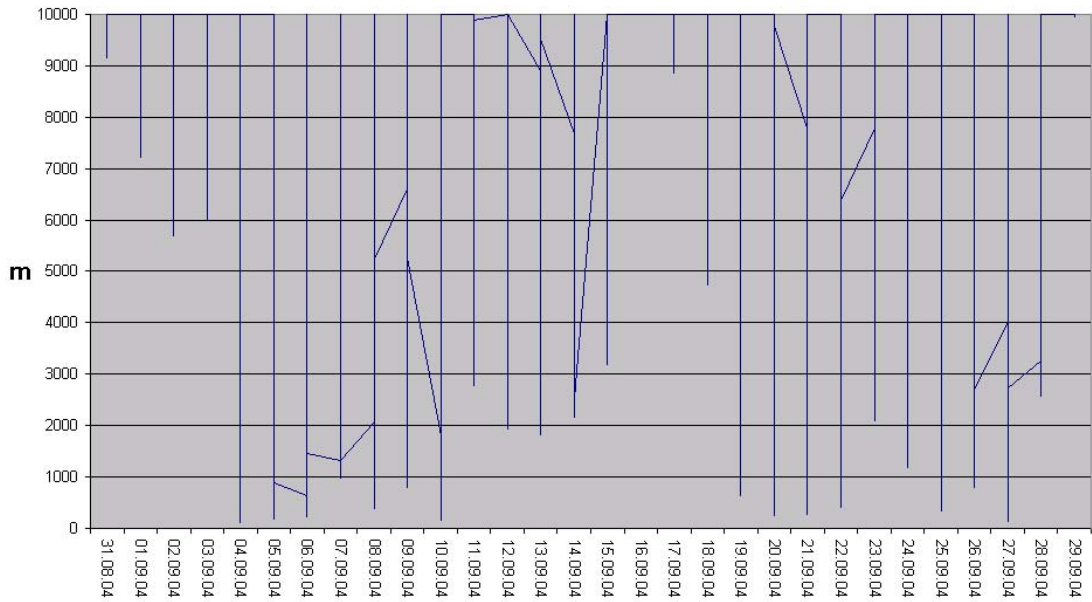


Fig. 3.3: Visibility: Measurements per 10 minutes; conditions changed also very fast.

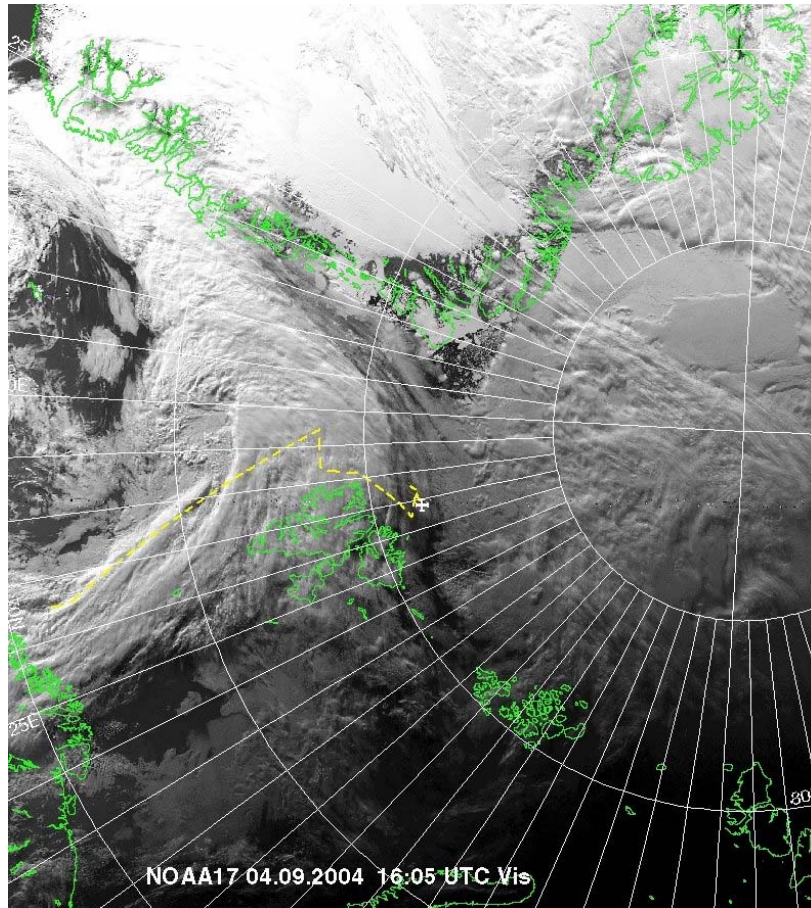


Fig. 3.4: A new low arriving; dashed line indicates course of “Polarstern”, cross her position.

The following weather period was determined by moist and rather mild air masses. The wind came from easterly directions and then, when the low had moved off, from northerly directions. It reached for a short time a wind force 8 to 9 Bft, accompanied by intermittent rain or drizzle with a temperature only barely exceeding the freezing point and thus inducing danger of icing - helicopter flights were not possible

From September 07 onwards, a new weather situation with cold air advection began. Snow was falling, and the air temperatures smashed below $-5\text{ }^{\circ}\text{C}$, later $-10\text{ }^{\circ}\text{C}$. Friendly periods with good visibility and convenient flight weather changed temporarily with some disturbances and shallow lows that arrived from northwest. Intermediately there fell snow.

When the temperature finally rose, the weather conditions for helicopter flights were difficult with a change of snow, rain and also freezing drizzle. The wind blew from northeast with 4 to 5 Bft (Fig. 3.1).

During the middle of the month the high pressure influence rose from Greenland. It was very cold, and due to the low condensation level and very low clouds, the ceiling of less than 300 ft was sometimes not sufficient for flights with the magnetic sensor more than 30 m below the helicopter.

The last part of the month was determined by cyclones, which moved slowly from Iceland to Scandinavia. The working area of "Polarstern" was between these cyclones and high pressure influence over Greenland and over the islands Svalbard, Franz Joseph Land and Novaja Semlja. Only shallow lows were able to influence us temporarily with low clouds, wet snow and poor visibility. Mostly it was cold with -3 to -9 °C. The wind blew from different directions and varied between 2 and 5 Bft.

In the last week of September a new cyclone, once it had been the hurricane "Karl", moved from Iceland to the middle of Norway. North of it "Polarstern" moved southeast, accompanied by mostly northerly, later on westerly winds blowing with 5 Bft. After passing the post cold-frontal weather, a short high pressure influence followed, then a short period during that "Polarstern" had to work against southerly winds 6 Bft and its waves.

"Polarstern" came back to Bremerhaven on October 03, 2004.

4. Sea-ice Observations

V. Shevchenko

“Polarstern” met sea ice on September 5 evening at 81°49.8’N, 9°12.4’E. During seismic profiling, “Polarstern” came to the area with strong ice conditions in the morning of September 6 at 82°20’N, 6°E. After that she came back to mostly open water at 82°N, 6°E and continued seismic studies. In the morning of September 7, regular visual ice observations from the ship’s bridge began. They continued till September 24. These observations were not performed during night time and during the work in ice-free waters. Variables like ice concentration, ice thickness, floe size, melt-pond coverage, ridge height and age, as well as the occurrence of ice-rafted sediments (“dirty ice”) and icebergs were recorded, representing ice conditions in an area of 500 to 1000 m around the ship similarly as it was done during the ARK XVII/2 expedition of “Polarstern” in August–September 2001 (Haas and Lieser, 2003). For most typical situations photos were made from the bridge (Fig. 4.1). In total 89 observations were carried out. Results of these observations are presented in the Annex (Chapter 12.3).

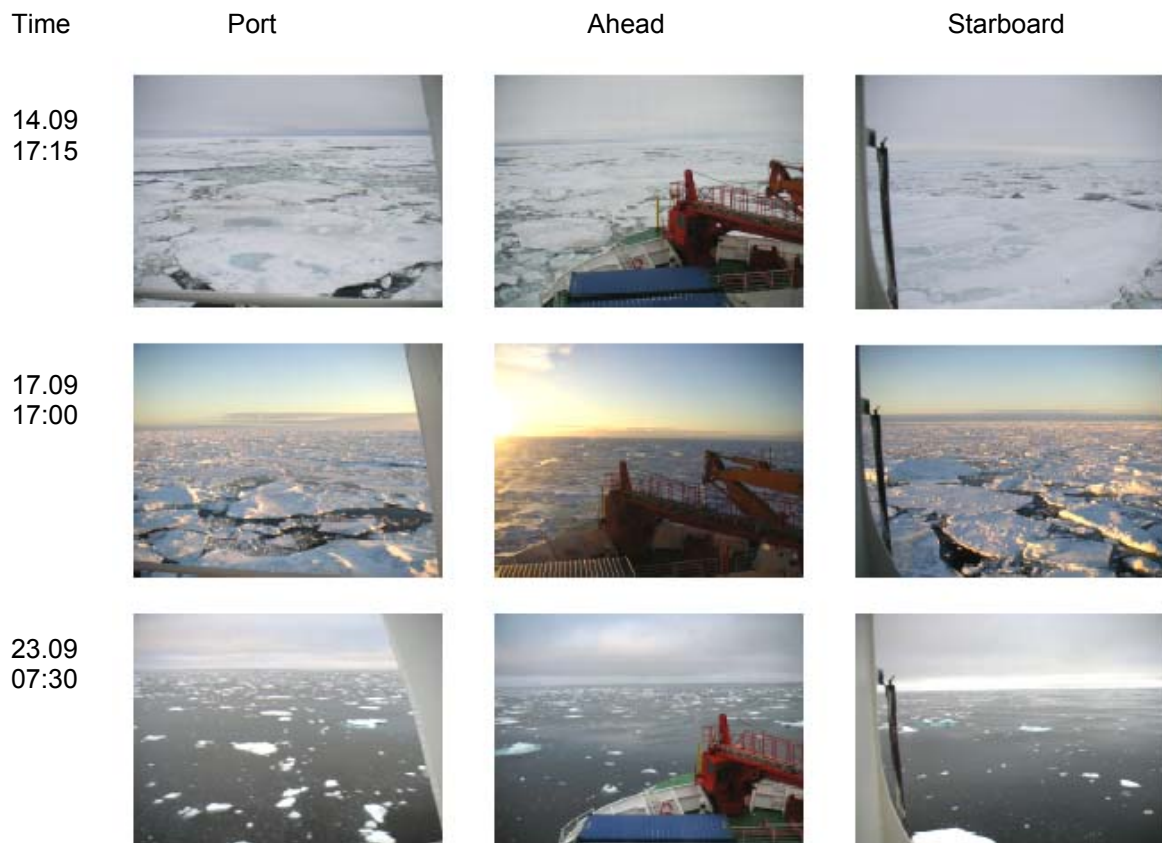


Fig. 4.1: Photos from the bridge of “Polarstern” (performed by R. Stein)

In the area of Yermak Plateau and Fram Strait we mostly worked in the ice-free zone or in the marginal ice zone (region within a hundred kilometres or so of the ice edge). In this region the ice tended to resemble a granular medium with relatively small floes, often densely packed (Hibler, 1989). The typical sizes of ice floes varied from 5 to 20 m, sometimes they were up to 50 m. The typical thickness of ice floes varied from 0.5 to 1 m, snow depth varied from 0 to 15 cm.

Melt ponds were not clearly expressed on the ice floes, probably due to recent snow cover. As it was shown earlier, with the beginning of snowfalls in September the identification of melt ponds by aerial photography and visual observations became difficult or impossible (Bareiss and Haas, 2002).

Ice-rafted sediments were very rare (for more details see Chapter 5). Even their search during the helicopter flights sometimes was not successful. It is possible, that part of these dirty patches on sea ice was covered by recent snow.

Often (see Annex, Chapter 12.3) brown ice was observed on the bottom of ice floes when "Polarstern" reversed them. This discoloration of ice is the result of active development of ice algae (ice algal bloom), that is typical for marginal ice zones (Smith, 1987).

During the expedition icebergs were observed. Photos of some icebergs are presented in Figure 4.2. Along the ship route in the Yermak Plateau area we observed few small icebergs (Fig. 4.2a). In the western part of the Fram Strait (NW part of the Greenland Sea) icebergs were more abundant. In the vicinity of point 79°42' N, 0°48' W three icebergs having sizes from 100 to 300 m, were registered. In the morning of September 23, we crossed a narrow field of old destroyed ice floes (79°12.10' N, 6°11.69' W) and observed three icebergs (largest of them had a size of 500 m to 600 m and 25 m height; Fig. 4.2b). Moving to the west we arrived in the area of detailed seismic studies on the East Greenland shelf, and at 79°02.67'N, 10°55.6'W we were close to an iceberg of 100 m length. This iceberg was reversed to its side, and layering was clearly seen. Dark layers are enriched by sediments (Fig. 4.2e–g). In the vicinity of point 79°03' N, 10°56' W, we observed 16 icebergs ranging in size from 100 to 2000 m and in height from 15 to 30 m (Fig. 4.2h–o).



Fig. 4.2: Photos of icebergs (from the archive of the expedition): a – September 13, 17.00, 82°05.3'N, 18°03.0'E; b – September 23, 07:45, 79°12.1'N, 6°27.0'W; c–d – September 23, 12:00, 79°0.32'N, 10°12.2'W; e–g – September 23, 13:00, 79°02.67'N, 10°55.6'W; h–o – group of icebergs on September 23, 18:30 around location 78°55.6'N, 11°17.5'W.

5. Sea-ice Sedimentology and Snow Chemistry

V. Shevchenko, N. Kukina

5.1. Ice-rafted Sediments

V. Shevchenko, N. Kukina

Sediment transport via sea ice is expected to contribute significantly to deep-sea sedimentation at least in regions of ice ablation (Pfirman et al., 1990; Nürnberg et al., 1994; Lisitzin, 2002) with potential importance also for the dispersal of pollutants (Pfirman et al., 1995; Meese et al., 1997). In the Arctic Ocean, sediments are transported by ice drifting mainly in two major surface current systems – the anticyclonic Beaufort Gyre in the Amerasian Basin and the Transpolar Drift in the Eurasian Basin.

As shown in many works, large amounts of sediments can be entrained into the ice cover through several processes: scavenging of suspended material from the water column by frazil-ice crystals, uplift of material by anchor ice, river spilling on sea ice and aeolian transport (e.g., Mulen et al., 1972; Reimnitz et al., 1987; Dethleth et al., 2000; Eicken, 2003). Now there are many evidences that much of its particulate load originates from the Siberian and specifically the Laptev Sea shelf (Pfirman et al., 1990; Wolenburg, 1993; Nürnberg et al., 1994; Eicken et al., 1997; Lindemann, 1998; Hölemann et al., 1999; Dethleff et al., 2000; Eicken, 2003). During its drift multi-year sea ice is exposed to the extensive surface melting which takes place each summer. Surface melting affects the distribution of particles in sediment-laden multi-year sea ice. Seasonal surface ablation of snow and sea ice and freezing of new ice at the base will result in surface accumulation of particles from the entire melted snow and sea-ice column, while “clean” ice is added underneath each winter that ice-floes are in the central Arctic (Pfirman, 1990).

Surface ablation of sediment-laden ice may form cryoconites (e.g. Pfirman et al., 1990). Cryoconite formation results in aggregation of particles at the base of cylindrical holes in the ice surface. With extensive freeze-thaw cycling, formation of more or less cohesive pellets may occur (Barnes et al., 1988). This process may shield particle accumulation from melt water wash-off and run-off and thus delay particle release until the bulk of the floe disintegrates. When released from the floe, cohesive cryoconite pellets may settle intact to the sea floor. Similar pellets found in sediment traps in the Fram Strait have been attributed to this process (Berner and Wefer, 1990).

Because incorporated material is concentrated mostly at the ice surface in multi-year floes, it appears likely that deposition on the sea floor will occur primarily along the drift path of the ice-floes as it finally disintegrates. Thus, the greatest potential for sediment deposition is expected to occur along the ice margin, near polynyas and large leads. Much of the ice-rafted sediments transported by the Transpolar Drift may be deposited along the axis of the East Greenland Current (Pfirman et al., 1989), with some inflow into the Barents Sea (Elverhøi et al., 1989; Dethleff, 1997).

Determination of the source is very difficult question. The main purpose of studies of ice-rafted sediments is to reveal the main sources of sediments in the area of Yermak Plateau and Fram Strait.

Table 5.1: Time and location of sampling of snow and ice-rafted sediments (IRS) in the Yermak Plateau area.

Date	Investigators	Ice station	Coordinates		No. of samples	
			Lat. (N)	Longitude	Snow	IRS
07.09.2004	Shevchenko V.	0	81°29.96'	08°43.61' E	1	1**
08.09.2004	Shevchenko V. Schäfer C.	1	81°46.0'	02°27.0' W	2*	
09.09.2004	Shevchenko V. Winkelmann D. Kukina N.	2	81°30.20'	03°39.12' E	3*	
10.09.2004	Shevchenko V. Schoster F. Mende I.	3	81°03.73'	03°09.22' E	4*	2
11.09.2004	Shevchenko V. Schneider J. Penshorn D.	4	81°07.25'	00°54.96' E	5	3**
13.09.2004	Shevchenko V. Yanina Ya. Saarswat R.	5	82°08.22'	17°20.31' E	6	
14.09.2004	Shevchenko V. Bahr B. Noffke H.	6	82°18.21'	25°56.27' E	7	4**
14.09.2004	Fricke N. Mende I.	DF	80°16.8'	24°24.4' E	8	
19.09.2004	Shevchenko V. Nam S. Puhr A.	7 8	82°12.23' 82°02.41'	05°41.76' E 05°55.67' E	9	5** 6**
21.09.2004	Shevchenko V. Winkler A. Mende I.	9	81°05.70'	02°00.60' E	10	7**

*Snow sampling for oxygen isotopy was also collected

**Subsamples of IRS for biomarker analysis were taken

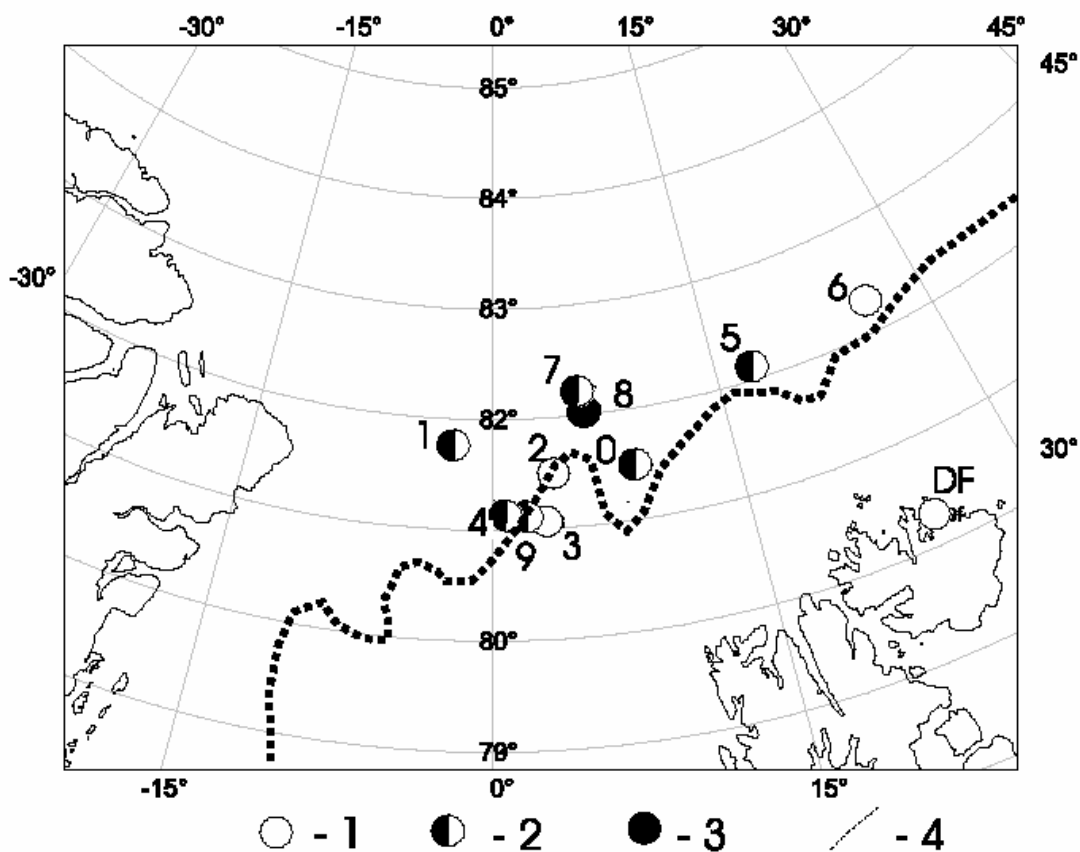


Fig. 5.1: Position of sampling sites: 1 – only snow; 2 – snow and ice-rafted sediments; 3 – only ice-rafted sediments; 4 – ice edge on September 15, 2004 according to satellite data (from www-site of Bremen University).

During the ARK-XX/3 Expedition, we collected samples of ice-rafted sediments on ice floes for multidisciplinary studies. Date, coordinates and short description of sampling sites are given in Table 5.1. Positions of sampling sites are shown in Figure 5.1. All sampling sites were accessed by helicopter. At six stations we found ice-rafted sediments in the form of cryoconite pellets 1–10 cm long dispersed in the 1–2 cm ice layer on the surface of ice ridges. Only at ice station 4, sediments formed a 2–5 mm thick crust on the surface of smooth ice ridges (1 m in height) (Fig. 5.2). Sampling of ice-rafted sediments was carried out by stainless knife and plastic shovel in plastic bottles for trace metal analysis and in stainless tanks for organic geochemistry (Fig. 5.3). Onboard “Polarstern”, ice enriched by sediment pellets was melted at +4°C, and after decantation sub-samples of sedimentary material for biomarker analysis were stored at –30°C and for other analyses at +4°C.



Fig. 5.2: Grey sediment-laden ice ridges at an ice floe in the Yermak Plateau area (Station 4, 81°07.25'N, 0°54.96'E).



Fig. 5.3: Sampling of sediment crust on the ice ridge (Station 4).

Smear slide analyses carried out on sea-ice sediments from seven stations (Table 5.1, Fig.5.1), were performed to estimate the grain size distribution and mineralogical composition of the material. In general, the sea-ice sediments are composed of fine-grained material with partly more than 80 % in the fraction less 63 μm (Table 5.2). Only from one station (Station 1) located in the western part of the Yermak Plateau, coarse-grained sea-ice sediments were sampled that consist of 18% of the sand fraction. The sandy material points to entrainment of surface deposits through anchor ice formation or bottom adfreezing. At other six ice floes we found sediments that more probably were entrained into the ice through scavenging of suspended material from the water column by frazil-ice crystals.

Table 5.2: Grain size distribution ice-rafted sediments (IRS) in %.

No. of IRS sample	Sand	Silt	Clay	Sediment type
1	18	46	36	sandy clayey silt
2	1.2	34.1	64.7	silty clay
3	2.1	41.9	56	silty clay
4	8.6	62	29.4	clayey silt
5	3.6	64	32.4	clayey silt
6	3.9	55	41.1	clayey silt
7	1.1	30.5	68.4	silty clay

Based on smear slide analyses, terrigenous particles dominate in the sea-ice sediments during ARK-XX/3. The principal minerals include quartz, feldspar, mica and clay minerals (Table 5.3). Quartz contents ranged from 16.9% (Station 2) to 36.6% (Station 6). Feldspar contents were up to 21%. The highest amounts of clay minerals (>20%) were observed in sea-ice sediments of stations 2, 3, and 7. The sea-ice sediments of western part of the Yermak Plateau (Stations 1, 2, 4, and 7) obtained less than 1.9% of volcanic glasses. The content of organic remains generally represented by diatoms, spores and plant debris, was between 3.7% and 15.9%.

Table 5.3: Results of smear slide analysis: Mineral composition of ice-rafted sediments in %

Number*	Quartz	Feldspars	Mica	Volc. glass
1	31	13,2	1,2	1,9
2	16,9	10,2	2,3	1,8
3	30,2	20,1	9,5	0
4	30,2	20,6	7,2	1,2
5	30,9	20,4	5,2	0
6	36,6	20,3	9,2	0
7	30,2	14,2	7,1	1,9
Number*	Clay minerals	Org. remains	Fe-hydroxide	Pyroxene
1	18	3,7	9,4	7,6
2	29,1	15,9	5,3	4,5
3	20	9,2	0	3,1
4	7,3	6,8	3,5	6,8
5	9,2	9,6	2,1	3,5
6	7,2	15,9	1,5	1,4
7	20,3	14,2	2,4	1,8
Number*	Amphibole	Garnet	Epidote	Black ores
1	2	1,8	4	5
2	2,6	3,5	1,1	3,5
3	1,6	2,1	2,2	1
4	5,2	3,5	2,1	3,1
5	7,9	9,2	0,1	1,3
6	1,3	3,2	0,2	0,9
7	2,2	2,8	0,8	1
Number*	Turmaline	Rutile	Pyrite	Opaque
1	0,1	0	0	1,1
2	0,7	1,1	0,4	1,1
3	0	0	0	1
4	0	1,8	0	0,7
5	0	0	0	0,6
6	0,4	0,6	0,5	0,8
7	0,4	0,2	0,2	0,3
*Number of IRS sample (see Table 5.1).				

Heavy minerals include pyroxenes, amphiboles, epidote, garnets, Fe-hydroxides and black ores. Pyroxenes and amphiboles dominate the spectrum although in sea-ice sediments of some stations (Stations 1 and 2) Fe-hydroxides dominate the association.

Further laboratory investigation of ice-rafted sediments will include determination of sand/silt/clay percentages (wet sieving and Atterberg separation), silt grain size distribution (Sedigraph), clay mineral assemblages (X-ray diffractometry), total and organic carbon and nitrogen content, biomarkers and elemental composition (instrumental neutron activation, atomic absorption, synchrotron radiation X-ray fluorescence analyses) as well as diatom analysis. Analytical work will be carried out in at the Alfred Wegener Institute for Polar and Marine Research Bremerhaven, the P.P. Shirshov Institute of Oceanology Moscow, the Murmansk Marine Biological Institute, and the United Institute of Geology, Geophysics and Mineralogy SB RAS Novosibirsk, and diatoms will be studied in Moscow State University.

At ice station 5 (82°08.22'N, 17°20.31'E) 1.5 kg of visually clean ice were collected from 2 m high ice ridge as reference sample of Arctic multi-year ice for comparative study of carbon and sulfur isotopes composition with tabular ground ice in the Russian Arctic. The sample is stored in refrigerator at -30°C, and it will be analysed in Institute of Oceanology RAS and P.P. Shirshov Institute of Oceanology RAS, Moscow.

5.2 Snow Chemistry

V. Shevchenko

Aeolian transport of particulate matter onto the Arctic sea ice is one of the sources of sedimentary material in the Arctic (Shevchenko et al., 2000; Shevchenko, 2003). Its role in sedimentation in the Arctic Ocean has been studied insufficiently. The drifting ice in the Arctic is a giant natural accumulator of the aeolian material and attendant pollutants, which first are deposited onto the ice and are transformed into cryosols. When the ice melts, often many thousands kilometres away from the places of their fallout, they are released into the water (mostly in Fram Strait and the Greenland Sea).

The main purpose of our work is to study composition of snow covering drifting ice in the remote arctic area to find sources of dissolved and particulate components. Most snow samples were collected on ice floes. One sample was taken on the shore of the Duvefiord, Spitsbergen. Date, coordinates and short description of sampling sites are given in Table 5.1, position of sampling site is shown in Figure 5.1. All sampling sites were accessed by helicopter at the distance more than 2 km upwind from the RV "Polarstern".

At most sites we collected upper 3-4 cm of snow, reworked by winds. Only on September 10, the upper 3 cm of really fresh snow were taken on an ice floe (Sample No. 4). Snow was collected in pre-cleaned plastic bags using a plastic shovel. Samples are stored in the refrigerator at -30°C till the analysis in the land laboratory.

In the laboratory snow will be melted at +18°C. After that pH will be measured, and ion chromatography will be carried out. Snow melt water will be filtered

through Whatman GF/F and pre-weighted Nuclepore (pore size of 0.45 μm) filters to determine concentrations of total particulate matter, particulate organic carbon, black carbon, particulate nitrogen. Qualitative composition of particulate matter will be studied by scanning electron microscopy. Most laboratory work will be carried out at the Alfred Wegener Institute for Polar and Marine Research, Bremerhaven and at the P.P. Shirshov Institute of Oceanology RAS, Moscow. Contents of black carbon will be determined at the Institute of Chemical Kinetics and Combustion SB RAS, Novosibirsk. The obtained data will be used for an estimation of the aeolian input of particulate matter and chemical components to the drifting ice.

At three ice floes snow for oxygen isotope composition analysis was collected (Table 5.1). After melting at $+4^{\circ}\text{C}$ water subsamples were mixed and combined. In total 30 l of water was obtained. It will be analysed at the Technical University of Freiberg, Germany.

6. Secchi Depth Measurements

V. Shevchenko

The Secchi disc was used for qualitative estimates of the concentration of suspended particulate matter (turbidity). The Secchi disc is a flat circular plate, 30 cm in diameter, all white. It is lowered through the water column in a horizontal attitude until it is observed just to disappear. The depth, at which this happens, is called the Secchi depth, and it depends on the turbidity of the water. The Secchi disc is both cheap and easily made, and it has been used by oceanographers for over a century as a rapid means of assessing water clarity (Seawater, 1995).

In our expedition nine measurements of the Secchi depth were carried out (Table 6.1). It varied from 13 to 18 m with an average of 14.7 m. It shows that the concentration of suspended particulate matter (SPM) in water is very low. The SPM concentration in the Yermak Plateau area in September 2004 was estimated using Secchi depth data and fitting power equation calculated from data of simultaneous SPM and Secchi disk measurements in the White Sea in April 2003 (V. Shevchenko and A. Filippov, unpublished data). Accordingly to these qualitative estimates SPM concentration in the upper 5 m of water column in the studied area varied from 0.23 to 0.37 mg/l (0.31 mg/l in average). For comparison, in the Kara Sea the 5-m transparency isoline shows the border of the main area of influence of the fresh turbid waters from Ob, Yenisey and other rivers (Lisitzin et al., 2000). Only in the outer part of the Kara Sea where the concentration of suspended matter is <0.5 mg/l the Secchi depth increases up to 15 m. In the Gakkel Ridge area in August–September 2001, the Secchi depth varied from 16 to 30 m with an average of 21 m (Shevchenko, 2002).

Table 6.1 Time, locations and results of Secchi depth measurements.

Station	Date	Time (UTC)	Coordinates		Secchi depth (m)
			Latitude (N)	Longitude (E)	
PS 66/318	12/09/2004	16:40	81°18.52'	12°2.55'	14
PS 66/321	13/09/2004	08:45	82°10.38'	18°15.02'	14
PS 66/322	13/09/2004	14:04	82°5.36'	18°5.27'	13
PS 66/325	15/09/2004	15:35	81°26.19'	25°59.85'	14
PS 66/326	16/09/2004	14:00	80°43.23'	15°52.85'	16
PS 66/327	16/09/2004	16:32	81°0.99'	17°9.54'	15
PS 66/333	19/09/2004	17:29	81°55.19'	8°35.81'	18
PS 66/336	20/09/2004	08:09	81°36.35'	6°47.74'	14
PS 66/337	20/09/2004	09:30	81°36.33'	7°1.32'	14

7. Bathymetric Investigations

B. Platten, R. Rathlau, A. Winkler

The main task of the bathymetric working group on this cruise was the support of the geological and geophysical working groups by creating bathymetric charts of their research areas by means of the Hydrosweep system developed by STN Atlas.

The deep-water sounding system Hydrosweep D2 (Fig. 7.1) on RV "Polarstern" DS2 stands out through a 90°/120° coverage angle in which the seafloor is recorded with 59 specific values for water depths (hard beams) perpendicular to the ship's long axis. The sonar beam has an accuracy of approximately 1% deviation from the real waterdepth after the correction of an automated crossfan calibration. The mean sound velocity over the vertical water column is determined by regular transmission and measurement of a sweep profile in the ship's longitudinal direction and comparison of the slant beams with the vertical beam. These data are used for the depth computation

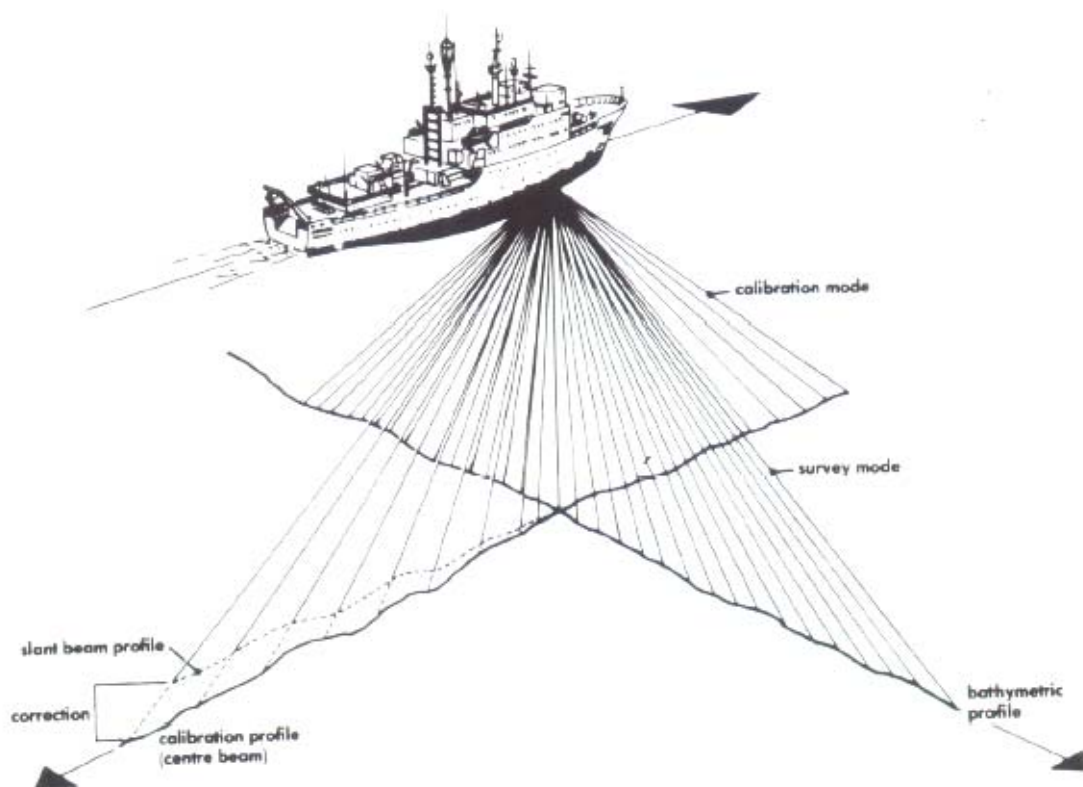


Fig. 7.1: Multibeam sonar system

The operation of the sonar system and the data processing made up the main part of the work. 12 days of the 27 days lasting survey were done under thick ice conditions. In order to prevent abnormal functioning and false measurements due to the thick ice conditions the mostly automatically working multibeam sonar system had to be observed continuously. The changing of the ship's speed and direction due to ice breaking as well as hydroacoustic disturbances caused faulty measurements. Even post-processing became difficult because of the ice conditions, so it was mandatory to check the positions, depths and the ship's attitude data continuously for outlier- or blunder-values. The corrections of the data as well as the general post-processing tasks were done with the software CARIS HIPS and SIPS v. 5.3.

Despite these difficulties the bathymetry working group managed to process all data so far that they now can be used for further examination directly at the AWI.

Beside the sonar operation and the data editing the analysis of multibeam data, the preparation of quick-look track plots and the creation of preliminary bathymetric charts were made. Further presentations of the sea bottom topography grids were calculated out of the edited data with the Generic Mapping Tool (GMT) software.

Based on the grids, contour line maps with a contour interval of 100 m and scales up to 1:150'000 were produced with colour coded depth ranges. These

maps allowed a vivid display of the oceanic ridge topography. The IBCAO Vol. 1 (grid spacing 2500 m) data set was used as background bathymetric data in the contour maps. But since the IBCAO in that region is based on sporadic single beam sonar tracks and bathymetry estimated from satellite data, there were substantial differences between the systematically surveyed maps and the IBCAO data. By the combination of previously recorded data with the new data from this cruise the working group bathymetry was able to close some major gaps in the existing data as well as to discover new examination areas.

Bathymetric issues have been very important for the geological investigations on this cruise as shown in three examples.

(1) The eastern slope Yermak Plateau and the North East Land shelf of Svalbard was of special interest due to a suspected megaslide in this area (See Chapter 9). The shelf and its eastern and western slopes (Fig. 7.2) could be surveyed by using the multibeam sonar system Hydrosweep. Altogether the sea-ice conditions were good, so that reasonable profile measurements could be done on the Yermak Plateau.

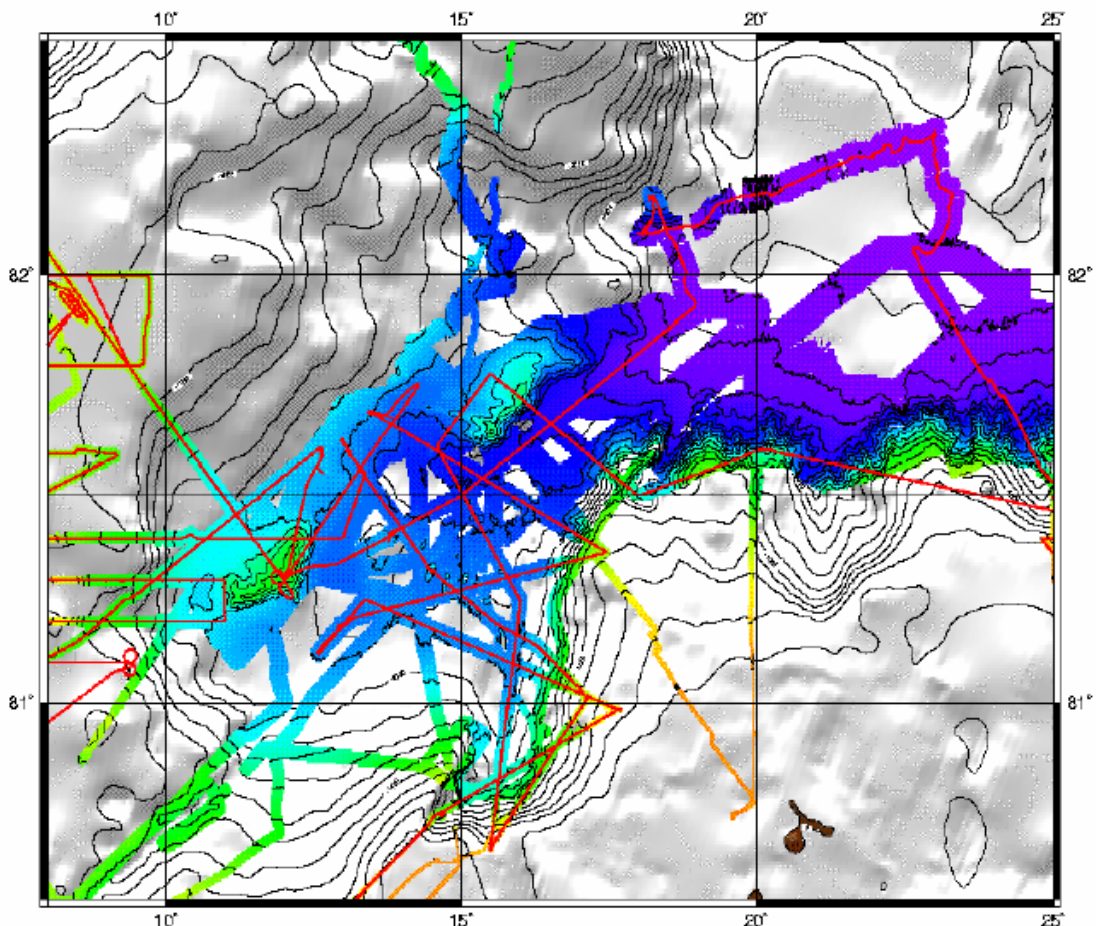


Fig. 7.2: Hydrosweep profiles in the Sophia Basin, southeast of the Yermak Plateau, and at the northern Svalbard continental margin

(2) On top of the central Yermak Plateau, probably out-cropped older sedimentary rocks should be sampled by means of the sediment dredge. The localization of petrologic sampling stations was accomplished based on the bathymetric maps (Fig. 7.3).

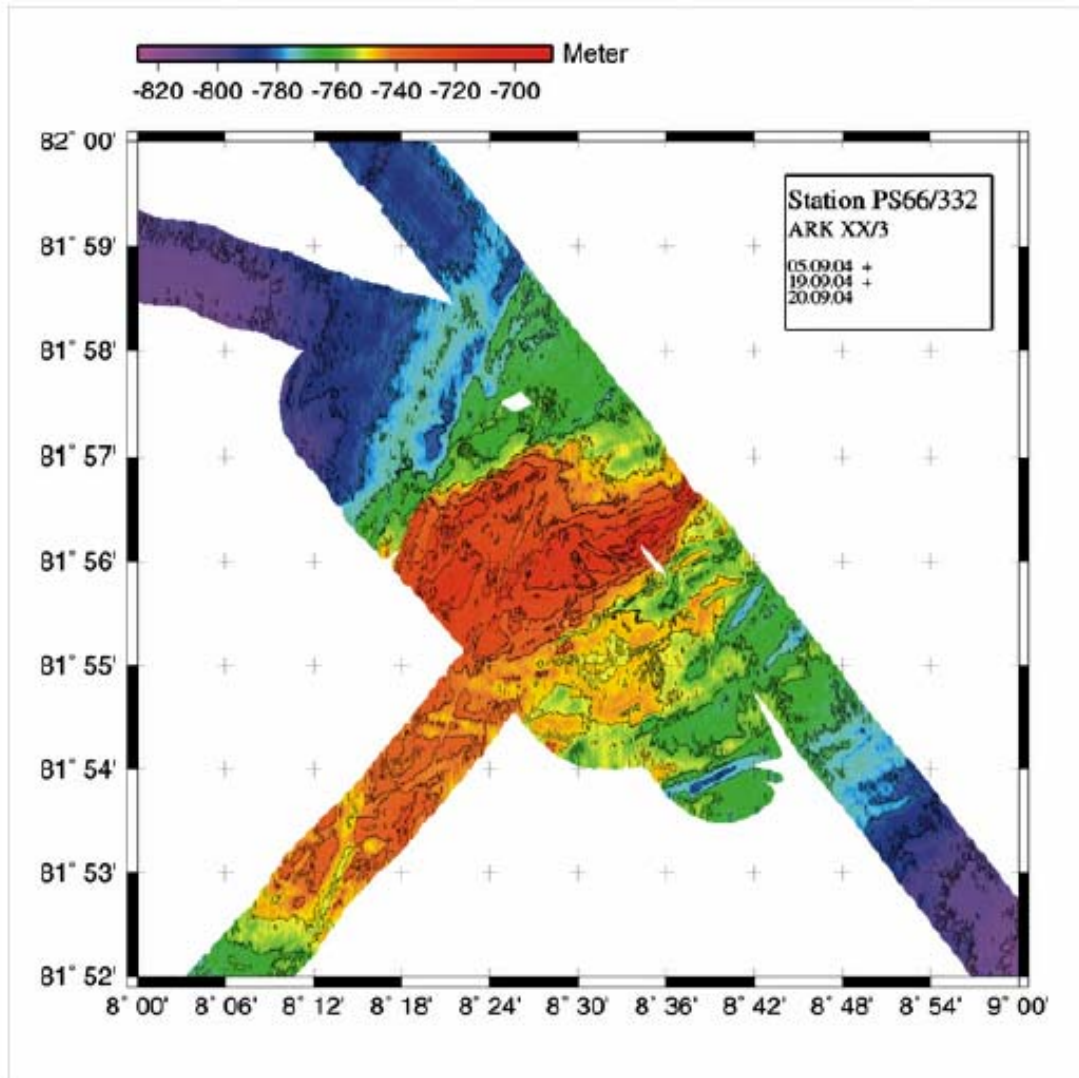


Fig. 7.3: Station PS 66/332 on the central Yermak Plateau, selected based on a bathymetric chart

(3) With systematic seismic profiles it was possible to determine the depth and course of iceberg plough marks on the Yermak plateau from the recorded bathymetric depth data (Fig. 7.4). On the western slope of the plateau the transition from the plateau area in Fram Strait-direction to the deep sea could be documented successfully.

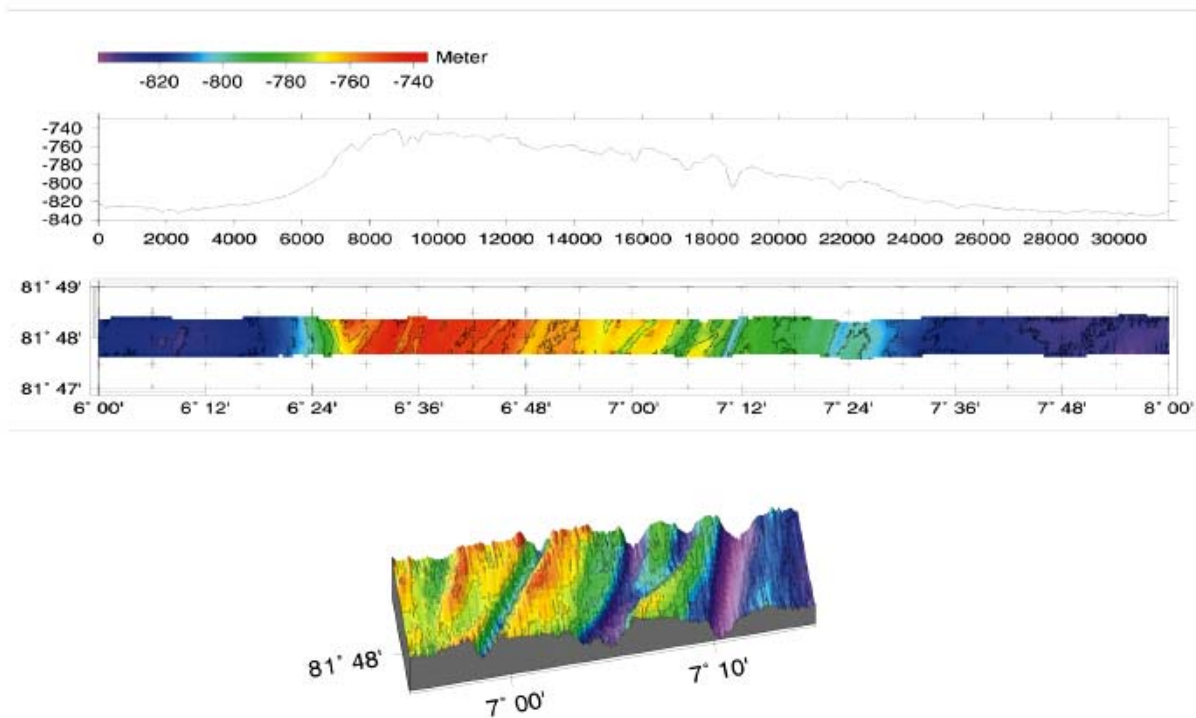


Fig. 7.4: Iceberg plough marks on Yermak Plateau

8. Marine Geophysics

W. Jokat, Y. Behr, H. Birnstiel, A. Gebauer, K. Gößling, D. Günther, H. Martens, N. Lensch, W. Raabe, M. Schmidt-Aursch, M. Schroeder, Th. Spengler

The only deep water connection of the Arctic Ocean with the world oceans is the Fram Strait. The deepest part of the Fram Strait hosts an active mid-ocean ridge, the Lena Trough. The spreading in the Lena Trough is the latest stage of the separation of Greenland and Svalbard, which started with large strike-slip movements some 50 Myr ago. According to published geodynamic models a deep-water connection for the Arctic Ocean was established some 10 to 15 Ma. This is inferred from reconstructions of the northern Atlantic and the relevant magnetic spreading anomalies in the North Atlantic and the Eurasia Basin. Details on the opening history of the Lena Trough, however, are not available, since spreading anomalies in the Fram Strait and across the southern basins (Greenland-Spitzbergen Sill, Boreas Basin) are missing.

The mid-ocean ridge in the Lena Trough is bounded by two prominent plateaus to the east and west: Yermak Plateau and Morris Jessup Rise. Based on the current knowledge these rises were formed some 35 Ma, when the relative

movements between Svalbard and Greenland became significant, and as a consequence, volcanic material erupted beneath the rises and/or formed them. There is no information available to constrain the amount of magmatic material that erupted during this time period. Speculations suggest that the north-eastern Yermak Plateau is oceanic in origin, while its southern part might consist of stretched continental crust. The same interpretations are valid for the Morris Jessup Rise. Most of these hypotheses base on aeromagnetic investigations, which show strong up to 1000 nT magnetic anomalies at both rises. Such strong anomalies are believed to be related to magmatism during continental break-up. However, no seismic data exist to constrain the interpretations in defining the nature of the crust.

The main scientific objective of this cruise was to enlarge the geophysical database in the Fram Strait to provide further constraints on the deeper structure and the evolution of this region. In detail the following problems should be addressed:

- Seismic investigations across the northern Yermak Plateau to identify the continent-ocean transition. The multichannel seismic network should be designed in a way that within a recent IODP preproposal the location of the sites can be determined in an optimum way.
- Deep seismic investigations to identify the deeper structure of the Yermak Plateau. With the wide-angle reflection data it should be possible to make estimates on the magmatic underplating, if any are present, of the Yermak Plateau.
- Try to sample basement rocks in order to date and constrain the evolution of the plateau.

Within the proposed IODP drilling proposal the following goals should be achieved:

- To find suitable locations to drill the basement in order to resolve the origin of the plateau and to understand the origin of the strong magnetic anomalies along the northern rim of the plateau.
- To find suitable locations to reach old drift sediments in the Fram Strait in order to resolve the palaeoceanographic history of the Arctic Gateway.

Experiment set-up, constraints and statistics

Before the expedition available ice maps showed already that during this season the ice edge in the Fram Strait retreated as far north as 82°N. Arriving in the research area of the north-eastern plateau this observation was more or less confirmed with the exception that compact ice fields drifting in the entire area were making seismic investigations difficult. To conduct deep seismic experiments in ice we needed ice floes with a sufficient snow cover to dig the geophones into it. Such kind of floes was completely missing. Almost no snow was left on the floes. Thus, the deep seismic experiments were not conducted since there was no chance to dig the geophones into the naked ice, and shelter them

against wind. As a consequence the geophysical experiments were concentrated on acquiring multi-channel seismic data with an 800 m long streamer. As source we used an airgun array with a total volume of 24 l. In addition, 20 long-range sonobuoys were deployed and successfully recovered (Table 8.2). Their signal ranges vary between 10 and 50 km.

The geophysical ship time can be split into three large portions a) the seismic network on the Yermak Plateau (Fig. 8.1, 260 h), b) dredging of basement highs on the Yermak Plateau (20 h), and c) the four site survey boxes along the East Greenland margin (Figs. 8. 2 and 8.3; 110 h). This sums up to 17 days of ship time including transit and seismic profiling. During this period in total 2920 km of new seismic data were acquired in the areas of investigation (Table 8.1). Despite an 5-10/10 ice cover the data quality is good, and there is a fair chance to suppress the seafloor multiple in order to image the basement of the Yermak Plateau along some profiles. The spacing of the W-E trending lines on the north-western part of the Yermak Plateau is approximately 11 km. Existing seismic networks acquired in 2002 and by Norwegian institutions were supplemented wherever possible. Areas south of 81°N were not investigated, since they are also accessible during normal sea ice seasons. Here, using a longer streamer of up to 3000 km is more appropriate, since a strong water bottom multiple has to be removed in order to image the thicker sediment packages.

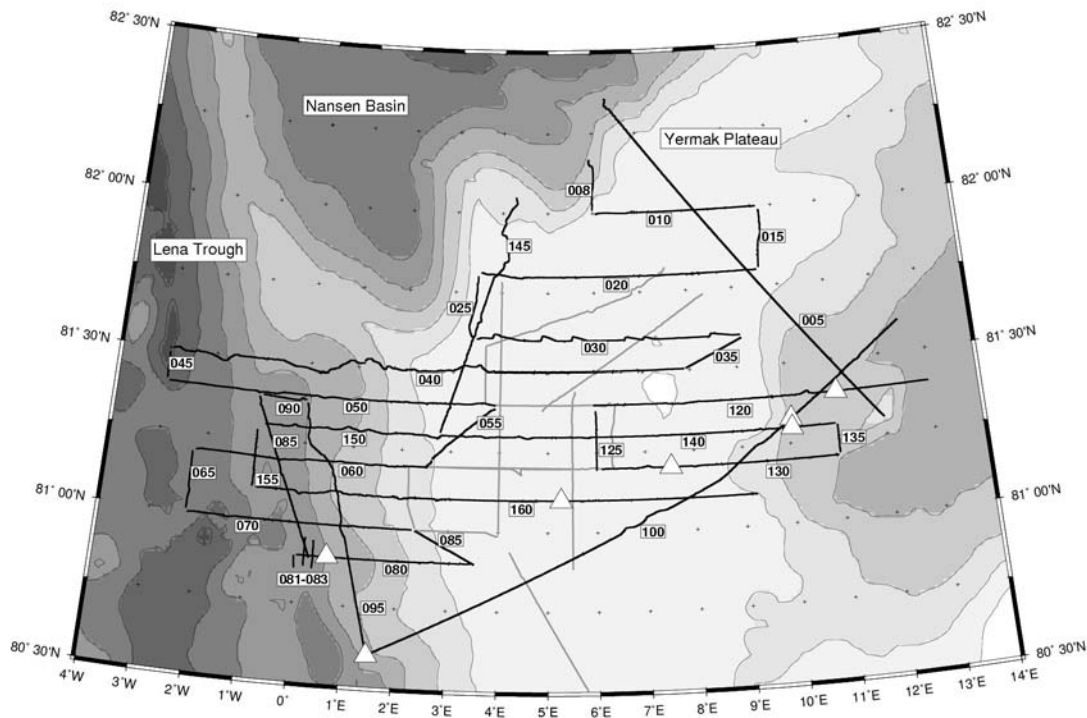


Fig.8.1: Location of the seismic profiles on the Yermak Plateau. The small triangles indicate the location of sonobuoy deployment.

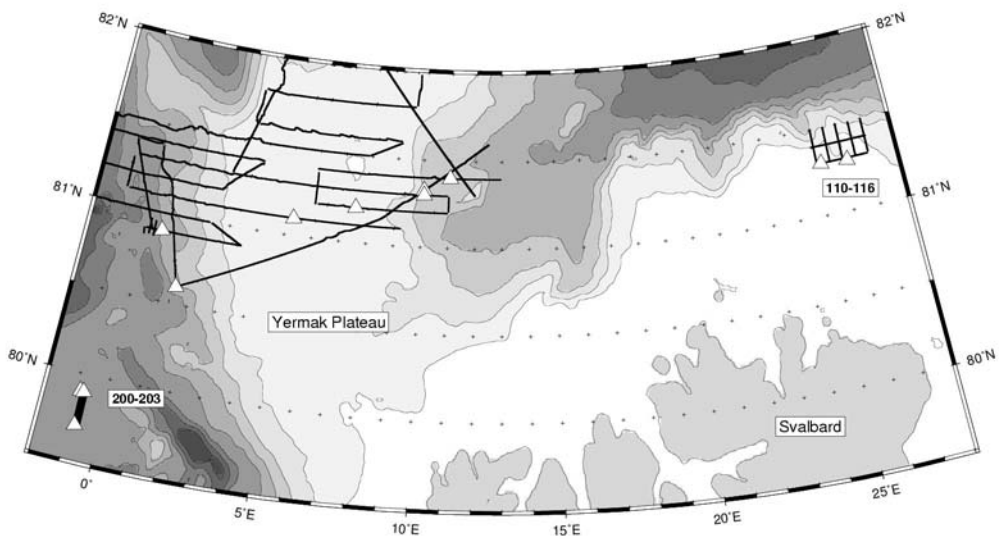


Fig. 8.2: Location of IODP site surveys on the Spitzbergen Sill and along the margin of Northern Svalbard

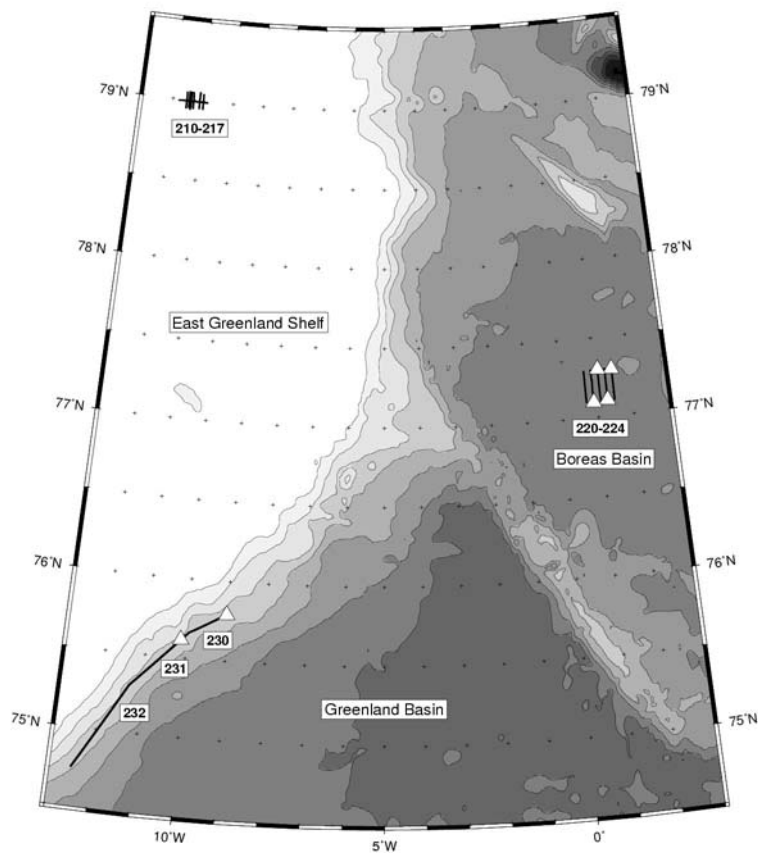


Fig. 8.3: Location of IODP site surveys along the East Greenland margin and on the East Greenland Shelf

Table 8.1: Profile and shot statistics

Profil	Beginn		End		Start		End		Shots	Length	Sonobuoys	Delay	Streamer	Lead In	Airgun	Chan	dx Chan
	Date	Time	Date	Time	Lon	Lat	Lon	Lat		[km]	Running Number	[s]	[m]	[m]			
20040005	05.09.2004	13:50:00	06.09.2004	04:35:00	81,3029	11,9847	82,3577	6,3005	3516	150,4	none	0	600	30	8x3l	96	6,25
20040008	06.09.2004	10:05:00	06.09.2004	11:57:00	82,1674	5,9172	82,0087	5,9910	446	18,7	none	0	600	30	8x3l	96	6,25
20040010	06.09.2004	12:07:00	06.09.2004	17:28:00	81,9977	6,0521	82,0005	9,6548	1276	56,35	none	0	600	30	8x3l	96	6,25
20040015	06.09.2004	17:38:00	06.09.2004	19:34:00	81,9890	9,7165	81,8071	9,6239	462	20,75	none	0	600	30	8x3l	96	6,25
20040020	06.09.2004	19:40:00	07.09.2004	05:14:00	81,8017	9,5782	81,8127	3,5446	2281	97,19	none	0	600	30	8x3l	96	6,25
20040025	07.09.2004	05:24:00	07.09.2004	07:30:00	81,8023	3,4816	81,6088	3,3753	502	22,4	none	1	600	30	8x3l	96	6,25
20040030	07.09.2004	07:41:00	07.09.2004	18:05:00	81,6045	3,4817	81,6003	9,1208	2246	98,11	none	1	600	30	8x3l	96	6,25
20040035	07.09.2004	18:16:00	07.09.2004	20:23:00	81,5908	9,1385	81,5055	7,9214	506	22,25	none	1	600	30	8x3l	96	6,25
20040040	07.09.2004	20:26:00	08.09.2004	16:25:00	81,5043	7,8922	81,5011	-2,9565	4436	191	none	3	600	30	8x3l	96	6,25
20040045	08.09.2004	16:37:00	08.09.2004	17:30:00	81,4869	-3,0025	81,4073	-2,9932	270	8,96	none	3	600	30	8x3l	96	6,25
20040050	08.09.2004	17:40:00	09.09.2004	05:16:00	81,3994	-2,9245	81,3979	3,9000	2765	116,1	none	4	600	30	8x3l	96	6,25
20040055	09.09.2004	05:25:00	09.09.2004	08:54:00	81,3881	3,9026	81,1968	2,4869	740	32,81	none	4	600	30	8x3l	96	6,25
20040060	09.09.2004	13:03:00	09.09.2004	21:27:00	81,1990	2,5337	81,1970	-2,2092	2003	82,28	none	0	600	30	8x3l	96	6,25
20040065	09.09.2004	21:36:00	09.09.2004	23:35:00	81,1883	-2,2743	81,0093	-2,2717	473	20,23	none	0	600	30	8x3l	96	6,25
20040070	09.09.2004	23:44:00	10.09.2004	07:28:00	80,9997	-2,2322	81,0003	2,2710	1842	79,48	none	0	600	30	8x3l	96	6,25
20040075	10.09.2004	07:35:00	10.09.2004	09:52:00	80,9974	2,3334	80,8976	3,5299	544	23,93	none	1	600	30	8x3l	96	6,25
20040080	10.09.2004	12:05:00	10.09.2004	18:30:00	80,9004	3,4686	80,8998	0,0110	1406	61,98	sb0401	0	600	30	8x3l	96	6,25
20040081	10.09.2004	18:36:00	10.09.2004	19:01:00	80,8978	-0,0406	80,8594	-0,0140	101	4,34	none	0	600	30	8x3l	96	6,25
20040082	10.09.2004	19:25:00	10.09.2004	20:25:00	80,8668	0,1661	80,9571	0,1667	231	10,17	none	0	600	30	8x3l	96	6,25
20040083	10.09.2004	20:50:00	10.09.2004	21:51:00	80,9498	0,3336	80,8596	0,3305	243	10,14	none	0	600	30	8x3l	96	6,25
20040085	10.09.2004	22:27:00	11.09.2004	04:30:00	80,8932	0,2574	81,3848	-1,0284	1436	60,34	none	0	600	30	8x3l	96	6,25
20040090	11.09.2004	04:39:00	11.09.2004	06:17:00	81,3904	-0,9523	81,3865	-0,0368	390	15,94	none	1	600	30	8x3l	96	6,25
20040095	11.09.2004	06:24:00	11.09.2004	15:33:00	81,3776	-0,0082	80,6089	1,4884	2085	93,54	sb0402	1	600	30	8x3l	96	6,25
20040100	11.09.2004	15:40:00	12.09.2004	13:22:00	80,6021	1,5312	81,5997	12,4949	5161	223,9	sb0402 / sb0403	2	600	30	8x3l	96	6,25
20040110	14.09.2004	15:45:00	14.09.2004	17:50:00	81,5010	25,0007	81,3009	25,0030	498	22,44	none	0	600	30	8x3l	96	6,25
20040111	14.09.2004	17:56:00	14.09.2004	20:59:00	81,2972	25,0379	81,3008	26,9711	727	32,83	sb0404	1	600	30	8x3l	96	6,25
20040112	14.09.2004	21:03:00	14.09.2004	23:07:00	81,3052	27,0002	81,4998	26,9996	494	21,83	sb0404	1	600	30	8x3l	96	6,25
20040113	15.09.2004	00:03:00	15.09.2004	02:07:00	81,5003	26,4956	81,3000	26,5033	494	22,47	sb0404	1	600	30	8x3l	96	6,25
20040114	15.09.2004	03:09:00	15.09.2004	05:23:00	81,2998	26,0019	81,5074	26,0028	533	23,29	sb0404 / sb0405	1	600	30	8x3l	96	6,25

Profil	Beginn		End		Start		End		Shots	Length	Sonobuoys	Delay	Streamer	Lead In	Airgun	Chan	dx Chan
	Date	Time	Date	Time	Lon	Lat	Lon	Lat		[km]	Running Number	[s]	[m]	[m]			
20040115	15.09.2004	06:14:00	15.09.2004	08:26:00	81,502	25,4988	81,2951	25,4972	525	23,21	sb0404 / sb0405	1	600	30	8x3l	96	6,25
20040116	15.09.2004	10:18:00	15.09.2004	13:38:14	81,3996	24,8971	81,4001	27,0641	749	36,34	none	2	600	30	8x3l	96	6,25
20040120	17.09.2004	08:54:00	17.09.2004	20:09:45	81,4002	12,9789	81,3995	5,9591	2679	118,93	sb0406	0	600	30	8x3l	96	6,25
20040125	17.09.2004	20:32:00	17.09.2004	22:32:00	81,3805	5,9898	81,1946	6,0015	477	20,88	sb0406	1	600	30	8x3l	96	6,25
20040130	17.09.2004	22:45:00	18.09.2004	06:40:00	81,1984	6,1144	81,2006	10,972	1865	83,79	sb0406 / sb0407	1	600	30	8x3l	96	6,25
20040135	18.09.2004	06:47:00	18.09.2004	07:43:00	81,2079	11,0016	81,2970	10,9967	221	10,02	sb0406 / sb0407	1	600	30	8x3l	96	6,25
20040140	18.09.2004	07:49:00	18.09.2004	21:33:00	81,3000	10,9570	81,2993	2,8190	3192	139,11	sb0406 / sb0407 / sb0408	2	600	30	8x3l	96	6,25
20040145	18.09.2004	21:44:00	19.09.2004	07:25:00	81,3099	2,7736	82,0513	4,2940	2293	92,32	none	3	600	30	8x3l	96	6,25
20040150	20.09.2004	16:45:00	20.09.2004	23:26:45	81,3008	2,8373	81,2991	-0,8591	1598	65,21	none	0	600	30	8x3l	96	6,25
20040155	21.09.2004	00:04:00	21.09.2004	02:06:00	81,2780	-1,0098	81,1008	-1,0027	486	20,19	none	0	600	30	8x3l	96	6,25
20040160	21.09.2004	02:24:00	21.09.2004	20:00:00	81,0979	-0,9011	81,1001	9,2497	4194	178,36	sb0411	1	600	30	8x3l	96	6,25
20040200	22.09.2004	10:43:00	22.09.2004	12:46:00	79,8994	-0,8598	79,7000	-0,8467	490	22,41	sb0412	0	600	30	8x3l	96	6,25
20040201	22.09.2004	13:00:00	22.09.2004	15:10:00	79,7005	-0,8001	79,9054	-0,7998	517	22,98	sb0412 / sb0413	0	600	30	2xG+1xGl	96	6,25
20040202	22.09.2004	15:21:00	22.09.2004	17:31:00	79,8998	-0,7522	79,6955	-0,7522	517	22,95	sb0412 / sb0413 / sb0414	0	600	30	2xG+1xGl	96	6,25
20040203	22.09.2004	17:42:45	22.09.2004	19:48:00	79,6983	-0,7009	79,9051	-0,7022	499	23,20	none	0	600	30	2xG+1xGl	96	6,25
20040204	22.09.2004	20:02:00	22.09.2004	22:17:00	79,8991	-0,6549	79,6986	-0,6492	537	22,49	none	1	600	30	2xG+1xGl	96	6,25
20040210	23.09.2004	14:13:00	23.09.2004	15:13:00	79,0476	-10,9979	78,9496	-10,9976	715	11,00	none	0	600	30	1x2,4l (G)	96	6,25
20040211	23.09.2004	15:37:00	23.09.2004	16:45:00	78,9499	-11,1114	79,0556	-11,1074	808	11,90	none	0	600	30	1x2,4l (G)	96	6,25
20040212	23.09.2004	17:14:00	23.09.2004	18:22:00	79,0547	-11,3299	78,9467	-11,3216	808	12,16	none	0	600	30	1x2,4l (G)	96	6,25
20040213	23.09.2004	18:40:00	23.09.2004	19:51:00	78,9371	-11,4034	79,0555	-11,3895	841	13,14	none	0	600	30	1x2,4l (G)	96	6,25
20040214	23.09.2004	20:00:00	23.09.2004	21:10:00	79,0537	-11,4242	78,9466	-11,4238	832	12,04	none	0	600	30	1x2,4l (G)	96	6,25
20040215	23.09.2004	21:22:00	23.09.2004	22:28:00	78,9497	-11,4579	79,0538	-11,4615	787	11,70	none	0	600	30	1x2,4l (G)	96	6,25
20040216	23.09.2004	22:48:00	23.09.2004	23:54:00	79,0504	-11,5496	78,9453	-11,5483	750	11,80	none	0	600	30	1x2,4l (G)	96	6,25
20040217	24.09.2004	00:54:00	24.09.2004	02:48:00	78,9928	-11,8007	78,9933	-10,8556	1354	20,31	none	1	600	30	1x2,4l (G)	96	6,25
20040220	25.09.2004	04:45:00	25.09.2004	06:25:00	77,2987	1,4938	77,1397	1,5025	399	17,86	sb0415	0	600	30	2xG+1xGl	96	6,25
20040221	25.09.2004	07:27:00	25.09.2004	09:41:00	77,0984	1,2958	77,3053	1,2994	533	23,19	sb0415 / sb0416	0	600	30	2xG+1xGl	96	6,25
20040222	25.09.2004	10:13:00	25.09.2004	12:29:00	77,3058	1,0962	77,0963	1,1070	541	23,52	sb0415 / sb0416 / sb0417	1	600	30	2xG+1xGl	96	6,25
20040223	25.09.2004	13:08:00	25.09.2004	15:20:00	77,1005	0,9036	77,3051	0,9002	525	22,96	sb0417 / sb0418	1	600	30	2xG+1xGl	96	6,25
20040224	25.09.2004	15:54:30	25.09.2004	18:06:00	77,3000	0,6998	77,0947	0,6990	524	23,04	sb0417 / sb0418	1	600	30	2xG+1xGl	96	6,25
20040230	26.09.2004	09:38:00	26.09.2004	12:25:00	75,8033	-8,9457	75,6611	-9,9653	665	32,43	sb0419	0	600	30	8x3l	96	6,25
20040231	26.09.2004	12:25:00	26.09.2004	17:55:00	75,6611	-9,9653	75,2996	-11,3196	1178	55,70	sb0419 / sb0420	0	600	30	8x3l	96	6,25
20040232	26.09.2004	17:55:00	27.09.2004	00:05:15	75,2996	-11,3196	74,7475	-12,4960	1472	70,69	none	0	600	30	8x3l	96	6,25

Table 8.2: Statistics on the sonobuoy deployments

Profil	Beginn		End		Sonobuoy			Shots	Length of Profil w hile registrating	Start of Registration		Airguns	Streamer
	Date	Time	Date	Time	Typ	Buoy	Number			Lon	Lat		
20040080	10.09.2004	12:34:48	10.09.2004	17:26:40	DOSH	sb1	sb0401	1033	44,97	80°52N	00°36E	VFL	600
20040095	11.09.2004	11:59:02	11.09.2004	15:33:00	DOSH	sb1	sb0402	802	37,43	80°36N	01°29E	VFL	600
20040100	11.09.2004	15:40:00	11.09.2004	18:49:20	DOSH	sb1	sb0402	752	33,66	81°36N	10°30E	VFL	600
	12.09.2004	08:36:43	12.09.2004	13:22:00	DOSH	sb1	sb0403	1126	45,80	81°36N	12°28E	VFL	600
20040111	14.09.2004	18:08:00	14.09.2004	20:59:00	DOSH	sb3	sb0404	681	30,73	81°17N	25°09E	VFL	600
20040112	14.09.2004	21:03:00	14.09.2004	23:07:00	DOSH	sb3	sb0404	494	21,83	81°19N	27°00E	VFL	600
20040113	15.09.2004	00:03:00	15.09.2004	02:07:00	DOSH	sb3	sb0404	494	22,47	81°30N	26°30E	VFL	600
20040114	15.09.2004	03:09:00	15.09.2004	05:23:00	DOSH	sb3	sb0404	533	23,29	81°18N	26°00E	VFL	600
	15.09.2004	03:10:00	15.09.2004	05:23:00	DOSH	sb1	sb0405	529	23,11	81°18N	26°00E	VFL	600
20040115	15.09.2004	06:14:00	15.09.2004	08:26:00	DOSH	sb3	sb0404	525	23,21	81°30N	25°30E	VFL	600
	15.09.2004	06:14:00	15.09.2004	08:21:00	DOSH	sb1	sb0405	505	22,26	81°30N	25°30E	VFL	600
20040120	17.09.2004	11:57:38	17.09.2004	20:09:45	DOSH	sb1	sb0406	1949	86,20	81°24N	11°01E	VFL	600
20040125	17.09.2004	20:32:00	17.09.2004	22:32:00	DOSH	sb1	sb0406	477	20,88	81°23N	05°59E	VFL	600
20040130	17.09.2004	22:45:00	18.09.2004	06:40:00	DOSH	sb1	sb0406	1865	83,79	81°12N	06°07E	VFL	600
	17.09.2004	01:03:00	18.09.2004	06:40:00	DOSH	sb3	sb0407	1317	60,45	81°12N	06°07E	VFL	600
20040135	18.09.2004	06:47:00	18.09.2004	07:43:00	DOSH	sb1	sb0406	221	10,21	81°13N	11°00E	VFL	600
	18.09.2004	06:47:00	18.09.2004	07:43:00	DOSH	sb3	sb0407	221	10,21	81°13N	11°00E	VFL	600
20040140	18.09.2004	07:49:00	18.09.2004	08:16:00	DOSH	sb1	sb0406	108	4,81	81°18N	10°57E	VFL	600
	18.09.2004	07:49:00	18.09.2004	17:22:00	DOSH	sb3	sb0407	2194	96,92	81°18N	10°57E	VFL	600
	18.09.2004	09:23:00	18.09.2004	17:00:00	DOSH	sb1	sb0408	1735	76,21	81°17N	9°58E	VFL	600
20040160	21.09.2004	13:35:00	21.09.2004	16:44:47	DOSH	sb2	sb0411	755	33,63	81°06N	5°16E	VFL	600
20040200	22.09.2004	10:43:00	22.09.2004	12:46:00	DOSH	sb1	sb0412	490	22,41	79°53N	0°52W	VFL	600
20040201	22.09.2004	13:00:00	22.09.2004	15:10:00	DOSH	sb1	sb0412	517	22,98	79°42N	0°48W	2xG+1xGI	600
	22.09.2004	13:00:00	22.09.2004	15:10:00	DOSH	sb2	sb0413	517	22,98	79°42N	0°48W	2xG+1xGI	600
20040202	22.09.2004	15:21:00	22.09.2004	16:28:00	DOSH	sb1	sb0412	267	12,15	79°54N	0°45W	2xG+1xGI	600
	22.09.2004	15:21:00	22.09.2004	16:43:00	DOSH	sb2	sb0413	326	14,76	79°54N	0°45W	2xG+1xGI	600
	22.09.2004	15:21:00	22.09.2004	17:30:00	DOSH	sb4	sb0414	513	22,78	79°54N	0°45W	2xG+1xGI	600
20040220	25.09.2004	04:47:00	25.09.2004	06:25:00	DOSH	sb1	sb0415	391	17,52	77°17N	1°29E	2xG+1xGI	600
20040221	25.09.2004	07:27:00	25.09.2004	09:41:00	DOSH	sb1	sb0415	533	23,19	77°06N	1°18E	2xG+1xGI	600
	25.09.2004	07:27:00	25.09.2004	09:41:00	DOSH	sb2	sb0416	533	23,19	77°06N	1°18E	2xG+1xGI	600
20040222	25.09.2004	10:13:00	25.09.2004	10:20:00	DOSH	sb1	sb0415	29	1,23	77°18N	1°06E	2xG+1xGI	600
	25.09.2004	10:13:00	25.09.2004	10:40:00	DOSH	sb2	sb0416	108	4,74	77°18N	1°06E	2xG+1xGI	600
	25.09.2004	10:16:00	25.09.2004	12:29:00	DOSH	sb4	sb0417	529	33,00	77°18N	1°05E	2xG+1xGI	600
20040223	25.09.2004	13:08:00	25.09.2004	15:20:00	DOSH	sb4	sb0417	525	22,96	77°06N	0°54E	2xG+1xGI	600
	25.09.2004	13:08:00	25.09.2004	15:20:00	DOSH	sb1	sb0418	525	22,96	77°06N	0°54E	2xG+1xGI	600
20040224	25.09.2004	15:54:30	25.09.2004	16:26:00	DOSH	sb4	sb0417	127	5,70	77°18N	0°42E	2xG+1xGI	600
	25.09.2004	15:54:30	25.09.2004	16:13:00	DOSH	sb1	sb0418	75	3,36	77°18N	0°42E	2xG+1xGI	600
20040230	26.09.2004	09:53:00	26.09.2004	12:25:00	DOSH	sb1	sb0419	605	29,39	75°47N	9°01W	VFL	600
20040231	26.09.2004	12:25:00	26.09.2004	13:58:00	DOSH	sb1	sb0419	237	11,27	75°40N	9°58W	VFL	600
	26.09.2004	13:39:00	26.09.2004	16:28:00	DOSH	sb2	sb0420	671	31,49	75°36N	10°15W	VFL	600

The Yermak Plateau east of 10°E was this season not accessible. Thick multi-year ice floes did not allow any single ship seismic investigations. This is also valid for the areas north of 82°N. Only on two profiles this part of the Arctic Ocean could be entered till the ship got stuck in thick ice floes.

Parallel to the seismic investigations gravity and magnetic data were continuously acquired by fixed installed instruments. Harbour values for the gravimeter were taken in Tromsø and Bremerhaven. Both instruments worked without any problems or failures.

Results

The ice conditions during this season allowed the first time to conduct a detailed seismic survey across the north-western part of the Yermak Plateau (Fig. 8.1). In addition two long almost N-S trending transect were acquired across the entire plateau, which provided a surprising image of the deeper structure of the Yermak Plateau at 10°E longitude. The seismic data show that the ancient topography is quite rough. Ridges and mountains with altitudes up to 1000 m are present. The present plateau-like shape is a consequence of continuous sedimentation mostly driven by currents, which filled the deep depressions between the topographic highs.

The seismic network west of 6°E indicates some kind of change in the style of drift deposition. Close to topographic highs the sedimentation pattern shows that currents were guided along these obstacles. The fast changes in the geometry of sediment drifts indicate quite dynamic processes, which are active till present. However, the drift sediment could build up only to a depth range of 600 to 800 m. In the shallowest parts the deposits were eroded by icebergs. More or less constant erosion by the icebergs prevented any formation of shallower sediment drifts. These processes caused on several locations that old drift sediments crop out at the surface or are only covered by a thin (200 m) sedimentary drape. Such locations are present on the Yermak Plateau, where old sedimentary units terminate close to the seafloor. However, their exact age is not known. From geodynamic models it can be assumed that the basement blocks were formed during the final split of the Yermak and Morris Jessup plateaus and/or during the earlier rifting period. Thus, the oldest sediments on the Yermak Plateau might be around 35 Ma old. The basement, if continental, might be as old as Devonian.

A different situation is found in the west towards the Lena Trough (Fig. 8.1). This mid-ocean ridge system actually forms the deep part of the Fram Strait and channels the deep-water exchange between the North Atlantic and the Arctic Ocean. Again the exact timing how this ridge evolved during the geological times is not known. The older oceanic crust is covered on both sides of the ridge by thick sediments. Magnetic spreading anomalies terminate north of 83°N. Thus, no detailed information on the development of the Lena Trough between 83°N and 80°N from the magnetic data is available. Especially this area is critical to all models, which deal with the initiation of the deep-water exchange of both oceans. The seismic profiles were planned to stretch from the central part of the Yermak Plateau to the present day rift shoulder of the Lena Trough.

Only one profile enters also the rift valley. Two observations from the seismic data are important:

- The geological history of both rift flanks seems not to be symmetric for the Greenland and the Svalbard margins. From the seismic data which were gathered in the last years, the North-Greenland margin is more rugged and is less covered by sediments than its counterpart on the Yermak Plateau. Models which suggest that the northward running Atlantic water carries more sediment load than the Arctic water masses are confirmed by the seismic data sets.
- Along the western margin of the Yermak Plateau large drift deposits were formed through the sediment load of the Atlantic water masses. They are around 2000 m thick and show a very constant depositional pattern. However, there are two exceptions. Close to the flank of the Lena Trough the sediments are slightly folded. More eastward an interesting area is indicated by a smooth change in the depth gradient of the sea floor. Below this stronger increase in water depth, the seismic units terminate or thin significantly. Old drift deposits, which might have formed during Miocene times, are close below the sea floor (Fig. 8.4, ca. 200 m drape). From the present stage of interpretation it is not clear what kind of process caused this image. A likely scenario is that the current speed increased due to a faster subsidence of the ridge or an increased amount of water exchange. Thus, the new drift sediments were deposited at greater depths and the older drift deposits were partly eroded.

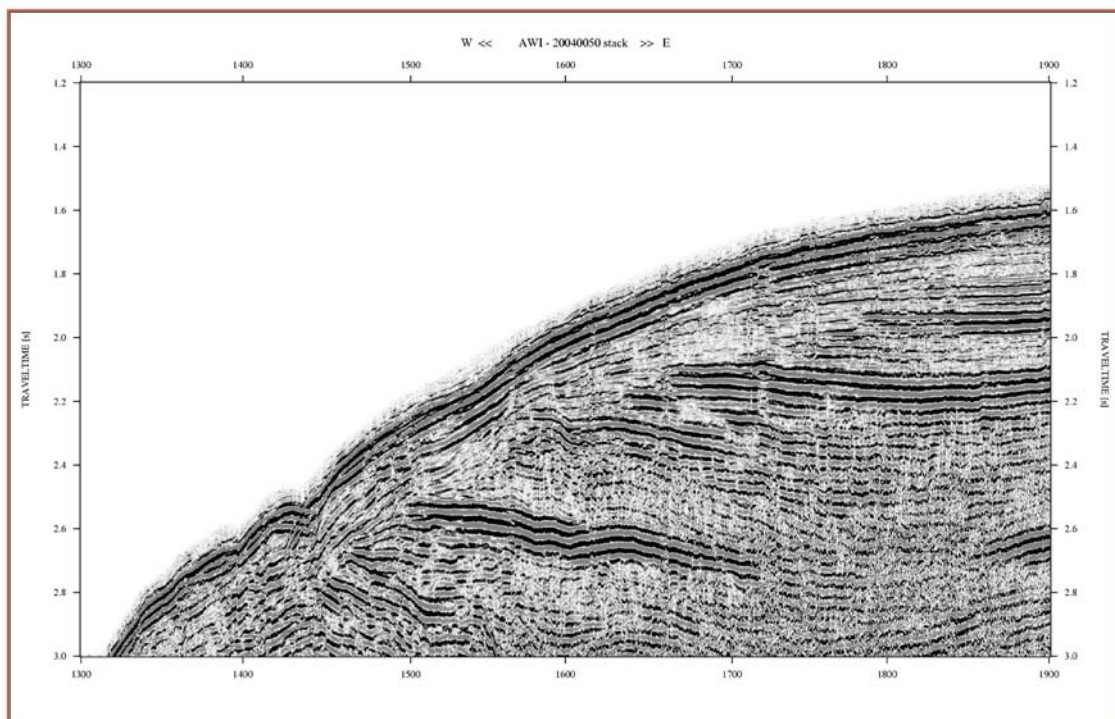


Fig.8.4: Seismic profile on the eastern flank of the Lena Trough. Please note that deeper strata terminate and/or thin towards the seafloor.

These first ideas on the explanation of the seismic images have to be verified during future analyses. An important aspect to do so is that the new seismic network has several tie lines to the existing ODP drill holes. Here, the drill hole 910 is of special interest since the oldest sediments were drilled of Plio/Pleistocene age. This information can be extrapolated into the seismic lines of the network to provide at least time constraints for the last 5 Mio. years.

To provide constraints on the crustal fabric of the Yermak Plateau some seismic refraction work was planned before the cruise. The intention was to place RefTek recording stations on ice floes and to shoot with a large volume airgun. It turned out that this season the ice floes in the area of investigation were to small and/or were not covered by any snow, which would allow to hide the geophones from the wind. Thus, the only wide-angle data were gathered with a new type of sonobuoys. These instruments do not directly transmit the data to the ship but store them on an internal disc. They have to be retrieved by helicopter. The advantage is that longer offsets can be recorded than the line of sight, which is typical at 25-35 km. The instruments recorded data up to 70 km. Longer offsets were not tested due to the profile planning. The signal quality is highly variable due to different geological settings and the level of environmental noise.

Helicopter-borne Magnetic Data

Parallel to the seismic profiling across the Yermak Plateau an aeromagnetic survey was performed by helicopter. The aim was to complete and fulfil planned lines of a past magnetic survey from 1999 (Fig. 8.5). The scientific goal was to densify the existing magnetic data sets in order to resolve more details on the magnetic structure of the Yermak Plateau, especially in the area of the strong positive anomalies (ca. 1000 nT strong anomalies). The complete area of interest has its boundaries along 81°N to 83°N and 5°W to 25°E. The block-corners were transformed to UTM coordinates and a central meridian of 21 was used. The line direction is on this longitude 0° which changes with higher distances to the central meridian. The line-spacing was 7.5 km. The flight altitude was mainly 100 m and the data were acquired at a speed of 80 ktms (~ 40 m/s). A new flying procedure was introduced. At the end of each line the pilots made a 270° turn and cross the lines in order to get more intersections. This will lead to an improvement for levelling the data.

Within nine days and 20 flights most of the survey area was successfully completed and more than 7250 line-kilometres were flown. An overview of flights per day and flying hours per day is given in Table 8.3. Unfortunately the profile lines could not be finished to the northern end due to bad weather and long transit respectively. Crossing the lines of the past survey gives us now the opportunity to level the data and combine them into one database.

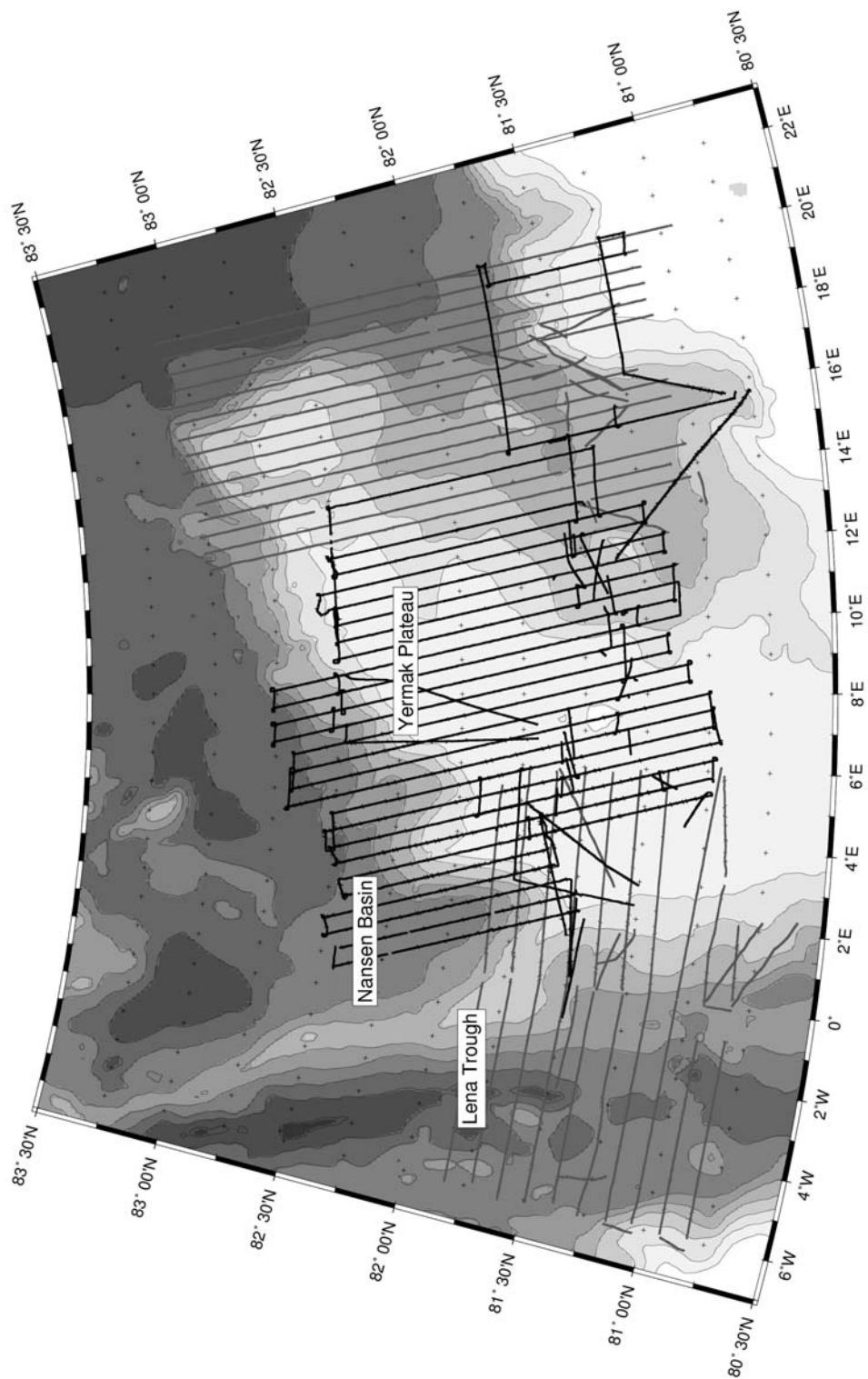


Fig. 8.5: Survey area for the magnetic measurements performed with the “Polarstern” helicopters

Table 8.3: Flight and data statistics for the magnetic survey

text filename	binary filename	line #	fiducial start	end	time start	end	flight #	ascii raw-filename
03.09.2004								
S4090310.T49	testflight	radartest						0409031.raw
07.09.2004								
S4090708.T17	S4090708.B17	110.ON	1	3331	08:18:55	09:14:25	1	0409071.raw
	S4090709.B13	120.OS	3332	5685	09:14:27	09:53:40		
S4090712.T04	S4090712.B04	???	1	1328	12:05:37	12:27:44	2	0409072.raw
S4090712.T27	S4090712.B27	130.ON	1	2461	12:29:19	13:10:19		0409073.raw
	S4090713.B08	140.OS	2462	4331	13:10:21	13:41:29		
S4090713.T40	S4090713.B40	140.OS	1	1077	13:42:09	14:00:05		0409074.raw
S4090714.T44	S4090714.B45	150.ON	1	3749	14:46:47	15:49:15	3	0409076.raw
	S4090715.B47	140.ON	3750	4088	15:49:17	15:54:55		
	S4090715.B53	150.OS	4089	4089	15:54:57	15:54:57		
	S4090715.B5D	160.OS	4090	7548	15:54:59	16:52:37		
924 km								
08.09.2004								
S4090808.T48	S4090808.B48	160.OS	1	22	08:50:40	08:51:01	1	0409081.raw
	S4090808.B49	150.OS	23	27	08:51:03	08:51:07		
	S4090808.B4J	140.OS	28	31	08:51:09	08:51:12		
	S4090808.B50	130.OS	32	1100	08:51:51	09:09:39		
	S4090809.B07	120.OS	1101	1102	09:09:41	09:09:42		
	S4090809.B0H	110.OS	1103	1106	09:09:44	09:09:47		
	S4090809.B0Y	100.ON	1107	4430	09:09:49	10:05:12		
	S4090810.B03	90.OS	4431	8845	10:05:14	11:18:48		
S4090811.T34	S4090811.B34	100.OS	1	25	11:36:11	11:36:35	2	0409083.raw
	S4090811.B3E	90.OS	26	27	11:36:37	11:36:38		
	S4090811.B3V	???	28	683	11:36:40	11:47:35		
S4090811.T48	S4090811.B49	90.ON	1	3	11:51:01	11:51:03		0409084.raw
	S4090811.B4J	???	4	971	11:51:05	12:07:12		
S4090812.T06	S4090812.B06	90.OS	1	12	12:08:38	12:08:49		0409085.raw
	S4090812.B0G	80.ON	13	856	12:08:51	12:22:54		
S4090812.T22	S4090812.B22	80.ON	1	720	12:24:18	12:36:17		0409086.raw
S4090812.T35	S4090812.B35	80.OS	1	5	12:37:38	12:37:42		0409087.raw
	S4090812.B3F	70.OS	6	934	12:37:44	12:53:12		
S4090812.T52	S4090812.B52	???	2	1048	12:54:54	13:12:20		0409088.raw
S4090813.T11	S4090813.B11	70.OS	1	1031	13:13:49	13:30:59		0409089.raw
S4090813.T30	S4090813.B30	70.ON	3	1221	13:32:58	13:53:17		0409080.raw
782 km								
09.09.2004								
S4090908.T27	S4090908.B28	60.ON	1	1105	08:30:28	08:48:52	1	0409091.raw
	S4090908.B46	160.OS	1106	2937	08:49:19	09:19:50		
	S4090909.B17	150.ON	2938	2941	09:19:52	09:19:55		
	S4090909.B1H	140.OS	2942	5369	09:19:57	10:00:24		
260 km								
10.09.2004								
	testflight	cable and radiotest						040910*.raw
12.09.2004								
S4091209.T12	S4091209.B12	290.ON	1	4441	09:15:42	10:29:42	1	0409121.raw
	S4091210.B26	280.OS	4442	7432	10:29:44	11:19:34		
S4091211.T46	S4091211.B47	280.ON	3	39	11:50:43	11:51:19	2	0409122.raw
	S4091211.B4H	290.OS	40	43	11:51:21	11:51:24		
	S4091211.B4Y	300.ON	44	3294	11:51:26	12:45:36		
	S4091212.B42	290.ON	3295	3310	12:45:38	12:45:53		
	S4091212.B4C	300.OS	3311	3646	12:45:55	12:51:30		
S4091212.T48	S4091212.B48	300.OS	1	7	12:52:08	12:52:14		0409123.raw
	S4091212.B4I	310.OS	8	26	12:52:16	12:52:34		
	S4091212.B49	320.OS	27	33	12:52:36	12:52:42		
	S4091212.B4J	330.OS	34	37	12:52:44	12:52:47		
S4091212.T49	S4091212.B50	330.OS	1	15	12:53:33	12:53:47		0409124.raw

text filename	binary filename	line #	fiducial start	end	time start	end	flight #	ascii raw-filename			
S4091214.T30	S4091212.B5A	340.0S	16	2692	12:53:49	13:38:25	3	0409125.raw			
	S4091213.B34	330.0S	2693	2695	13:38:26	13:38:29					
	S4091213.B35	320.0S	2696	2698	13:38:31	13:38:33					
	S4091213.B3F	310.0S	2699	2701	13:38:35	13:38:37					
	S4091213.B3W	300.0N	2702	4122	13:38:39	14:02:19					
	S4091214.B30	300.0N	1	2	14:33:49	14:33:50					
	S4091214.B3A	290.0N	3	4	14:33:52	14:33:53					
	S4091214.B3R	280.0N	5	5	14:33:55	14:33:55					
	S4091214.B3c	270.0N	6	6	14:33:57	14:33:57					
	S4091214.B3t	260.0N	7	3962	14:33:59	15:39:54					
S4091216.T22	S4091215.B36	270.0S	3963	6657	15:39:56	16:24:51		0409126.raw			
	S4091216.B23	270.0S	1	741	16:26:33	16:38:54					
14.09.2004	testflight	radiotest									
16.09.2004											
S4091608.T51 S4091609.T11	S4091608.B51	350.0N	1	1129	08:55:06	09:13:54	1	0409162.raw 0409163.raw			
	S4091609.B11	350.0N	1	910	09:15:53	09:31:02					
	S4091609.B27	360.0N	911	912	09:31:04	09:31:05					
	S4091609.B2H	370.0N	913	914	09:31:07	09:31:08					
	S4091609.B2Y	380.0N	915	916	09:31:10	09:31:11					
	S4091609.B2j	390.0N	917	917	09:31:13	09:31:13					
	S4091609.B2a	400.0N	918	918	09:31:15	09:31:15					
	S4091609.B2b	410.0N	919	920	09:31:17	09:31:18					
	S4091609.B2c	420.0N	921	924	09:31:20	09:31:23					
	S4091609.B2d	430.0N	925	928	09:31:25	09:31:28					
	S4091609.B2e	440.0N	929	931	09:31:30	09:31:32					
	S4091609.B2g	460.0S	936	3074	09:31:39	10:07:17					
	S4091610.B03	450.0S	3075	6399	10:07:19	11:02:43					
	S4091610.B58	440.0S	6400	6402	11:02:45	11:02:47					
	S4091610.B5I	430.0S	6403	6404	11:02:49	11:02:50					
	S4091610.B5Z	420.0S	6405	6407	11:02:52	11:02:54					
	S4091610.B59	410.0N	6408	6410	11:02:56	11:02:58					
	S4091610.B5J	400.0N	6411	6414	11:03:00	11:03:03					
	S4091611.B00	360.0S	6415	8443	11:03:58	11:37:46					
	S4091611.T55	S4091611.B55	360.0N	1	4	11:59:57			12:00:00	2	0409164.raw
S4091611.B56		350.0N	5	1887	12:00:01	12:31:25					
S4091612.B27		340.0S	1888	1890	12:31:27	12:31:29					
S4091612.B2H		330.0S	1891	1893	12:31:31	12:31:33					
S4091612.B2Y		320.0S	1894	1895	12:31:35	12:31:36					
S4091612.B2j		310.0S	1896	1897	12:31:38	12:31:39					
S4091612.B2a		300.0N	1898	3616	12:31:40	13:00:19					
S4091612.B56		290.0N	3617	4617	13:00:21	13:00:21					
S4091613.B13		280.0S	4618	5907	13:00:22	13:38:32					
S4091613.B34		270.0S	5908	8850	13:38:34	14:27:36					
									859 km		
17.09.2004											
S4091708.T05		S4091708.B05	310.0N	1	107	08:10:00	08:11:46	1	0409171.raw		
	S4091708.B07	300.0N	108	136	08:11:48	08:12:16					
	S4091708.B08	310.0N	137	2672	08:12:18	08:54:33					
	S4091708.B50	300.0S	2673	2673	08:54:34	08:54:34					
	S4091708.B5A	290.0S	2674	2674	08:54:35	08:54:35					
	S4091708.B5R	280.0S	2675	2675	08:54:36	08:54:36					
	S4091708.B5c	270.0S	2676	2676	08:54:37	08:54:37					
	S4091708.B5t	260.0S	2677	2677	08:54:38	08:54:38					
	S4091708.B5U	250.0S	2678	7565	08:54:45	10:16:12					
	S4091710.T30	S4091710.B3B	250.0N	1	28	10:35:11	10:35:38			2	0409172.raw
S4091710.B3S		240.0N	29	2816	10:35:40	11:22:07					
S4091711.T18	S4091711.B18	240.0N	1	759	11:22:49	11:35:27		0409173.raw			
S4091711.T31	S4091711.B31	240.0N	1	27	11:35:46	11:36:12		0409174.raw			

text filename	binary filename	line #	fiducial start	end	time start	end	flight #	ascii raw-filename
S4091713.T07	S4091711.B32	230.0S	28	4350	11:36:14	12:48:16	3	0409175.raw
	S4091712.B44	240.0N	4351	4986	12:48:18	12:58:53		
	S4091713.B07	240.0N	1	3	13:11:56	13:11:58		
	S4091713.B0H	230.0N	4	6	13:12:00	13:12:02		
	S4091713.B0Y	220.0N	7	3162	13:12:04	14:04:39		
	S4091714.B00	210.0S	3163	7293	14:04:41	15:13:31		
	S4091715.B09	220.0N	7294	8351	15:13:33	15:31:10		
1149 km								
18.09.2004								
S4091808.T43	S4091808.B43	240.0S	2	920	08:47:35	09:02:54	1	0409182.raw
	S4091808.B58	250.0S	921	921	09:02:55	09:02:55		
	S4091808.B5I	260.0N	922	2344	09:02:58	09:26:40		
	S4091809.B22	250.0S	2345	4017	09:26:42	09:54:34		
	S4091809.B50	240.0S	4018	4022	09:54:36	09:54:40		
	S4091809.B5A	230.0N	4023	4991	09:54:42	10:10:50		
	S4091810.B06	220.0S	4992	4997	10:10:52	10:10:57		
	S4091810.B0G	210.0S	4998	5002	10:10:59	10:11:03		
	S4091810.B0X	200.0S	5003	6648	10:11:05	10:38:30		
	S4091810.B34	190.0N	6649	8228	10:38:32	11:04:51		
S4091811.T21	S4091811.B21	200.0N	1	3315	11:25:50	12:21:04	2	0409183.raw
	S4091812.B16	190.0S	3316	7654	12:21:06	13:33:24		
S4091813.T43	S4091813.B43	190.0S	1	5	13:47:45	13:47:49	3	0409184.raw
	S4091813.B4D	180.0N	6	3305	13:47:51	14:42:50		
	S4091814.B38	170.0S	3306	9114	14:42:52	16:19:40		
1160 km								
20.09.2004								
S4092008.T09	S4092008.B09	200.0N	3	2069	08:14:09	08:48:35	1	0409203.raw
	S4092008.B44	210.0N	2070	2994	08:48:37	09:04:01		
	S4092008.B59	220.0S	2995	4237	09:04:03	09:24:45		
	S4092009.B20	230.0N	4238	5352	09:24:47	09:43:21		
	S4092009.B38	240.0S	5353	8599	09:43:22	10:37:29		
S4092010.T50	S4092010.B50	240.0S	1	9	10:55:36	10:55:44	2	0409204.raw
	S4092010.B51	230.0S	10	10	10:55:46	10:55:46		
	S4092010.B5B	220.0S	11	12	10:55:48	10:55:49		
	S4092010.B5S	210.0S	13	14	10:55:51	10:55:52		
	S4092010.B5d	200.0S	15	16	10:55:00	10:55:00		
	S4092010.B5u	190.0S	17	17	10:55:56	10:55:56		
	S4092010.B5x	180.0S	18	18	10:55:59	10:55:59		
	S4092010.B5y	170.0S	19	21	10:56:01	10:56:03		
	S4092010.B5z	160.0S	22	2019	10:56:04	11:29:22		
	S4092011.B24	170.0N	2020	2021	11:29:24	11:29:25		
	S4092011.B2E	180.0N	2022	3511	11:29:26	11:54:16		
	S4092011.B49	170.0S	3512	4918	11:54:18	12:17:44		
	S4092012.B13	160.0N	4919	4920	12:17:46	12:17:47		
	S4092012.B1D	150.0N	4921	7108	12:13:11	12:49:40		
	S4092012.B49	140.0S	7109	8364	12:17:49	13:15:13		
S4092013.B10	130.0N	8365	9369	13:15:15	13:31:59			
851 km								
21.09.2004								
S4092112.T09	S4092112.B09	130.0S	1	10	12:14:27	12:14:36	1	0409211.raw
	S4092112.B0J	120.0N	11	2468	12:14:38	12:55:35		
	S4092112.B50	130.0S	2469	4654	12:55:37	13:32:02		
	S4092113.B27	140.0N	4655	5928	13:32:04	13:53:17		
301 km								

9. Marine Geology

R. Stein, F. Niessen, F. Schoster, B. Bahr, C. Gebhardt, N. Kukina, N. Lensch, S. Nam, H. Noffke, D. Penshorn, A. Puhr, R. Saraswat, Chr. Schäfer, J. Schneider, J. Thiele, D. Winkelmann, Y. Yanina

9.1 Introduction

One of the key marine-geology objectives was the study of sediment dynamics of megaslides along the Svalbard continental margin (as part of the ESF Program „EUROMARGINS“), using Hydrosweep (bathymetry) and PARASOUND profiling data, multi-sensor-core-logging data, and long sediment cores. In this context, the characterization of sediment facies within debris flow and turbidite sequences as well as undisturbed pelagic sequences, the dating of sediment mass flows and estimates of sediment tray budgets are of interest. Furthermore, detailed multidisciplinary (i.e., sedimentological, mineralogical, micropaleontological, and geochemical) studies will be performed on the sediment cores for high-resolution reconstructions of paleoclimate, paleoceanic circulation patterns, paleosea-ice cover, and paleoproductivity and their variability during late Quaternary times. In order to reach these goals, an intensive sampling program was performed using large-volume box corer, multicorer, gravity corer, and kastenlot corer. In addition, gravity cores were taken from the central part of the Yermak Plateau as well as the East Greenland continental margin as part of the IODP Site survey work. All geological stations are shown in Fig. 9.1 (for details see station list, Chapter 12.1, Annex).

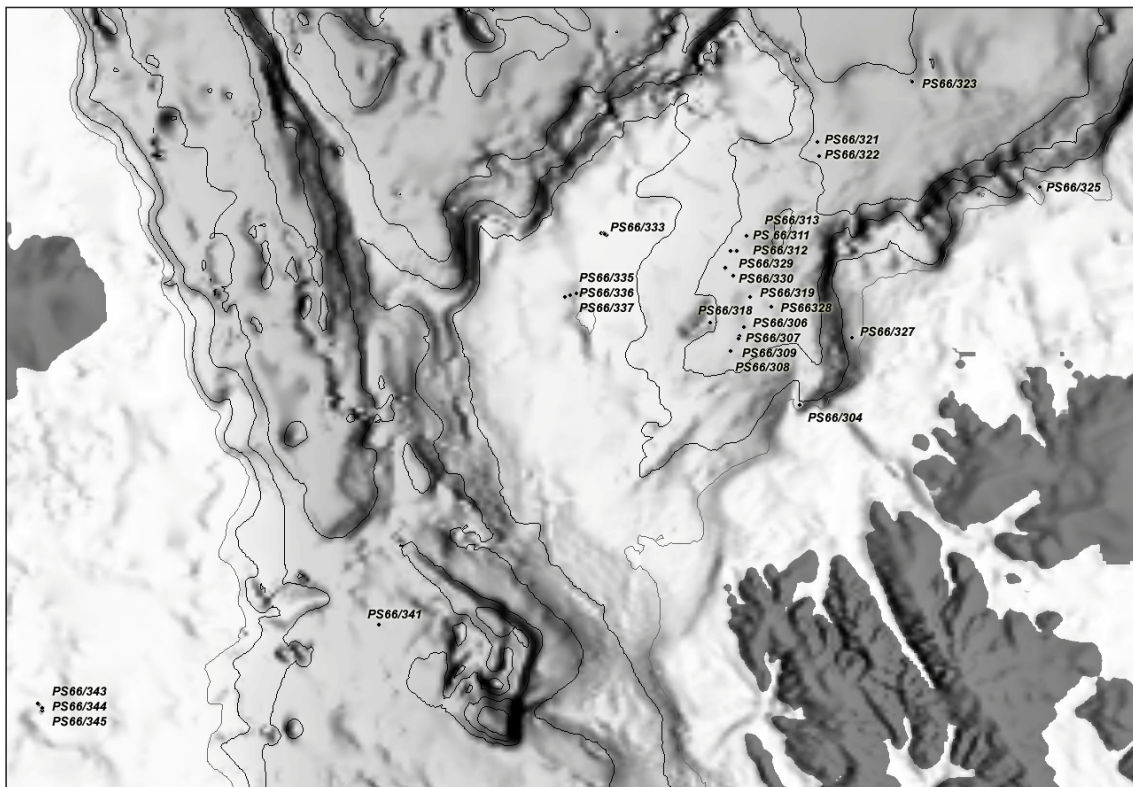


Fig. 9.1: Location map of geological stations of „Polarstern“ Cruise ARK-XX/3

9.2. Marine Sediment Echosounding using PARASOUND

F. Niessen, J. Rogenhagen and F. Schoster

Scientific objectives, technical settings and operation conditions

Bottom and sub-bottom reflection patterns obtained by PARASOUND characterize the uppermost sediments in terms of their acoustic behavior. This can be used to interpret the sedimentary environments and their changes in space and time. The use and basic principles of the system are described in Spiess (1992). During ARK XX/3 the aims of PARASOUND profiling were (i) to select coring locations for gravity and box cores, (ii) to identify lateral differences in sedimentary facies with particular emphasis on submarine slides and debris flows north of Svalbard. (iii) to characterize the topmost sedimentary cover at locations proposed for IODP drilling as part of seismic site-survey work carried out during the cruise in the framework of various IODP-preproposals.

The hull-mounted PARASOUND sediment echosounder was in 24-hour operation along all cruise tracks starting from 2 September 2004, 15:35 UTC (77° 34.79'N, 05° 55.260'E) until after the completion of the seismic survey on 27 September 2004, 10:00 UTC (73° 35.336'N, 10° 35.663'W). The PARASOUND system (ATLAS Hydrographic, GmbH, Bremen, Germany) generates two primary frequencies between 18 and 23.5 kHz transmitting in a narrow beam of 4° at high power. As a result of the interaction of the primary frequencies within the water column, a secondary frequency is created based on the parametric effect. The parametric frequency is the difference frequency of the two primary waves transmitted. As a result of the longer wave length, the parametric frequency allowed sub bottom penetration up to 70m with a vertical resolution of ca. 30 cm. The parametric pulse length was set to 2 under normal operating conditions. Under extreme conditions, such as above steep slopes and while operating in heavy sea ice, the pulse length was increased up to 6. In water depth shallower than 2000m the mode of operation was PAR. At water depth larger than 2000m operation modes was PAR, NBS-PAR or PAR-pilot. In general, the operating conditions during the cruise were excellent due to mostly ice-free areas and relatively calm sea. Only in the most northerly areas the data acquisition was affected by moderate sea ice conditions causing noisy records with some traces missing.

The new ATLAS PARASOUND-DS2 system onboard "Polarstern"

Before the start of the first cruise leg of ARK-XX, the "Polarstern" PARASOUND system received a major upgrade by installation of ATLAS PARASOUND-DS2. This equipment consists of the transmitter/receiver electronics and its control/data acquisition system. The former remained mostly unchanged as compared to the previous version, whereas the latter was completely replaced by an operator personal computer (PC) working as control, processing, display and recording unit. The function of the new system was checked during the Sea Acceptance Test (SAT) carried out during ARK-XX/1. The results are published in Budeus (in prep.). The basic elements of the entire system are summarized in a flow diagram (Fig. 9.2) and described in full details in the different reference manuals (ATLAS Hydrographic, 2004a, 2004b, 2004c). The first ATLAS PARA-

SOUND-DS2-system was installed onboard RV "Academic Boris Petrov" in 2003. The basic principles and first results using the system during cruise "Karas Sea 2002" are described in Dittmers and Schoster (2003).

The ATLAS PARASOUND-DS2 system comprises of the following essential components (Fig. 9.2):

- (1) Transducer arrangement SW 6051 G 003
- (2) Transceiver Cabinets GE 6019 A 003 and 004
- (3) Control Unit GE 6030
- (4) User interface in form of an Operator PC containing the control software ATLAS HYDROMAP SERVER, ATLAS HYDROMAP CONTROL and the data acquisition software ATLAS PARASTORE-3

The RV "Polarstern" PARASOUND-system is equipped with additional components:

- (5) Two colour printers HP Business Inkjet 1100 for printing of echograms and auxiliary data (navigation, depth and PARASOUND settings), respectively
- (6) Data Storage PC for data management, recording and data replay in off-line mode
- (7) Spare PC of the Operator PC as hardware backup but fully installed in the winch control room echogram in order to provide track plot and single trace information for station work
- (8) Flat-Screen Monitor for duplication of echogram information of the Operator PC on the bridge
- (9) black and white chart recorder ATLAS Deso-25 as slave

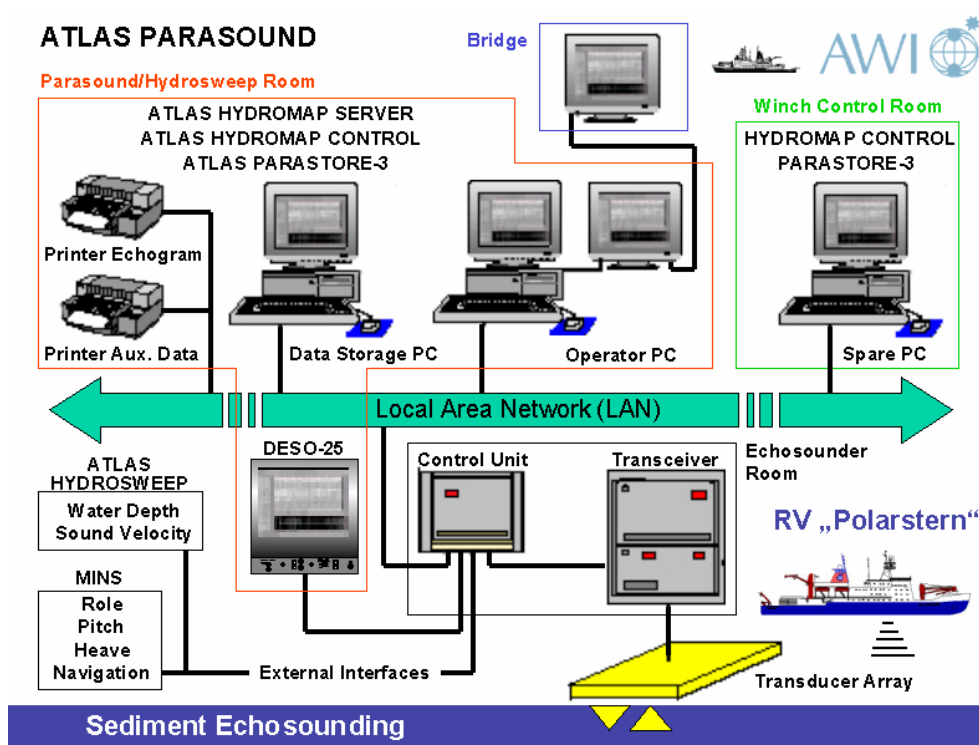


Fig. 9.2 Schematic overview of different hardware components of the new system PARASOUND DS-2 onboard RV "Polarstern"

The Data Storage PC and the Spare PC are equipped with the same software components (except for the ATLAS HYDROMAP SERVER installed on the Operator PC only) and linked to printers and Control Unit via a Local Area Network (Fig. 9.2). One major advantage of the new system is that several units of the former system were replaced by modern standard equipment for the benefit of easier handling, maintenance and repair. The former control unit (COLOR-SCOPE) has been replaced by a standard Windows-XP-based PC together with the new Control Unit GE 6030, which mostly contains of-the-shelf products. The equipment is now controlled by means of the ATLAS HYDROMAP CONTROL software via Operator PC (Fig. 9.2). The operating elements affect the system according to their functions (e.g. parametric frequency, pulse length, depth range, modes PAR/NBS-PAR/PAR-pilot, Narrow Beam Sounder (NBS) operation modes, beam steering, depth control and others).

The hardware and software configuration onboard "Polarstern" using two Windows-based PC's for system control and data management (Fig. 9.2), respectively, offers a lot of additional functions by means of the ATLAS PARASTORE-3 software via both Operator and Data Storage PC. ATLAS PARASTORE-3 provides a user-friendly graphical interface and has been designed to acquire, visualize, process, store, convert, quality control, replay and print data from ATLAS PARASOUND-DS2 profiles. This includes not only the sub-bottom parametric data but also the primary narrow single-beam signal (NBS, 18 kHz). The recorded data of both parametric and NBS signals are stored in a hybrid raw data format (ASDF format) in either a ring buffer or into user selected folders on hard disc. The important improvement compared to the previous system is the acquisition of full soundings of both signals and not only data selected in specific depth windows by the operator. Optionally, the parametric data can be converted on-line into standard SEG-D format for further processing using industrial post-processing software. In addition, the parametric data can be stored in the formerly used PS-3 format (Paradigma). This function, however, requires careful watch keeping because only data kept in a selected depth window of commonly 200m length is stored. In addition to data acquisition, ATLAS PARASTORE-3 provides the following functions:

- (10) simultaneous operation of parametric signal and narrow beam signal
- (11) data storage reduction by user selectable input of wait times (e.g. during station work)
- (12) colour-coded visualization of parametric and NBS data in arbitrary number of windows with different scales including single-trace visualization
- (13) appropriate processing algorithms such as bandpass filtering, clipping, negative flank subtraction and threshold filtering
- (14) colour-coded online print of echograms on user selectable scales
- (15) Table print of navigation data and PARASOUND system settings in user-selectable time intervals (auxiliary data)
- (16) information window for all system parameters combined with navigation information
- (17) visualization of ships track information on user selectable map scales
- (18) storage of auxiliary data in user selectable time intervals on hard disc

- (19) storage of meta information for each echogram window for monitoring operator activity during the survey on hard disc
- (20) network capability
- (21) replay of recorded data in off-line mode including visualization, processing, printing and storage in SED-D and/or PS3-formats

We have used the Operator PC for system control, data acquisition and storage as well as visualization of data in on-line mode. Both parametric and NBS signals were acquired. The stronger backscatter of the NBS-signal turned out to be very useful for keeping the echo in the selected time window when the sediment character or slope steepness did not allow sufficient reception of parametric reflections. The data storage PC was used for data management and replay of signals in off-line mode. Data transfer was carried out via Local Area Network (Fig. 9.2). This has allowed rapid visualization of previously stored PARASOUND data from ARK-XX/3 as well as PARASOUND data (PS-3 format) from previous cruises. In replay modes we have used software PARASTORE-3 and SENT (H. van Loom, University of Bremen). Unfortunately, the PARASOUND SEG-D data format was unreadable by shipboard seismic software "Focus".

Data Management

The capabilities of the ATLAS PARASTORE-3 software in acquiring the PARASOUND data are two-fold: (i) simultaneously as raw data from the parametric channel and the NBS channel for full trace length including the water column, and, (ii) selected in specific depth windows, in PS3 and SEG-D formats. Because all the data can be produced and stored simultaneously, a well-organized data management is necessary. As outlined above the full soundings of the parametric and NBS signals are transferred from the Control Unit to the Operator PC and may be acquired there with the ATLAS PARASTORE-3 software and converted to PS3 and SEG-D format. So, it is possible to store parametric, NBS, PS3 and SEG-D data of the same profile. In addition, the newly implemented replay option of PARASTORE-3 gives the opportunity to replay the soundings of parametric data and/or NBS data and record them again as PS3 and/or SEG-D data, for example, for specifically defined profiles. In order to avoid confusion with the different formats and the status of the data, the data management was carried out by one designated person.

Taking into account the amount of hard disk space and/or storage media, the user has to decide what kind of data set is recorded and stored. The minimum data set would be the PS3 data of a specific depth window, mostly 200 m, and leads to a data amount of 30 to 60 MB per hour (dependent of the sounding rate) or 0.7 to 1.5 Gbyte per day. This could be further reduced with a functional resample option during storage, which is not yet implemented in PARASTORE-3. Keeping only PS3 data requires that the depth window is always manually adjusted to the topographic variations of the seafloor.

The other extreme is keeping all raw data and subsets of PS3 and SEG-D data, selected by a depth window of again 200 m. This data amount is ranging between 500 and 700 MB per hour (12 to 16 GByte per day), again dependent of the sounding rate. Hard disk capacity of the Data Storage PC is around 138

GByte, and would last for nine to ten days of PARASOUND measurement. Including the hard disk capacity of the Operator PC this time span can be doubled.

Both PC's are equipped with a DVD Writer and an LTO High Density Tape Drive, which allows the use of mass storage media. During cruise ARK XX/3, we decided to store the full data set of parametric and NBS raw data. NBS data has not been stored previously but the experience of this cruise showed that it also contains valuable information on the sediment structure especially in regions with steep slopes and irregular sea-floor topography such as measured at the surface of the Mega Slide. In addition, the PARASOUND system was monitored online all the time and the depth window adjusted, so that the out coming PS3 data were of good quality and stored as well. Because, according to testing, the converted SEG-D data from PARASTORE-3 could not be handled by other standard seismic software, we refrained from acquiring this data during the cruise.

The data storage was organized in such a way that the parametric raw data (.asd files) and the subsequent data set of PS3 data (.ps3) were recorded on DVD and LTO tapes, while the NBS data (.asd files) were recorded on LTO Tapes only. For backup reasons the LTO tapes were copied.

First Results with examples from the different working areas

There are six working areas, where PARASOUND profiling was of interest (from east to west, Fig. 9.3):

- (1) The IODP preproposal NSB-01A site survey grid north of North-Eastland (Svalbard)
- (2) The mega-slide area covering most of the Sophia Basin north of the Hinlopen Strait
- (3) A relatively small subbasin characterized by pelagic sediments between the Sophia Basin and the Yermak Plateau which also includes the sediment covered Mosby Seamount
- (4) The Yermak Plateau including its eastern and western slopes together with IODP preproposal site survey grids YP-03A and LE-01A
- (5) The central Fram Strait locations of the IODP preproposal FR-01A and FR-02A site survey grids
- (6) The East Greenland Shelf area of the IODP preproposal GR-01A-GR-05A site survey grid

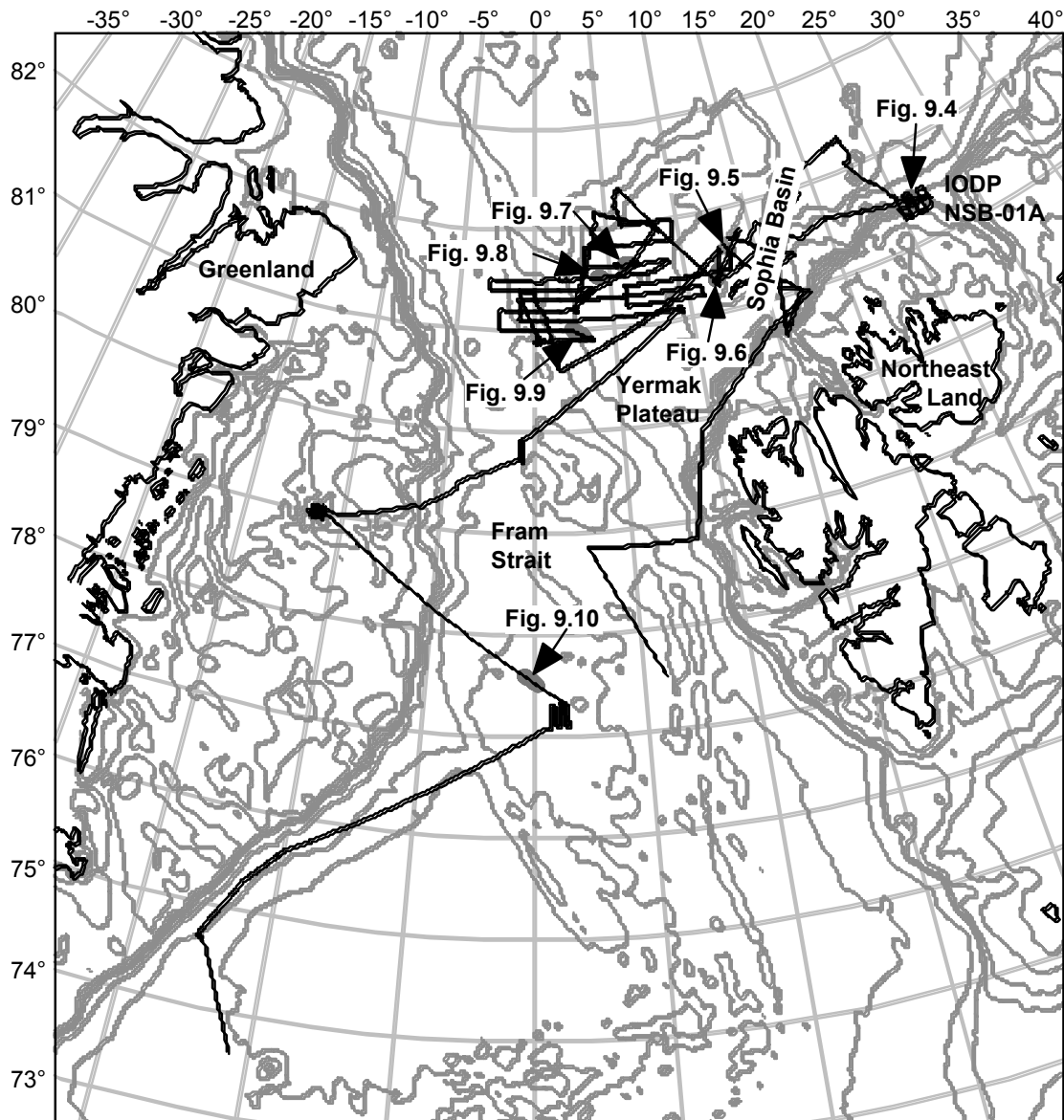


Fig. 9.3: Track map of RV "Polarstern" Cruise ARK-XX/3 during which PARASOUND was in operation and location of selected sections presented as examples in this report

In this report, examples from the different areas above are presented and described in brief including some preliminary interpretation. In particular, for areas (2), (3) and (4), the reader is referred to previous reports (Stein and Fahl, 1997; Jokat, 2000), in which PARASOUND profiles are presented from the same areas recorded during earlier "Polarstern" cruises. In order to avoid repetition, the examples described here give new information about the sedimentary environment and do not always represent the overall character of the different regions above. The locations of the PARASOUND profile examples presented are highlighted in the track lines along which PARASOUND was in operation during the entire cruise (Fig. 9.3).

The example from area (1) including the location of coring station PS66/325, exhibits a typical situation adjacent to IODP coring location outlined in preproposal NSB-01A (Fig. 9.4). An upper undisturbed and continuous sediment unit

is defined by a strong basal reflector of maximum amplitude. In the profile presented (Fig. 9.4), there is a general S-to-N-decrease in thickness of this unit from the Svalbard side (about 10m) towards the Nansen Basin (about 2m). The underlying strata is well-stratified in the deeper area of the profile (>860m water depth), but may be invisible along the southern slope as a result of limited sound penetration. In places, lenticular-shaped debris flows, are intercalated at the boundary between the upper and lower unit (Fig. 9.4), and suggest a south to north flow direction.

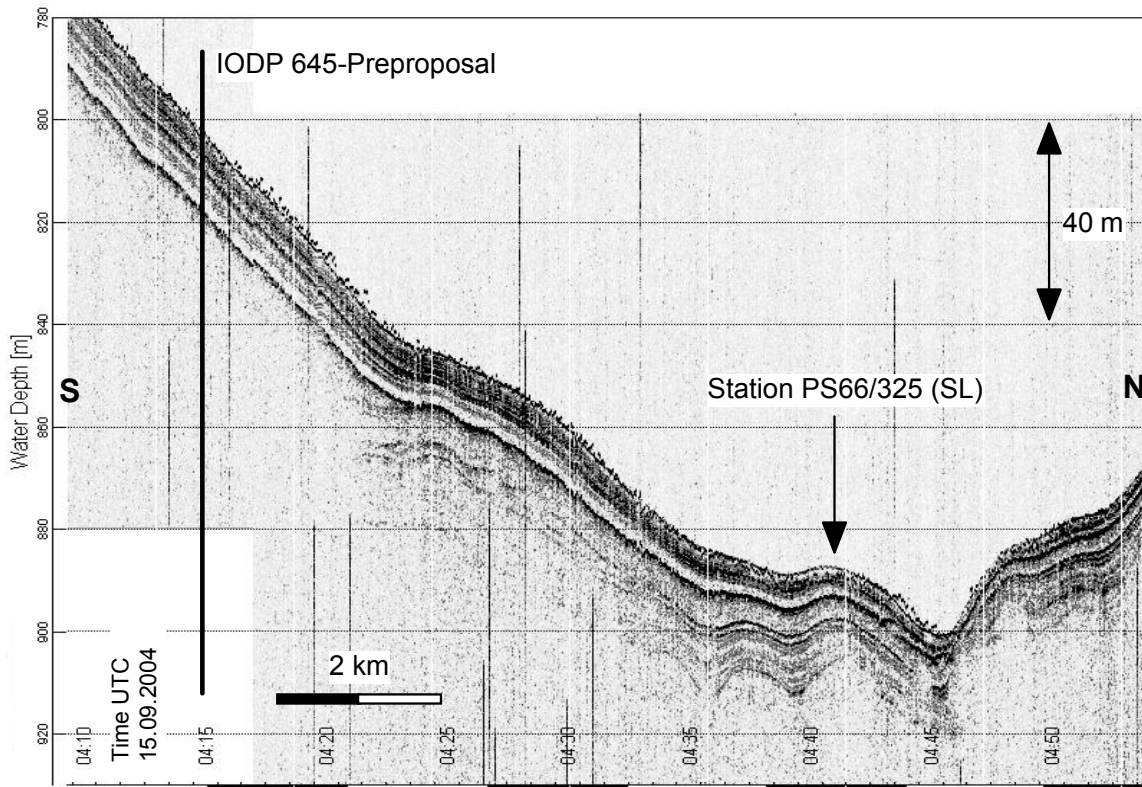


Fig. 9.4: PARASOUND example from the area of IODP preproposal NSB-01 including coring location of PS66/325. Note that the dots plotted just above the sediment surface are an artefact caused by malfunction of the PARASOUND DS2-System (Bottom TVC)

The transition from area (2), the western end of the mega-Slide, to pelagic sediments west of the Sophia basin (3) exhibits hummocky relief with no or limited penetration. The slide is grading into a distal debris-flow tongue of transparent acoustic character overlying pelagic sediments before lensing out at the western end of the profile (Fig. 9.5). Although of complete appearance, well-stratified pelagic sediments built up a hummocky relief too, possibly as a result of post-sedimentary overprint by the adjacent slide. The latter may have caused overloading of pelagic sediments buried by the slide and subsequent hummocky gravitational deformation and uplift west of the slide in areas largely uncovered by debris.

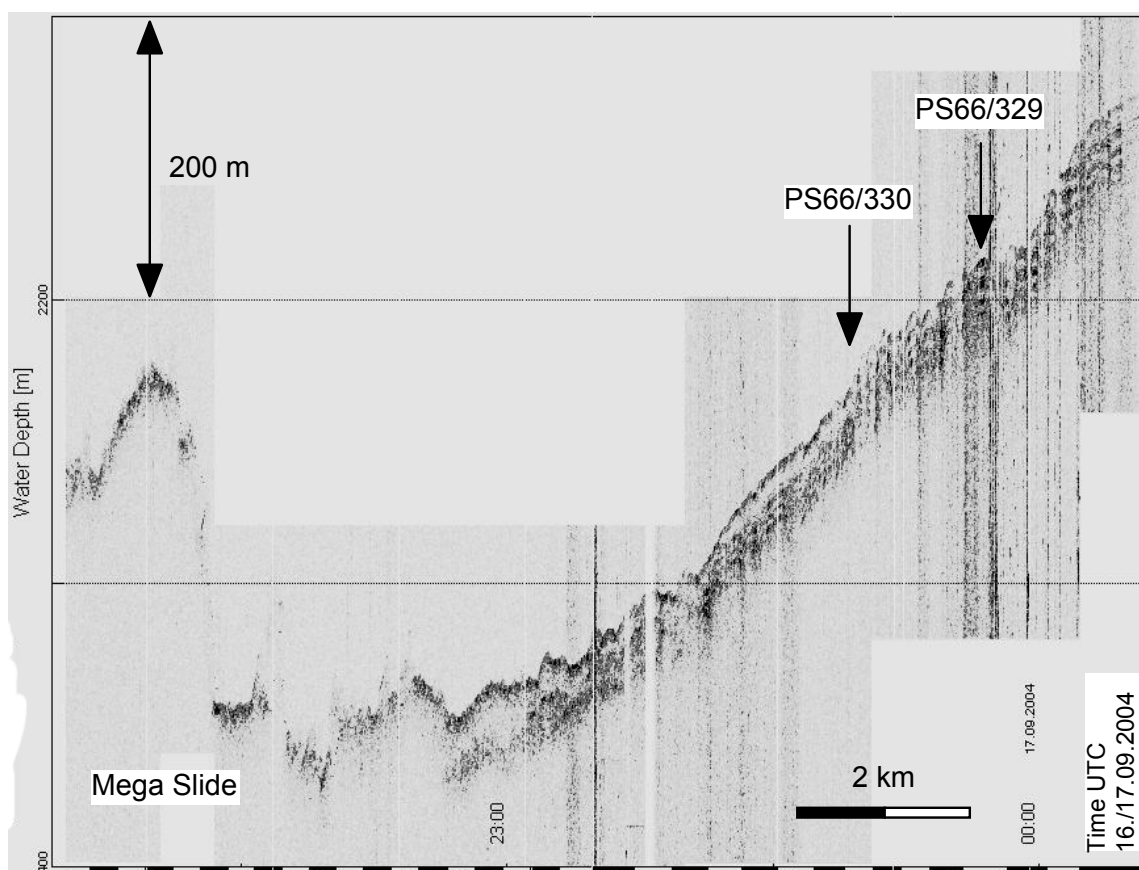


Fig. 9.5: PARASOUND example from the western end of the mega slide grading into pelagic sediments including coring locations PS66/329 and /330.

A chain of small seamounts are located in S-N-direction along the boundary between the Sophia Basin (2) and the small sub basin (3) towards the west. According to the PARASOUND data, one of them, the Mosby Seamount (Fig. 9.6) is covered by well-stratified sediments. Along the profile across the mount, the uppermost sediments decrease in thickness over a relatively small lateral distance from 30m (1350m water depth) to <5m (1250m water depth) on the top of the mount. The observed condensation of the sedimentary record is associated with increase in reflector amplitudes. This may suggest that currents have a stronger influence on sedimentation over the top of the mount compared to the flanks thereby decreasing sedimentation rates and possibly leading to the formation of lag-deposits with high acoustic reflectivity towards the top. The steeper N-E slope of the mount is marked by slump scars (Fig. 9.6 left).

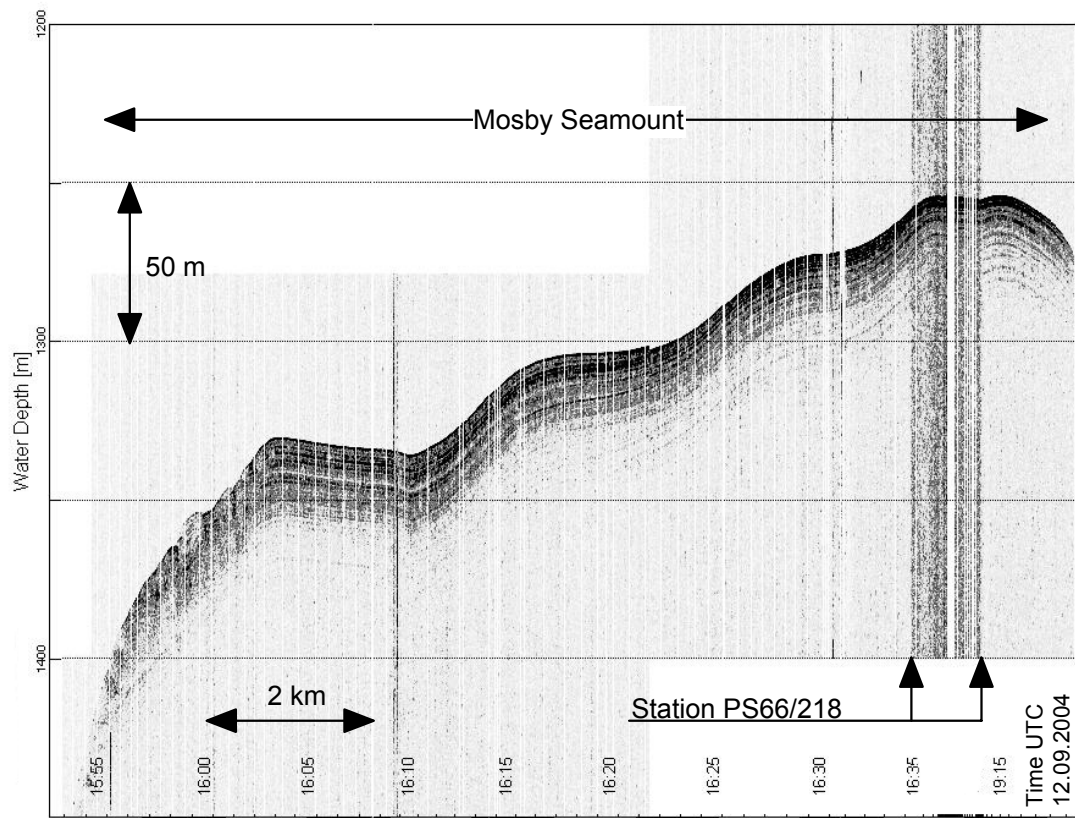


Fig. 9.6: PARASOUND example from the top area of the Mosby Seamount including coring location PS66/318

The topography of the Yermak Plateau (4) is marked by a number of small sub-plateaus which appear to be uplifted areas or relicts of basement reaching into relatively shallow water. In places, along the steep flanks of these sub-plateaus, PARASOUND indicates well-stratified sediments, which decrease in thickness significantly over short lateral distances down-slope from 60m in 820m water depth to less than 1m in 940m water depth directly adjacent to steep slopes (Fig. 9.7). In places, these deeper areas may also be marked by erosional discontinuities at the sediment surface. The overall character of the pattern is typical for marine drift deposits, which are controlled by the influence of bottom currents. On the shallowest areas of the Yermak Plateau (Fig. 9.8) the relief is characterized by deep furrows. The fact that PARASOUND exhibits a pelagic cover of well-stratified sediments overlying furrows and hummocks suggests a paleo-relief possibly formed by massive ice-berg gouging during earlier glaciations with intensive ice-berg drift (e.g. Vogt et al., 1994).

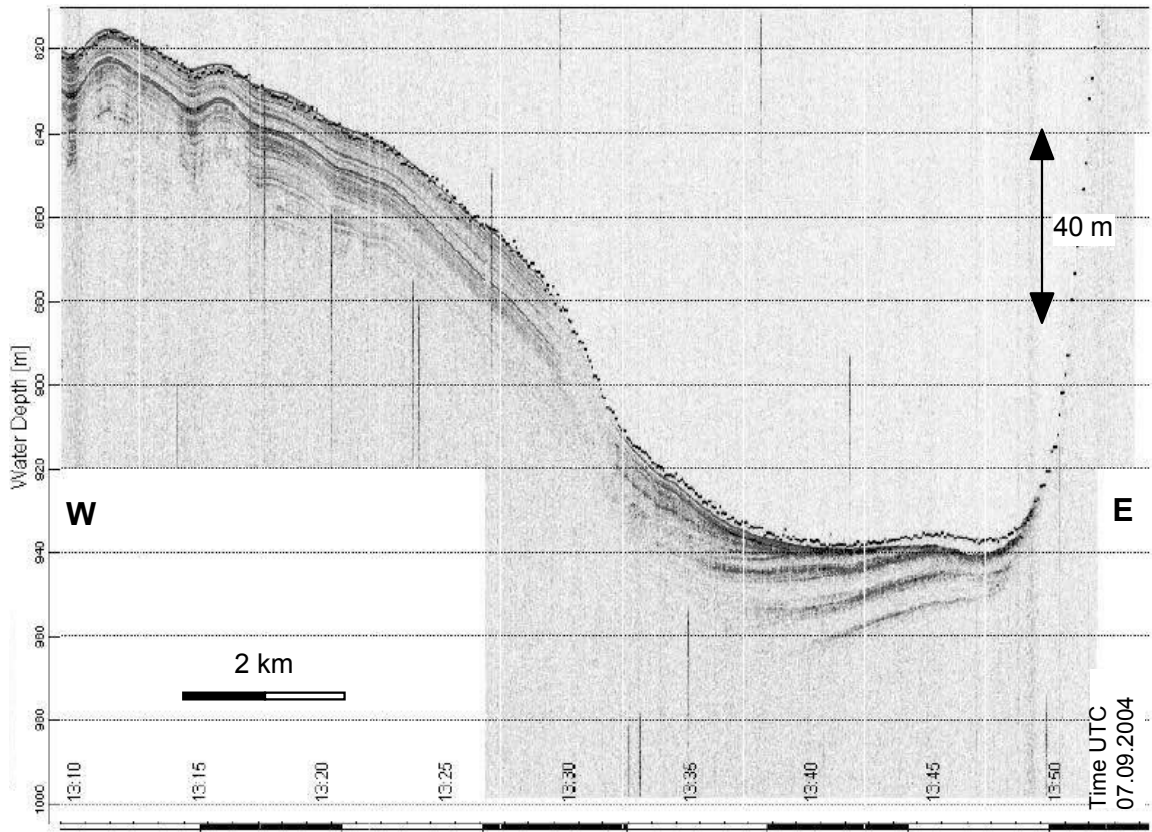


Fig. 9.7: PARASOUND example from the eastern part of the Yermak Plateau indicating drift deposits adjacent to steep slopes of elevated basement. Note that the dots plotted just above the sediment surface are an artefact caused by malfunction of the PARASOUND DS2-System (Bottom TVC).

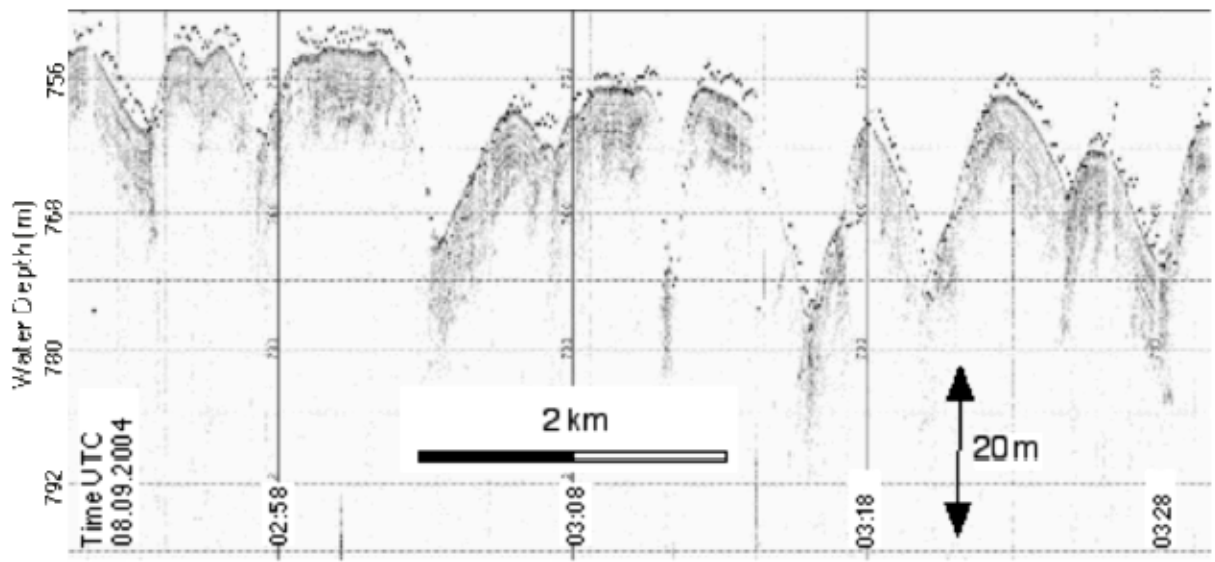


Fig. 9.8: PARASOUND example from the top of the Yermak Plateau showing sediment-covered furrows related to ice erosion. Note that the dots plotted just above the sediment surface are an artefact caused by malfunction of the PARASOUND DS2-System (Bottom TVC).

The western slope of the Yermak Plateau (4) towards the Fram Strait (5) is often characterized by well-stratified pelagic sediments intercalated with up to 20m thick transparent debris-flow deposits (Fig. 9.9). These debris flows are rarely found directly at the sediment surface but are mostly covered by packages of undisturbed sediments of 5 to 10m in thickness including several distinct sub-parallel reflectors (Fig. 9.9).

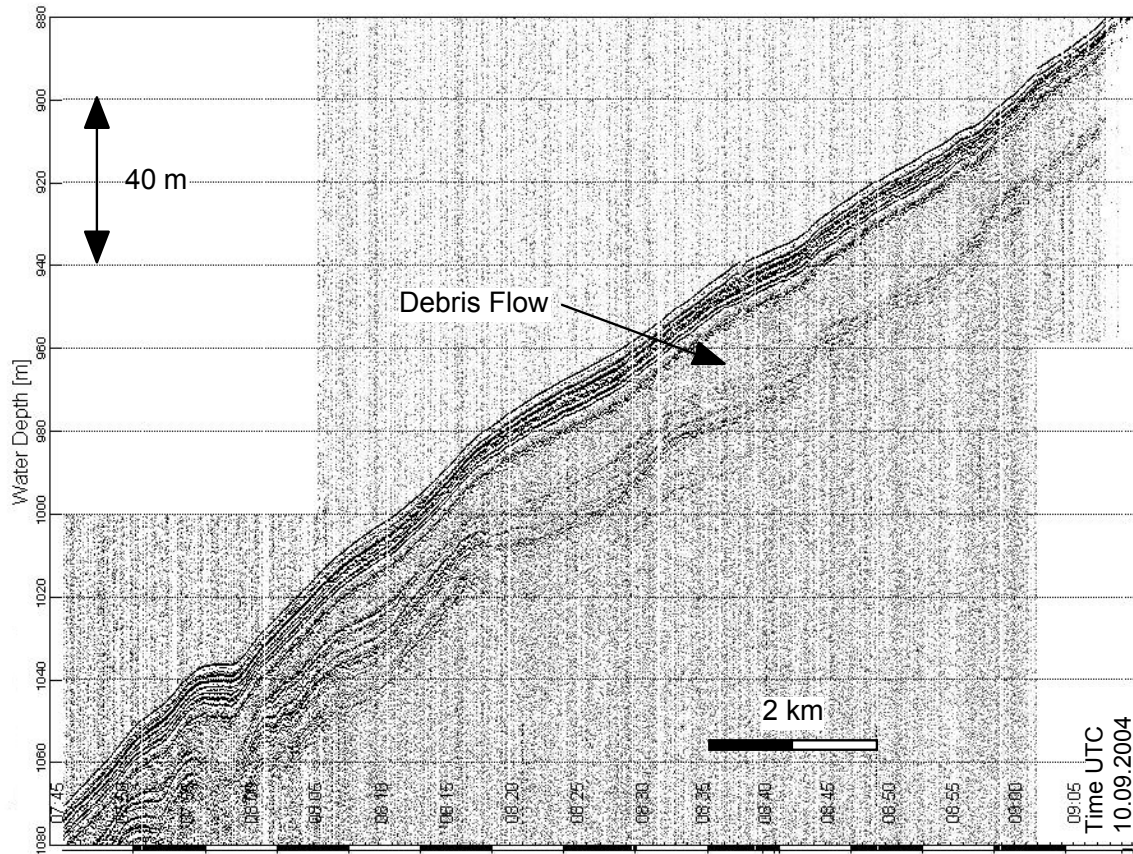


Fig. 9.9: PARASOUND example from the western slope of the Yermak Plateau showing typical intercalation of pelagic sediments with debris flows

The presence of debris-flow deposits is also common off the slope of the East Greenland Shelf and in the area of the Southern Fram Strait (6). The sequence of pelagic sediments intercalated with debris flows is in places laterally interrupted by diapirs visible as acoustic voids but forming distinct hummocks on the sediment surface up to 20m high (Fig. 9.10). Possibly the source of the diapirs are muds of high porosity/low density derived from debris-flow deposits in greater depth (not visible in Fig. 9.10 as a result of limited sound penetration). In places, these muds were uplifted in diapirs due to overburden of denser pelagic sediments. The general pattern is typical for marine slopes and basins off formerly glaciated continental margins. In the presented example the primary 18 kHz NBS-record is compared to the secondary parametric 4 kHz PARASOUND signal. Note the differences in resolution and penetration (Fig. 9.10).

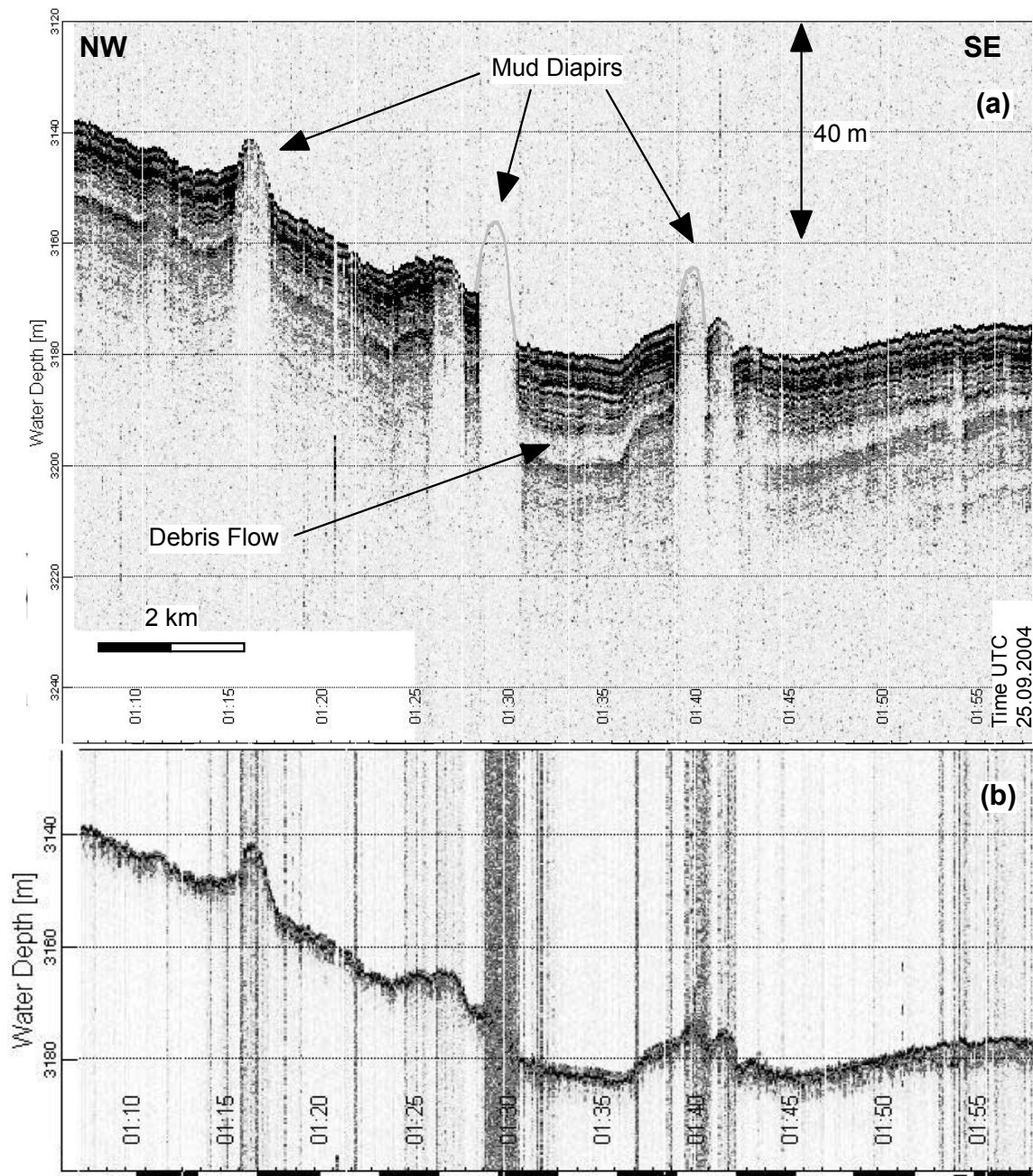


Fig. 9.10: PARASOUND example from the southern Fram Strait indicative of mud diapirs cutting through pelagic sediments and debris flows

9.3 Physical Properties and Core Logging

F. Niessen, J. Rogenhagen, C. Gebhardt, D. Penshorn, J. Schneider, D. Winkelmann

9.3.1 Multi-sensor Core Logging

F. Niessen, J. Rogenhagen, C. Gebhardt, J. Schneider, D. Penshorn

The physical properties of whole sediment cores (gravity cores and box cores) were measured in one-meter sections using a GEOTEK 'Multi-Sensor-Core-Logger' (MSCL). P-wave travel times, magnetic susceptibility, and γ -ray-absorption were measured simultaneously including control measurements of core diameter and sediment temperature. From these data, the physical properties density, magnetic susceptibility, fractional porosity, P-wave velocity, and impedance can be calculated using the MSCL software package. The technical description of the system is given in Table 9.1.

Table 9.1: Technical specifications of the GEOTEK MSCL14

P-wave velocity and core diameter Plate-transducer diameter: 4 cm Transmitter pulse frequency: 500 kHz Pulse repetition rate: 1 kHz Received pulse resolution: 50 ns Gate: 5000 Delay: 0 μ s
Density Gamma ray source: Cs-137 (1983) Activity: 356 MBq Energy: 0.662 MeV Collimator diameter: 5.0 mm Gamma detector: Gammasearch2, Model SD302D, Ser. Nr. 3043 , John Count Scientific Ltd., 10 s counting time
Fractional porosity Mineral grain density = 2.75, water density = 1.026
Magnetic susceptibility Loop sensor: BARTINGTON MS-2C, Ser. Nr. 208 Loop sensor diameter: 14 cm Point sensor: BARTINGTON MS-2F, Ser. Nr. 139 Alternating field frequency: 565 Hz, counting time 10 s, precision $0.1 \cdot 10^{-5}$ (SI) Magnetic field intensity: ca. 80 A/m RMS Krel: 1.56 (SL, 12 cm core- \emptyset), 0.60 (KAL, cross section 50.27 cm ² , = 8 cm core- \emptyset) Loop sensor correction coefficient: 6.391 (SL) for 10^{-6} (SI), 16.689 (KAL) for 10^{-6} (SI) Point sensor: BARTINGTON MS-2F, Ser. No. 139 counting time 10 s

In addition, measurements of magnetic susceptibility using a Bartington point sensor were performed on split cores. For practical reasons, the point sensor was hooked up on the GEOTEK Colour-Line-Scan-Logger. Data acquisition was carried out in combination with colour scans of split-cores surfaces. The latter is described in more detail under 9.3.2. of this report. The step intervals of the measurements were 0.5 or 1.0 cm (see appendix for more details). Gravity cores were measured in coring liners, whereas Kastenlot cores were measured in sub-cores retrieved from the original core using length-wise open transparent plastic boxes of 1000mm length and 75 x 75 mm cross section (outside includ-

ing 2 x 2.5 mm plastic wall thickness). In order to allow for magnetic-susceptibility sensor correction (according to the Bartington correction requirements), the rectangular cross section of the box was equalised to an size-equivalent circular section, of which a fictive core diameter was calculated as input parameter for loop-sensor correction coefficient (Table 9.1). For both gravity and Kastenlot cores, the density calibration was carried out using a set of defined mixtures of aluminium and distilled water in a gravity liner and Kastenlot sub-sampling box, respectively (Best and Gunn, 1999).

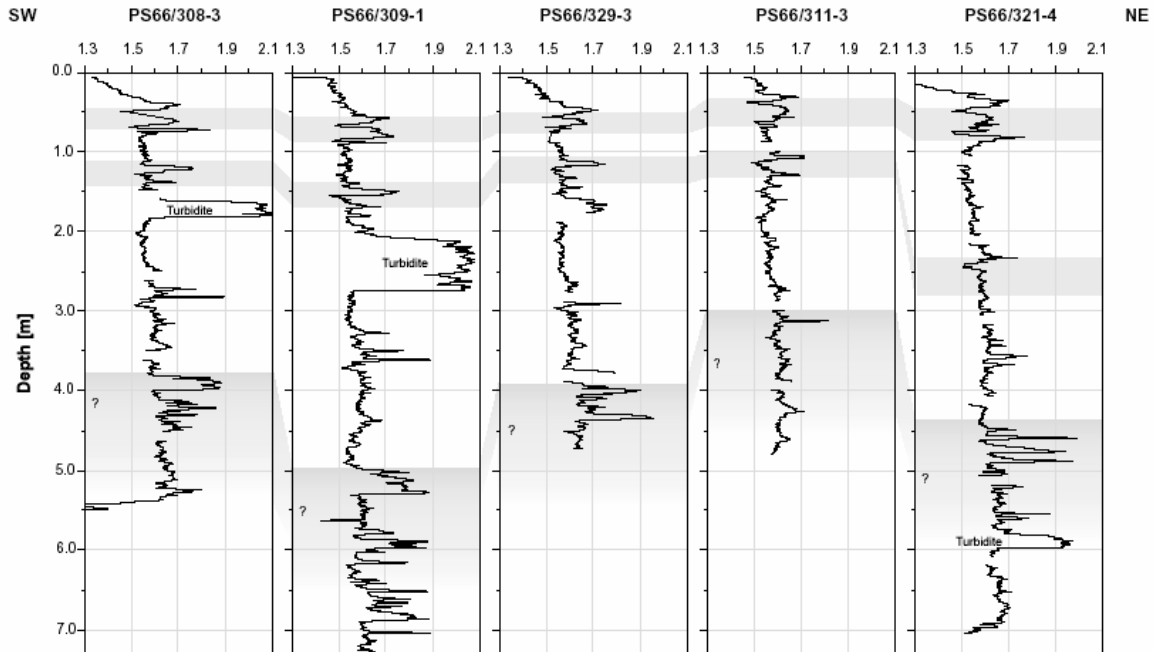


Fig. 9.11: Lateral core-correlation using wet-bulk density (g/cm^3).

Physical properties are commonly used for lateral core correlation. For the area of the Fram Strait and Yermak Plateau, wet bulk density proved to function as useful correlation parameter for gravity and Kastenlot cores obtained during a previous "Polarstern" expedition (ARK-XIII/2; Stein and Fahl, 1997). For the area under investigation during this cruise wet-bulk density again exhibits distinct down-core pattern of variability, which is found in several cores obtained from pelagic facies. For the pelagic sediments west of the Sophia Basin, largely covered by the mega-slide, a wet-bulk density-correlation for a cross section from core PS66/308-3 (south-west) to core PS66/321-4 (north-east) is presented as example (Fig. 9.11). Some distinct density wiggles can be correlated along the entire profile, whereas peaks with maximum densities are observed in turbidites of cores PS66/308-3 and PS66/309-1 only (Fig. 9.11). This local occurrence of turbidites is related to distal deposition caused by the mega-slide. Thus, the physical property records reveal an ideal tool to put the slide event into a first stratigraphic framework. Along the same profile, an overlay of the density correlation onto magnetic susceptibility data indicates that some density wiggles coincide with depth intervals, in which susceptibility exhibits distinct fluctuations too (Fig. 9.12). The latter, however, do not occur in exactly the same core-depth levels suggesting that the fluctuation of magnetic susceptibility is not purely a function of variation in density/porosity but has its own signature.

Also, it appears that the correlation using magnetic susceptibility is less clear than that of density, and, for some depth intervals weak or even invisible (Fig. 9.12). Again, very high magnetic susceptibility is mostly measured in turbidites (Fig. 9.12). The down-core pattern of all physical properties measured during the cruise is presented in the Appendix of this report.

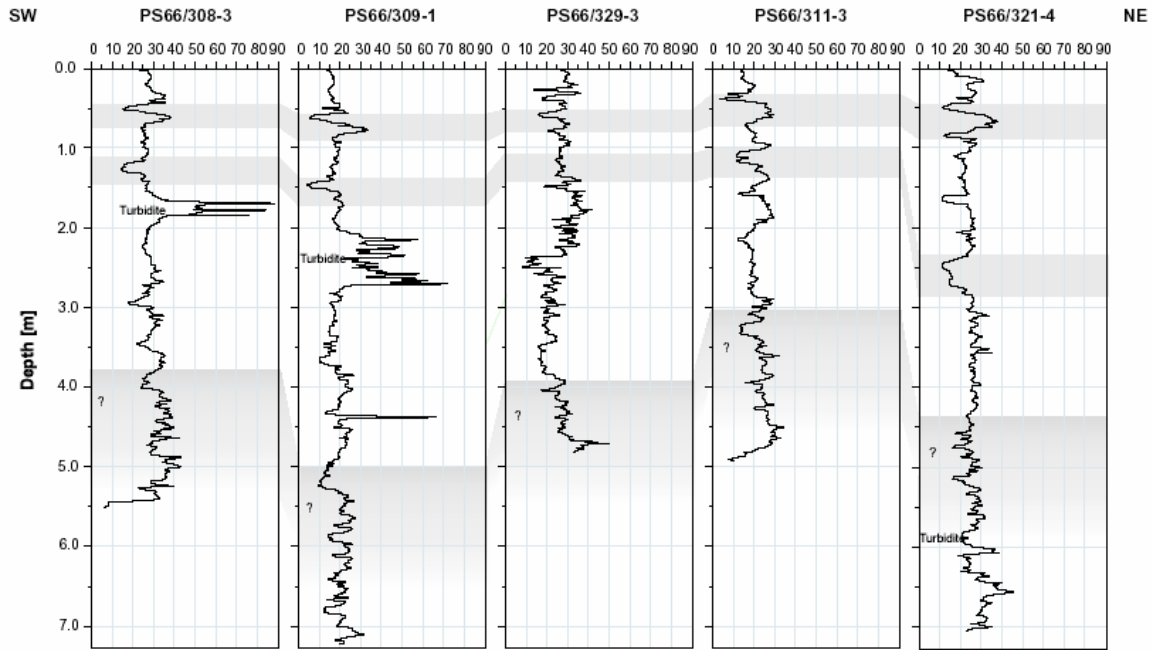


Fig. 9.12: Lateral core-correlation of magnetic susceptibility (point-sensor data in 10^{-6} SI; sensor susceptibility not converted to sediment volume). Note that correlation of grey-shaded areas is an overlay obtained by density data (Fig. 9.11) in order to test the core correlation for consistency.

9.3.2 Colour Scan Logging

A. C. Gebhardt, F. Niessen, D. Penschorn, J. Schneider

In combination with the magnetic susceptibility point sensor measurements (see Chapter 9.3.1), all split-core surfaces were colour-scanned with a resolution of 10 to 20 scan lines per millimetre in vertical and 1000 pixels in horizontal direction to have a digital downcore colour signal of the fresh sediment. The GEOSCAN camera was installed on an MSCL array and calibrated as described in the GEOTEK Multi-Sensor Core Logger Manual (2000). The camera uses a diachronic colour interference filter and three line-scan device arrays (1024 pixels each) to continuously record the three red-green-blue (RGB) colour channels. Its aperture was set to maximize contrast for the lightest-coloured sediment of each core. Synchronisation between the camera and the track is achieved by using the stepper motor pulses to trigger the line acquisition of the camera. Camera data is demultiplexed in the interface box, and 24-bit data is transmitted differentially to the PC interface card. In the PC data are corrected for convergence, gain and offset with the previously set calibration parameters. Profiles for each RGB channel were produced by averaging pixels in 6 cm x 1 cm and 8 cm x 1 cm rectangles for Kastenlot and gravity cores, respectively, along the central axis of the core using GEOTEK MSCL imaging software.

As an example, results from colour-scan logging of Kastenlot Core PS66/309-1 are shown in Fig. 9.13. Further records are presented in Chapter 12.5 (Annex).

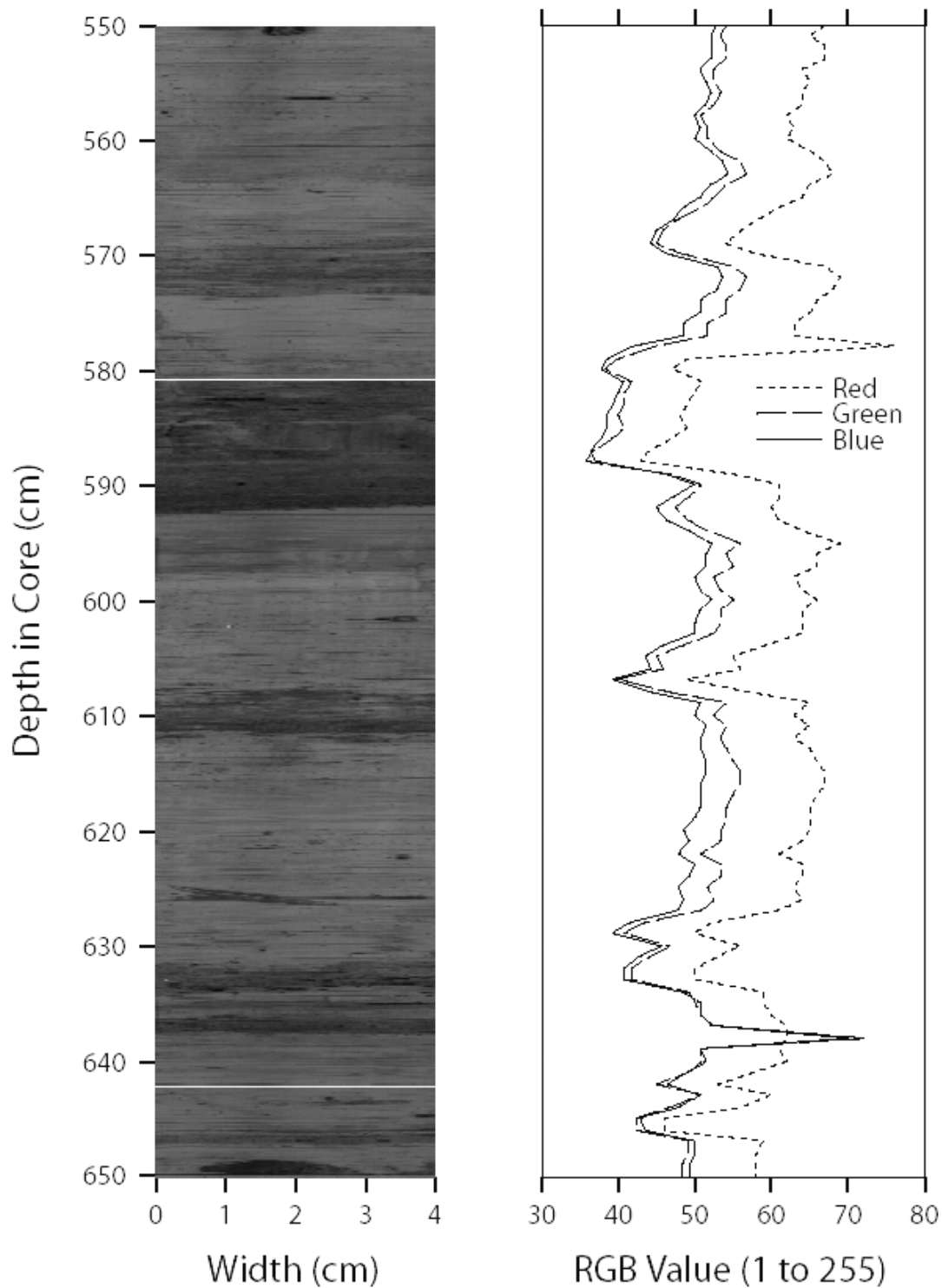


Fig. 9.13: Gray-value image of Core PS66/309-1, depth 550 to 650 cm, and RGB values of this section.

9.3.3 Shear Strength

D. Winkelmann, D. Penshorn

Shear strength measurements of undrained marine sediment (commonly silty clays) have been carried out by using both the fall-cone device Geotechnik g-200 and for comparison the Haake Rotovisco RV-12/500M on material from selected gravity kastenlot cores.

The fall cone method originally developed by John Olsson, member of the technical commission of the Swedish Royal Railway, in 1915, was used to determine the consistency of clays. The penetration of the fall cone into the clay or soil is considered to be directly proportional to its weight. According to Hansbo (1957) the relation between undrained shear strength s and the penetration h of a cone of the weight m can be written as:

$$s = K * m * h^{-2}$$

The constant K represents the angle of the cone and the sensivity of the clay. For comparison to the SI system gravity has to be considered as:

$$T_j = s * g$$

The rotovisco method uses a winged wheel pressed into the sediment followed by rotational momentum applied to it until the wheel turns. The relation of the rotational momentum and shear strength T_j can be written as:

$$T_j = f * a$$

The shape factor f represents a proportionality constant [$f = 1/(2*\pi*h*R^2)$] while a is the rotational momentum per scale unit.

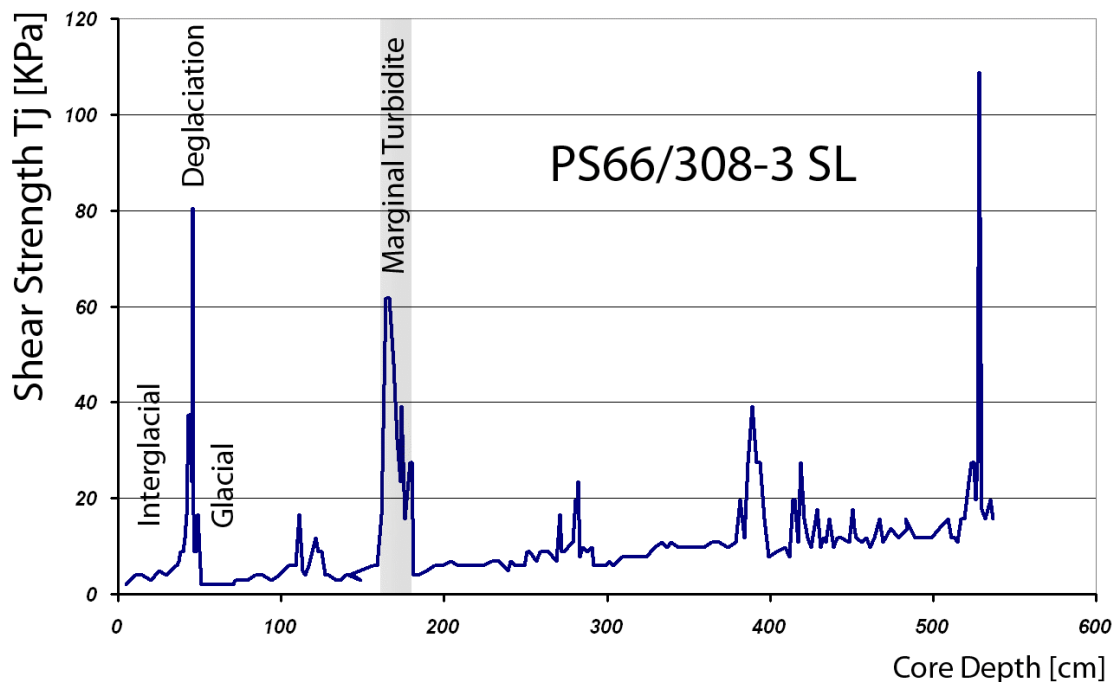


Fig. 9.14: Shear strength plot of core PS66/308-3 SL from the northern Svalbard continental margin close to the mega-slide margin.

Variability of measured shear strength can be attributed to major lithological changes within the sediment core mirroring glacial and interglacial conditions or turbidites from the adjacent submarine slide (Fig. 9.14). In some sediment cores from the Greenland shelf extraordinary shear strength characterises overconsolidated diamictos from an extensive glaciation (Fig. 9.15).

Problems of the method arise from sandy layers within the sediment cores. Due to dewatering effects the fall cone method overestimates the shear strength of such layers. Secondly, the application of both methods to the same core material leaves the second method with a slightly altered sediment resulting in lower or higher shear strength values.

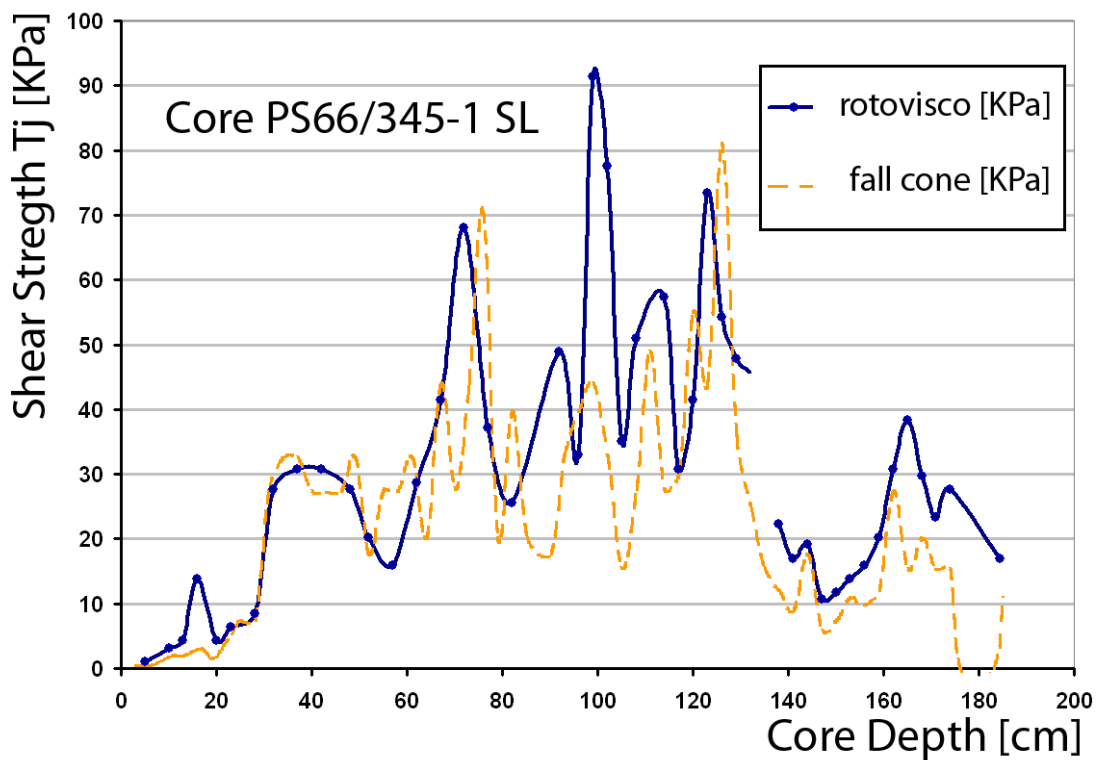


Fig. 9.15: Shear strength record from Core PS66/345-1, East Greenland continental margin. Comparison of parameters from the two methods applied for determination of the shear strength.

9.4 Geological Sampling, Description, and Methods Applied

F. Schoster, B. Bahr, C. Gebhardt, N. Kukina, N. Lensch, S. Nam, H. Noffke, D. Penshorn, A. Pühr, R. Saraswat, Chr. Schäfer, J. Schneider, R. Stein, J. Thiele, D. Winkelmann, Y. Yanina)

Surface and near-surface sediment sampling

Surface and near-surface sediment sampling was carried out by using a giant box corer and a multicorer.

The Giant Box Corer (weight of ca. 500 kg; volume of sample 50*50*60 cm; manufactured by Fa. Wuttke, Henstedt-Ulzburg, Germany) was successfully used 14 times at 16 stations. Two times there was no recovery due to technical problems. From the box corer surface sediments and three sediment cores (diameter 12 cm) for (1) sedimentology, mineralogy, geochemistry, (2) heavy minerals, and (3) archiving were taken. The second core was logged (MSCL, colour, magnetic susceptibility; see Chapter 9.3), opened and sampled for heavy mineral determination (MMBI) and bulk parameters like total organic carbon, total carbon, carbonate, and Rock-Eval analysis (AWI). The following samples were obtained from the surface sediments:

10x10 cm ²	(100cc)	Foraminifera (IfM-GEOMAR)
10x10 cm ²	(100cc)	Org. Geochemistry (AWI)
10x10 cm ²	(100cc)	Sedimentology (AWI)
10x10 cm ²	(100cc)	Micropaleontology (KIGAM)
3x3 cm ²	(ca. 10 cc; freeze-drying onboard)	TOC (AWI)
10x10 cm ²	(100cc)	Sedimentology (IORAS)

The standard 8-tubes-version multicorer (manufactured by Fa. Wuttke, Henstedt-Ulzburg, Germany) with an inner tube diameter of 10 cm was used. The penetration weight was always 250 kg. The multicorer was successfully used 6 times at 7 stations, and usually recovered undisturbed surface sediments and overlying bottom water. One multicorer was empty due to a technical problem. In general, the multicorer cores were sampled for the following investigations in slices of 1cm throughout the whole core:

3 cores	Org. Geochemistry (IfBM Hamburg)
2 cores	Micropaleontology (AWI)
2 cores	Org. Geochemistry-Sedimentology (AWI)
1 Core (Only surface 0-1 cm)	TOC, freeze-drying onboard (AWI)

Sampling of long sediment cores

Long sediment cores were taken by a gravity corer and a kastenlot. The gravity corer (GC or "Schwerelot", SL) has a penetration weight of 1.5 t. It was successfully used in variable barrel lengths of 3, 5, or 10 m at 26 stations (33 cores; see Table 9.1 for details). The recovery of the gravity corer varied between 0.1 and 7.11 m, the penetration between 0.1 and 11 m (Table 9.2).

The kastenlot (Kögler, 1963), a gravity corer with a rectangular cross section of 30x30 cm, has a penetration weight of 3.5 t and a corebox segment sized 30x30x575 cm (manufactured by Hydrowerkstätten Kiel). The length of the kastenlot boxes used was 11.75 m plus about 30 cm for the core catcher. The great advantage of this kastenlot is the wall-thickness of only 0.2 cm. Because of the great cross-sectional area (900 cm²) and the small thickness of the walls, the quality of the cores was generally excellent. The kastenlot was successfully used at 3 stations. The recovery of the kastenlot cores varied between 2.80 and 7.27 m (Table 9.2, Fig. 9.16).

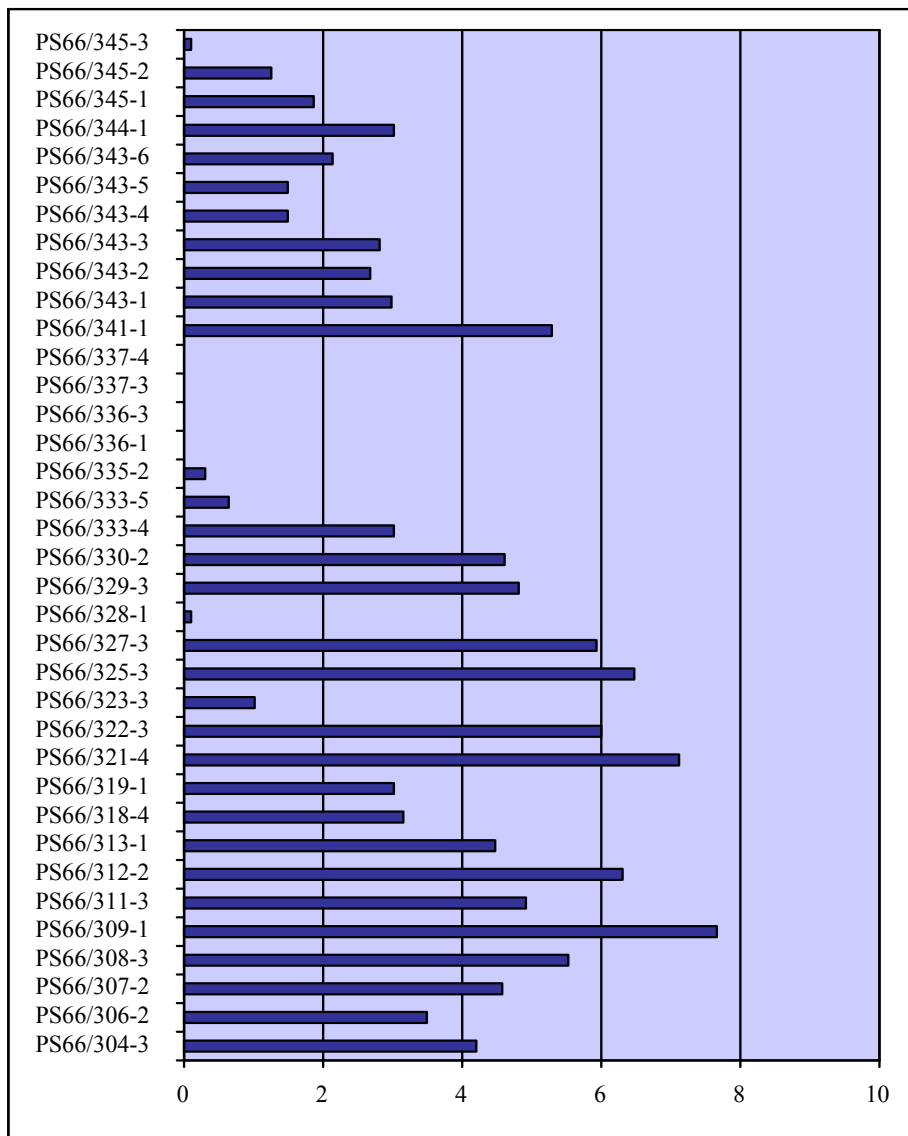


Fig. 9.16: Recovery of the gravity and kastenlot cores (in m). For location of cores see Fig. 9.1.

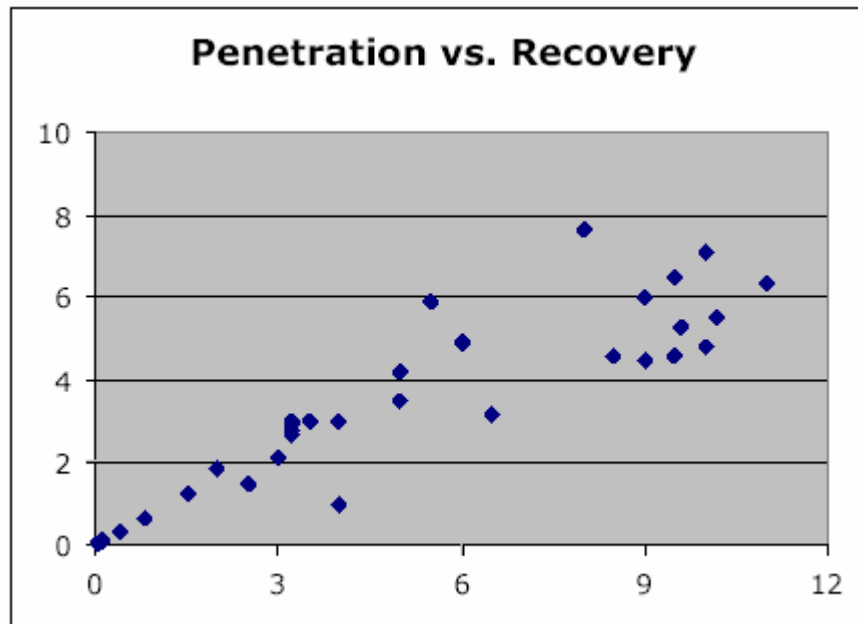


Fig. 9.17: Penetration (m) vs. recovery (m) of the gravity and kastenlot cores.

Fig. 9.17 shows the relation between recovery and penetration of the gravity and kastenlot cores.

All gravity cores and kastenlot cores were logged (MSCL, colour, magnetic susceptibility; Chapter 9.3). Most of them were opened, described (see Chapter 9.6.4. and Annex), and sampled for heavy minerals (MMBI) and bulk parameters like total organic carbon, total carbon, carbonate, and Rock-Eval parameters (AWI). Core PS66/309-1 KAL was also sampled for coarse fraction and foraminifera determination (see Chapter 9.6.3.). From all opened cores slices were taken in order to do X-ray photographs (see Chapter 9.6.1.).

Table 9.2: Gravity and kastenlot cores from ARK XX/3 with penetration and recovery values. Cores opened during the expedition, are marked with an "x".

Station	Date	Time	Latitude	Longitude	Depth [m]	Gear	Penetration	Recovery	Opened
PS66/304-3	03.09.04	17:40	80°43,20'N	14°38,02' E	1095,0	GC-5	5	4,19	x
PS66/306-2	04.09.04	03:34	81°14,56' N	13°18,62' E	2268,0	GC-5	5	3,5	x
PS66/307-2	04.09.04	06:21	81°11,94' N	13°2,68' E	2275,0	GC-10	8,5	4,57	x
PS66/308-3	04.09.04	10:47	81°7,30' N	12°35,97' E	2218,0	GC-10	10,2	5,54	x
PS66/309-1	04.09.04	13:44	81°11,22' N	12°59,08' E	2269,0	KAL	8	7,65	x
PS66/311-3	05.09.04	02:53	81°41,78' N	13°28,20' E	2192,0	GC-5	6	4,93	x
PS66/312-2	05.09.04	05:30	81°41,24' N	13°42,65' E	2275,0	GC-10	11	6,32	x
PS66/313-1	05.09.04	07:35	81°45,56' N	14°16,31' E	2298,0	GC-10	9	4,49	x
PS66/318-4	12.09.04	18:46	81°18,60' N	12°2,71' E	1262,0	KAL	6,5	3,15	x
PS66/319-1	12.09.04	22:26	81°24,49' N	13°48,79' E	2178,0	GC-3	4	3	x
PS66/321-4	13.09.04	11:51	82°10,27' N	18°13,47' E	2360,0	GC-10	10	7,11	x
PS66/322-3	13.09.04	16:16	82°5,40' N	18°5,25' E	3028,0	GC-10	9	6	x
PS66/323-3	14.09.04	06:06	82°18,44' N	22°59,67' E	3913,0	GC-3	4	1	x
PS66/325-3	15.09.04	16:32	81°26,18' N	25°59,86' E	895,5	GC-10	9,5	6,48	x
PS66/327-3	16.09.04	17:18	81°0,92' N	17°9,39' E	701,0	KAL	5,5	5,92	x
PS66/328-1	16.09.04	21:03	81°19,25' N	14°30,88' E	1979,0	GC-5	0,1	0,1	x
PS66/329-3	17.09.04	03:44	81°36,31' N	13°6,13' E	2211,0	GC-10	10	4,82	x
PS66/330-2	17.09.04	06:44	81°32,88' N	13°21,71' E	2305,0	GC-10	9,5	4,6	x
PS66/333-4	19.09.04	22:30	81°56,42' N	8°30,17' E	725,5	GC-3	3,5	3	x
PS66/333-5	19.09.04	23:26	81°56,10' N	8°31,50' E	719,1	GC-3	0,8	0,63	x
PS66/335-2	20.09.04	06:47	81°36,05' N	6°34,06' E	654,8	GC-3	0,4	0,32	x
PS66/336-1	20.09.04	07:40	81°36,48' N	6°45,14' E	505,2	GC-3	0,05	0,05	x
PS66/336-3	20.09.04	08:22	81°36,41' N	6°47,40' E	505,9	GC-3	0,05	0,05	x
PS66/337-3	20.09.04	10:29	81°36,30' N	7°1,44' E	503,0	GC-3	0,05	0,05	x
PS66/337-4	20.09.04	11:12	81°36,61' N	7°3,18' E	587,8	GC-3	0,05	0,05	x
PS66/341-1	22.09.04	23:43	79°44,07' N	0°44,97' W	2822,0	GC-10	9,6	5,28	x
PS66/343-1	24.09.04	03:50	79°0,83' N	11°6,91' W	216,2	GC-3	3,2	2,97	
PS66/343-2	24.09.04	04:20	79°0,98' N	11°6,82' W	226,0	GC-3	3,2	2,67	
PS66/343-3	24.09.04	04:49	79°1,05' N	11°6,88' W	227,2	GC-3	3,2	2,8	
PS66/343-4	24.09.04	05:18	79°1,17' N	11°7,12' W	240,9	GC-3	2,5	1,49	
PS66/343-5	24.09.04	05:44	79°1,31' N	11°6,80' W	252,2	GC-3	2,5	1,49	
PS66/343-6	24.09.04	06:09	79°1,44' N	11°6,84' W	264,2	GC-3	3	2,14	
PS66/344-1	24.09.04	06:48	79°2,55' N	11°6,65' W	338,7	GC-3	3,2	3,02	
PS66/345-1	24.09.04	07:30	79°3,58' N	11°15,11'W	317,9	GC-3	2	1,86	x
PS66/345-2	24.09.04	08:08	79°3,58' N	11°16,03' W	313,3	GC-3	1,5	1,27	x
PS66/345-3	24.09.04	08:40	79°3,58' N	11°17,37' W	308,6	GC-3	0,1	0,1	x

Sampling of crystalline basement

In order to collect samples from outcropping crystalline basement a dredge (chain bag) was successfully used two times on three stations (Table 9.3). At one station the overlying sediment layer was too thick. The chain bag was 0.95 x 0.35 x 0.40 m large and had a weight of 100 kg. The rope length during dredging was three times the water depth.

At station PS66/333-2 and PS66/335-1 stones were collected. The stones varied in size and composition, some of them were covered by a black layer (Fe-Mn-crust?). Identification and quantification will take place in the home laboratories.

Table 9.3. Positions of the dredges during ARK XX/3.

Station	Date	Time	Latitude	Longitude	Waterdepth [m]	Gear	Action
PS66/333-2	19.09.04	17:54	81° 55.54' N	8° 34.29' E	751.5	DRG_C	Dredge Beginn
PS66/333-2	19.09.04	19:05	81° 56.32' N	8° 31.62' E	720.8	DRG_C	Dredge Ende
PS66/333-3	19.09.04	20:45	81° 56.53' N	8° 22.74' E	718.5	DRG_C	Dredge Beginn
PS66/333-3	19.09.04	21:34	81° 56.49' N	8° 22.77' E	716.8	DRG_C	Dredge Ende
PS66/335-1	20.09.04	05:08	81° 35.99' N	6° 32.00' E	863.7	DRG_C	Dredge Beginn
PS66/335-1	20.09.04	05:29	81° 36.02' N	6° 35.42' E	558.5	DRG_C	Dredge Ende

9.5 Characteristics of Surface Sediments

S. Nam, N. Kukina, R. Saraswat, J. Thiele, Y. Yanina

During ARK-XX/3 expedition, at a total of 14 geological stations the giant box corer (GKG) was deployed to take undisturbed surface sediments from water depths varying between 503 and 3910 m. Recovery of GKG cores ranges between 16 and 55 cm in length. A total of 11 box cores were mostly undisturbed, while the surface sediments of two cores (PS66/306-1GKG and PS66/323-1GKG) were strongly and/or probably disturbed, respectively (Table 9.4). In general, the mostly undisturbed surface sediments mainly consist of brown to olive brown silty clay to mud. Core PS66/336-4 comprised many black-coloured (black coating?) dropstones overlying nearly undisturbed surface sediments. Core PS66/337-2GKG, retrieved from the shelf of the Yermak Plateau, mainly contained high amounts of dropstones with strongly varying sizes between gravel and boulder, and a little amount of coarse sand. The majority of dropstones of gravel to boulder sizes seem to be also black-coloured (basalts? and/or black-coated sedimentary rocks?). Table 9.4 shows general information about all box core sediments collected during this expedition.

Table 9.4: General overview of box cores collected during ARK-XX/3.

Core (GKG)	Core length (cm)	Water depth (m)	Sampling No.			Color & lithology	Remarks
			100cm ³	biomarker	tube		
PS66/306-1	51	2271	1	X	2	brown silty clay	abundant benthic forams (<i>Pyro</i>)
PS66/307-1	48	2276	6	1	3	brown silty clay	abundant benthic forams (<i>Pyro</i>)
PS66/308-1	53	2217	6	1	3	brown silty clay	moderate benthic forams (<i>Pyro</i>), worms
PS66/311-1	-	2195	6	1	3	brown silty clay	traces of benthic organisms, not described
PS66/312-1	51	2273	6	1	3	brown silty clay	worms, abundant benthic forams (<i>Pyro</i>), traces of benthic organisms
PS66/321-2	25	2359	6	1	3	brown silty clay	traces of benthic organisms, sponge
PS66/322-2	23	2992	6	1	3	brown silty clay	traces of benthic organisms, shell fragments, benthic forams
PS66/323-1	24	3910	x	x	2	brown silty clay	probably surface disturbed
PS66/325-2	53	896	6	1	3	olive gray to brown silty clay	abundant benthic organisms and its traces, sea-stars of <~1 cm, worms, bivalve shell (~2 cm) with flat form
PS66/327-2	55	701	6	1	3	olive gray to brown silty clay	abundant benthic organisms, i.e. sea-stars, nematodes and/or annelids, bird feather
PS66/329-1	52	2209	6	1	3	brown mud	various benthic organisms including sea-stars, nematodes and/or annelids, benthic forams
PS66/330-1	50	2306	6	1	3	brown mud	dropstone of ca. 25 cm long
PS66/336-4	16	505	X	X	3	gravelly sand mud	abundant dropstones of gravel to boulder, abundant benthic organisms (forams, brittle stars, bivalves, worms, etc.)
PS66/337-2	51	2271	X	X	X	gravel	abundant dropstones of gravel to boulder

Prior to opening the box cores onboard, wet bulk density and P-wave velocity and magnetic susceptibility (10⁻⁵ SI) were determined in 1 cm intervals using Multi Sensor Core Logger (MSCL-14) on all box cores. The box cores were then split in two halves one each for archive and working. The working half was used for preliminary description. Both half cores were photographed. The colors and magnetic susceptibility (10⁻⁵ SI) of the archive cores were additionally logged in 0.5 cm intervals using Color Scanner. Sediment colors were visually noted using Munsell Soil Color Charts (1954). Lithological changes and primary structures of sediment were also described with an exception of core PS66/311-1GKG. X-radiographs were made for the determination of sedimentary structures and to estimate the contents of IRD. Generally, the sediments of box cores are composed mainly of brown to dark grayish brown homogenous mud and silty clay. However, slightly bioturbated and/or laminated structures are also observed in several cores (see Chapter 12.3, Annex).

Table 9.5: Bulk minerals of surface (0-1cm) sediments

Stations	Quartz	Feldspar	Mica	Terr. carbonate	Volcanic glass	Clay minerals	Org. remains	Biog. Carbonate	Fe-hydroxide	Other Heavy
PS66/304-2MUC	30,2	18,1	7,3	4,1	1,6	5,3	8,8	2,1	10,2	12,3
PS66/307-1GKG	28,2	20,6	7,8	0	2,1	7,3	8,9	1,1	4,1	19,9
PS66/308-1GKG	30,2	10,1	6,2	1,1	2,1	15,4	20,1	4,9	2,1	7,8
PS66/311-1GKG	20,8	11,2	5,3	1,1	1,5	11,1	12,2	2,2	25,5	9,1
PS66/312-1GKG	26,3	10,1	5,3	1,2	0	21,2	11,3	4,6	3,2	16,8
PS66/321-2GKG	33,5	14,2	8,6	0	0	10,2	8,5	3,6	6,6	14,8
PS66/322-2GKG	22,1	8,2	7,2	0	0	25	11,2	1,1	12	13,2
PS66/325-2GKG	22,6	11,1	8,8	0	0	26,6	9,1	0	14,1	7,7
PS66/327-2GKG	19	6,4	4,3	6,4	2,2	17,2	18,3	2,2	7,5	16,5
PS66/329-1GKG	28,1	14,2	6,3	1	0	20,3	18	0,5	4,6	7
PS66/330-1GKG	20,3	8,9	9,3	0	0	5,6	25	8	6	16,9
PS66/336-4GKG	30,1	10,8	7,1	0	0	18,3	5,9	2,5	6,8	18,5
PS66/337-2GKG	25,3	11,2	8,9	1,2	0	6,9	9,9	12,2	8,1	16,3

Table 9.6: Heavy minerals of surface (0-1cm) sediments

Stations	Pyroxene	Amphibole	Epidote	Clorite	Garnet	Black ores	Opaque
PS66/304-2MUC	38,1	31	9,2	2,6	5,8	6,2	7,1
PS66/307-1GKG	38,7	25,1	12,6	4,4	6,9	7,2	5,1
PS66/308-1GKG	22,6	41,1	5,6	0	14,2	11,3	5,2
PS66/311-1GKG	21,5	39,9	2,8	0	8,9	16,3	10,6
PS66/312-1GKG	40	39	6,3	0	5,2	3,2	6,3
PS66/321-2GKG	38,4	29,6	7,9	0	3,3	10,6	10,2
PS66/322-2GKG	32,2	30	8,9	2,2	8,2	15,3	3,2
PS66/325-2GKG	40,1	30,1	11,2	2,6	5,5	7,8	2,7
PS66/327-2GKG	23,8	28,6	9,5	0	4,8	19	14,3
PS66/329-1GKG	30	35,2	4,8	0	12,2	14,6	3,2
PS66/330-1GKG	39	28,3	4,6	2,1	2,5	12,3	11,2
PS66/336-4GKG	40	30	5	1,8	2,1	14,2	6,9
PS66/337-2GKG	32,7	21,2	5,8	3,8	9,6	9,6	17,3

Surface (0-1cm) sediments from 13 box cores collected during the ARK-XX/3 cruise were investigated with smear slides. Results of smear slide analysis are given in Table 9.5 and 9.6. Smear slide analysis shows that major surface sediments are comprised of quartz and clay minerals with minor amounts of feldspars, heavy minerals and Fe-oxides/hydroxides. The abundance of heavy minerals varies from 11.0% (PS66/329-1) to 34.6% (PS66/311-1). The increase in the amount of heavy minerals is on account of Fe-oxides/hydroxides. The biogenic components and diatoms are almost absent in all the samples.

Quartz, feldspar and mica constitute the majority of the light minerals. In all surface sediments quartz content is higher than feldspar content. The Q/Fsp ratio is more than 2.0 in seven samples (PS66/308-1, PS66/312-1, PS66/322-2, PS66/325-2, PS66/330-1, PS66/336-4, PS66/337-2) and between 1.0 and 2.0 at the other stations. Terrigenous carbonates were found to be significant at two stations (PS66/304-2 and PS66/327-2, 4.0% and 6.4%, respectively).

In most of the studied samples the heavy minerals include pyroxenes, amphiboles and black ore minerals (almost everywhere more than 15%). The garnet and epidote content also exceeds 10% in some of the samples investigated on-board. The concentration of other minerals does not reach 10%.

9.6. Characteristics of ARK-XX/3 Sediment Cores

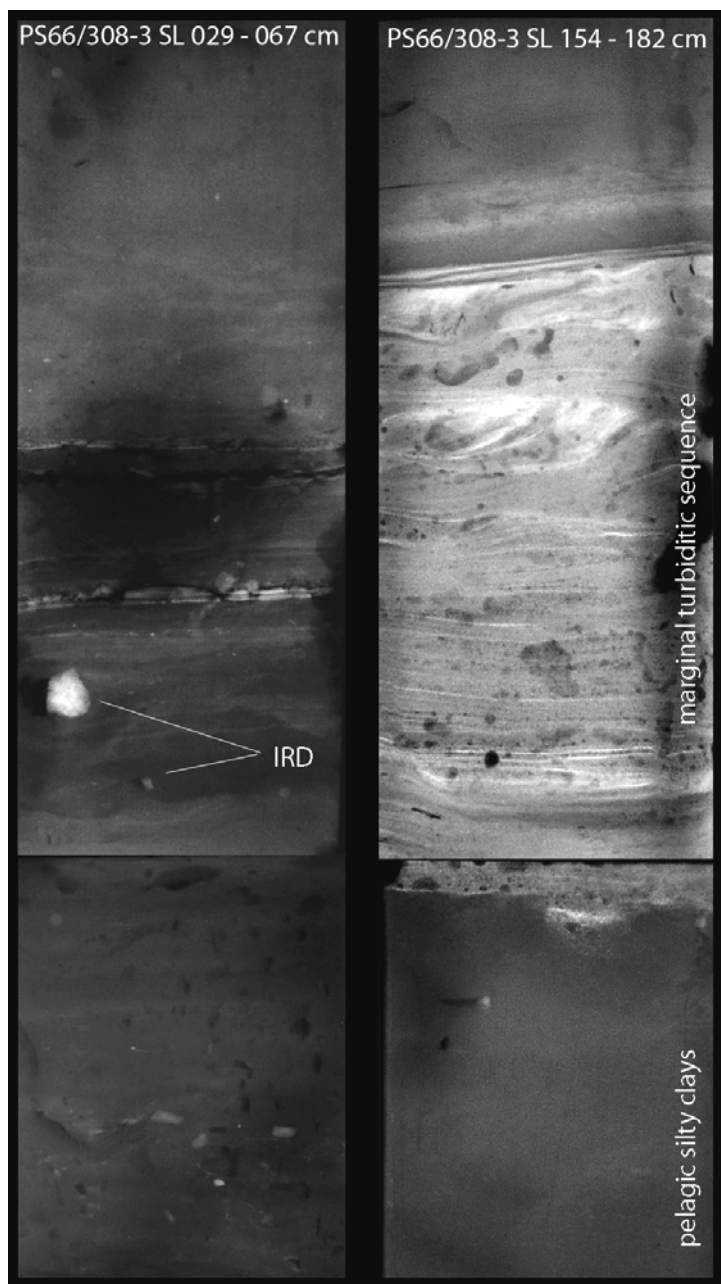
R. Stein, N. Kukina, H. Noffke, A. Pühr, Chr. Schäfer, D. Winkelmann, Y. Yanina

9.6.1 X-ray Photographs: Sediment Structure and IRD Content

D. Winkelmann, H. Noffke, A. Pühr, Chr. Schäfer

X-ray imagery of sediment sections has become a common tool in accessing the internal structure of soft marine sediments. Standard slices (10x25x1cm) of sediment continuously taken downcore from all long gravity and kastenlot cores as well as from short cores, have been processed onboard. The structures identified on the photographs reflect marine sedimentary environments ranging from

partly bioturbated pelagic glacio-marine deposits, turbidites and debris flows to diamicton.



Examples of x-ray images from gravity core PS66/308-3 SL situated near the western margin of the mega-slide in the Sophia Basin north of Svalbard are shown in Figure 9.18. The marginal debris flow / turbidite is visible as unit of sandy silty material (brighter in the image due to lower penetration of the x-rays) with cross bedding and fining upwards sequences indicating higher velocities of current speed (right column of figure). The unit displays individual pulses of sediment accumulation presumably from a single event. The “normal” pelagic sediments partly bioturbated with IRD mirror glacio-marine conditions while layers of higher silt/sand content often laminated may point towards deglacial conditions further up in the core (left column of figure).

Fig. 9.18: Examples of x-ray images from gravity core PS66/308-3 SL situated near the western margin of the mega-slide in the Sophia Basin north of Svalbard (For core location see Figure 9.1).

From the Kastenlot Core PS66/327-3 sediment slices have been taken every ten centimetre to cover large sediment structures of the full core width (Fig. 9.19). The core displays tilted sediment layers as well as sediment folding. Hence standard slices have been taken in 10 centimetres interval to cover almost the full width of the kastenlot. Note the scale of deformational features which would make their identification in a standard gravity core (e.g. Gravity corer with a core barrel of 10 cm in diameter) very unlikely.

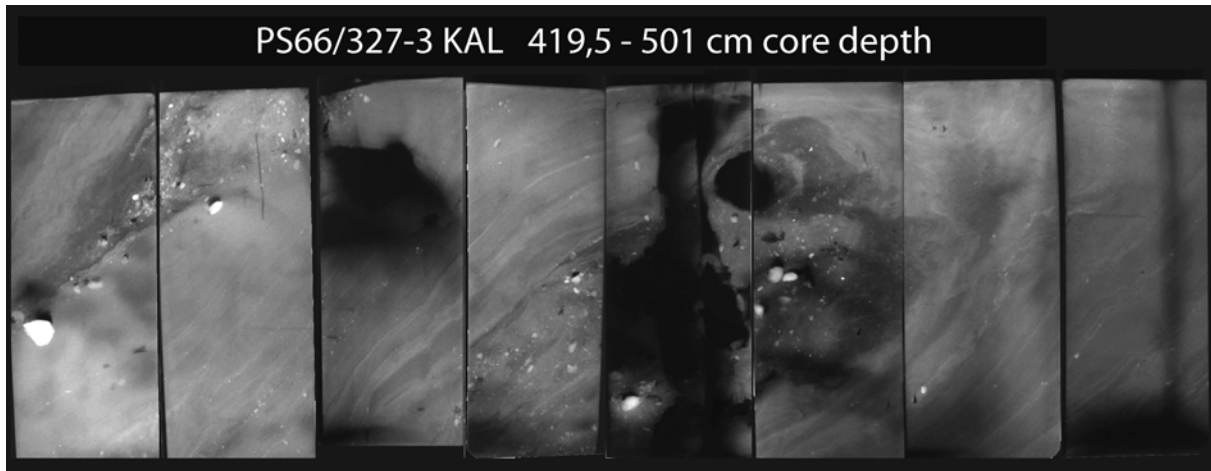


Fig. 9.19: Examples of x-ray images from Kastenlot Core PS66/327-3 KAL, northern Svalbard continental slope (For core location see Figure 9.1).

The x-ray photographs have also been used for quantification of ice rafted debris (IRD). According to the method of Grobe (1987) the IRD content can be evaluated by counting lithogenic particles with more than one millimetre diameter per ten cubic centimetre (per cm sediment slice). In the IRD records from selected sediment cores, distinct changes in IRD abundances occur (Fig. 9.20), which are probably related to glacial/interglacial variability in extension of glaciation on Svalbard.

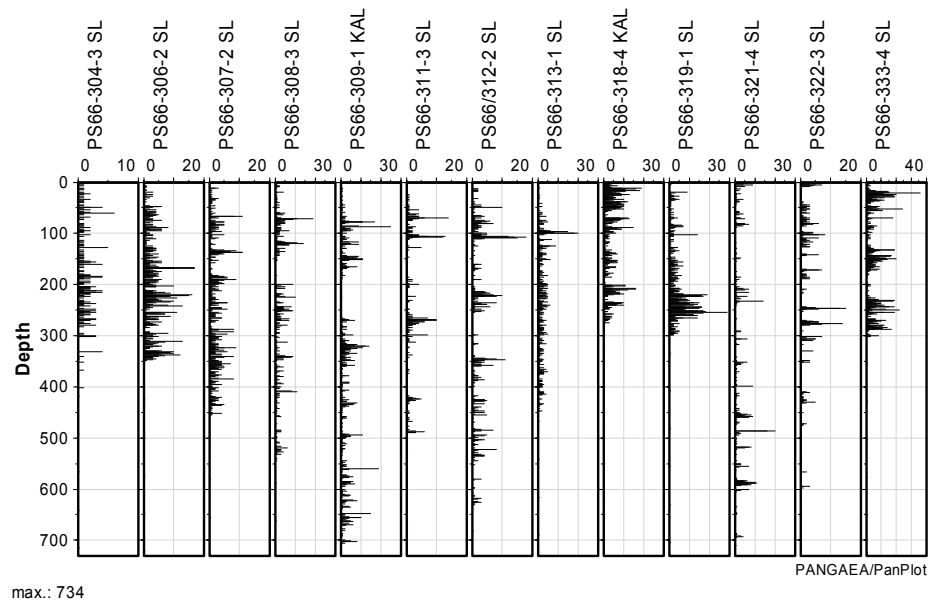


Fig. 9.20: IRD record of selected gravity and kastenlot cores recovered during Cruise ARK-XX/3 (For core locations see Figure 9.1).

9.6.2 Results of Smear-slide Analysis

N. Kukina

Description of the smear slides allow to indicate mineral associations and contents of terrigenous and biogenous components. The results of smear-slide estimates in cores PS66/304, PS66/308, PS66/309, PS66/312, PS66/318, PS66/319, PS66/325, and PS66/333 are shown in Figures 9.21 to 9.28 (for location of cores see Fig. 9.1). In these figures, on one hand the abundances of quartz, feldspars, mica, terrigenous carbonate, volcanic glass, clay minerals, organic remains, Fe-hydroxides, and heavy minerals (summed up to 100%) are shown. On the other hand, the composition of heavy minerals (summed-up to 100%) is shown in separate graphs of the figures. Tables of the smear-slide data are listed in Chapter 12.4 (Annex).

Based on smear-slide analysis, the main minerals are quartz, feldspar, terrigenous carbonates, mica and clay minerals. The heavy minerals are presented by pyroxenes, amphiboles, epidote, garnets, Fe-oxides/hydroxides and black ores. Pyroxenes and amphiboles dominate, but in some intervals the Fe-oxides and hydroxides are enriched.

The study of the mineral composition and lithological description allowed to distinguish the following types of sediments (units), ordered from core top to bottom:

The type 1 sediments are composed of dark brown and dark grayish brown soft silty clay. Clay minerals and quartz dominate in the mineralogical composition. Amphiboles, Fe oxides/hydroxides and black ores increase, terrigenous carbonates and organic remains decrease. The heavy minerals concentration changes from 10% (PS66/308) to 23% (PS66/309).

The type 2 sediments have very dark brown color, and oxidations, Fe-Mn nodules, sandy silt with gravel grain-size composition ("hard ground") were found. The mineral composition is characterized by much higher abundances of Fe oxides/hydroxides in these sediments. Terrigenous and biogenic carbonates are absent. Contents of pyroxenes and epidote increase from 20% to 35%.

The type 3 sediments are characterized by strong variability of lithological parameters. The sediments are dark olive gray sandy silty clay. In the upper part of the unit elevated content of sand were observed. With increase of sand content the heavy minerals content increase also. The terrigenous and biogenic carbonates were completely absent. Only rare amount of organic remains was found. The content of amphiboles and garnets increases.

Type 4 sediments, composed of very viscous gray or dark gray silty clay, are observed in cores PS66/308, -329, and -330. Quartz and feldspar are the main minerals, pyroxenes, epidotes and chlorites dominate in the heavy fraction.

The type 5 sediments (PS66/306, -309, -311, -313) are different from the other units due to high grad of compaction and fine to coarse grain-size. Color changes from dark grayish brown to olive brown and to olive gray are typical.

The sediment is laminated. In the mineralogical composition, a relatively high content of volcanic glass and organic remains and a decrease of content of the heavy minerals were determined.

The type 6 sediments (Cores PS66/308 and 309) are of brown, olive gray and dark grayish brown colours and bioturbated, contain some lenses of olive gray sand and dropstones. The main minerals are quartz, feldspar and mica. Volcanic glass and biogenic carbonates are absent.

Type 7 sediments are generally fine-grained and have gray and dark gray colours with black points. Description of smear slide showed increased abundances of sulphides and opaques. There are more amphiboles than pyroxenes. The content of terrigenous and biogenic carbonates is increased (to 16-18% in cores PS66/318 and 319).

Future studies of mineral assemblages and grain-size composition have to be performed to describe the sediment type and to identify lithological units in more detail.

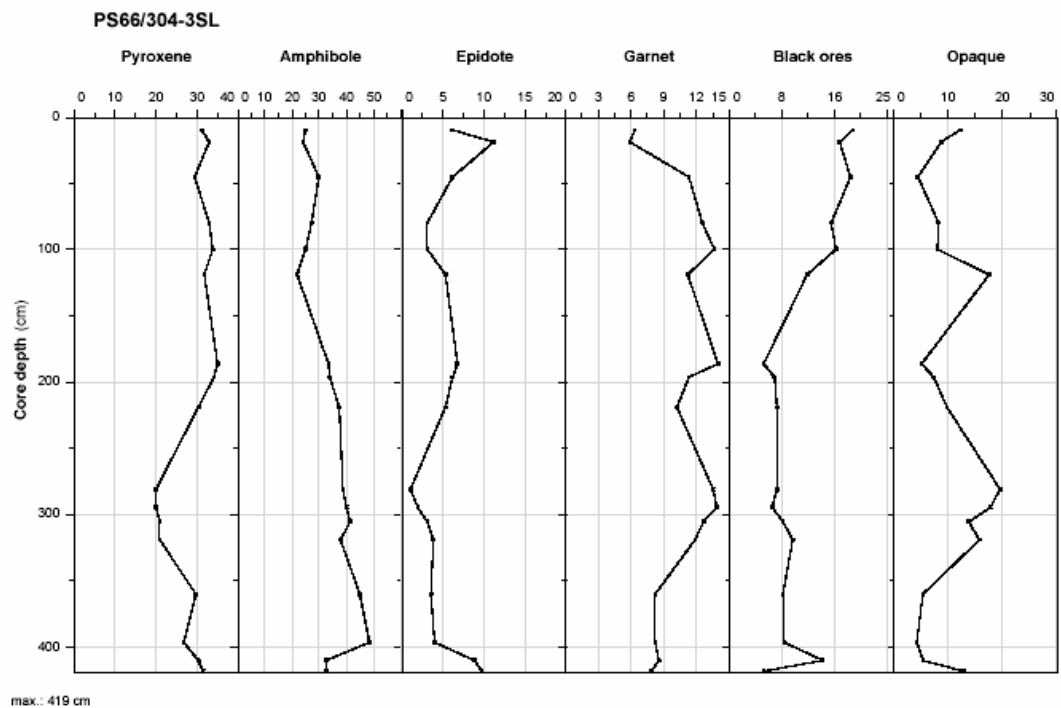
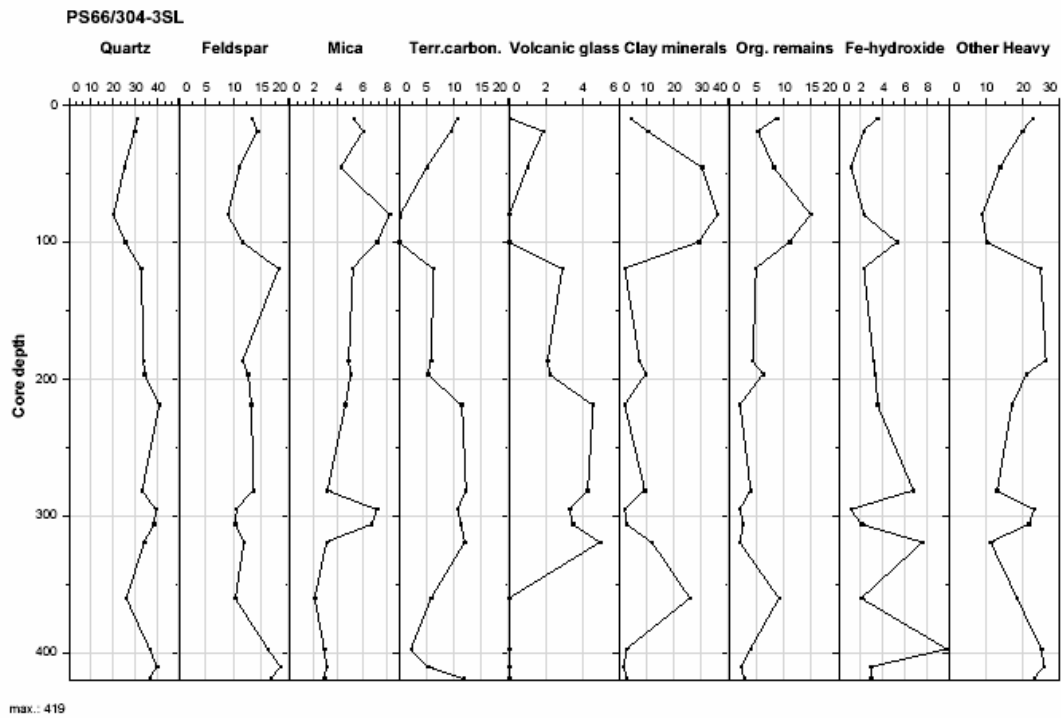


Fig. 9.21: Mineralogical composition of sediments of Core PS66/304, based on smear-slide estimates.

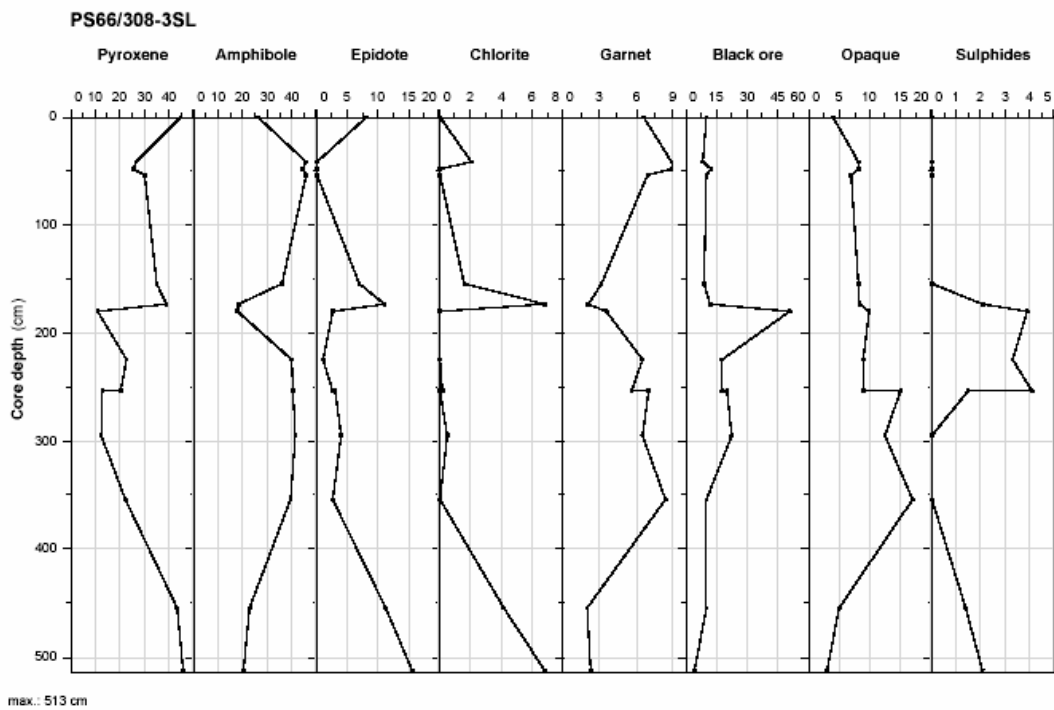
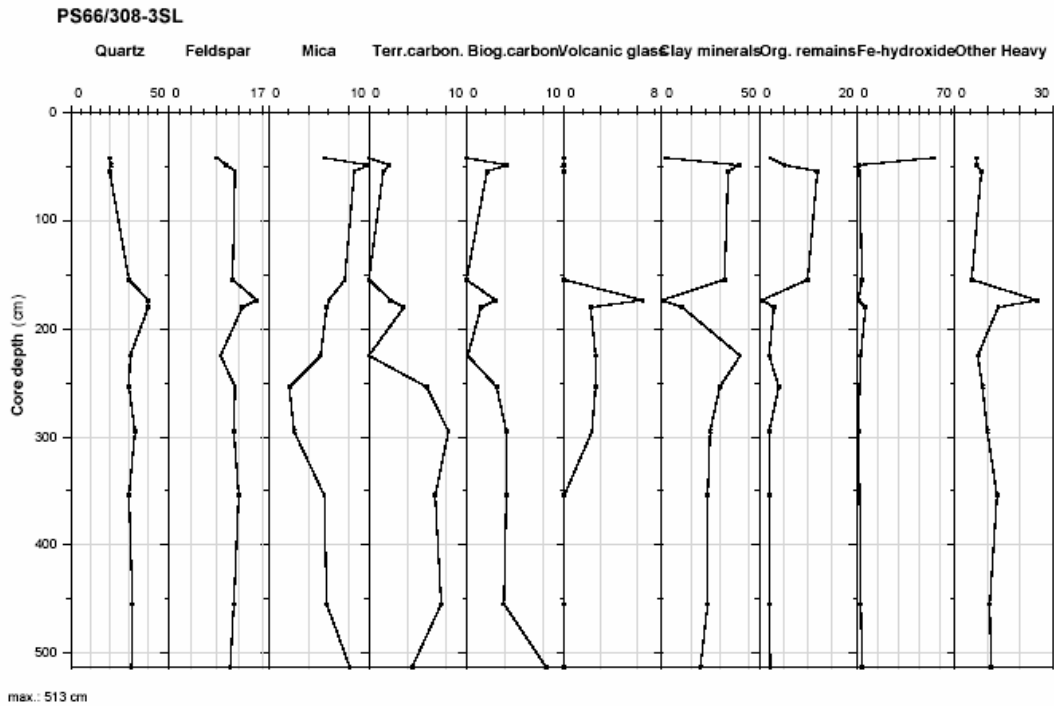


Fig. 9.22: Mineralogical composition of sediments of Core PS66/308, based on smear-slide estimates.

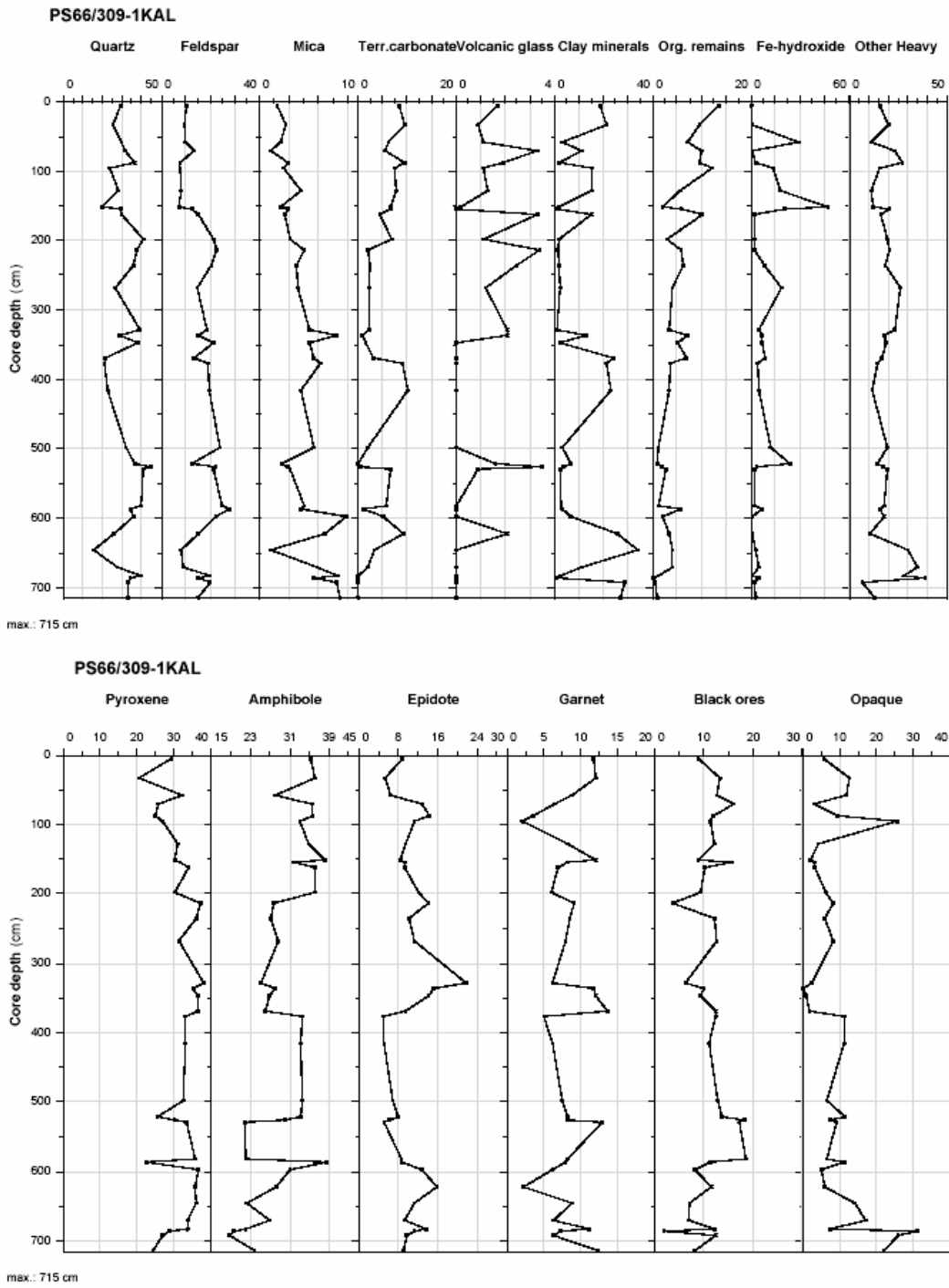
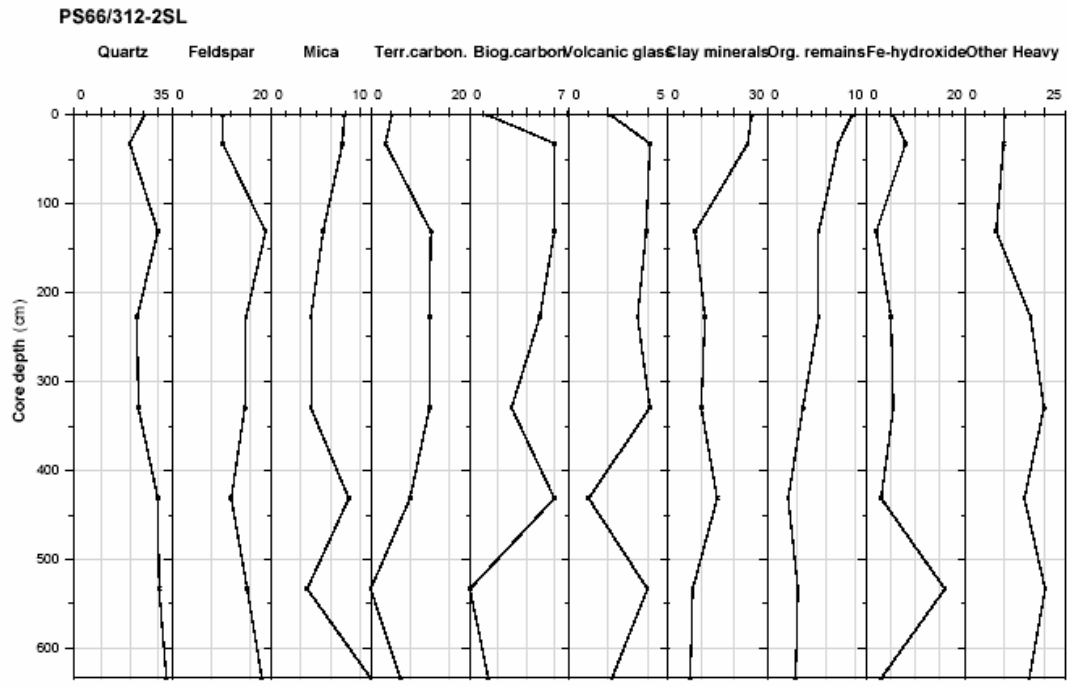
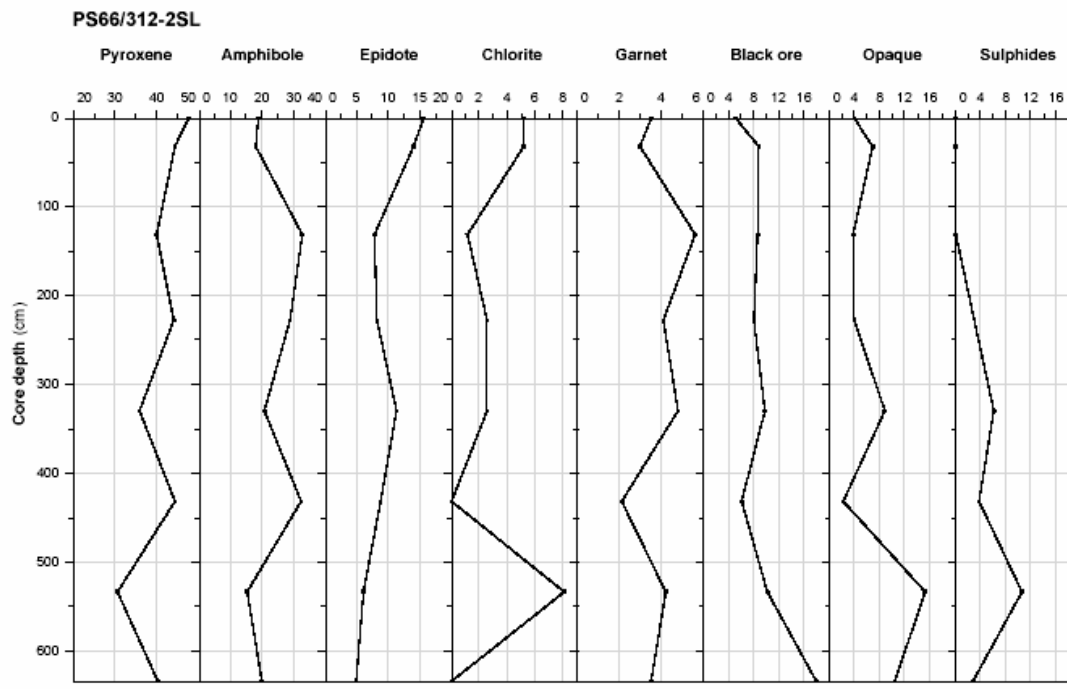


Fig. 9.23: Mineralogical composition of sediments of Core PS66/309, based on smear-slide estimates.



max.: 633 cm



max.: 633 cm

Fig. 9.24: Mineralogical composition of sediments of Core PS66/312, based on smear-slide estimates.

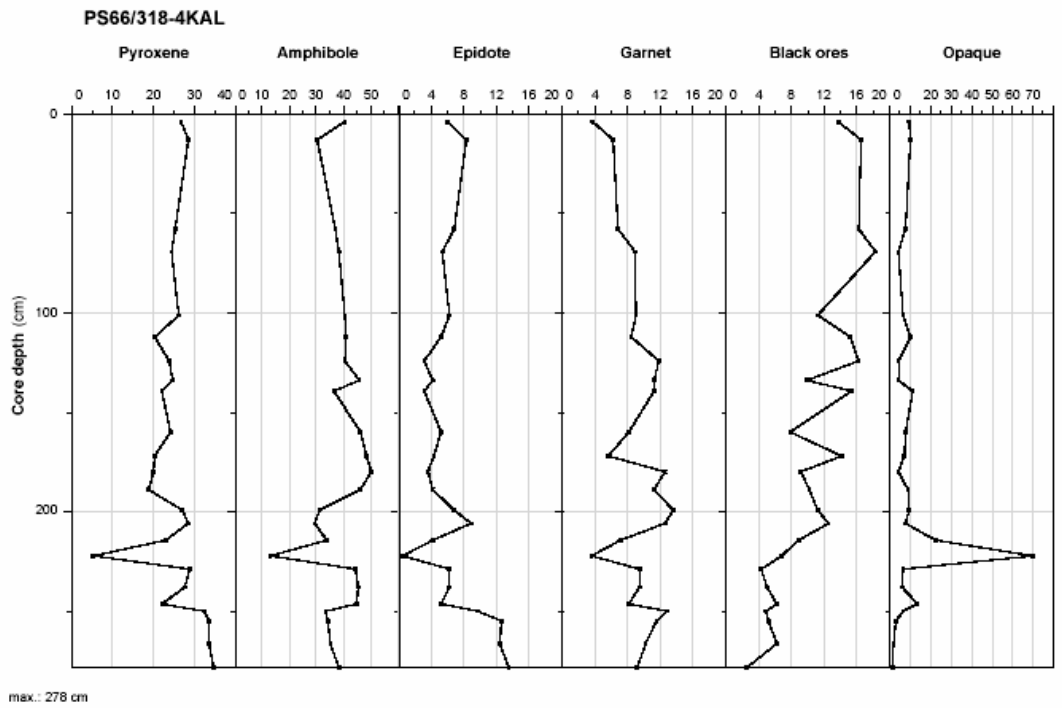
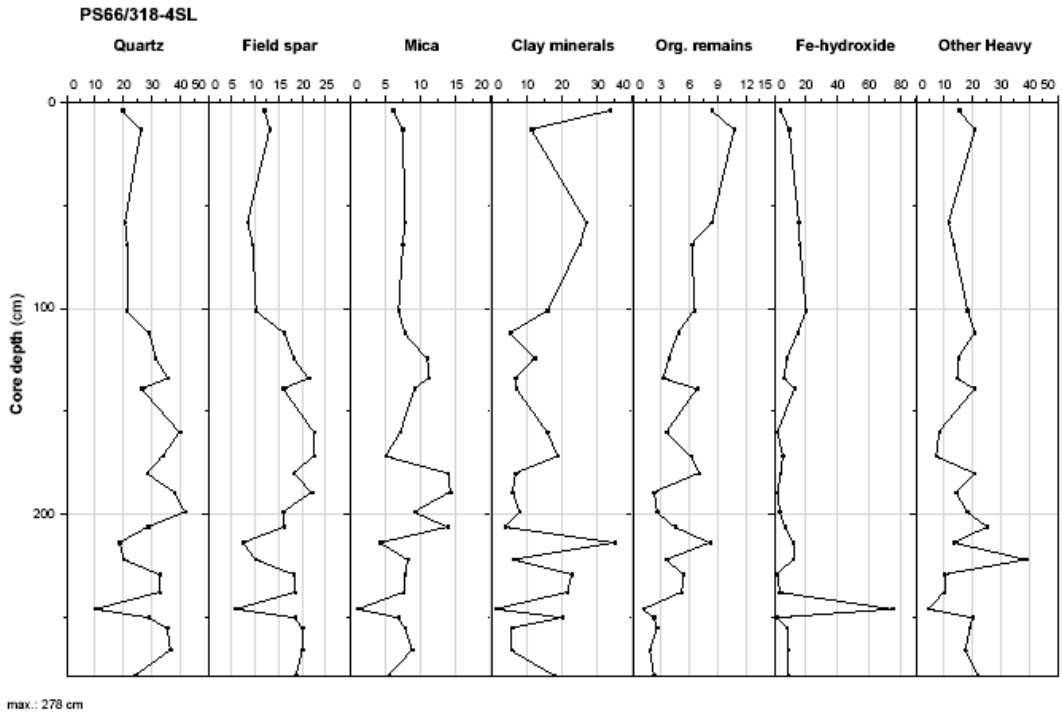


Fig. 9.25: Mineralogical composition of sediments of Core PS66/318, based on smear-slide estimates.

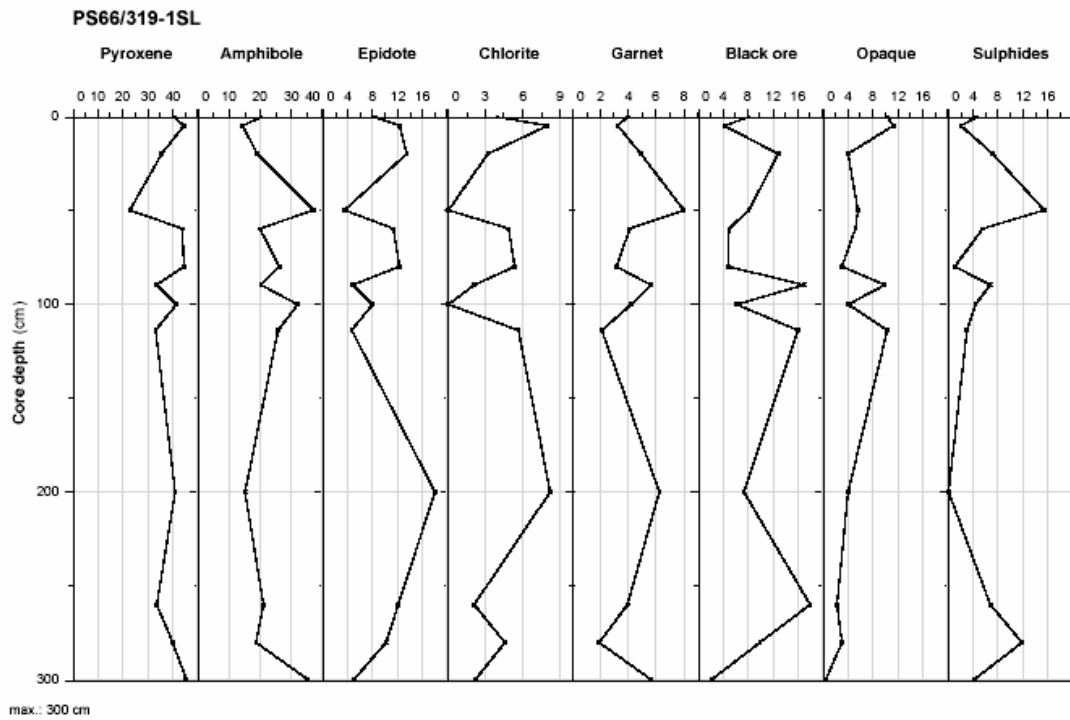
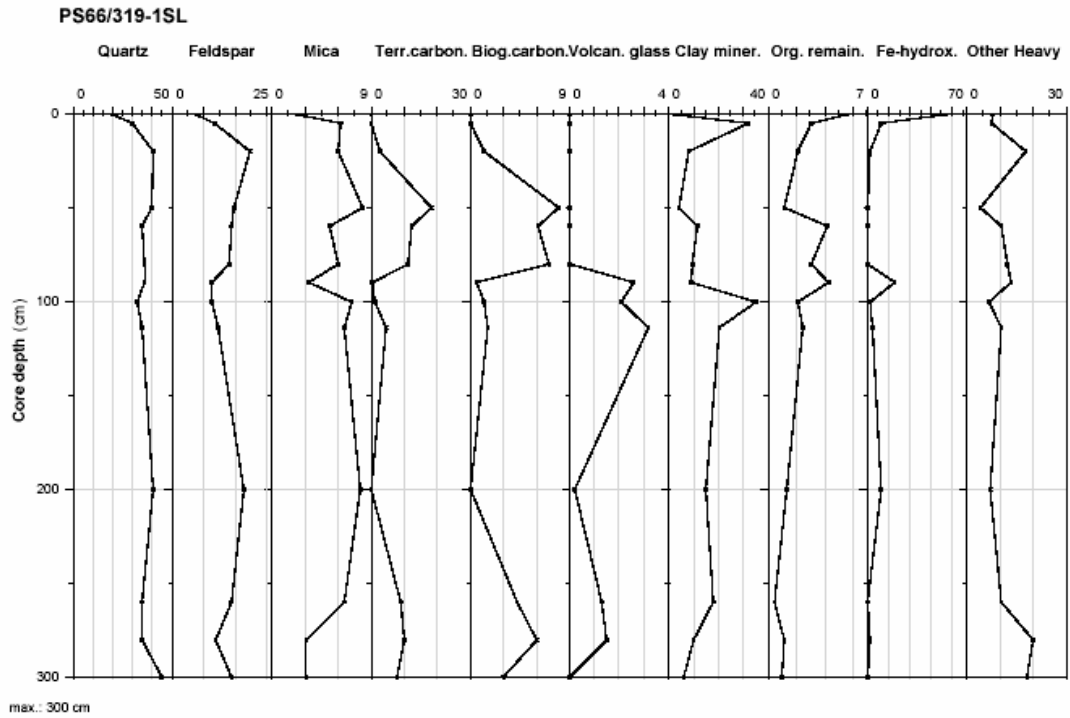


Fig. 9.26: Mineralogical composition of sediments of Core PS66/319, based on smear-slide estimates.

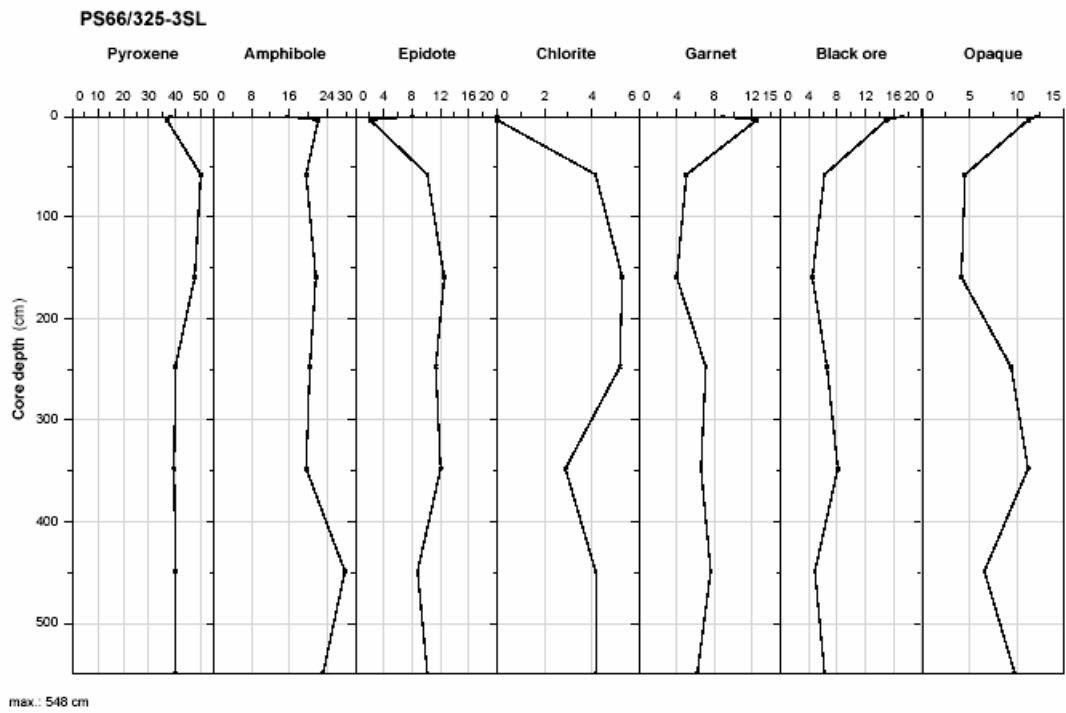
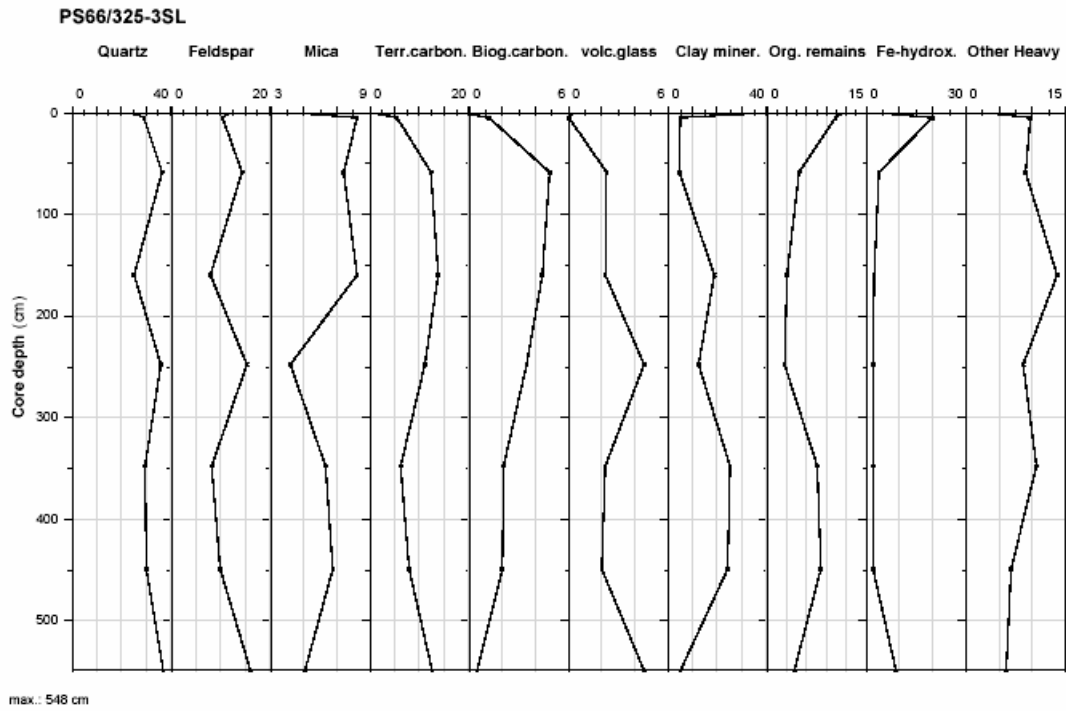


Fig. 9.27: Mineralogical composition of sediments of Core PS66/325, based on smear-slide estimates.

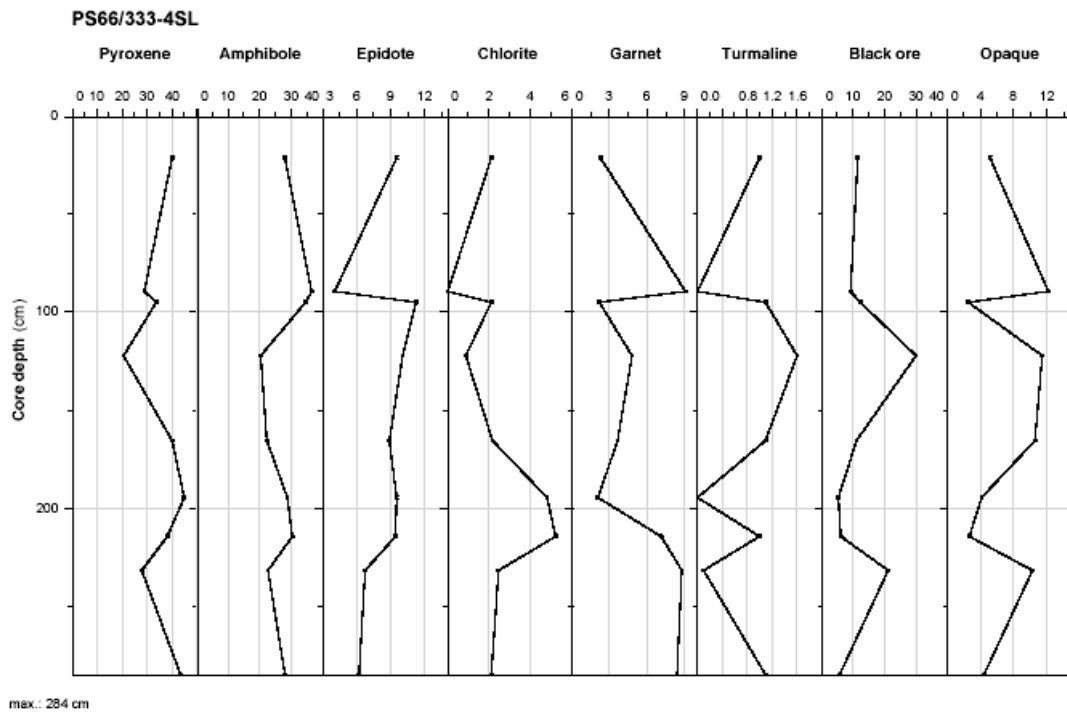
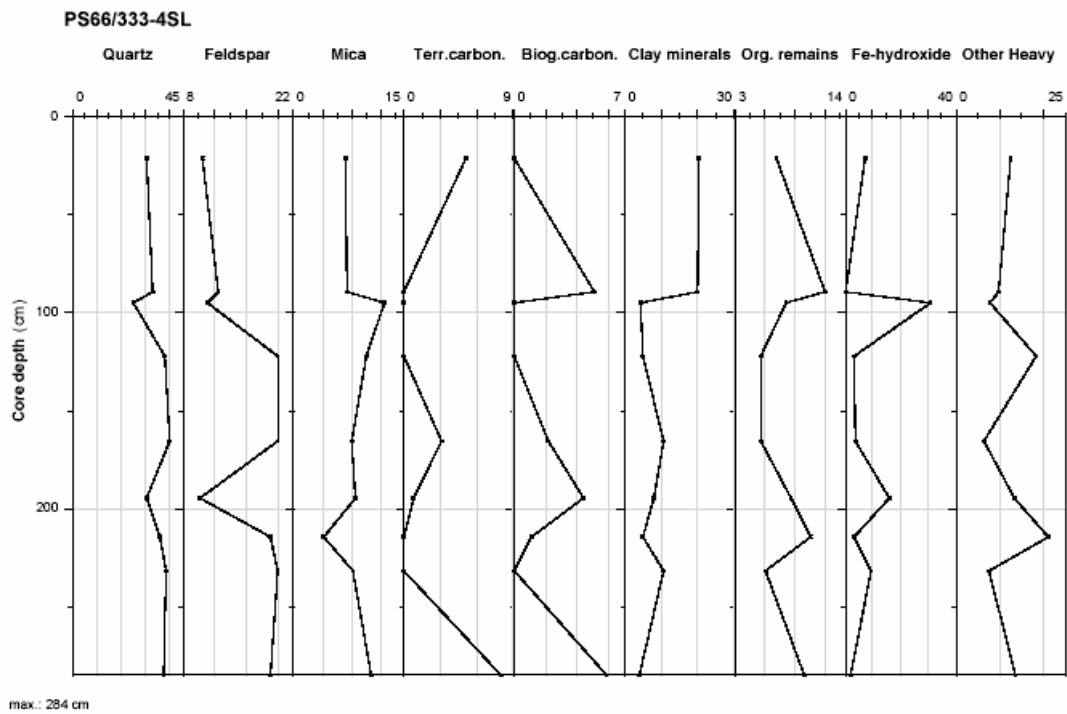


Fig. 9.28: Mineralogical composition of sediments of Core PS66/333, based on smear-slide estimates.

9.6.3 Results of Coarse Fraction Analysis

J. Thiele, R. Saraswat

Foraminifers (unicellular, almost exclusively marine protists), have been used extensively for paleoclimatic reconstructions and are extremely helpful in providing the chronology based on their oxygen and carbon isotopic composition. Keeping the objective of reconstructing the past climatic variations and especially the dating of megaslides in view, a preliminary analysis of the coarse fraction was carried out onboard.

The longest Kastenlot core PS66/309-1 recovered during "Polarstern" Cruise ARK XX/3 was investigated in order to assess the coarse-fraction composition of different lithologies. This core was recovered from the north of Spitsbergen (see Figure 9.1 and annex for location details). Based on the differences in colour and also to get an overview of the complete core, 24 samples were processed for coarse fraction analysis as per prescribed procedures (freeze-drying followed by wet sieving over 63 μ m and 125 μ m sieves). A small representative fraction from the >125 μ m fraction was taken with the help of splitter, in order to count a minimum of 300 particles. A total of 15806 particles were counted. The particles were grouped into two categories, i.e., biogenic and abiogenic origin. The abiogenic fraction constituted the larger part of the majority of samples (Fig 9.29). In the abiogenic fraction, quartz grains with angular to subangular edges were most abundant. In few samples, considerable numbers of pyritized worm tubes were also found. The biogenic fraction mainly consists of planktic foraminiferal tests with few benthic foraminifers and rare sponge spiculae. As reported earlier the planktonic foraminiferal assemblage was dominated by *Neogloboquadrina pachyderma*, the polar bear of planktonic foraminifers. The planktonic foraminiferal assemblage is almost monospecific. The benthic foraminiferal component is represented by few agglutinated specimens along with considerably large specimens of *Pyrgo* and few specimens of *Cibicidoides*.

From the intervals where sufficient planktonic foraminifers were available, specimens of *N. pachyderma* were picked for AMS dating (five in number) as well as stable isotopic analysis (24 in number).

The correlation of the major constituents at different intervals with the colour of the sediments shows that some of the brown coloured sediments are devoid of biogenic components while some of the gray coloured intervals are high in biogenic components, mainly composed of planktonic foraminiferal tests. Out of the total of 24 samples analysed onboard, the maximum amount of biogenic components (approx. 92%), was reported in the very dark brown coloured silty clay sediments at 179 cm interval. One of the samples (249-252cm) taken from the sandy sediment layer that probably is the result of debris flow, is low in biogenic components. Further analysis of sandy sediments showed the presence of few shallow water benthic foraminifers, probably indicating the transport of sediments from the shelf to the deeper regions from where the core has been recovered. This needs to be confirmed by detailed species identification and subsequent grouping into foraminiferal assemblages.

This preliminary onboard analysis provides an overview of the composition (biogenic and abiogenic) of the different lithologies. For detailed reconstruction of the past climatic events, closer spaced sample analysis has to be carried out.

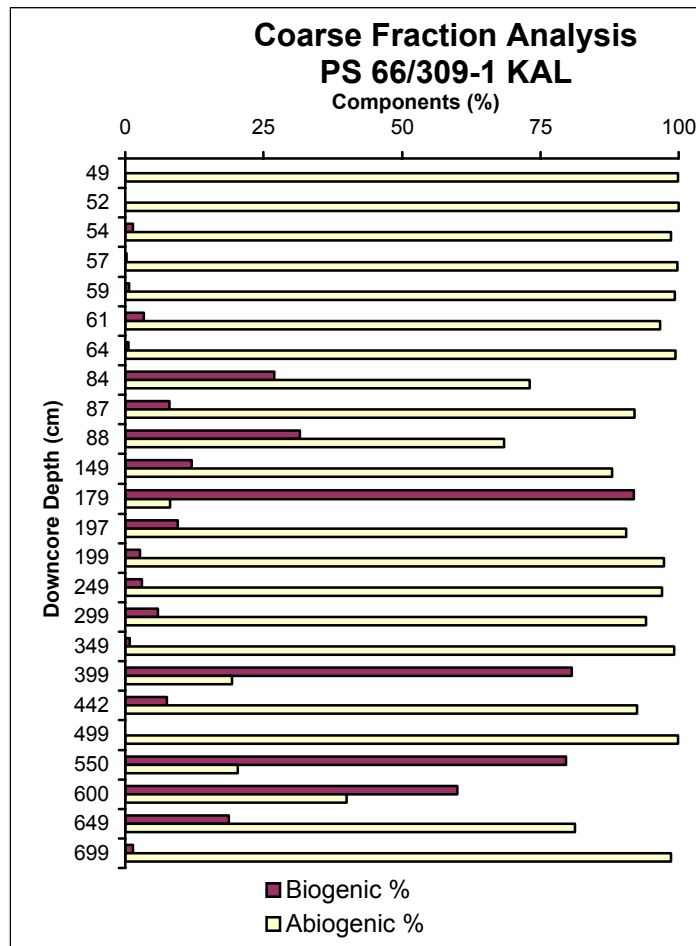


Fig 9.29: Down-core plot of abundance of biogenic and abiogenic components in 24 samples taken for preliminary onboard coarse fraction (>125 μ m) analysis. The figure shows the broad overview of the composition of different lithologies.

9.6.4 Main Lithologies and Preliminary Interpretation of ARK-XX/3 Sediment Cores

R. Stein

During the „Polarstern“ Cruise ARK-XX/3, sediment cores were taken at 26 stations in total (see Chapter 9.4 for details). In the following, the main lithologies of the recovered sediments are described and preliminary interpretations are given. The detailed lithological core descriptions are presented in Chapter 12.3 of the Annex.

Lithostratigraphy of sediment cores from the Svalbard continental margin and eastern slope of the Yermak Plateau

One of the main targets of the ARK-XX/3 geology program is the study of sediment dynamics of mega-slides along the Svalbard continental margin (as part of the ESF Program „EUROMARGINS“) (Fig. 9.30). In this context, the characterization of sediment facies within debris flow and turbidite sequences as well as undisturbed (hemi-) pelagic sequences, the dating of sediment mass flows, and estimates of sedimentary budgets are of interest. In order to sample sedimentary sequences within the mega-slide area as well as the adjacent undisturbed (hemi-) pelagic facies, detailed PARASOUND and Hydrosweep surveys have been carried out (see Chapters 7 and 9.2) to select optimum coring stations. At the southwestern flank of the mega-slide area, several couples of sediment cores representing slide-influenced facies and (hemi-) pelagic facies were taken (Fig. 9.31).

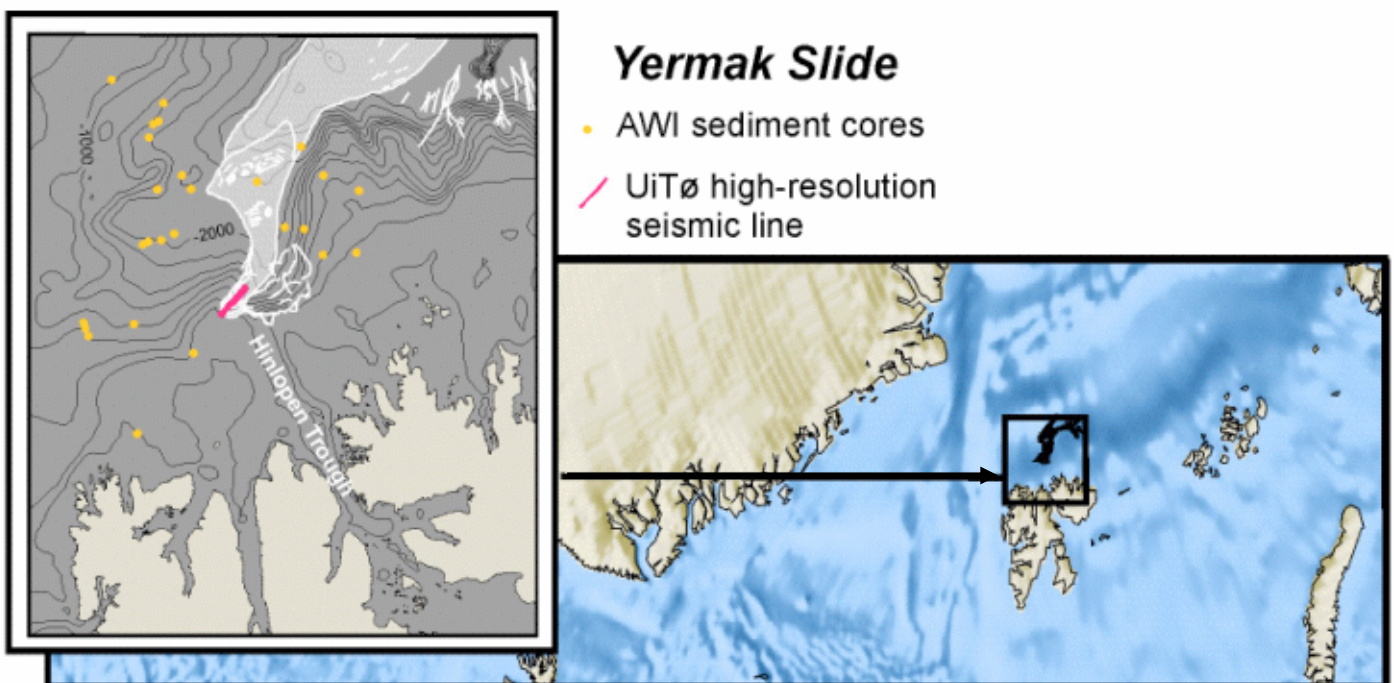


Fig. 9.30: Assumed extension of the mega-slide („Yermak Slide“) area north of Svalbard (light gray area in the left figure) (Figure taken from ESF-EUROMARGINS proposal on „Slope Stability on Europe’s Passive Continental Margins“, coordinated by J. Mienert, Tromsø University, Norway).

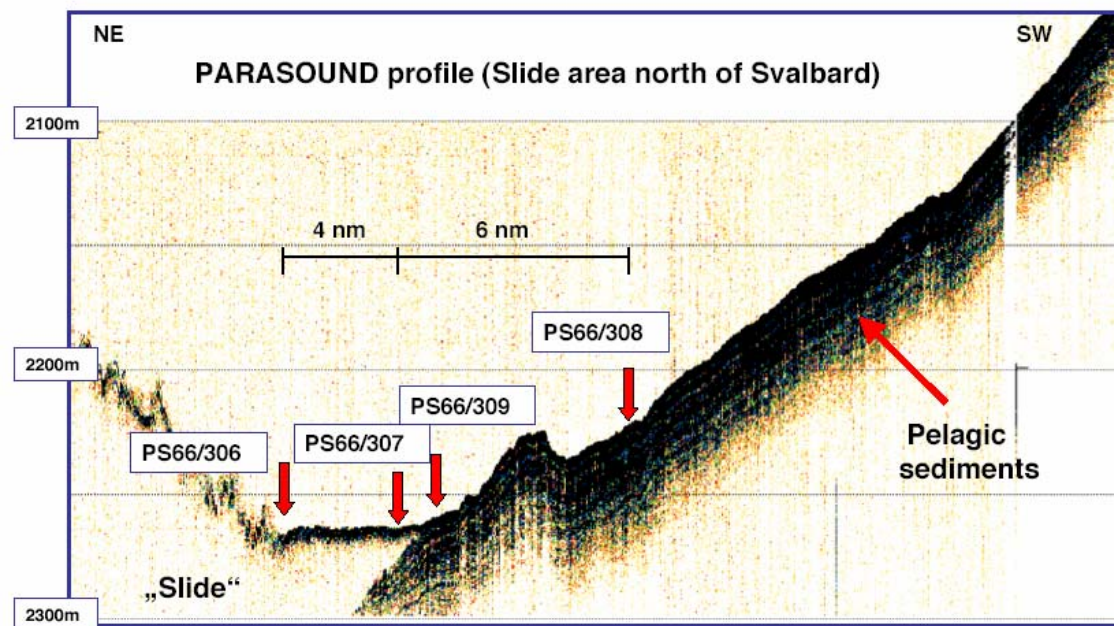


Fig. 9.31: PARASOUND profile and locations of cores PS66/306 to PS66/309 as an example for the sampling strategy. Cores PS66/306 and PS66/307 were taken inside the slide area, PS66/309 at the marginal part, and PS66/308 in the (hemi-) pelagic facies outside the slide area.

A key core within our research will be Kastenlot Core PS66/309-1 obtained close to the edge of the mega slide (Fig. 9.31). This core is composed of very different lithologies as shown in Figure 9.32 (for detailed lithological core description see Chapter 12.3, Annex). Based on sediment colour and texture, the sequence can be divided into nine units. Unit I (0 to 61 cm) is composed of brown and very dark brown silty clay with some layers of mud clasts. Underneath an about 20 cm thick interval of dark gray to very dark gray silty clay is obvious (Unit II). Unit III (89 – 138 cm) is an olive brown, partly bioturbated silty clay. Unit IV (138 – 204 cm) and Unit VI (272 – 299 cm) consist of olive gray silty clay. Between these two units, an interval characterized by dark gray sandy silty clay and sand alternation and fining-upwards sequences (Unit V). This turbidite unit has a sharp (erosional?) contact to the underlying Unit VI. Unit VII (299 – 510 cm) is mainly composed of dark grayish brown, partly bioturbated silty clay with occasional occurrence of very dark gray layers and dropstones. Unit VIII (510 – 641 cm) is characterized by alternation of olive/dark olive gray and dark gray/very dark gray (sandy) silty clay. The uppermost part of this unit is more coarse-grained, and at the bottom of this unit (636 – 641 cm) gray and dark olive brown beds occur. The lowermost unit (Unit IX; 641 – 765 cm) consists of dark gray to very dark gray silts clay.

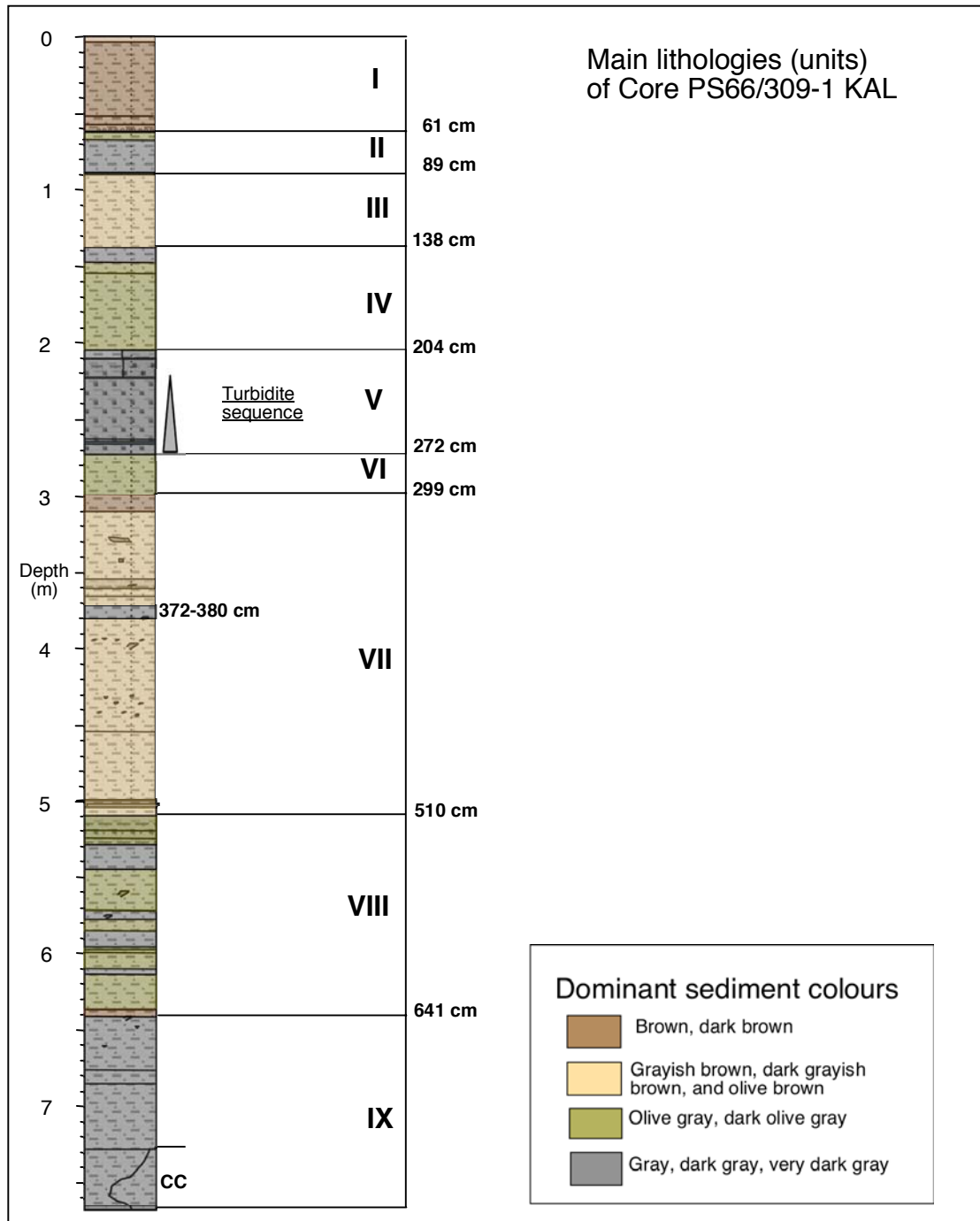


Fig. 9.32: Major lithologies of Kastenlot Core PS66/309-1

The distinct changes in sediment colour (and grain size) in the record of Core PS66/309-1 may represent glacial/interglacial variability (with the dark gray/dark olive gray intervals such as the lower part of the sedimentary sequence probably representing glacial and the brownish intervals probably representing interglacial intervals; e.g., Jakobsson et al. 2000). The turbidite sequence (Unit V) is related to the mega-slide event. The turbidites occur in reduced thickness also in the more distal Core PS66/308 (Fig. 9.33). If a precise dating of the sedi-

ments under- and overlying the turbidite unit can be done, this gives the unique possibility to reconstruct the history of the mega-slide event at the northern Svalbard continental margin.

Similar lithologies as described for Core PS66/309-1 were also recorded in the other (pelagic) cores obtained in the study area during this cruise. Based on the lithological core description, a correlation between these cores is possible (Fig. 9.33). In general, this correlation is also supported by the wet bulk density and magnetic susceptibility records (see Chapter 9.3.1, Figs. 9.11 and 9.12).

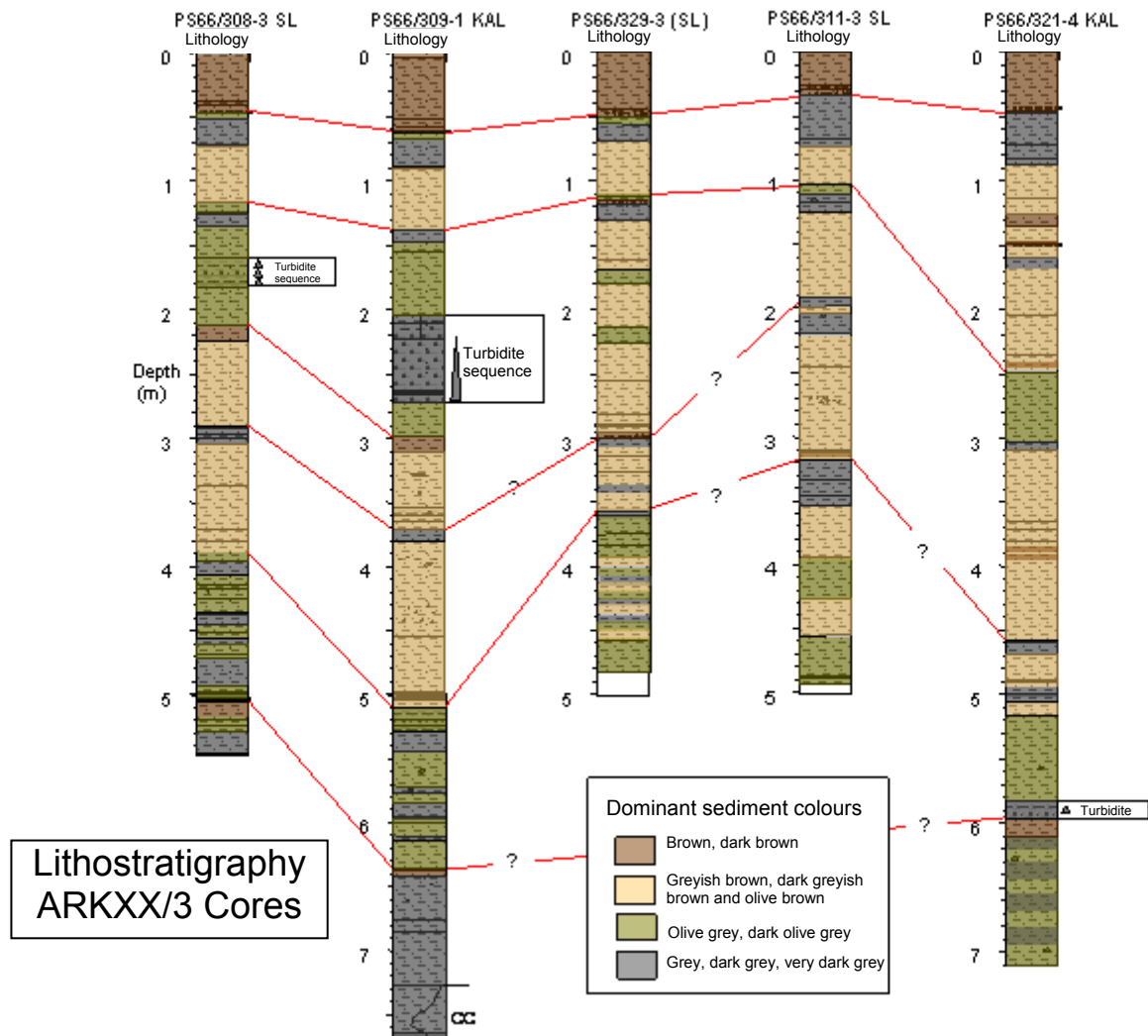


Fig. 9.33: Major lithologies of cores PS66/308-3, PS66/309-1, PS66/311-3, PS66/321, and PS66/329 (For core locations see Figure 9.1).

The lithology of Core PS66/325-3 taken from the continental slope north of North East Land at a water depth of 895 m, differs from those described above. Except the uppermost dark brown-coloured silty clay, very dark gray and dark olive gray silty clay and sandy silty clay are the dominant type of sediment (Fig.

9.34; for details see Annex 12.3). The sedimentary sequence can be divided into six main lithological units. Unit I (0 to 10 cm) is composed of very dark brown silty clay with mud clasts in the lower part. Units II (10 – 230 cm), IV (274 – 516 cm) and VI (545 – 648 cm) consist of very dark gray to olive gray silty clay. In between these units, two more coarse-grained (sandy silty clay) units are intercalated: Unit III (230 – 274 cm) and Unit V (516 – 545 cm). The upper part of Unit V (516 – 524 cm) is a diamicton-type sediment. These two more coarse-grained units probably represent glacial stages. Furthermore intervals with significant amount of ice-rafted debris (IRD), especially in Units III and V, are obvious (Fig. 9.34). These pulses of maximum IRD input may be related to advances of the near-by Svalbard-Northern Barents Sea Icesheet, as described for Marine Isotope Stages (MIS) 6, 5d, 4, and 2 (e.g., Mangerud et al. 1996).

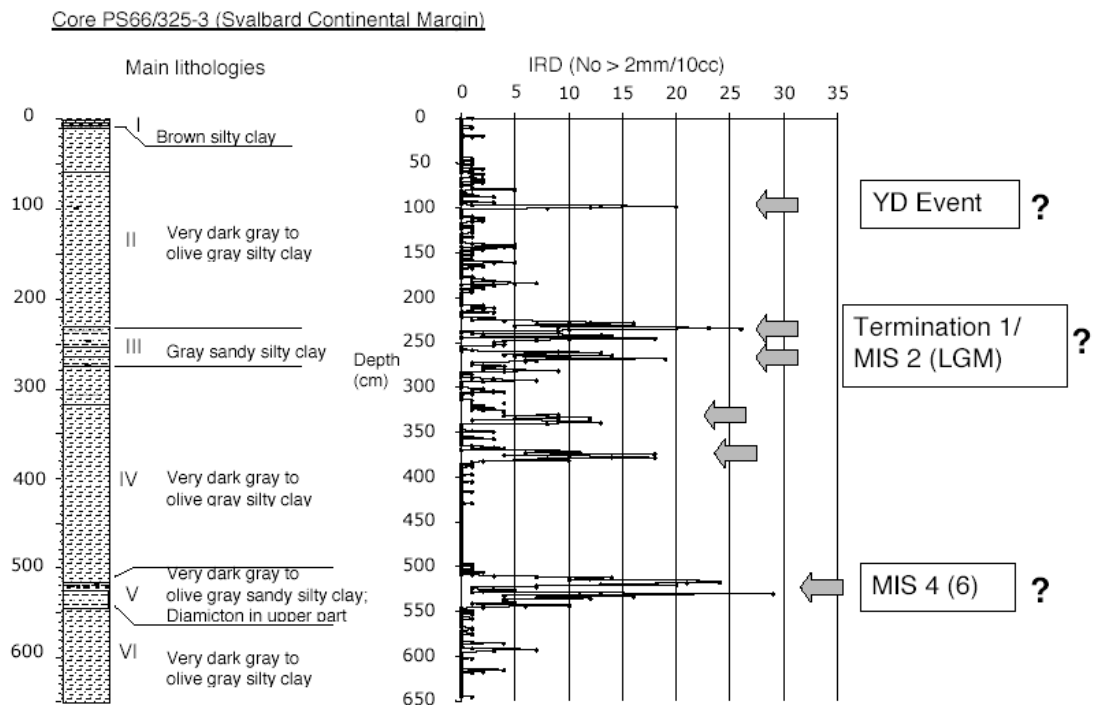


Fig. 9.34: Major lithologies (Units I to VI) and amount of ice-rafted debris (IRD) of Core PS66/325-3. Arrows indicate maxima in IRD input, probably related to fluctuations (advances) of the Svalbard-Northern Barents Sea Icesheet during glacial stages.

Future sedimentological, micropaleontological, and geochemical studies and, especially, the dating of the sediment cores are needed for more detailed interpretation in terms of paleoenvironmental history.

Sediments and rocks from the top of the central Yermak Plateau: Implications for basement origin?

As outlined in Chapter 8, it is assumed that the northeastern Yermak Plateau is oceanic in origin, while its southern part might consist of stretched continental crust. Thus, on top of the central Yermak Plateau where old strata (basement?) probably terminate close to the seafloor, the sediment dredge as well as the giant box corer and the gravity corer was used for sampling at several stations (Fig. 9.35). The sampling stations were selected based on detailed PARASOUND and Hydrosweep profiling. For this purpose, steep slopes and peak elevations with lacking young soft sediments on top were of interest (Fig. 9.36).

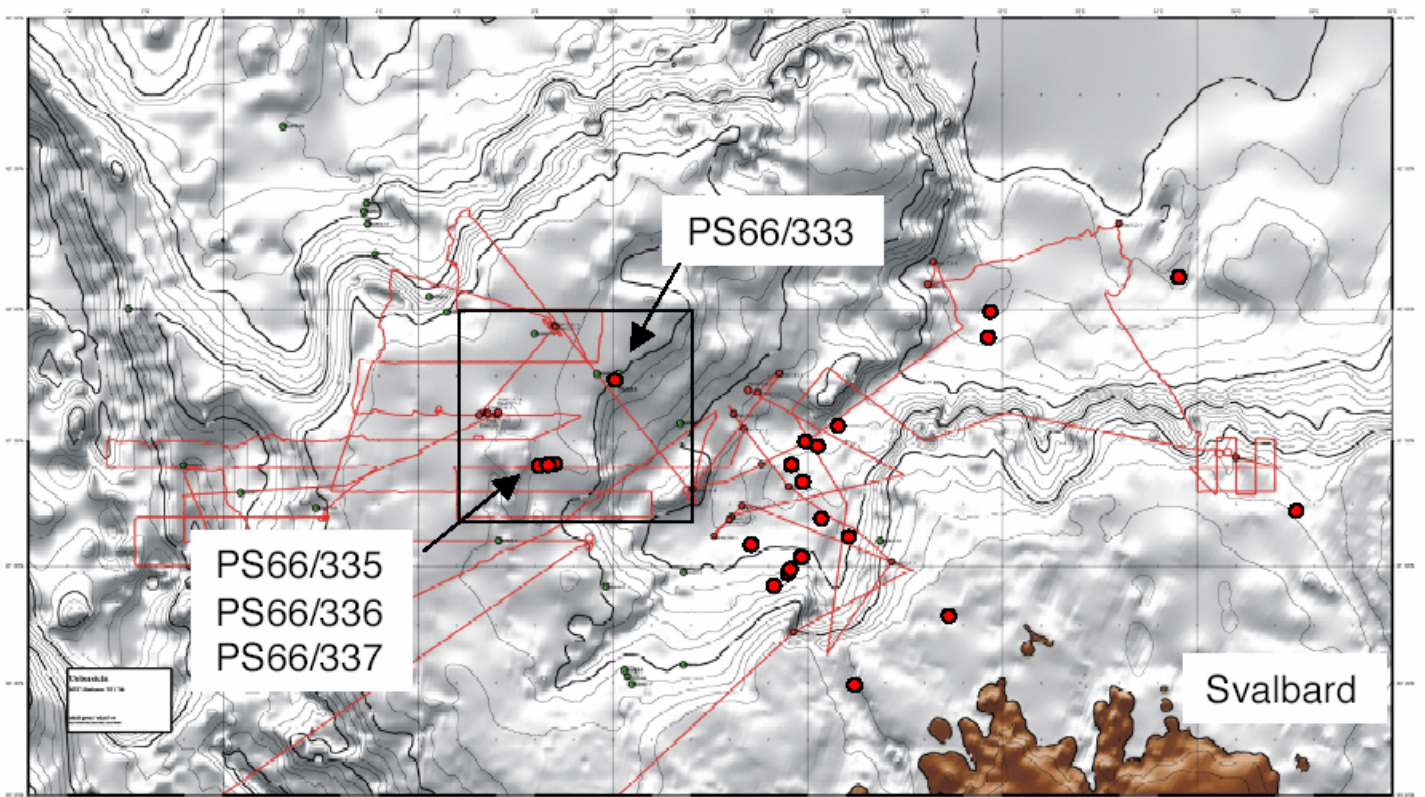


Fig. 9.35: Stations of „basement sampling“ on top of the central Yermak Plateau

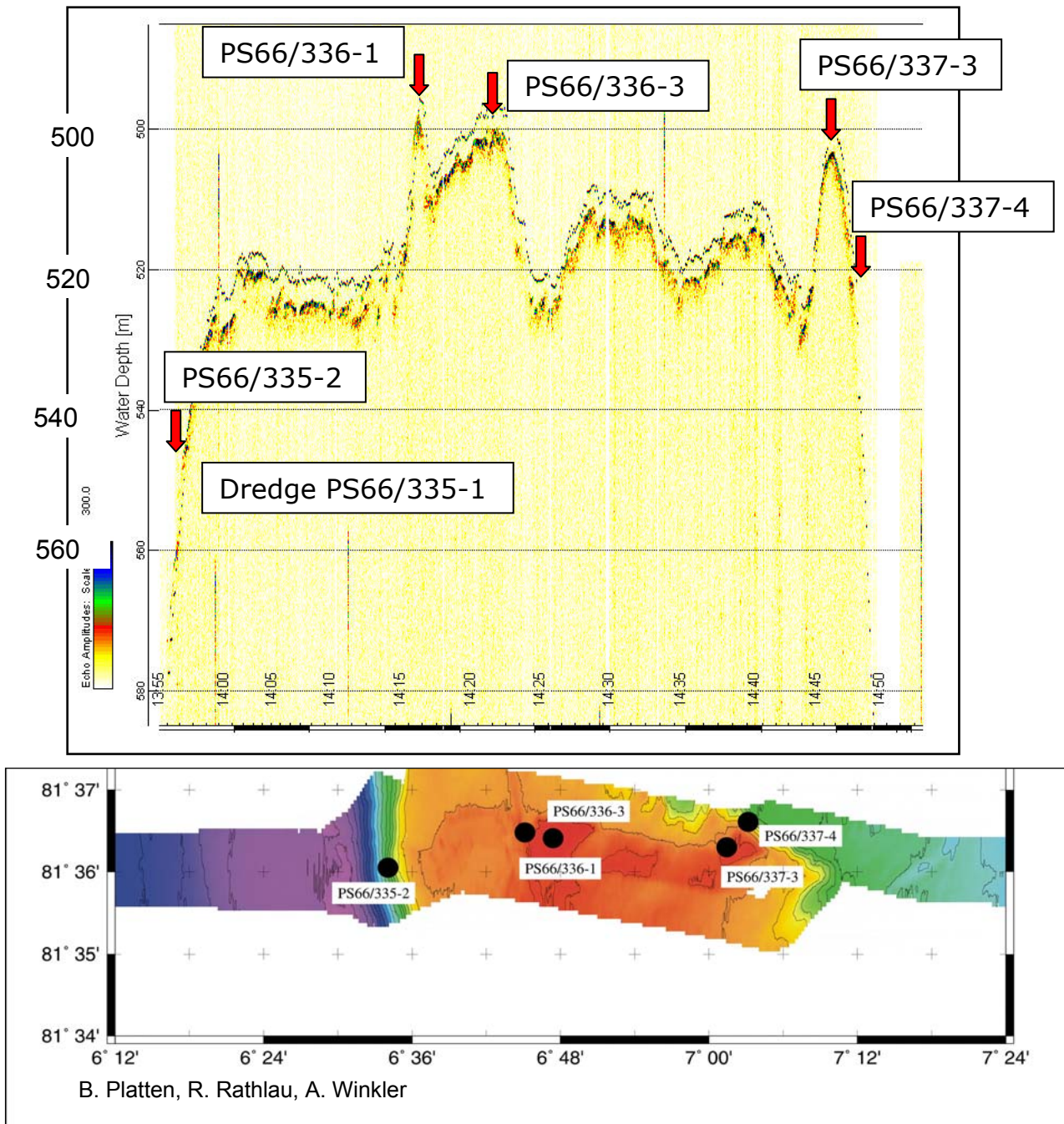


Fig. 9.36: PARASOUND and Hydrosweep profiles across the central part of the Yermak Plateau with sampling stations.

At the western steep slope (location PS66/335), huge amounts of stones have been dredged (Fig. 9.37; for exact dredge location see Table 9.3). The majority of stones is black-coloured/-coated. After cutting, however, a large number of stones were identified as red sandstones. At the same location, also a gravity core (PS66/335-2) was taken. In this core, only 32 cm of sediments were recovered. Part of the recovered sequence is composed of – for this area – non-typical red-coloured sediments (Fig. 9.38).



Fig. 9.37: Dredged rocks at Station PS66/335, central Yermak Plateau

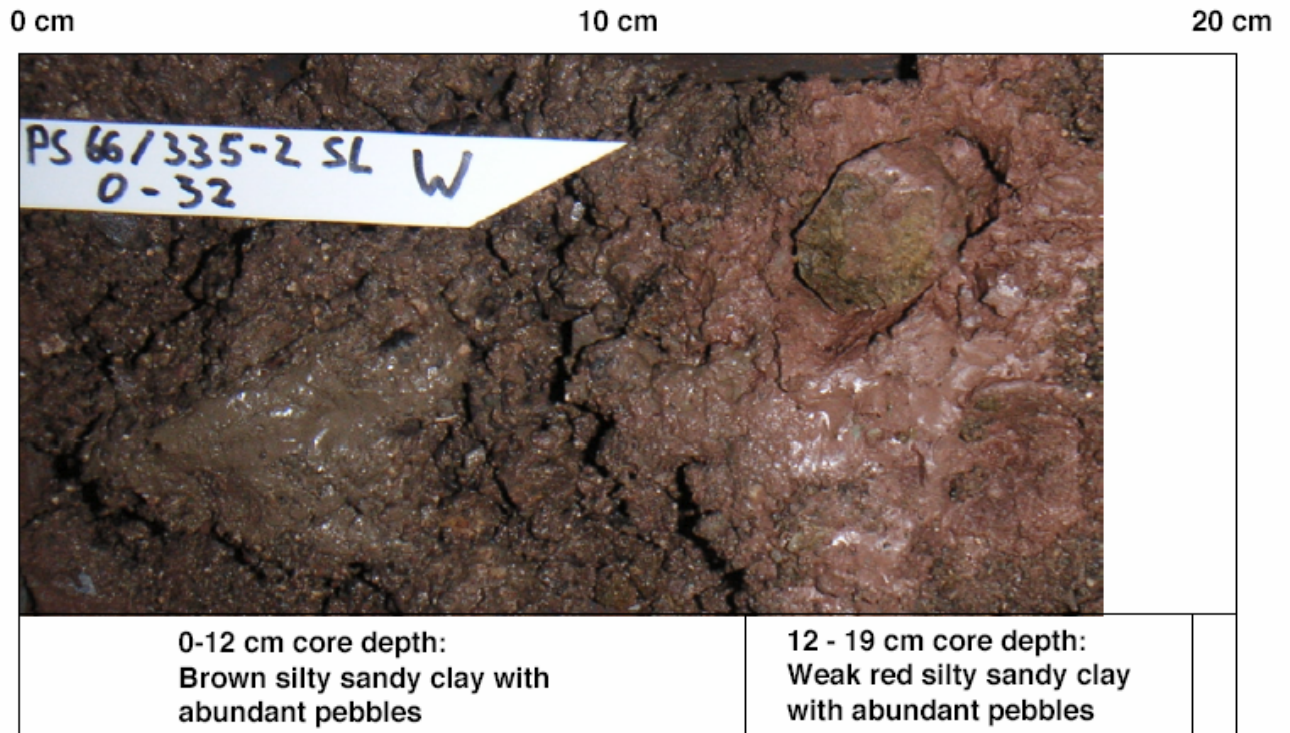


Fig. 9.38: Sediments recovered in gravity core PS66/335-2, central part of the Yermak Plateau

At sites PS66/337-3 and PS66/337-4 located in the eastern part of the profile (Fig. 9.36), no penetration with the gravity corer was possible. At Site PS66-337-3 the core catcher of the gravity corer even became damaged when hitting the hard “basement” rocks at the seafloor. In the core catcher of both cores, mainly black (basalt-like looking crystalline) stones or fragments of them were recovered.

Based on these very preliminary results and still speculative interpretation, the basement may have a continental origin (Devonian Old-Red sandstones?) at the western slope of the profile whereas in the eastern part basaltic material may be cropping out, indicating an oceanic origin. Of course, more detailed work on the petrology of the dredged material should be performed before a more precise interpretation about the basement origin of the Yermak Plateau in this area can be done.

Sediments from the East Greenland continental shelf: Pre-Quaternary basement and Quaternary paleoenvironment

As part of the IODP site survey, seismic profiling was carried out on the east Greenland shelf during this expedition (see Chapter 8). In this area, seismic data reveal the presence of a prominent salt province and suggest that Mesozoic sediment are cropping out at the surface (Schmitz and Jokat, 2005). In order to sample these old strata, 10 gravity cores (using the short 3m core barrel) were taken. The location of the cores was selected based on PARASOUND profiling (Fig. 9.39). Based on comparison with the seismic profile, faulted old sediment strata and a salt diapir can also be assumed in the PARASOUND profile.

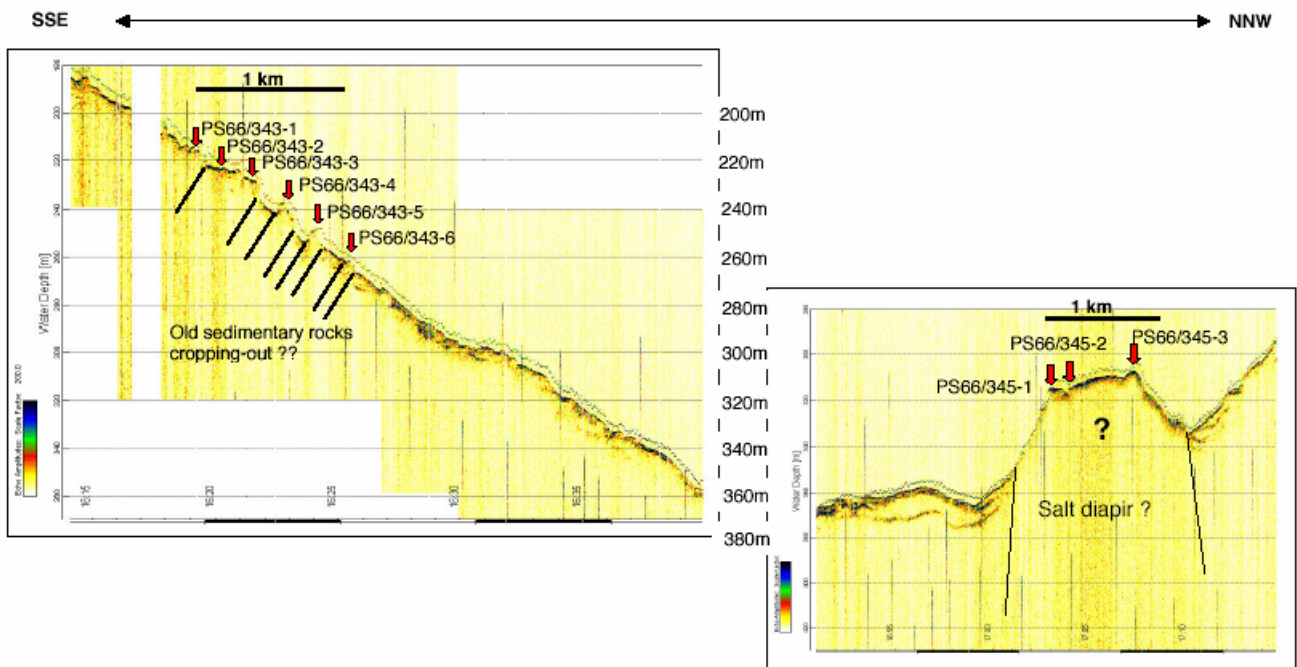


Fig. 9.39: PARASOUND profile and core locations, East Greenland Shelf (for location of area see Fig. 9.1).

In the southern part of the profile (PS66/343-1 to PS66/343-6), where pre-Quaternary (Mesozoic?) sediments should be sampled, unfortunately only soft (young) sediments were recovered (Fig. 9.40). Some of the gravity corers even over-penetrated into the seafloor. At Site PS66/345 located on top of the assumed salt diapir structure (Fig. 9.39), however, coring of old strata was successful. At Station PS66/345-2, a 1.5 m long gravity core was recovered (Fig. 9.41). In the lowermost part of the sequence (core catcher), small light gray „crystals“ and one large white-orange „crystal“ of about 4 cm in diameter were found (Fig. 9.42-A). X-Ray analysis of the large „crystal“ indicates that it is pure gypsum (Fig. 9.42-B). This may suggest that the gravity corer may have hit the (Permian?) salt diapir surface (or came at least very close to it). This important finding may support the interpretation of the seismic data of Schmitz and Jokat (2005).

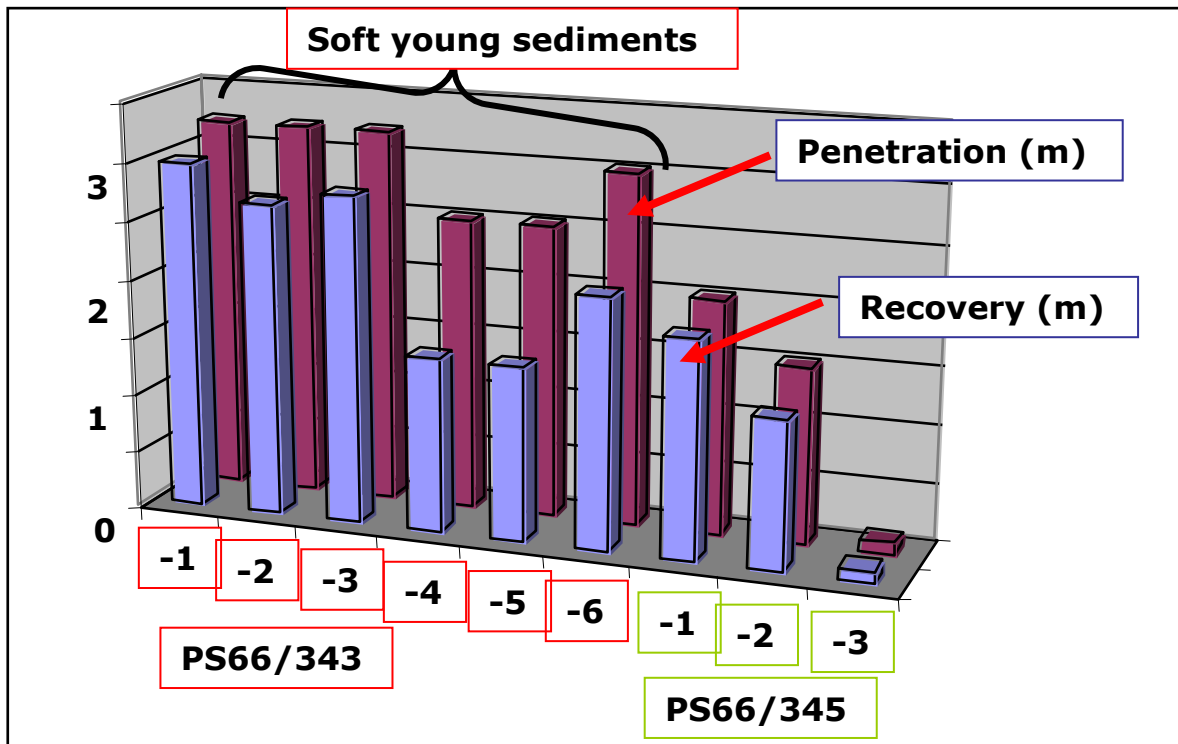


Fig. 9.40: Corer penetration and core recovery of gravity cores from the East Greenland Shelf.

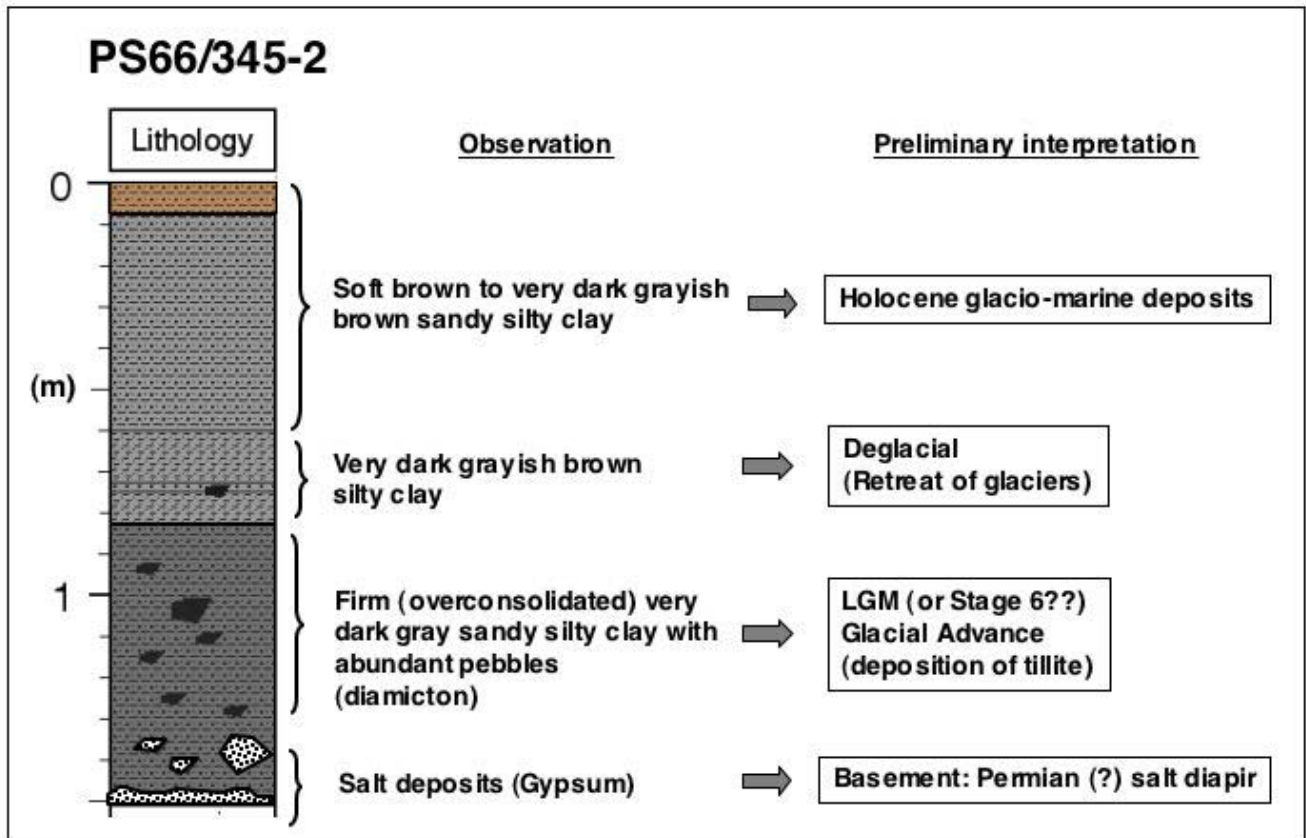


Fig. 9.41: Lithology and preliminary interpretation (Core PS66/345-2, East Greenland Shelf)

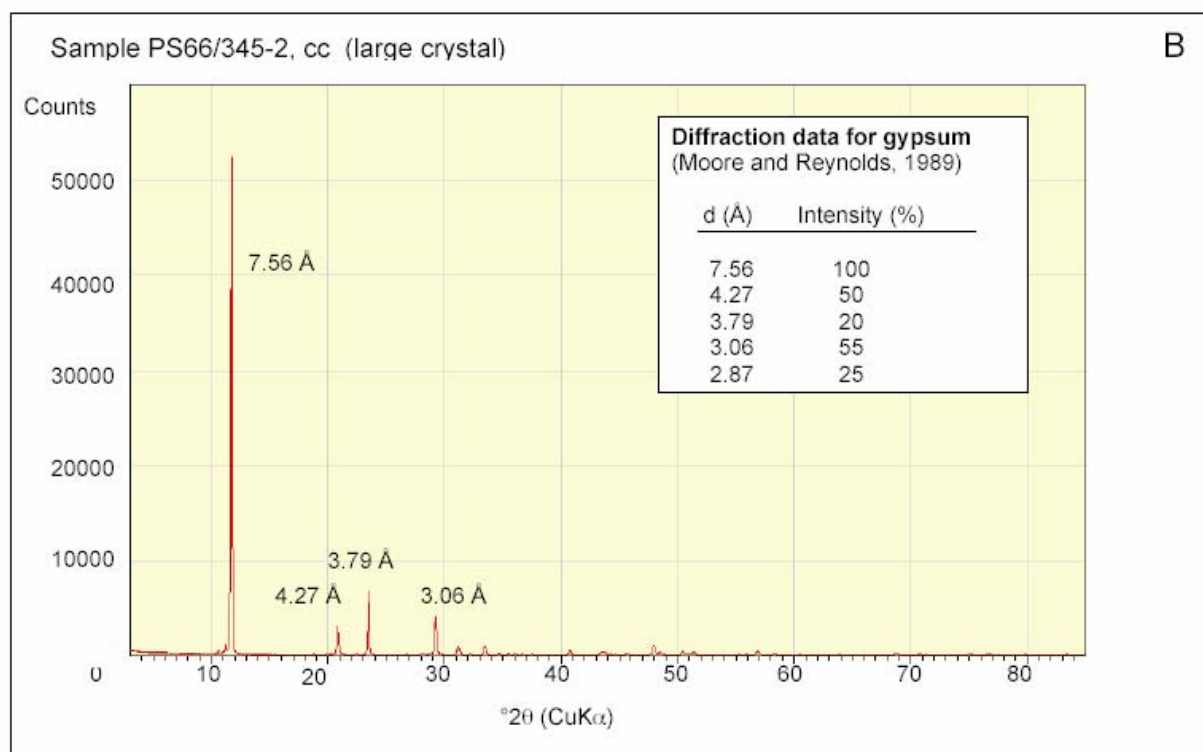
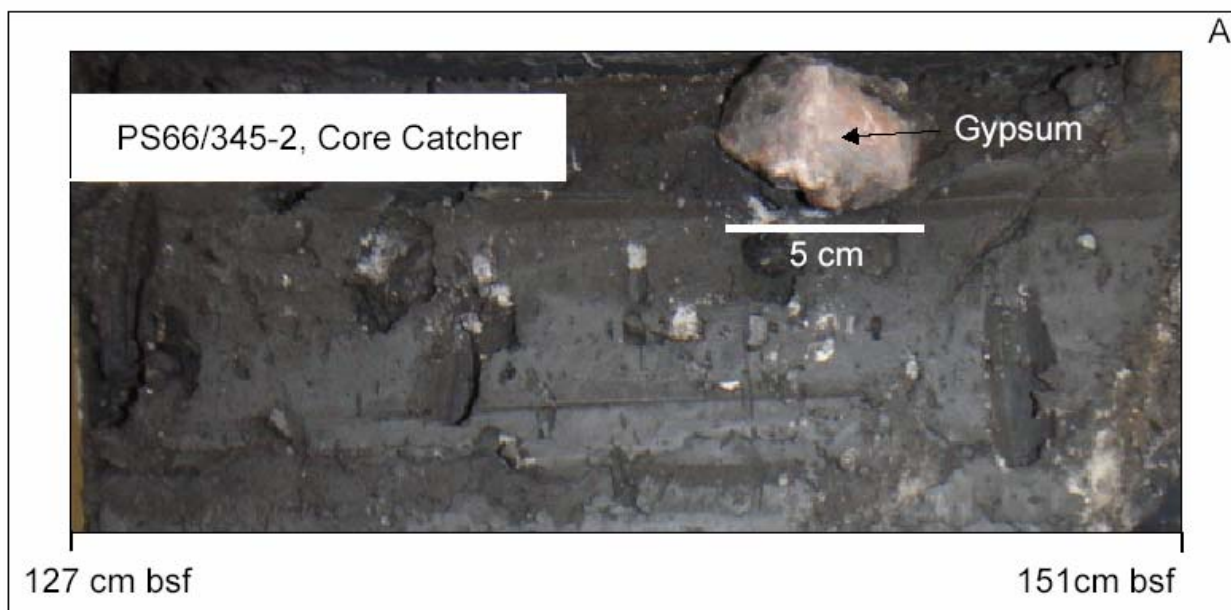


Fig. 9.42: (A) Photograph of core catcher sediments recovered in gravity core PS66/345-2 (East Greenland shelf). Common small white rock fragments („crystals“) and one large „crystal“ of about 4 cm in diameter are obvious. (B) X-Ray diffractogram of the large crystal found in the core catcher, identified as gypsum (X-Ray analysis has been performed by Chr. Vogt, Bremen University).

The main part of the sedimentary record of Core PS345-2 that is certainly of Quaternary age can be divided into three main units (Fig. 9.41).

- Unit I (0 - 60 cm): soft brown to very dark grayish brown sandy silty clay
- Unit II (60 - 83 cm): very dark grayish brown silty clay
- Unit III (83 – base): firm (overconsolidated) very dark gray sandy clay with abundant pebbles (diamicton)

From correlation with similar sequences from the East Greenland continental margin (e.g., Stein et al., 1993; Hubberten et al., 1995; Funder et al., 1999), these lithologies can be interpreted in terms of East Greenland glacial history. The sediments of Unit III (a tillite) probably represent the Last Glacial Maximum (LGM) glacial advance. The site was overridden by glaciers as shown by overconsolidation. Overconsolidated sediments are also reflected in the shear-strength record (see Chapter 9.3.3, Fig. 9.15). The deglacial retreat of glaciers is documented in the sediments of Unit II. The uppermost Unit may represent the glacial-marine post-glacial (Holocene) time interval. Finally, it has to be mentioned that it cannot be excluded at this stage, that the diamicton of Unit III may be related to older (Marine Isotope Stage 6?) glaciations. AMS¹⁴C datings are needed to give a more precise interpretation of the sedimentary record of Core PS66/345.

10. The Lost Deutsche Arktische Expedition 1912: A Pilot Study in the North East Land of Spitsbergen

N.Fricke, I.Mende

In 1912, the world's attention focussed around events in the Antarctic: Scott and Amundsen's race to the South Pole. Almost simultaneously similar heroic, pathetic and tragic events unfolded on Spitsbergen – the lost Deutsche Arktische Expedition (DAE) 1912, also known as Schroeder Stranz expedition: a trial expedition to the North East Land of Spitsbergen (Fig. 10.1) thought to be a forerunner of the ambitious plan to cross the North East passage. The ill-prepared expedition ended in chaos and disintegration. Of the 10 German members, 7 including lieutenant Schroeder Stranz, died. It became Germany's most tragic polar expedition.

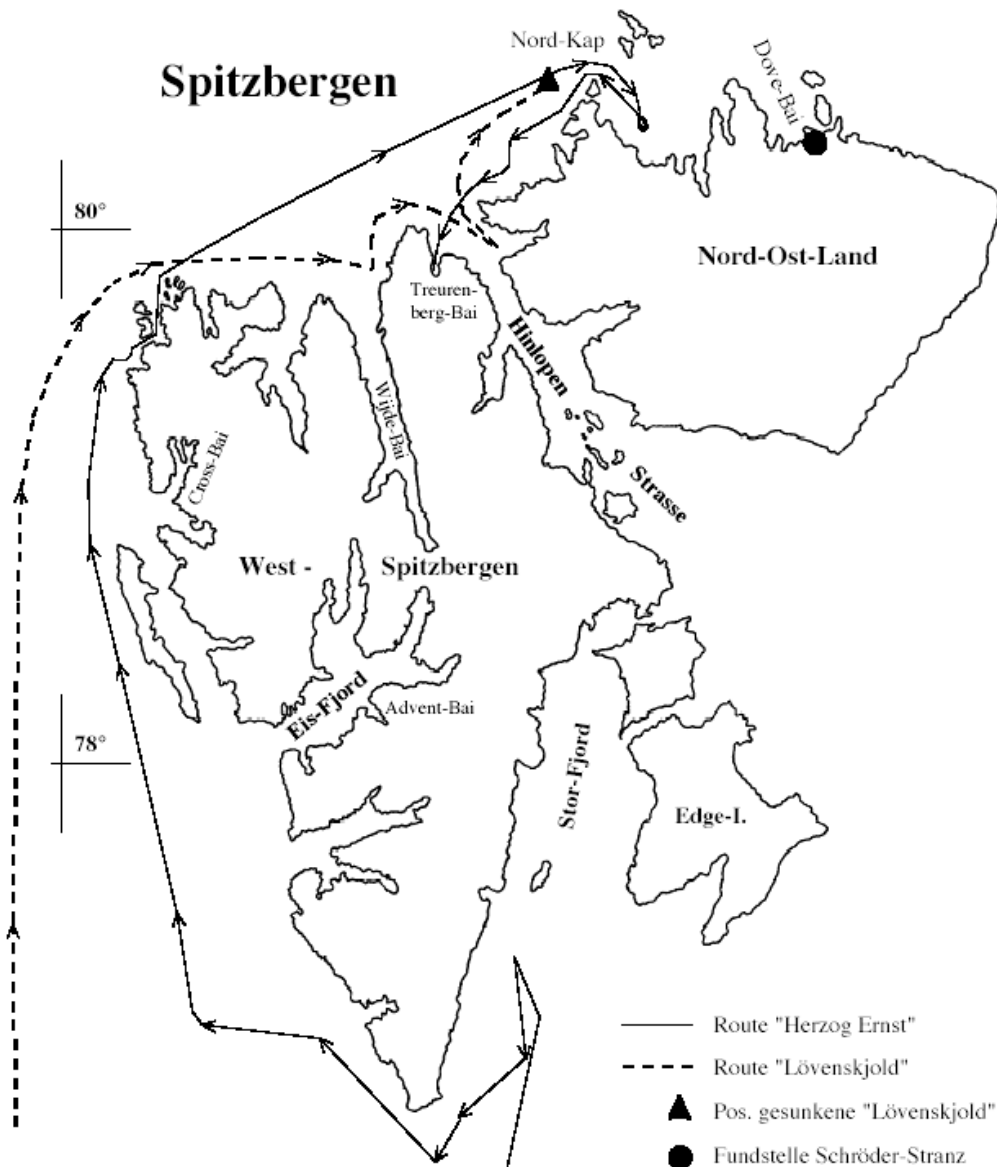


Fig. 10.1: Locations and tracks of lost „Deutsche Arktis Expedition 1912 (DAE)“

One of the objectives of the present pilot study during the “Polarstern” Cruise ARK-XX/3 was to get preliminary information and to confirm some of the positions of the Schroeder Stranz Expedition of 1912 and the Lerner Expedition of 1913, as available in the literature.

Our first search point was Cape Rubin situated at the western side of the North Cape of North East Land (Fig. 10.1). We were interested in this place, since in 1913 the German expedition lead by Theodor Lerner and organized to search the lost German Artic expedition, the “Schroeder Stranz Expedition” of 1912, started from the North East Land of Svalbard. The participants of Lerner’s expedition built a base at Cape Rubin and spent two month in this camp and searched around 600 km of coastline, unfortunately without any success.

The expedition vessel “Loevenskiold“ of Lerner got entrapped in the pack ice and sunk off the Beverlysund near the North Cape. This wreck is the most northern wreck of the world. It is important to know the precise position of the place, where the ship sank. The information available about the Lerner’s expedition included the latitude and the water depth of the place of accident from the ships’ logbook as well as from historical pictures shot by the participants of the Lerner expedition. The pictures shot from the land, show the “Loevenskiold” in the ice, whereas in other pictures taken from the ship, the camp with rock formations in the background is shown. These pictures helped in locating the place of accident.

On September 03, when “Polarstern” was near to the first search point, we flew to North Cape/Cape Rubin (Fig. 10.1). Supported by a helicopter and the pictures we had, we could locate the place of the camp. We found some remains of the camp, which included old clothes, wooden snow-shoes (Fig. 10.2a), shekels (Fig. 10.2b) and cartridge cases (Fig. 10.2c). Though taking a bearing is not an appropriate way to find this wrack, the coordinates we got from the present pilot study will definitely help to find the shipwreck later with the submarine “Jago” and other appropriate techniques.

a)



b)



c)



Fig. 10.2: Remains of the camp at Cape Rubin
(a) wooden snow-shoes, (b) shekels, and (c) cartridge cases

Our second search location was the assumed position where remains of the Schroeder Stranz Expedition were reported in 1937. The fisherman Amandus Wilhelmsen found equipment of the 1912 expedition in the Duvefjord (Dove Bay) area (Fig. 10.1). He gave coordinates as well as the description of the place. But the coordinates and the description of the place as given by Amandus Wilhelmsen do not fit together. In the planning of our project we selected three possible locations that we wanted to confirm.

In search for this place, first we flew to the Schroeder Stranz Eldet (Fig. 10.3) on September 14. Fortunately, this seems to be a place which is concurrent with the description of Wilhelmsen. But, unfortunately, we could not find any fur-

ther remains of the expedition because of bad weather. Fresh snow covered the ground, and continuous heavy snowfall made a long stay with a substantial search almost impossible. We shot some films and photographs at this place. One hour later we flew to the two other possible locations. From the helicopter we observed that these two places did not at all fit to the description of the place where Amandus Wilhelmsen found the remains.



Fig. 10.3: Schroeder Stranz Eldet, Duvefjord area, North East Land

Our next point of interest was from where Wilhelm Dege, a soldier of the secret German weather station “Haudegen”, made an interesting discovery in 1945, few dishes that were later on recognised by Prof. Dr. Hans Fricke (MPI Seewiesen) as the remains of Schroeder Stranz Expedition. The place of recovery of these remains is known. Unfortunately, we could stay there only for five minutes because of the bad weather conditions. After taking some pictures and making video sequences we had to leave.

In summary, the major goals of this pilot study were reached. We could (1) precisely document the place of recovery of the remains from the Lerner expedition of 1913, (2) ascertain the coordinates where the “Loevenskiold” sunk, (3) locate the place where Amandus Wilhelmsen found remains of the Schroeder Stranz Expedition and (4) collect video clippings and photographs of the region around Cape Rubin and Dove-Bay. The results will help in the more exact planning of the multidisciplinary submersible expedition of the shallow shelf and fjords of North Spitsbergen in 2006.

11. References

- ATLAS Hydrographic, 2004a. ATLAS PARASOUND DS-2 Control Unit GE 6030, Service Manual 1.0 (May 2004). ATLAS HYDROGRAPHIC, Bremen, Germany
- ATLAS Hydrographic, 2004b. ATLAS HYDROMAP CONTROL User Manual 1.8 (May 2004). ATLAS HYDROGRAPHIC, Bremen, Germany
- ATLAS Hydrographic, 2004c. ATLAS PARASTORE-3 User Manual (July 2004). ATLAS HYDROGRAPHIC, Bremen, Germany
- Bareiss, J. and Haas, C., 2002. Spectral albedo and areal coverage of various surface types. *Berichte zur Polar- und Meeresforschung*, 421: 70–75.
- Barnes, P.W., Kempema, E.M., and Reimnitz, E., 1988. Source, characteristics and significance of sediment pellets formed on the sea ice of the Arctic Basin. *EOS Trans. Amer. Geophys. Union*, 69: 1263.
- Barnes, P.W., Kempema, E.M., and Reimnitz, E., 1988. Source, characteristics and significance of sediment pellets formed on the sea ice of the Arctic Basin. *EOS Trans. Amer. Geophys. Union*, 69: 1263.
- Berner, H. and Wefer, G., 1990. Physiographic and biologic factors controlling surface sediment distribution in the Fram Strait. In: *Arctic and Antarctic comparisons. Geological History of the Polar Oceans: Arctic versus Antarctic*. Bleil U. and Thiede J. (Eds.). Kluwer Academic Publishers: 317–335.
- Best, A. I. and Gunn, D.E., 1999. Calibration of marine sediment core loggers for quantitative acoustic impedance studies. *Marine Geology*, 160, 137–146
- Budeus, G., 2005. The Expedition ARK-XX/1 of "Polarstern" in 2004. Reports on Polar and Marine Research, in prep.
- Dethleff, D., 1997. Sea-ice sediments. *Berichte zur Polarforschung*, 255: 90–96.
- Dethleff, D., Rachold, V., Tintelnot, M., and Antonow, M., 2000. Sea-ice transport of riverine particles from the Laptev Sea to Fram Strait based on clay mineral studies. *International Journal of Earth Sciences*, 89: 496–502.
- Dittmers, K. and Schoster, F., 2003. Acoustic facies in the southern Kara Sea: new results by PARASOUND echosounding. In: Schoster, F., Levitan, M. (eds.) *Scientific Cruise Report of the joint Russian-German Kara Sea Expedition in 2002 with RV "Akademik Boris Petrov"*, Reports on Polar and Marine Research, 450, 109pp
- Eicken H., 2003. The role of Arctic sea ice in transporting and cycling terrigenous organic matter. In Stein, R., Macdonald, R.W. (Eds). *The Organic Carbon Cycle in the Arctic Ocean*. Springer, Berlin: 45–53.
- Eicken, H., Reimnitz, E., Alexandrov, V., Martin, T., Kassens, H., and Viehoff, T., 1997. Sea-ice processes in the Laptev Sea and their importance for sediment export. *Cont. Shelf Res.*, 17: 205–233.
- Elverhøi, A., Pfirman, S., Solheim, A., and Larsen, B.B., 1989. Glaciomarine sedimentation in epicontinental seas exemplified by the northern Barents Sea. *Marine Geology*, 85: 225–250.

- Funder, S., Hjort, C., Landvik, J.Y., Nam, S., Reeh, N., and Stein, R., 1998. History of a Stable Ice Sheet Margin - East Greenland During the Middle and Upper Pleistocene. In: Elverhoi, A. et al. (Eds.), *Glacial and Oceanic History of the Polar North Atlantic Margins*. Quaternary Science Review, 17: 77-124.
- GEOTEK, 2000. Multi-Sensor Core Logger. <http://www.geotek.co.uk/>
- Grobe, H., A simple method for the determination of ice rafted debris in sediment cores, *Polarforschung* 57(3), 123-126.
- Haas, C. and Lieser, J.L. (compilers), 2003. Sea ice conditions in the Transpolar Drift in August/September 2001. Observations during POLARSTERN cruise ARKTIS XVII/2. *Berichte zur Polar- und Meeresforschung*, 441: 123 pp.
- Hansbo, S., 1957, A New Approach to the Determination of the Shear Strength of Clay by the Fall-Cone Test. Sw. Geot. Inst. Pub. No. 14, Stockholm.
- Hibler, W.D., III, 1989. Arctic ice-ocean dynamics. In: Herman, Y. (Ed.), *The Arctic Seas: Climatology, Oceanography, Geology, and Biology*. Van Nostrand Reinhold Company, New York: 47–91.
- Hubberten, H.-W., Grobe, H., Jokat, W., Melles, M., Niessen, F., and Stein, R., 1995. Glacial History of East Greenland Explored. *EOS*, Vol. 76, p. 353-356.
- Jokat, W., 2000. The Expedition ARKTIS-XV/2 of "Polarstern" in 1999, Reports on Polar Research, Alfred Wegener Institut for Polar and Marine Research, Bremerhaven, 368, 128pp.
- Jakobsson, M., Løvlie, R., Al-Hanbali, H., Arnold, E., Backman, J., and Mörth, M., 2000. Manganese/ color cycles in Arctic Ocean sediments constrain Pleistocene chronology. *Geology* 28: 23-26.
- Lindemann, F., 1998. Sedimente im arktischen Meereis – Eintrag, Charakterisierung und Quantifizierung. *Berichte zur Polarforschung*, 283: 124 pp.
- Lisitzin, A.P., 2002. *Sea-ice and Iceberg Sedimentation in the Ocean: Recent and Past*. Berlin, Heidelberg: Springer-Verlag, 563 pp.
- Lisitzin, A.P., Shevchenko, V.P. and Burenkov, V.I., 2000. Hydrooptics and suspended matter of Arctic seas. *Atmosph. Oceanic Optics*, 13: 61–71.
- Mangerud, J., E. Jansen, and J.Y. Landvik, 1996. Late Cenozoic history of the Scandinavian and Barents Sea ice sheets. In: Solheim, A., F. Riis, A. Elverhøi, J.J. Faleide, L.N. Jensen and S. Cloetingh (Eds.): *Impact of Glaciations on Basin Evolution: Data and Models from the Norwegian Margins and Adjacent Basins*. *Global and Planetary Change*, Special Issue, 12: pp. 11-26
- Meese, D.A., Reimnitz, E., Tucker, W.B., Gow, A.J., Bischof, J., and Darby, D., 1997. Evidence for radionuclide transport by sea ice. *The Science of the Total Environment*, 202: 267–278.
- Moore, D.M. and Reynolds, R.C., 1989. *X-Ray diffraction and the identification and analysis of clay minerals*. Oxford University Press, Oxford, 332 pp.
- Mullen, R.E., Darby, D.A. and Clark, D.L., 1972. Significance of atmospheric dust and ice rafting for Arctic Ocean sediment. *Geol. Soc. America Bull.*, 83: 205–212.
- Nürnberg, D., Wollenburg, I., Dethleff, D., Eicken, H., Kassens, H., Letzig, T., Reimnitz, E. and Thiede, J., 1994. Sediments in Arctic sea ice: Implica-

- tions for entrainment, transport and release. *Marine Geology*, 119: 185–214.
- Pfirman S.L., Eicken H., Bauch D. and Weeks W.F., 1995. The potential transport of pollutants by Arctic sea ice. *The Science of the Total Environment*, 159: 129–146.
- Pfirman, S., Gascard, J.-C., Wollenburg, I., and Mudie, P.J., 1989. Particle-laden Eurasian Arctic sea ice, observations from July and August 1987. *Polar Research*, 7: 59–66.
- Pfirman, S., Lange, M.A., Wollenburg, I. and Schlosser, P., 1990. Sea ice characteristics and the role of sediment inclusions in deep-sea deposition: Arctic and Antarctic comparisons. In: Bleil U. and Thiede J. (Eds.). *Geological History of the Polar Oceans: Arctic versus Antarctic*. Kluwer Academic Publishers: 187–211.
- Reimnitz, E., Kempena, E.W. and Barnes, P.W., 1987. Anchor ice, seabed freezing, and sediment dynamics in shallow arctic seas. *J. Geophys. Res.*, 92: 14671–14678.
- Schmitz, T. and Jokat, W., 2005. Evidence for a salt province beneath the North-East Greenland shelf north of 79°N, *Geology*, *subm.*
- Shevchenko, V., 2002. Secchi depth measurements. *Berichte zur Polar- und Meeresforschung*, 421: 89–90.
- Shevchenko, V., 2003. The influence of aerosols on the oceanic sedimentation and environmental conditions in the Arctic. *Berichte zur Polar- und Meeresforschung*, 464, 149 pp.
- Shevchenko, V.P., Lisitzin, A.P., Vinogradova, A.A., Smirnov, V.V., Serova, V.V. and Stein, R., 2000. Arctic aerosols. Results of ten-year investigations. *Atmos. Oceanic Optics*, 13: 510–533.
- Smith, W.O., Jr., 1987. Phytoplankton dynamics in marginal ice zones. *Oceanogr. Mar. Biol. Rev.*, 25: 11–38.
- Spiess, V., 1992. *Digitale Sedimentechographie - Neue Wege zu einer hochauflösenden Akustostratigraphie*. Berichte aus dem Fachbereich Geowissenschaften der Universität Bremen, Nr.35, 199pp.
- Stein, R. and Fahl, K., 1997. Scientific Cruise Report of the Arctic Expedition ARK-XIII/2 of RV "Polarstern" in 1997. Reports on Polar Research, Alfred Wegener Institut for Polar and Marine Research, Bremerhaven , 255, 235 pp.
- Stein, R., Grobe, H., Hubberten, H., Marienfeld, P., and Nam, S., 1993. Latest Pleistocene to Holocene changes in glaciomarine sedimentation in Scoresby Sund and along the adjacent East Greenland Continental Margin: Preliminary results. *Geo-Mar. Lett.*, Vol. 13, 9-16.
- Vogt, P. R., Crane, K., and Sundvor, E., 1994. Deep Pleistocene iceberg plowmarks on the Yermak Plateau; sidescan and 3.5 kHz evidence for thick calving ice fronts and a possible marine ice sheet in the Arctic Ocean, *Geology (Boulder)*, vol.22, no.5, pp.403-406
- Wollenburg, I., 1993. Sedimenttransport durch das arctische Meereis: die rezente lithogene und biogene Materialfracht. *Berichte zur Polarforschung*, 127. 159 pp.

Table 12.1: Station List

Station	Date	Time	Position Lat.	Position Long.	Depth [m]	Gear	Remarks
PS66/300-1	01.09.04	00:25	70° 31,46' N	19° 16,14' E	190,4	M	start- magnetic turncircels
PS66/300-1	01.09.04	01:07	70° 31,33' N	19° 16,33' E	187,2	M	end-magnetic turncircels
PS66/301-1	02.09.04	22:22	78° 50,25' N	2° 48,20' E	2496,0	PIES 71	
PS66/302-1	03.09.04	00:45	78° 49,87' N	5° 0,93' E	2707,0	PIES 141	
PS66/303-1	03.09.04	04:15	78° 50,03' N	8° 19,91' E	793,0	PIES 61	
PS66/304-1	03.09.04	16:07	80° 43,36' N	14° 39,37' E	1098,0	GKG	
PS66/304-2	03.09.04	16:57	80° 43,21' N	14° 38,47' E	1093,0	MUC	
PS66/304-3	03.09.04	17:40	80° 43,20' N	14° 38,02' E	1095,0	GC	
PS66/305-1	03.09.04	18:03	80° 42,95' N	14° 38,91' E	1058,0	HS_PS	start track
PS66/305-1	04.09.04	01:38	81° 14,62' N	13° 18,90' E	2269,0	HS_PS	profile end
PS66/306-1	04.09.04	02:17	81° 14,58' N	13° 18,96' E	2271,0	GKG	
PS66/306-2	04.09.04	03:34	81° 14,56' N	13° 18,62' E	2268,0	GC	
PS66/307-1	04.09.04	05:11	81° 11,95' N	13° 2,74' E	2277,0	GKG	
PS66/307-2	04.09.04	06:21	81° 11,94' N	13° 2,68' E	2275,0	GC	
PS66/308-1	04.09.04	08:22	81° 7,28' N	12° 35,96' E	2217,0	GKG	
PS66/308-2	04.09.04	09:38	81° 7,31' N	12° 36,16' E	2217,0	MUC	
PS66/308-3	04.09.04	10:47	81° 7,30' N	12° 35,97' E	2218,0	GC	
PS66/309-1	04.09.04	13:44	81° 11,22' N	12° 59,08' E	2269,0	KAL	
PS66/310-1	04.09.04	14:40	81° 12,20' N	13° 7,40' E	2271,0	HS_PS	start track
PS66/310-1	04.09.04	23:38	81° 41,50' N	13° 28,00' E	2198,0	HS_PS	profile end
PS66/311-1	05.09.04	00:20	81° 41,76' N	13° 28,25' E	2192,0	GKG	
PS66/311-2	05.09.04	01:33	81° 41,79' N	13° 28,45' E	2193,0	MUC	
PS66/311-3	05.09.04	02:53	81° 41,78' N	13° 28,20' E	2192,0	GC	
PS66/312-1	05.09.04	04:18	81° 41,26' N	13° 42,48' E	2273,0	GKG	
PS66/312-2	05.09.04	05:30	81° 41,24' N	13° 42,65' E	2275,0	GC	
PS66/313-1	05.09.04	07:35	81° 45,56' N	14° 16,31' E	2298,0	GC	
PS66/314-1	05.09.04	11:35	81° 17,87' N	11° 59,47' E	1337,0	M	start- magnetic turncircels
PS66/314-1	05.09.04	12:21	81° 17,83' N	11° 59,10' E	1347,0	M	end-magnetic turncircels
PS66/315-1	05.09.04	13:11	81° 16,46' N	12° 6,91' E	1708,0	SEISREFL	Streamer into water
PS66/315-1	05.09.04	13:37	81° 17,36' N	12° 3,00' E	1477,0	SEISREFL	airguns in the water
PS66/315-1	05.09.04	13:40	81° 17,50' N	12° 2,39' E	1440,0	SEISREFL	profile start
PS66/317-1	10.09.04	10:00	80° 53,75' N	3° 34,35' E	791,4	M	start- magnetic turncircels
PS66/316-1	10.09.04	10:01	80° 53,73' N	3° 34,76' E	787,1	SEISREFL	array on deck
PS66/317-1	10.09.04	11:24	80° 54,38' N	3° 41,51' E	761,5	M	end-magnetic turncircels
PS66/316-1	10.09.04	11:39	80° 55,05' N	3° 39,79' E	763,0	SEISREFL	airguns in the water
PS66/316-1	10.09.04	13:24	80° 54,01' N	2° 50,47' E	978,9	SEISREFL	cont. Profile
PS66/316-1	12.09.04	13:22	81° 35,98' N	12° 29,68' E	2073,0	SEISREFL	end of profile
PS66/316-1	12.09.04	13:39	81° 36,50' N	12° 34,26' E	2085,0	SEISREFL	streamer on deck
PS66/316-1	12.09.04	13:48	81° 36,77' N	12° 36,70' E	2091,0	SEISREFL	array on deck
PS66/318-1	12.09.04	16:40	81° 18,52' N	12° 2,55' E	1261,0	SD	
PS66/318-2	12.09.04	17:09	81° 18,60' N	12° 2,39' E	1261,0	GKG	
PS66/318-3	12.09.04	18:00	81° 18,58' N	12° 2,87' E	1260,0	MUC	
PS66/318-4	12.09.04	18:46	81° 18,60' N	12° 2,71' E	1262,0	KAL	
PS66/319-1	12.09.04	22:26	81° 24,49' N	13° 48,79' E	2178,0	GC	
PS66/320-1	12.09.04	23:00	81° 24,60' N	13° 48,96' E	2175,0	HS_PS	start track
PS66/320-1	13.09.04	08:38	82° 10,34' N	18° 15,35' E	2361,0	HS_PS	profile end
PS66/321-1	13.09.04	08:45	82° 10,38' N	18° 15,02' E	2359,0	SD	
PS66/321-2	13.09.04	09:21	82° 10,38' N	18° 14,89' E	2359,0	GKG	
PS66/321-3	13.09.04	10:40	82° 10,32' N	18° 14,36' E	2360,0	MUC	
PS66/321-4	13.09.04	11:51	82° 10,27' N	18° 13,47' E	2360,0	GC	
PS66/322-1	13.09.04	14:04	82° 5,36' N	18° 5,27' E	3041,0	SD	
PS66/322-2	13.09.04	14:47	82° 5,47' N	18° 4,13' E	2992,0	GKG	
PS66/322-3	13.09.04	16:16	82° 5,40' N	18° 5,25' E	3028,0	GC	
PS66/323-1	14.09.04	02:12	82° 18,48' N	22° 58,77' E	3910,0	GKG	
PS66/323-2	14.09.04	04:14	82° 18,69' N	22° 59,40' E	3914,0	MUC	
PS66/323-3	14.09.04	06:06	82° 18,44' N	22° 59,67' E	3913,0	GC	
PS66/324-1	14.09.04	14:52	81° 32,62' N	24° 54,50' E	1513,0	SEISREFL	Streamer into water
PS66/324-1	14.09.04	15:15	81° 31,81' N	25° 2,30' E	1402,0	SEISREFL	airguns in the water
PS66/324-1	14.09.04	15:45	81° 30,07' N	25° 0,00' E	846,1	SEISREFL	profile start
PS66/324-1	14.09.04	18:08	81° 18,00' N	25° 9,70' E	305,8	SEISREFL	Sono-buoy

Station	Date	Time	Position Lat.	Position Long.	Depth [m]	Gear	Remarks
PS66/324-1	15.09.04	03:10	81° 18,07' N	26° 0,17' E	537,8	SEISREFL	Sono-buoy
PS66/324-1	15.09.04	13:31	81° 24,01' N	26° 59,71' E	871,2	SEISREFL	end of profile
PS66/324-1	15.09.04	13:52	81° 23,96' N	27° 8,43' E	870,5	SEISREFL	streamer on deck
PS66/324-1	15.09.04	13:56	81° 23,95' N	27° 9,44' E	869,2	SEISREFL	array on deck
PS66/325-1	15.09.04	15:35	81° 26,19' N	25° 59,85' E	896,7	SD	
PS66/325-2	15.09.04	15:57	81° 26,17' N	25° 59,86' E	896,2	GKG	
PS66/325-3	15.09.04	16:32	81° 26,18' N	25° 59,86' E	895,5	GC	
PS66/326-1	15.09.04	17:00	81° 26,31' N	25° 56,93' E	864,7	HS_PS	start track
PS66/326-1	16.09.04	13:28	80° 43,05' N	15° 51,42' E	642,4	HS_PS	profile break
PS66/326-1	16.09.04	14:22	80° 43,30' N	15° 52,45' E	655,1	HS_PS	continue the profile
PS66/326-1	16.09.04	16:30	81° 1,04' N	17° 9,11' E	703,5	HS_PS	profile end
PS66/327-1	16.09.04	16:32	81° 0,99' N	17° 9,54' E	702,0	SD	
PS66/327-2	16.09.04	16:47	81° 0,93' N	17° 9,60' E	701,0	GKG	
PS66/327-3	16.09.04	17:18	81° 0,92' N	17° 9,39' E	701,0	KAL	
PS66/328-1	16.09.04	21:03	81° 19,25' N	14° 30,88' E	1979,0	GC	
PS66/329-1	17.09.04	01:08	81° 36,25' N	13° 6,19' E	2209,0	GKG	
PS66/329-2	17.09.04	02:25	81° 36,27' N	13° 6,14' E	2207,0	MUC	
PS66/329-3	17.09.04	03:44	81° 36,31' N	13° 6,13' E	2211,0	GC	
PS66/330-1	17.09.04	05:37	81° 32,87' N	13° 21,77' E	2306,0	GKG	
PS66/330-2	17.09.04	06:44	81° 32,88' N	13° 21,71' E	2305,0	GC	
PS66/331-1	17.09.04	08:16	81° 26,53' N	13° 5,68' E	2302,0	SEISREFL	Streamer into water
PS66/331-1	17.09.04	08:33	81° 25,53' N	13° 3,20' E	2306,0	SEISREFL	airguns in the water
PS66/331-1	17.09.04	11:57	81° 24,01' N	11° 2,03' E	1940,0	SEISREFL	Sono-buoy
PS66/331-1	18.09.04	01:10	81° 12,02' N	7° 31,45' E	787,2	SEISREFL	Sono-buoy
PS66/331-1	18.09.04	09:24	81° 17,97' N	9° 57,31' E	1784,0	SEISREFL	Sono-buoy
PS66/331-1	18.09.04	11:27	81° 17,97' N	8° 42,59' E	1205,0	SEISREFL	end of profile
PS66/331-1	18.09.04	11:37	81° 17,98' N	8° 36,95' E	1035,0	SEISREFL	profile start
PS66/331-1	19.09.04	01:08	81° 35,23' N	3° 21,56' E	843,4	SEISREFL	Sono-buoy
PS66/331-1	19.09.04	08:26	82° 8,01' N	4° 19,07' E	2105,0	SEISREFL	end of profile
PS66/331-1	19.09.04	08:37	82° 8,38' N	4° 18,88' E	2116,0	SEISREFL	streamer on deck
PS66/331-1	19.09.04	08:41	82° 8,40' N	4° 18,81' E	2116,0	SEISREFL	array on deck
PS66/332-1	19.09.04	15:10	81° 58,10' N	8° 19,62' E	791,0	HS_PS	start track
PS66/332-1	19.09.04	17:14	81° 54,55' N	8° 29,17' E	752,0	HS_PS	profile end
PS66/333-1	19.09.04	17:29	81° 55,19' N	8° 35,81' E	747,0	SD	
PS66/333-2	19.09.04	17:54	81° 55,54' N	8° 34,29' E	751,5	DRG_C	start dredging
PS66/333-2	19.09.04	19:05	81° 56,32' N	8° 31,62' E	720,8	DRG_C	stop dredging
PS66/333-3	19.09.04	20:45	81° 56,53' N	8° 22,74' E	718,5	DRG_C	start dredging
PS66/333-3	19.09.04	21:34	81° 56,49' N	8° 22,77' E	716,8	DRG_C	stop dredging
PS66/333-4	19.09.04	22:30	81° 56,42' N	8° 30,17' E	725,5	GC	
PS66/333-5	19.09.04	23:26	81° 56,10' N	8° 31,50' E	719,1	GC	
PS66/334-1	20.09.04	03:02	81° 36,99' N	6° 39,26' E	536,7	HS_PS	start track
PS66/334-1	20.09.04	04:39	81° 36,32' N	6° 32,22' E	819,5	HS_PS	profile end
PS66/335-1	20.09.04	05:08	81° 35,99' N	6° 32,00' E	863,7	DRG_C	start dredging
PS66/335-1	20.09.04	05:29	81° 36,02' N	6° 35,42' E	558,5	DRG_C	stop dredging
PS66/335-2	20.09.04	06:47	81° 36,05' N	6° 34,06' E	654,8	GC	
PS66/336-1	20.09.04	07:40	81° 36,48' N	6° 45,14' E	505,2	GC	
PS66/336-2	20.09.04	08:09	81° 36,35' N	6° 47,74' E	502,6	SD	
PS66/336-3	20.09.04	08:22	81° 36,41' N	6° 47,40' E	505,9	GC	
PS66/336-4	20.09.04	08:56	81° 36,39' N	6° 47,69' E	504,5	GKG	
PS66/337-1	20.09.04	09:30	81° 36,33' N	7° 1,32' E	505,1	SD	
PS66/337-2	20.09.04	09:43	81° 36,32' N	7° 1,38' E	503,3	GKG	
PS66/337-3	20.09.04	10:29	81° 36,30' N	7° 1,44' E	503,0	GC	
PS66/337-4	20.09.04	11:12	81° 36,61' N	7° 3,18' E	587,8	GC	
PS66/338-1	20.09.04	16:11	81° 19,05' N	3° 2,82' E	855,2	SEISREFL	airguns in the water
PS66/338-1	20.09.04	16:15	81° 18,96' N	3° 1,54' E	855,7	SEISREFL	Streamer into water
PS66/338-1	20.09.04	16:30	81° 18,51' N	2° 55,19' E	887,4	SEISREFL	airguns in the water
PS66/338-1	21.09.04	13:36	81° 6,01' N	5° 16,66' E	661,7	SEISREFL	Sono-buoy
PS66/338-1	21.09.04	20:00	81° 6,00' N	9° 14,96' E	1082,0	SEISREFL	end of profile
PS66/338-1	21.09.04	20:14	81° 5,99' N	9° 19,67' E	1131,0	SEISREFL	streamer on deck
PS66/338-1	21.09.04	20:18	81° 5,95' N	9° 20,57' E	1141,0	SEISREFL	array on deck
PS66/339-1	21.09.04	20:21	81° 5,94' N	9° 22,12' E	1157,0	M	start- magnetic turncircels
PS66/339-1	21.09.04	22:09	81° 5,96' N	9° 24,00' E	1178,0	M	end-magnetic turncircels
PS66/340-1	22.09.04	10:15	79° 55,10' N	0° 41,87' W	2747,0	SEISREFL	Streamer into water

Station	Date	Time	Position Lat.	Position Long.	Depth [m]	Gear	Remarks
PS66/340-1	22.09.04	10:32	79° 54,58' N	0° 48,57' W	2766,0	SEISREFL	airguns in the water
PS66/340-1	22.09.04	10:43	79° 53,97' N	0° 51,64' W	2775,0	SEISREFL	profile start
PS66/340-1	22.09.04	13:03	79° 42,26' N	0° 47,94' W	2821,0	SEISREFL	Sono-buoy
PS66/340-1	22.09.04	22:17	79° 41,92' N	0° 38,95' W	2826,0	SEISREFL	end of profile
PS66/340-1	22.09.04	22:33	79° 41,26' N	0° 39,08' W	2823,0	SEISREFL	streamer on deck
PS66/340-1	22.09.04	22:36	79° 41,18' N	0° 39,13' W	2826,0	SEISREFL	array on deck
PS66/341-1	22.09.04	23:43	79° 44,07' N	0° 44,97' W	2822,0	GC	
PS66/342-1	23.09.04	13:17	79° 3,51' N	10° 57,87' W	357,9	SEISREFL	airguns in the water
PS66/342-1	23.09.04	13:27	79° 4,04' N	10° 57,85' W	354,8	SEISREFL	array on deck
PS66/342-2	23.09.04	13:41	79° 5,22' N	10° 59,11' W	345,6	SEISREFL	Streamer into water
PS66/342-2	23.09.04	13:59	79° 3,85' N	10° 59,04' W	360,0	SEISREFL	airguns in the water
PS66/342-2	23.09.04	14:11	79° 3,03' N	10° 59,50' W	358,9	SEISREFL	profile start
PS66/342-2	24.09.04	02:45	78° 59,59' N	10° 52,84' W	281,9	SEISREFL	end of profile
PS66/342-2	24.09.04	03:02	78° 59,58' N	10° 48,25' W	313,7	SEISREFL	streamer on deck
PS66/342-2	24.09.04	03:07	78° 59,77' N	10° 47,95' W	319,7	SEISREFL	array on deck
PS66/343-1	24.09.04	03:50	79° 0,83' N	11° 6,91' W	216,2	GC	
PS66/343-2	24.09.04	04:20	79° 0,98' N	11° 6,82' W	226,0	GC	
PS66/343-3	24.09.04	04:49	79° 1,05' N	11° 6,88' W	227,2	GC	
PS66/343-4	24.09.04	05:18	79° 1,17' N	11° 7,12' W	240,9	GC	
PS66/343-5	24.09.04	05:44	79° 1,31' N	11° 6,80' W	252,2	GC	
PS66/343-6	24.09.04	06:09	79° 1,44' N	11° 6,84' W	264,2	GC	
PS66/344-1	24.09.04	06:48	79° 2,55' N	11° 6,65' W	338,7	GC	
PS66/345-1	24.09.04	07:30	79° 3,58' N	11° 15,11' W	317,9	GC	
PS66/345-2	24.09.04	08:08	79° 3,58' N	11° 16,03' W	313,3	GC	
PS66/345-3	24.09.04	08:40	79° 3,58' N	11° 17,37' W	308,6	GC	
PS66/346-1	25.09.04	04:08	77° 19.27' N	1° 21.36' E	3261.0	SEISREFL	Streamer into water
PS66/346-1	25.09.04	04:24	77° 18.75' N	1° 24.87' E	3261.0	SEISREFL	airguns in the water
PS66/346-1	25.09.04	10:16	77° 18.09' N	1° 5.88' E	3261.0	SEISREFL	Sono-buoy
PS66/346-1	25.09.04	13:06	77° 5.81' N	0° 54.19' E	3255.0	SEISREFL	Sono-buoy
PS66/347-1	26.09.04	09:51	75° 47.56' N	9° 1.76' W	1699.0	SEISREFL	Sono-buoy
PS66/347-1	26.09.04	13:35	75° 36.94' N	10° 8.72' W	1576.0	SEISREFL	Sono-buoy
PS66/347-1	27.09.04	00:07	74° 44.70' N	12° 30.10' W	1983.0	SEISREFL	end of profile
PS66/347-1	27.09.04	00:48	74° 42.27' N	12° 30.61' W	2125.0	SEISREFL	streamer on deck
PS66/347-1	27.09.04	00:55	74° 41.70' N	12° 30.62' W	2167.0	SEISREFL	array on deck
PS66/348-1	27.09.04	01:03	74° 40.77' N	12° 30.64' W	2234.0	M	start- magnetic turncircels
PS66/348-1	27.09.04	02:45	74° 40.60' N	12° 30.56' W	2246.0	M	end-magnetic turncircels

Date of September	Time UTC	Latitude, N	Longitude	True wind speed (m/s)	True wind direction (°)	Air temperature (°C)	Ship speed (kn)	Number of engines	Operation mode: channel=0, lead=1, floe ice=3, ramming=4	Total ice concentration (%)	Conc. of thin ice <30 cm (%)	Typical sea ice thickness (m)	Snow thickness (cm)	Typical floe diameter (m)	Max. floe diameter (m)	Melt pond coverage (%)	Typical pond diameter (m)	Maximum pond diameter (m)	Dirty ice concentration (%)	Lead width (m)	Lead floes, diameter (m)	Typical ridge height (m)	Max. ridge height (m)	Typical ridge spacing (m)	Ridges: new=0, old=1, both=2	Rubble fields, coverage (%)	Icebergs, number of	
9	8	81°13.93'	2°39.82' E	7.1	330	-5.6	4.5	3	3	40		1	10	15	30													
	10	81°12.05'	2°41.72' E	9.3	315	-6.6	4.0	3	3	50																		
	13	81°11.87'	2°32.80' E	7.1	300	-6.5	5.9	3	3	30																		
	14	81°11.86'	2°00.05' E	5.5	320	-6.5	6.0	3	3	70	10	1	5	15	50							1	1.5		1			
	16	81°12.00'	0°51.30' E	9.2	350	-6.0	3.3	3	3	40		1.5	10	15	30							1	1.5		1			
	19	81°11.70'	0°48.10' W	8.4	5	-6.6	6.4	3	3	5		1	5	15	30							1	1.5		1			
	20	81°11.95'	1°22.80' W	6.0	340	-6.7	5.2	3	3	5		0.5	5	10	20													
	22	81°09.02'	2°16.42' W	4.7	10	-6.0	5.0	3	3	5		0.5	5	10	20													
10	8	80°58.63'	2°34.80' E	4.0	45	-6.9	5.7	3	3	30		1	5	15	30							1	2		1			
	10	80°53.70'	3°36.00' E	1.3	50	-6.0	5.3	3	3	30		1	10	10	20							1	1.5		1			
	12	80°53.90'	3°22.00' E	6.6	35	-4.9	5.0	3	3	40		1	5	15	30							1	2		1		1	
	16	80°54.00'	1°18.80' E	7.9	350	-4.5	6.0	3	3	10		0.8	5	10	25							1	2		1			
	19	80°51.54'	0°00.75' W	15.1	45	-0.7	5.1	3	3	5		0.5	5	10	20							1	2		1			
	21	80°56.00'	0°20.10' E	13.7	40	-1.9	6.0	3	3	5		0.5	10	10	20							1	2		1			

Date of September	Time UTC	Latitude, N	Longitude	True wind speed (m/s)	True wind direction (°)	Air temperature (°C)	Ship speed (kn)	Number of engines	Operation mode: chanel=0, lead=1, floe ice=3, ramming=4	Total ice concentration (%)	Conc. of thin ice <30 cm (%)	Typical sea ice thickness (m)	Snow thickness (cm)	Typical floe diameter (m)	Max. floe diameter (m)	Melt pond coverage (%)	Typical pond diameter (m)	Maximum pond diameter (m)	Dirty ice concentration (%)	Lead width (m)	Lead floes, diameter (m)	Typical ridge height (m)	Max. ridge height (m)	Typical ridge spacing (m)	Ridges: new=0, old=1, both=2	Rubble fields, coverage (%)	Icebergs, number of	
18	18	81°18.00'	4°50.20' E	9.6	160	-0.1	5.7	3		0																		
	20	81°17.89'	3°40.75' E	5.3	165	-0.4	6.3	3	3	50		1	15	15	50							1	1.5		1			
19	8	82°06.00'	4°16.83' E	7.2	160	-1.2	4.8	4	3	90		1.2	15	20	50							1	1.5		1			
	14	82°00.94'	7°16.00' E	8.3	145	-0.6	8.8	3	3	40		1	10	15	30				1			1.5	3		1			
	16	81°54.85'	8°34.00' E	5.9	175	+0.1	5.1	3	3	80	30	0.6	10	15	30							1	2		1			
	18	81°55.70'	8°32.74' E	4.5	160	-0.5	1.7	3	3	50	10	0.5	10	15	40							1.5	3		1			
	20	81°57.08'	8°19.16' E	7.2	175	-0.6	0.2	3	3	75	20	0.8	10	15	30													
20	8	81°36.38'	6°47.64' E	6.6	60	-1.6	0.6	3		0																		
	12	81°34.10'	6°28.10' E	7.7	65	-0.7	10.0	3		<1		0.5	5	5	10													
	14	81°25.91'	4°43.98' E	7.1	65	-1.0	10.0	3	3	5		0.5	10	2	10													
	16	81°19.54'	3°09.10' E	6.4	35	-1.6	8.0	3	3	25		1	15	5	20				1			1	3		1			
	18	81°18.07'	2°06.80' E	6.0	50	-1.9	5.8	3	3	50		1	15	15	40							1	2		1			
	20	81°18.37'	0°58.63' E	5.5	15	-5.0	4.2	3	3	95		1.5	15	20	70							2	5		2			

Comments to Table 12.2

07.09.2004

20:00. POLARSTERN goes in open water along the ice margin which is situated at the distance about 1 mile from the ship.

09.09.2004.

14:00. Some ice floes are slightly brownish at their bottom – traces of algal bloom.

13.09.2004

08:00. Strong algal bloom (bottoms of ice floes are brown).

14:00. Strong algal bloom at the bottom of ice floes.

20:00. Strong algal bloom at the bottom of ice floes.

14.09.2004

08:00. Strong algal bloom at the bottom of ice floes.

14:00. In small ice floe (5 m) there is log (wood) 1.5 long.

16.09.2004.

08:00. Rare small peaces of rotten ice (1–2 m).

17.09.2004.

16:00. Weak algal bloom at the bottom of ice floes.

19.09.2004.

08:00. Weak algal bloom at the bottom of ice floes.

14: 00. Weak algal bloom at the bottom of ice floes.

20.09.2004.

14:15. Ice 40%, 10% are sediment-laden (“dirty”), but the sizes of ice floes are small (5–15 m) and landing of helicopters on them is impossible.

12.3.1 Graphical Core Description of Giant box cores
S. Nam

PS66/306-1 (GKG)

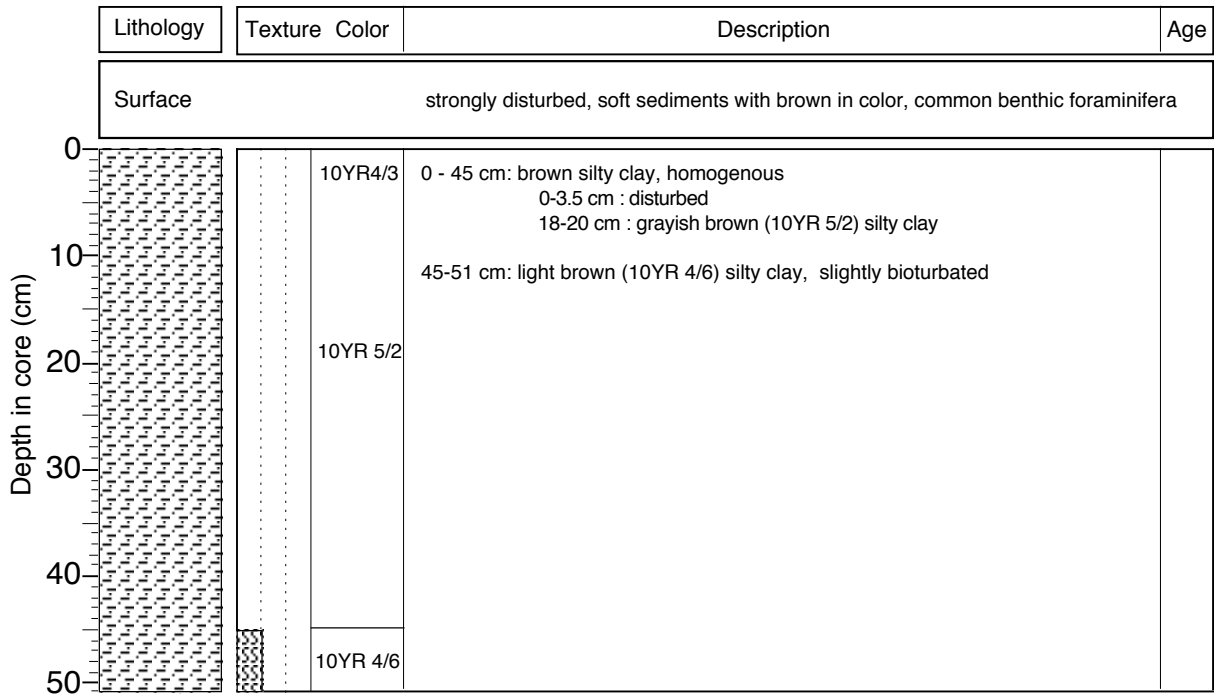
Yermak Plateau

ARK XX/3 (ARCTIC 04)

Recovery: 0.51 m

80°14.58'N, 13°18.96'E

Water depth: 2271 m



PS66/307-1 (GKG)

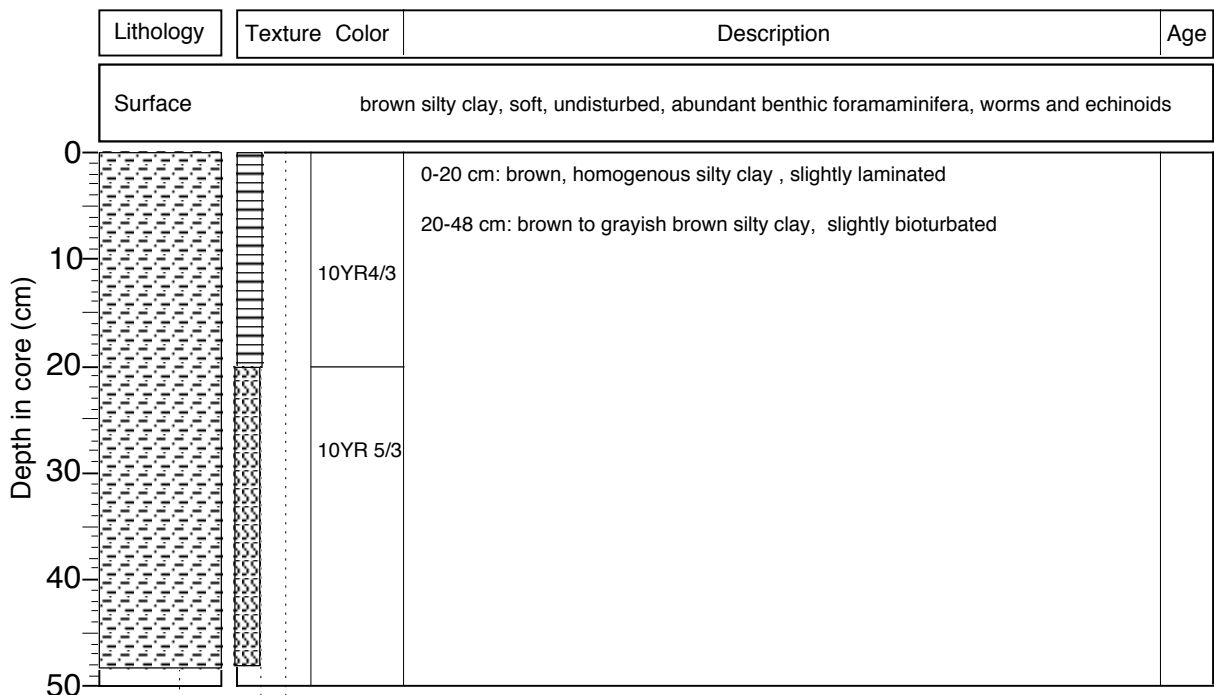
Yermak Plateau

ARK XX/3 (ARCTIC 04)

Recovery: 0.48 m

81°11.95'N, 13°2.74'E

Water depth: 2276 m



PS66/308-1 (GKG)

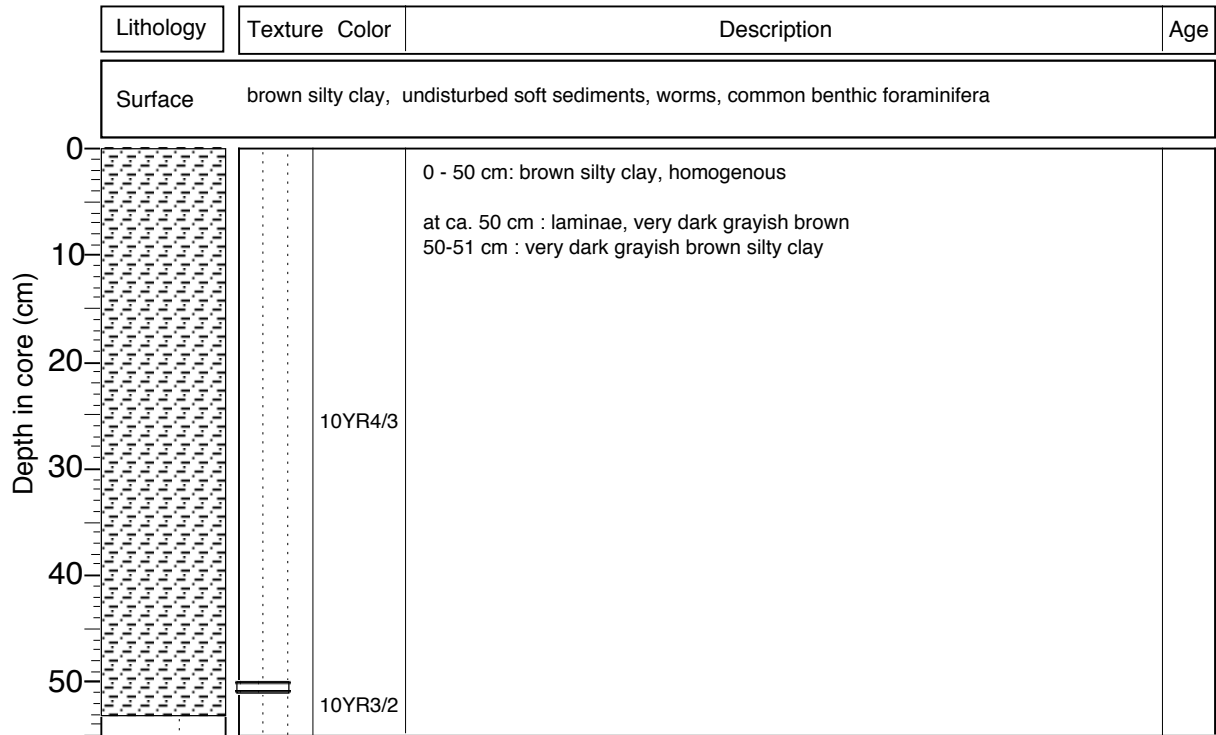
Yermak Plateau

ARK XX/3 (ARCTIC 04)

Recovery: 0.53 m

81°7.28'N, 12°35.96'E

Water depth: 2217 m



PS66/312-1 (GKG)

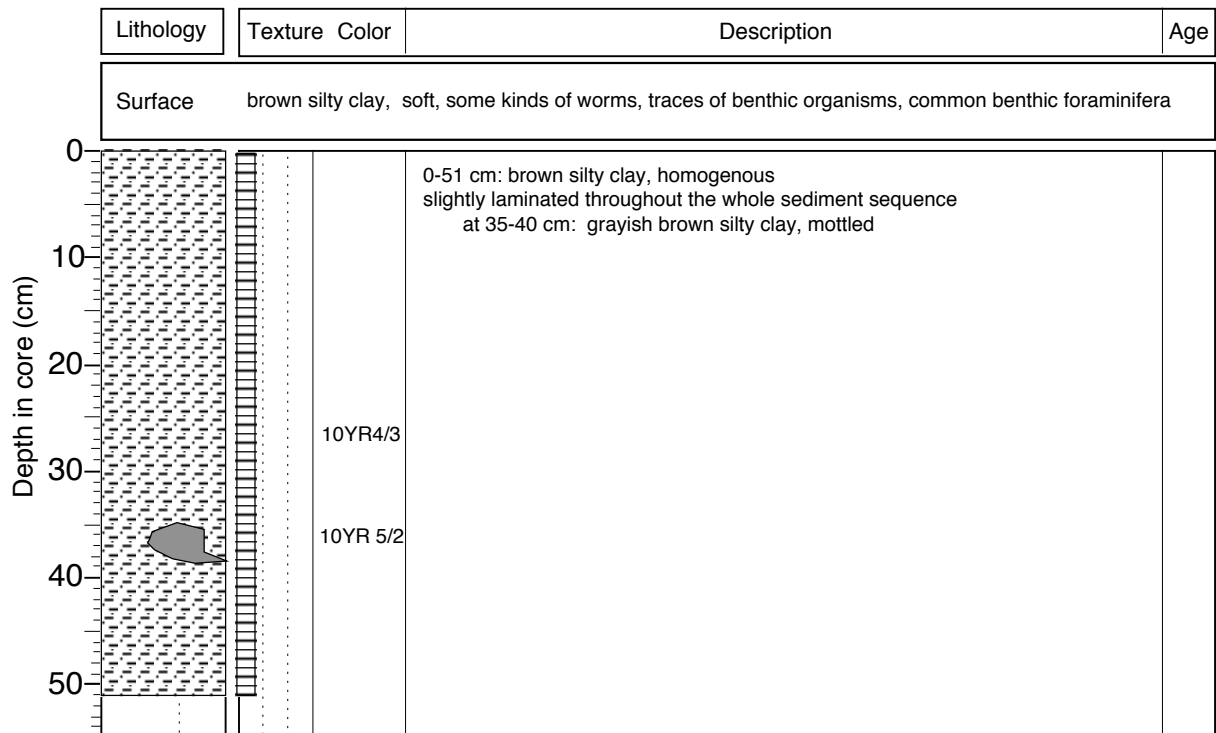
Yermak Plateau

ARK XX/3 (ARCTIC 04)

Recovery: 0.51 m

81°41.26'N, 13°42.48'E

Water depth: 2273 m



PS66/321-2 (GKG)

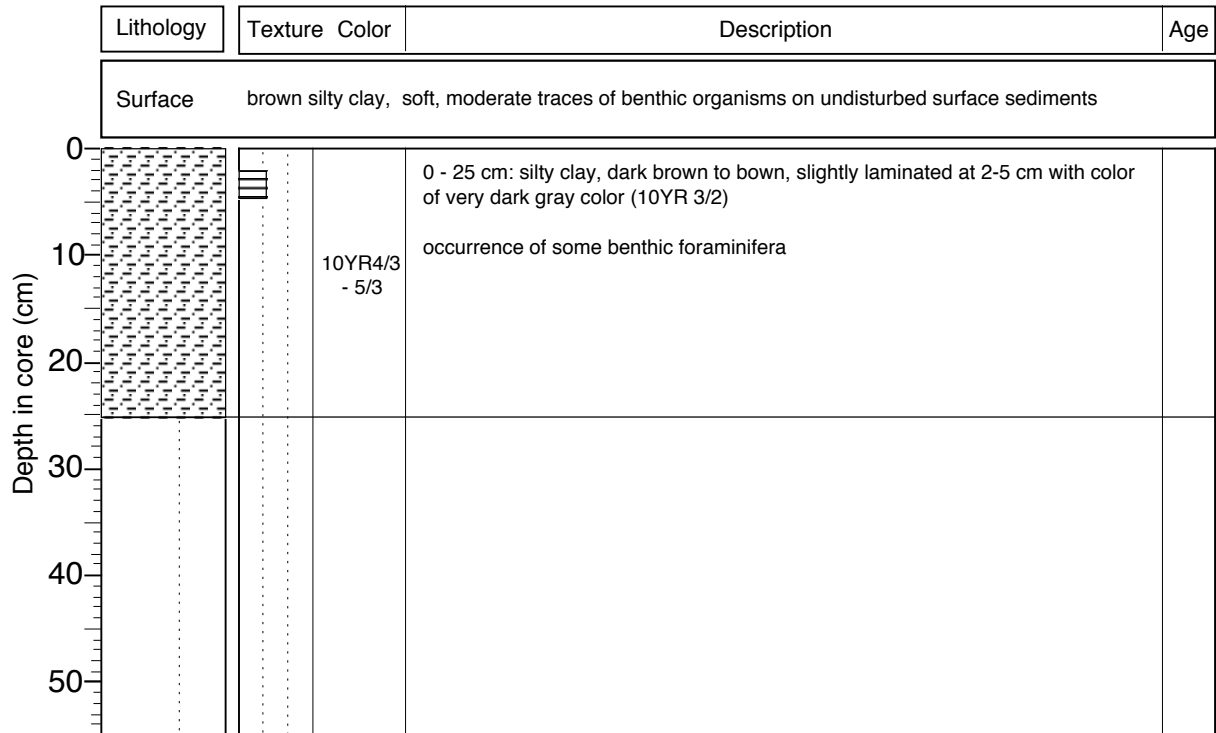
Yermak Plateau

ARK XX/3 (ARCTIC 04)

Recovery: 0.25 m

82°10.38'N, 18°14.89'E

Water depth: 2359 m



PS66/322-2 (GKG)

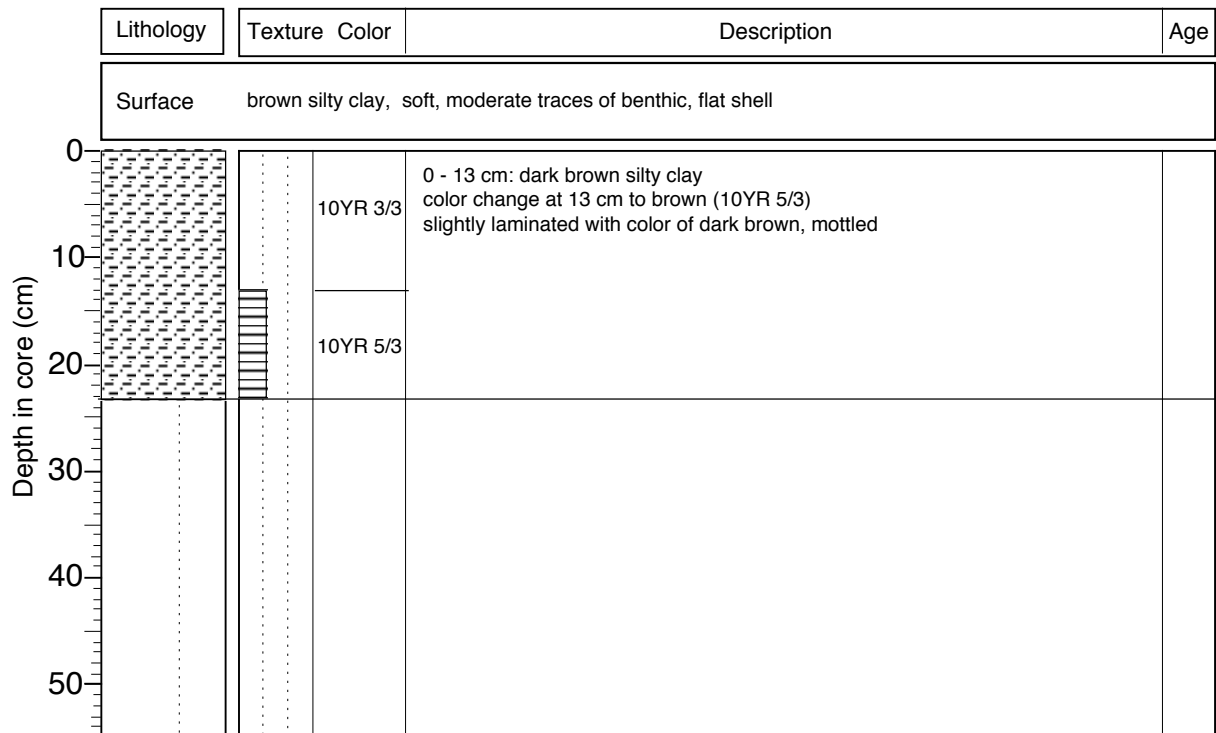
Yermak Plateau

ARK XX/3 (ARCTIC 04)

Recovery: 0.23 m

82°5.47'N, 18°4.13'E

Water depth: 2992 m



PS66/323-1 (GKG)

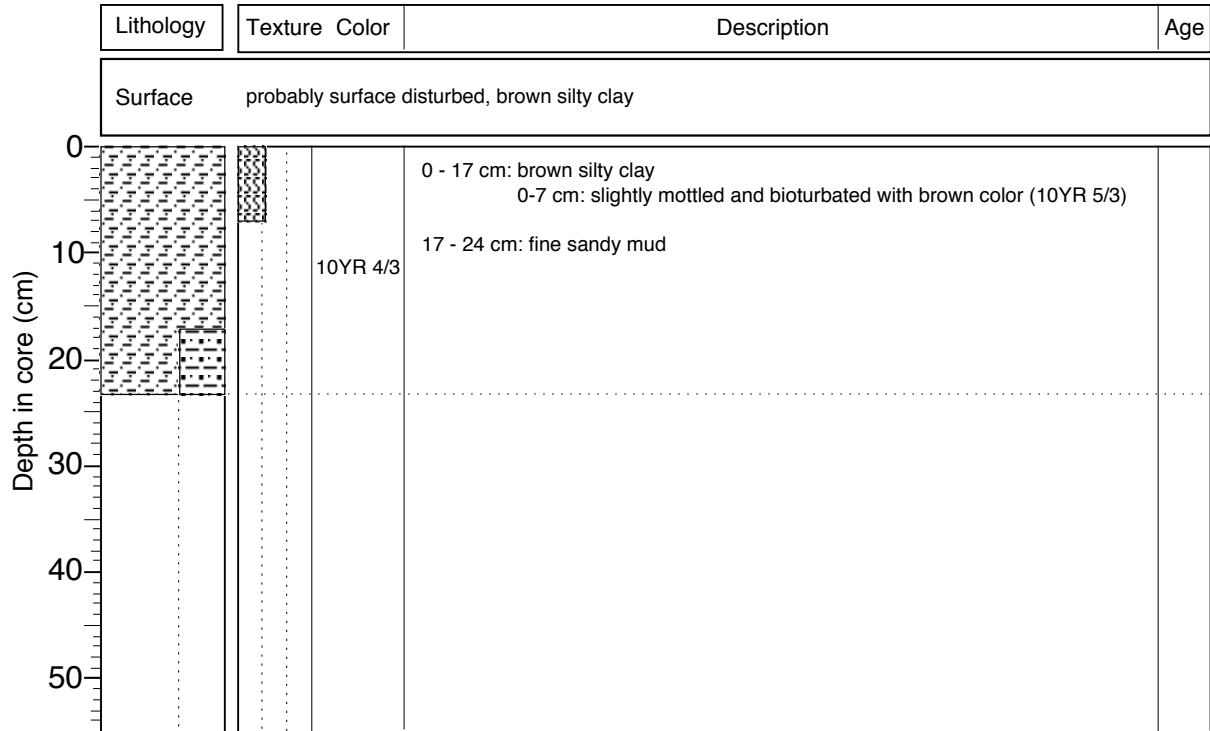
Yermak Plateau

ARK XX/3 (ARCTIC 04)

Recovery: 0.24 m

82°18.48', 22°58.77'

Water depth: 3910 m



PS66/325-2 (GKG)

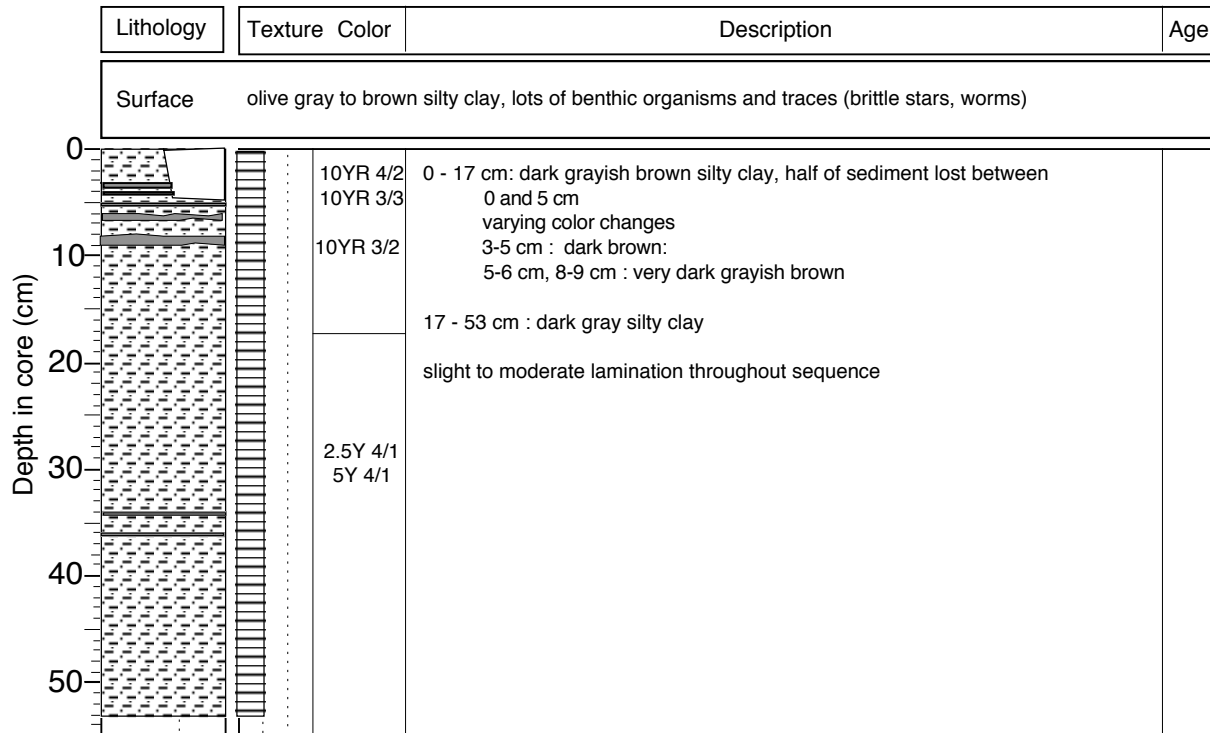
Yermak Plateau

ARK XX/3 (ARCTIC 04)

Recovery: 0.53 m

81°26.17'N, 25°59.86'

Water depth: 896 m



PS66/327-2 (GKG)

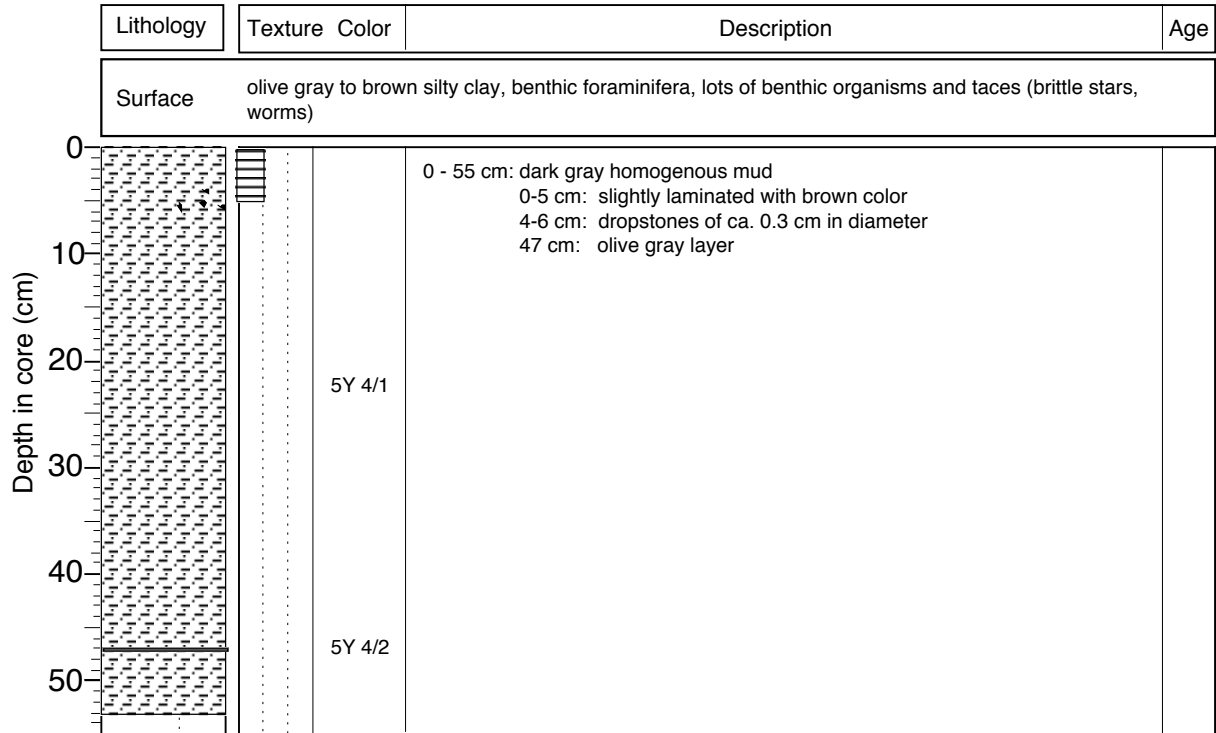
Yermak Plateau

ARK XX/3 (ARCTIC 04)

Recovery: 0.55 m

81°0.93'N, 17°9.60'E

Water depth: 701 m



PS66/329-1 (GKG)

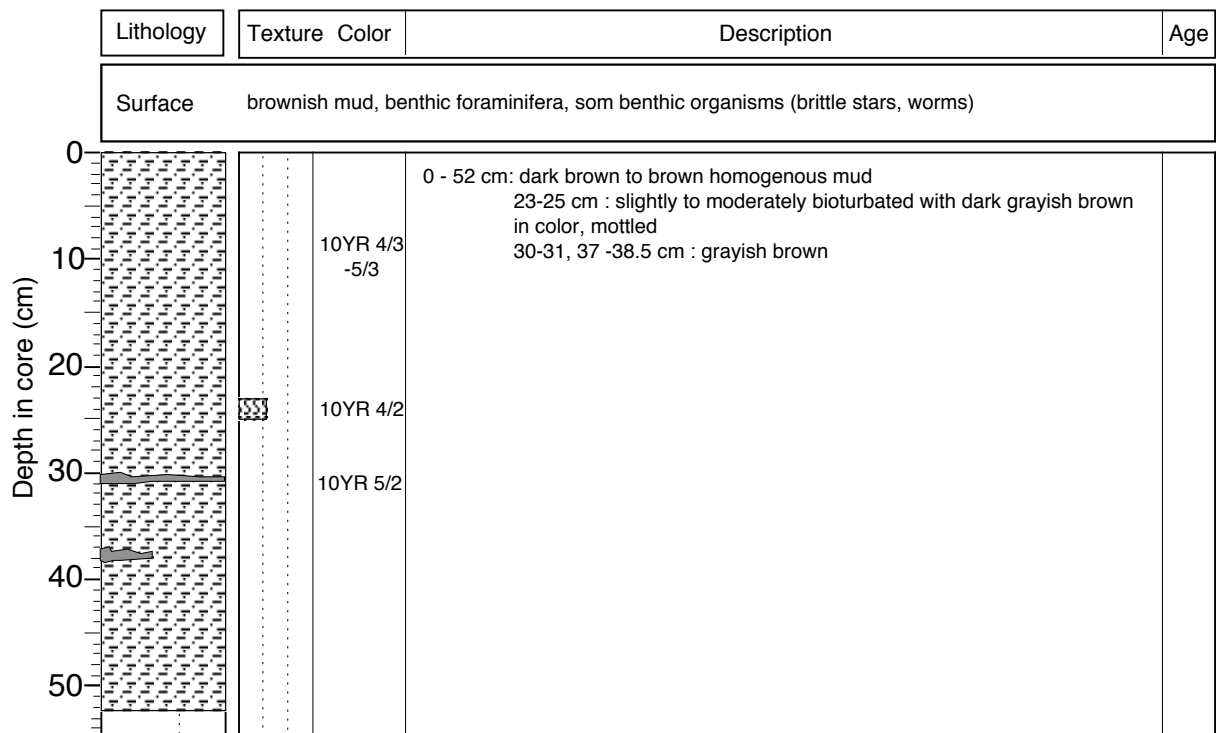
Yermak Plateau

ARK XX/3 (ARCTIC 04)

Recovery: 0.52 m

81°36.25'N, 13°6.19'E

Water depth: 2209 m



PS66/330-1 (GKG)

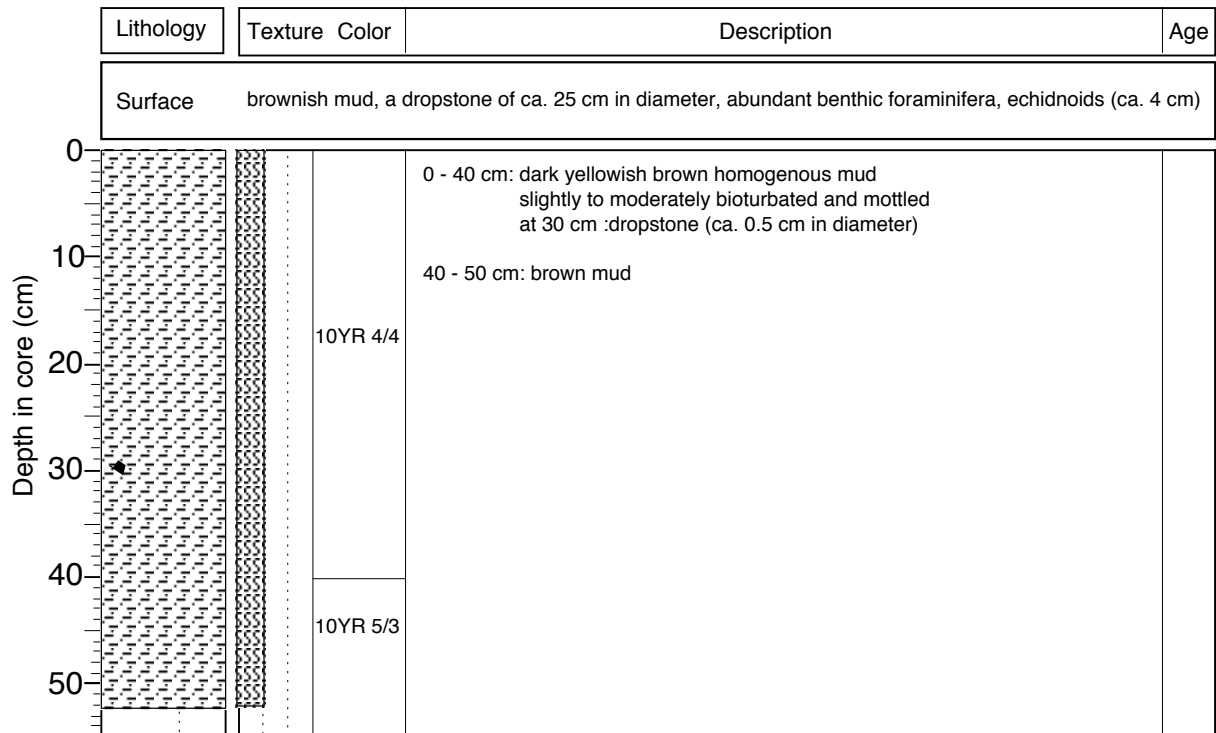
Yermak Plateau

ARK XX/3 (ARCTIC 04)

Recovery: 0.50 m

81°32.87'N, 13°21.77'E

Water depth: 2306 m



PS66/336-4 (GKG)

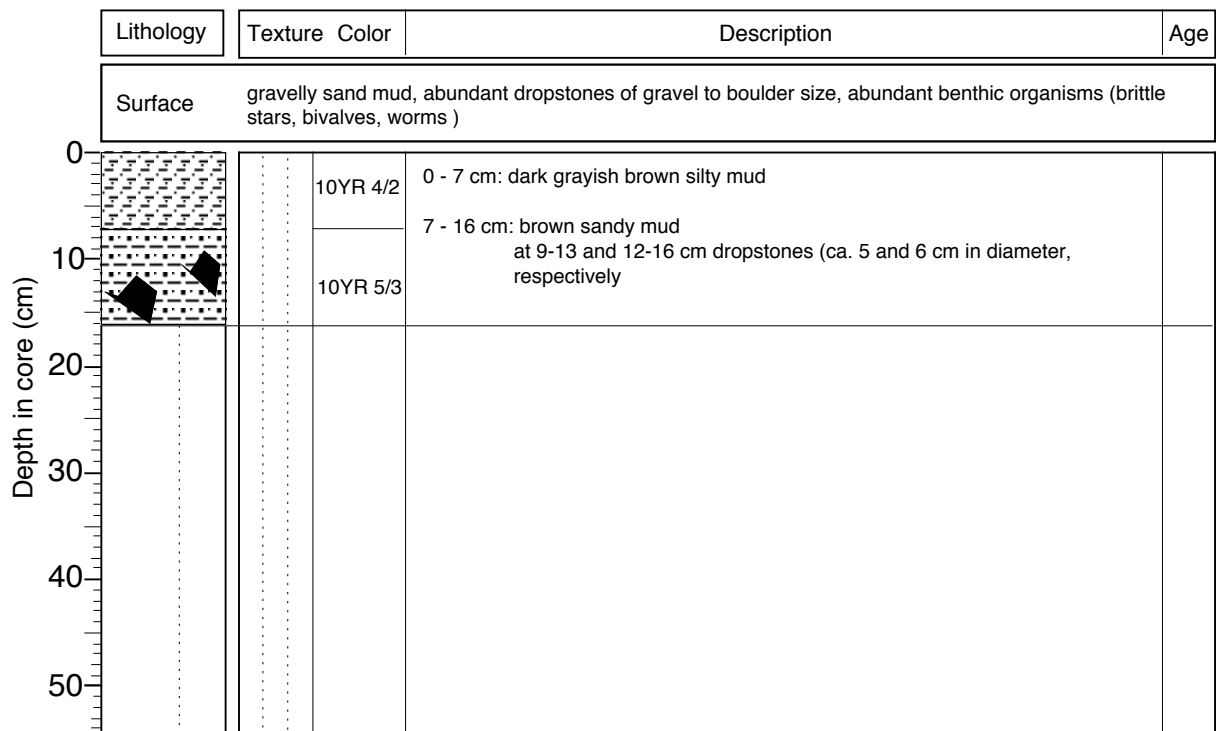
Yermak Plateau

ARK XX/3 (ARCTIC 04)

Recovery: 0.16 m

81°36.39'N, 6°47.69'E

Water depth: 505 m



12.3.2 Graphical Core Description – Gravity Cores (SL) and Kastenlot Cores (KAL)

R. Stein

PS66/304-3 (SL)

Recovery: 4.19 m

Svalbard Continental Margin

80° 43.20' N, 14° 38.02' E

ARK XX/3

Water depth: 1095 m

	Lithology	Texture Color	Description	Age	
0		5Y 3/2	0 - 64 cm: dark olive gray silty sandy clay 0-5 cm, 10-19cm), silty clayey sand (5-10 cm), and sandy silty clay (19-64 cm), large dropstone (5 cm in diameter) at 5-10 cm 64 - 83 cm: dark reddish gray silty clay, slump structure (folded/disturbed)? 83 - 92 cm: laminated, 0.1-0.5 cm thick layers of dark reddish gray and dark olive gray silty clay ("pink" layers?) 92 - 98 cm: dark reddish gray and dark olive gray silty clay, folded 98 - 319 cm: dark grayish brown (sandy) silty clay, partly laminated between 170 and 240 cm, sandy laminae at 149, 295-297, 306-307, and 311 cm; small dropstone at 109 cm, black (coal?) lenses at 282 cm		
1		5YR 4/2 and 5Y 3/2	319 - 419 cm: dark olive gray to dark grayish brown sandy silty clay, 328 - 350 cm black spots; sandy intervals at 355-356, 359, 360-362, 365-366, 369, 376, 378, 384, 385, 386, 394, 396, 397, 399, 401, 404, 405, 407, 410, 412, and 415 cm (= alternation of sandy silty clay and sandy layers, turbidites?); 360-362 coarse sand		
2		2.5Y 4/2			
3		2.5Y 4/2 and 5Y 4/2			
4					
5					

PS66/306-2

Svalbard Continental Margin

ARK XX/3

Recovery: 3.50 m

81° 14.56' N, 13° 18.61' E

Water depth: 2210 m

Depth in core (m)	Lithology	Texture	Color	Description	Age
	0			10YR4/3	0 - 26 cm: brown silty clay 26 - 28 cm: very dark brown (10YR 2/2) silty clay 28 - 31 cm: dark brown (10YR3/3) silty clay 31 - 34 cm: light olive brown and dark olive brown laminae
			2.5Y 4/4	34 - 43 cm: olive brown silty clay	
			2.5Y 4/0	43 - 50 cm: dark gray silty clay	
			5Y 5/1	50 - 53 cm: gray silty clay	
			2.5Y 4/4	53 - 88 cm: olive brown silty clay 88 - 92 cm: olive gray silty clay 92-93 cm: very dark brown silty clay	
			5Y 4/2	93-96 cm: dark olive gray silty clay	
			5Y 5/2	96 - 105 cm: olive gray silty clay	
			2.5Y 5/6	105 - 114 cm: light olive brown silty clay	
			2.5Y 5/0	114 - 129 cm: gray silty clay 129 - 156 cm: dark silty clay	
			2.5Y 4/0	156 - 206 cm: olive gray and dark gray silty clay, disturbed 206 - 213 cm: olive gray silty clay	
			5Y 5/2 and 2.5Y 4/0	213 - 252 cm: dark gray and gray silty clay, laminated, black spots 252 - 256 cm: olive gray silty clay; thin sand layer at base 256 - 285 cm: dark gray silty clay; thin gray laminae at 270, 272, 275, 276, 280, and 284 cm, black sand lense at 63-66 cm	
			2.5Y 5/3	285 - 291 cm: olive gray silty clay; sandy layer at base 291 - 300 cm: dark gray silty clay	
			2.5Y 4/0 and 2.5Y 5/0	300 - 305 cm: olive silty clay, block of dark gray and olive silty clay layers 305 - 327 cm: alternation of 1-2 cm thick dark gray, olive gray, and blueish gray silty clay intervals	
			2.5Y 4/0	327 - 330 cm: dark olive gray silty clay 330 - 350 cm: dark gray sandy silty clay, 340-345 more sandy	
			5Y 5/2 and 2.5Y 4/0	black coal (?) fragments at 310 and 313 cm dropstone (2 cm in diameter) at 333 cm	
			2.5Y 4/0		
3					
4					
5					

PS66/307-2 (SL)

Svalbard Continental Margin

ARK XX/3

Recovery: 4.57 m

81° 11.94' N, 13° 02.68' E

Water depth: 2275 m

	Lithology	Texture	Color	Description	Age
0			10YR 4/3	0 - 44 cm: brown silty clay, dark brown layer at 43 cm 44 - 51 cm: alternation of very dark brown and dark yellowish brown silty clay coarser layers at 47-48 and 50-51 cm ("cottage cheese") 51 - 56 cm: olive gray silty clay 56 - 77 cm: dark gray silty clay 77 - 113 cm: light olive brown silty clay; dropstone (2 cm in diameter) at 76-78 113 - 124 cm: yellowish brown silty clay 124 - 133 cm: olive silty clay 133 - 139 cm: dark olive gray silty clay, 138-139 mud clasts ("cottage cheese") 139 - 142 cm: very dark silty clay 142 - 152 cm: gray silty clay 152 - 161 cm: dark grayish brown silty clay 161 - 173 cm: grayish brown silty clay 173 - 189 cm: light olive brown silty clay, sand lense at 182-188 cm 189 - 199 cm: gray and dark gray silty clay 199 - 206 cm: grayish brown silty clay, some dark olive gray laminae 206 - 211 cm: dark gray and very dark gray silty clay layers 211 - 231 cm: grayish brown silty clay; dropstone (2 cm in diameter) at 217-219 cm 231 - 243 cm: gray and very dark gray silty clay, folded? 243 - 257 cm: grayish brown silty clay, dark olive gray layers at 247 and 252 cm 257 - 351 cm: alternation of dark grayish brown, grayish brown, gray and dark gray silty clay, laminated 351 - 357 cm: very dark gray silty clay, grayish brown "fold" 357 - 443 cm: dark grayish brown, grayish brown, and very dark gray silty clay very dark gray interval (424-432 cm), disturbed (slump?); large dropstone (3 cm in diameter) at 380-382 cm 443 - 448 cm: very dark gray and dark grayish brown silty clay, laminated 448 - 457 cm: grayish brown silty clay	
			5Y 4/2		
			2.5Y 4/0		
1			2.5Y 5/4		
			10YR 5/4		
			5Y 4/3		
			5Y 5/1		
			2.5Y 4/2		
			2.5Y 5/2		
			2.5Y 5/4		
			2.5Y 3/0		
2			2.5Y 5/2		
			2.5Y 5/2		
			2.5Y 5/0-3/0		
			2.5Y 5/2		
3			2.5Y 4/2, 2.5 Y 3/0 2.5Y 5/0, 2.5Y 5/2		
			2.5Y 3/0		
4			2.5Y 4/2, 2.5 Y 3/0 2.5Y 5/0, 2.5Y 5/2		
			2.5Y 4/2,3/0 2.5Y 5/2		
5					

PS66/308-3 SL

Yermak Plateau

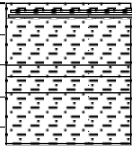
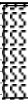
ARK XX/3

Recovery: 5.54 m

81° 07.30' N, 12° 35.97' E

Water depth: 2218 m

Lithology	Texture	Color	Description	Age
		10YR 4/3	0 - 37 cm: brown silty clay, homogeneous, large dropstone (6x2x3 cm in diameter) at 0-3 cm	
			37 - 38 cm: very dark brown silty clay	
			38 - 41 cm: brown silty clay	
			41 - 42 cm: very dark grayish brown silty clay	
		5Y 4/3	42 - 46 cm: dark brown and dark yellowish brown silty clay, laminated; mud clasts ("cottage cheese") at the base	
		5Y 4/1	46 - 50 cm: olive to dark olive gray silty clay	
			50 - 73 cm: dark gray silty clay; some lamination in lower part	
		2.5Y 4/4	73 - 117 cm: olive brown silty clay	
			117 - 123 cm: olive gray silty clay, some bioturbation	
			123 - 126 cm: very dark gray to dark olive gray silty clay	
			126 - 135 cm: dark gray silty clay	
		5Y 4/2	135 - 160 cm: olive gray silty clay	
		5Y 4/1	160 - 171 cm: olive gray silty sand, some brownish intervals, fining-upwards cycles	
			171 - 180 cm: dark gray (very) coarse and at base, fining upwards, erosional contact	
		5Y 5/2	180 - 212 cm: olive gray silty clay, some lamination	
			212 - 224 cm: dark yellowish brown silty clay, some bioturbation	
		5Y 4/1	224 - 289 cm: dark grayish brown to olive brown silty clay, partly bioturbated; dark gray intervals at 249-250, 252-254, 270-271 and 280-281 cm	
		5Y 5/2	289 - 292 cm: very dark grayish brown silty clay	
			292 - 297 cm: dark gray silty clay	
			297 - 302 cm: gray silty clay	
		10YR 4/2	302 - 337 cm: dark grayish brown to olive brown silty clay, some bioturbation	
			337 - 380 cm: olive brown, dark yellowish brown to light olive brown silty clay; dark brown to very dark brown layers at 337-338 and 371-372 cm	
		2.5 Y 4/4 to 4/2	380 - 389 cm: dark grayish brown silty clay	
			389 - 396 cm: dark olive gray silty clay	
			396 - 398 cm: very dark gray silty clay	
			398 - 406 cm: dark gray silty clay	
			406 - 414 cm: gray silty clay	
			414 - 415 cm: dark olive gray silty clay	
	2.5Y 3/2	415 - 436 cm: olive gray silty clay		
	2.5Y 4/0	dropstone (1 cm in diameter) at 420 cm		
	2.5Y 5/0	436 - 438 cm dark olive gray silty clay		
		438 - 447 cm: very dark gray silty clay		
	2.5Y 4/2 to 2.5Y 4/4	447 - 452 cm: dark olive gray silty clay; pink laminae at 454 cm		
		452 - 454 cm: very dark gray silty clay		
		454 - 459 cm: dark gray silty clay		
		459 - 466 cm: olive gray silty clay		
	2.5Y 4/4 to 2.5Y 5/4	466 - 470 cm: very dark gray silty clay		
		470 - 493 cm dark gray silty clay		
		493 - 500 cm: olive gray silty clay		
		500 - 504 cm: olive gray silty clay		
	2.5Y 4/2	504 - 512 cm: olive gray silty clay		
	5Y 3/2	512 - 515 cm: brown silty clay		
	5Y 4/1	515 - 521 cm: olive gray silty clay		
	5Y 5/1	521 - 525 cm dark olive gray silty clay, black spots		
	5Y 4/2	525 - 528 cm: olive gray silty clay		
	5Y 5/2	528 - 545 cm: dark gray silty clay, bioturbation between 490 and 530 cm		
		2.5Y 4/0		
		5Y 3/2		
		2.5Y 4/0		
		5Y 4/2		
		5Y 4/1		
		5Y 4/2		

	Lithology	Texture	Color	Description	Age
5			5Y 4/2 10YR 4/3 5Y 4/2 5Y 3/2 5Y 4/1		
6					
7					
8					
9					
10					

PS66/309-1 KAL

Yermak Plateau

ARK XX/3

Recovery: 7.65 m

81° 11.22' N, 12° 59.07' E

Water depth: 2270 m

	Lithology	Texture	Color	Description	Age
0				0 - 4 cm coring lost	
			10YR 4/3	0 - 52 cm: brown silty clay, homogeneous, some bioturbation 52 - 61 cm: very dark brown to dark yellowish brown silty clay; coarser layer with mud clasts ("cottage cheese") at 57 and 61 cm	
			10YR 3/3/2	61 - 67 cm: olive silty clay	
			5Y 4/3	67 - 89 cm: dark gray silty clay; 88 - 89 cm coarser and very dark gray	
			5Y 4/1	89 - 138 cm: olive brown silty clay, slightly bioturbated 138 - 147 cm: olive gray silty clay, some bioturbation	
			5Y 4/2	147 - 155 cm: dark olive gray silty clay 155 - 190 cm: olive gray silty clay, some bioturbation; very dark brown (10YR 4/2) intervals at 157 and 178-179 cm	
1			2.5Y 4/4	190 - 204 cm: dark grayish brown silty clay, in upper part some bioturbation 204 - 210 cm: alternation of dark grayish brown silty clay and olive gray sandy clayey silt	
			5Y 4/2	210 - 223 cm: alternation of dark gray to very dark gray sandy silty clay and sand	
			5Y 3/2	223 - 254 cm: dark gray sand, fining upwards; lower part (246 - 254 cm) silty sand and sand alternation	
			5Y 5/2	254 - 272 cm: dark gray to very dark gray coarse sand; 3 silty sand layers between 263 and 265 cm; very sharp (erosional?) contact	
			2.5Y 4/2	272 - 299 cm: olive gray silty clay, some bioturbation 299 - 310 cm: very dark brown silty clay, strongly mottled/bioturbated	
2			5Y 5/1 to 5Y 4/1	310 - 354 cm: dark grayish brown silty clay, partly bioturbated; dark brown layers at 312, 317, 320, 333 - 336, and 339 - 400 cm; very dark gray layers at 323 - 325, 327 - 328, and 347 - 349 cm; large dropstone (7x2x4) at 327-329 cm, coal fragment at 341-342 cm	
			5Y 5/2	354 - 360 cm: dark grayish brown silty sandy clay, dark spots, bioturbated dropstone (diameter of 2 cm) at 358-360 cm	
			5Y 5/1 to 5Y 4/1	360 - 365 cm: alternation of very dark brown silty clay and dark grayish brown silty clay	
			5Y 5/2	365 - 372 cm: very dark grayish brown silty (sandy) clay 372 - 380 cm: dark gray to very dark gray silty clay; dropstone (diameter of 1 cm) at 380 cm	
3			10YR 4/2	380 - 454 cm: dark grayish brown silty clay, partly mottled bioturbated (especially in the upper part); very dark brown layers at 426 - 428, 447, 448, 451, and 452 cm; large dropstone (diameter of 3 cm) at 394 - 397 cm, several small dropstones at 392 - 394 and 430 - 443 cm	
			2.5Y 4/2	454 - 510 cm: dark grayish brown to light olive brown silty clay; between 464 - 485 cm very dark brown layers/mottling, dark gray clayey silty sand layers at 497, 501, and 503 cm	
			2.5Y 3/2	510 - 520 cm: dark olive gray sandy silty clay and clayey sandy silt	
			2.5Y 4/0	520 - 525 cm: very dark olive gray clayey silty sand and sandy silt layers, sharp base	
			2.5Y 4/2	525 - 528 cm: very dark gray clayey sandy silt	
			2.5Y 3/2	528 - 545 cm: dark olive gray silty clay, very dark gray mottling	
4			2.5Y 4/0	545 - 572 cm: olive gray silty clay, few black spots; large dropstone (6x3x2) at 560 - 562 cm	
			2.5Y 4/2	572 - 578 cm: very dark gray to dark olive gray sandy silty clay; mottled dropstone (4 cm in diameter) at 575 - 576 cm	
			2.5Y 4/2	578 - 585 cm: olive gray silty clay	
			2.5Y 4/2	585 - 596 cm: dark olive gray sandy silty clay, mottled	
			2.5Y 4/2	596 - 598 cm: gray silty clay	
			2.5Y 4/2	598 - 600 cm: dark olive gray silty clay	
			2.5Y 4/2	600 - 610 cm: olive gray silty clay	
			2.5Y 4/2	610 - 614 cm: very dark gray to dark olive gray sandy silty clay	
5			2.5Y 4/2 to 2.5Y 5/4	614 - 636 cm: dark olive gray silty clay	

	Lithology	Texture	Color	Description	Age			
5			5Y 3/2	636 - 641 cm: alternation of gray (5Y 5/1) and dark olive brown (10YR 3/2) silty clay				
			5Y 4/2					
			5Y 4/1	641 - 676 cm: dark gray silty clay; very dark gray intervals at 648 - 649 and 666 - 667 cm; dropstones (diamter of 1 cm) at 649 and 660 cm				
			5Y 4/2					
			5Y 3/1	676 - 685 cm: very dark gray silty clay				
			5Y 4/2					
			5Y 3/1	685 - 727 cm: dark gray silty clay				
			5Y 4/2					
			5Y 3/1	727 - 765 cm: Core catcher, dark gray and yellowish brown silty clay; coring disturbance; sandy material at bottom of the CC				
			5Y 4/2					
			6				5Y 3/1	
							5Y 4/2	
							5Y 3/1	
							5Y 4/2	
							2.5Y 3/0	
							5Y 3/2	
7			5Y 4/1					
			5Y 3/1					
			5Y 4/1					
			5Y 4/1					
7.65		Core Catcher	5Y 4/1	Note: sand found at base of CC				
			10YR 5/2					
8								
9								
10								

PS66/311-3 (SL)

Yermak Plateau

ARK-XX/3

Recovery: 4.93 m

81° 41.78' N, 13° 28.20' E

Water depth: 2192 m

Depth in core (m)	Lithology	Texture	Color	Description	Age
	0			10YR4/3	0-25 cm: brown silty clay
			10YR3/2	25-27 cm: very dark brown silty clay, lamination	
			5/4	27-34 cm: yellowish brown and dark brown silty clay, coarser darker layers at 28 and 31 cm ("cottage cheese")	
			2.5Y4/0	34-68 cm: dark gray silty clay	
			2.5Y5/0	68-73 cm: gray silty clay	
			2.5Y5/2	73-103 cm: grayish brown silty clay	
			2.5Y5/0	103-112 cm: dark olive gray silty clay, small dropstone (0.5 cm) at base	
			2.5Y5/2	112-118 cm: gray silty clay	
			2.5Y5/2	118-125 cm: (light) gray silty clay	
1			2.5Y5/2	125-189 cm: grayish brown silty clay, brownish layer at 153-154 cm	
			5Y3/2	189-200 cm: gray silty clay	
			2.5Y5/0	200-204 cm: grayish brown silty clay (brown at top and base)	
			2.5Y6/0	204-220 cm: gray silty clay; small dropstone at 204 cm	
			2.5Y5/2	220-245 cm: grayish brown silty clay	
			2.5Y5/2	245-318 cm: (dark) grayishbrown silty clay;	
			2.5Y5/2	gray and dark gray silty clay lense at 257-259 cm (burrow?);	
			2.5Y5/2	small mud clasts at 268 and 272 cm; brownish layers at	
			2.5Y5/2	311-312 cm (sandy), 314-315 cm, and 317-318 cm	
			2.5Y5/2	318-334 cm: dark gray silty clay	
			2.5Y5/2	334-346 cm: gray silty clay	
			2.5Y5/2	346-354 cm: light gray silty clay	
			2.5Y5/2	354-393 cm: grayish brown silty clay; brownish layers at 372, 375, and	
			2.5Y5/2	378 cm	
2			2.5Y5/2	393-430 cm: olive gray silty clay, black spots; brown layer at 427 cm	
			2.5Y5/0	430-455 cm: (dark) grayish brown silty clay, some bioturbation	
			2.5Y5/2	455-493 cm: olive gray silty clay; sandy layer at 489 cm	
			2.5Y5/2		
			2.5Y4/2		
3			2.5Y4/2		
			2.5Y4/0		
			2.5Y5/0		
			2.5Y6/0		
			2.5Y5/2		
4			5Y4/2		
			2.5Y4/2		
			5Y4/2		
5	End of core				

PS66/312-2 SL

Yermak Plateau

ARK XX/3

Recovery: 6.33 m

81° 41.24' N, 13° 42.65' E

Water depth: 2275 m

	Lithology	Texture	Color	Description	Age
0				0 - 42 cm: brown silty clay, homogeneous	
				42 - 44 cm: dark grayish brown silty clay	
				44 - 45 cm: very dark grayish brown silty clay	
				45 - 50 cm: brown and dark grayish brown silty clay, laminated; mud clasts ("cottage cheese")	
				50 - 54 cm: dark olive gray silty clay	
				54 - 75 cm: dark gray silty clay	
				75 - 80 cm: gray silty clay	
				80 - 106 cm: grayish brown silty clay, some bioturbation	
				106 - 112 cm: dark olive gray silty clay; two dropstones (0.5 cm) at 106 cm	
				112 - 117 cm: olive gray and dark olive gray silty clay, laminated	
				117 - 133 cm: grayish brown silty clay, olive gray layers at 122 and 123 cm	
				133 - 146 cm: olive gray silty clay	
				146 - 154 cm: grayish brown silty clay	
				154 - 179 cm: alternation of pale brown and brown silty clay (1 cm thick horizons); dark brown layers at 154-155 and 174-179 cm	
				179 - 225 cm: grayish brown silty clay, partly bioturbated	
				225 - 228 cm: dark grayish brown silty clay	
				228 - 266 cm: dark grayish brown silty clay; dark gray and dark brown horizons (1 cm thick) at 37-38, 43-44, 50, 54-55 (sandy), 59, 62, 65 (mud clasts), and 66 cm (mud clasts)	
				266 - 275 cm: dark gray silty clay	
				275 - 282 cm: gray silty clay	
				282 - 288 cm: light gray silty clay	
288 - 295 cm: olive gray silty clay					
295 - 326 cm: grayish brown silty clay, partly bioturbated					
326 - 329 cm: dark grayish brown silty clay					
329 - 430 cm: grayish brown silty clay, some bioturbation; weak red (10R 5/3) layer at 51-52 cm					
430 - 433 cm: dark olive gray sandy silty clay					
433 - 436 cm: grayish brown silty clay					
436 - 443 cm: olive gray silty clay					
443 - 455 cm: dark olive gray silty clay					
455 - 457 cm: very dark gray silty clay					
457 - 468 cm: dark gray silty clay					
468 - 485 cm: gray silty clay					
485 - 489 cm: very dark olive gray silty clay					
489 - 495 cm: olive silty clay					
495 - 501 cm: very dark olive gray silty clay, some amount of sand					
501 - 503 cm: gray silty clay, thin very dark gray laminae on top					
503 - 506 cm: very dark olive gray silty clay; dropstone at 505 cm					
506 - 512 cm: olive silty clay					
512 - 514 cm: very dark olive gray silty clay, dark gray horizon at 513 cm					
514 - 522 cm: olive silty clay					
522 - 533 cm: alternation of very dark gray, dark gray, and dark olive gray silty clay, some amount of sand					
533 - 537 cm: dark olive gray silty clay					
537 - 539 cm: gray silty clay					
539 - 545 cm: very dark gray silty clay					
545 - 547 cm: gray silty clay					
547 - 550 cm: very dark gray silty clay					
550 - 574 cm: alternation of dark olive gray and very dark gray silty clay (2-3 cm thick layers)					
574 - 592 cm: olive gray silty clay					
592 - 598 cm: gray silty clay, homogeneous					
598 - 633 cm: olive gray silty clay; brownish horizon at 616-617 cm					
1					
2					
3					
4					
5					

		Lithology	Texture	Color	Description	Age					
5	Depth in core (m)			5Y 5/2							
				5Y 5/2							
				2.5Y 4/0-5/0							
				5Y 3/2							
				5Y 3/2 and 2.5Y 4/0							
				5Y 4/2							
				5Y 5/1							
				5Y 5/2							
				6							
				7							
8											
9											
10											

PS66/313-1

Yermak Plateau

ARK XX/3

Recovery: 4.49 m

81° 45.56' N, 14° 16.31' W

Water depth: 2298 m

	Lithology	Texture Color	Description	Age
0		10YR4/3	0 - 43 cm: brown silty clay, homogeneous; very dark brown layer at 39-40 cm	
		2.5Y 4/0	43 - 49 cm: alternation of brown and very dark brown silty clay, grayish brown layers/laminae (0.1-0.5 cm thick), lowermost layer "semi-lithified"?	
		5Y 4/2	49 - 54 cm: brown silty clay	
		5Y 4/2	54 - 68 cm: dark gray silty clay	
		5Y 4/2	68 - 96 cm: olive gray silty clay	
		5Y 4/2	96 - 100 cm: dark olive gray silty clay	
		5Y 4/2	100 - 102 cm: very dark gray silty clay	
		5Y 4/2	102 - 365 cm: olive gray silty clay, partly bioturbated	
		5Y 4/2	silty sand layer at 134-136 cm, black lenses at 319-325 cm, very dark gray intervals/parts between 249 and 260, 274 and 278, and 346 and 349 cm; dropstone (1 cm in diameter) at 309-310 cm	
		5Y 4/2	365 - 370 cm: dark olive gray more sandy interval	
		5Y 5/1	370 - 449 cm: olive gray silty clay, very dark gray layers/spots throughout	
		2.5Y 4/3	disturbed between 390 and 400 cm and below 435 cm	
5				

PS66/318-4

Yermak Plateau

ARK XX/3

Recovery: 3.15 m

81° 18.60' N, 12° 02.71' E

Water depth: 1262 m

Depth in core (m)	Lithology	Texture Color	Description	Age
0			0 - 6 cm: light olive brown clayey silty sand 6 - 11 cm: light olive brown clayey sandy silt 11-14 cm: light olive brown silty sand 14-15 cm: light olive brown sandy clayey silt, sharp contact at base 15-23 cm: light olive brown silty sand 23-32 cm: light olive brown sandy clayey silt 32-36 cm: light olive brown silty sand 36-41 cm: light olive brown sandy silty clay 41-50 cm: light olive brown sandy clayey silt to clayey silty sand 50-67 cm: light olive brown to brown sandy silty clay 67-71 cm: (olive) gray (sandy) silty clay, sharp erosional base 71-80 cm: olive gray silty sand, dropstone (2 cm in diameter) at 51-53 cm 81-85 cm: dark yellowish brown sandy clayey silt 85-89 cm: light olive (sandy) silty clay, sharp erosional contact 89-100 cm: light olive brown silty sand, coarsening upwards 100-103 cm: dark brown silty clay, mud clast layer ("cottage cheese") 103-118 cm: alternation of light olive brown and very dark brown silty clay, laminated	
		2.5Y 5/4		
		2.5Y 5/4-10YR 5/3		
		5Y 5/1		
		5Y 5/2		
		10YR 4/4		
1		2.5Y 5/4		
		5Y 5/1 to 5Y 4/1		
		10YR 5/6		
		2.5Y 5/2		
		2.5Y 4/2		
		2.5Y 3/2		
		2.5Y 3/0		
2		2.5Y 4/0		
		5Y 5/2		
		2.5Y 5/0		
		2.5Y 4/2		
		2.5Y 3/0		
		5Y 4/2-3/2		
3		CC		
			217-233 cm: olive gray silty sand, very large dropstone/gneiss (11x5x4cm), dark gray shist (2x2x7 cm), common smaller dropstones, black coarse sand lense 233-244 cm: gray clayey silty sand, small dropstones 244-258 cm: grayish brown sandy silty clay, mud clasts, small dropstones, large dropstone/mud clast (5x3x2 cm) 258-261 cm: brown clayey sandy silt, mud clasts 261-270 cm: clayey silty sand, small dropstones 270-280 cm: olive gray and dark olive gray sandy clayey silt, disturbed	
			+ 35 cm Core Catcher (olive gray and dark olive gray sandy clayey silt, disturbed)	
4				
5				

PS66/319-1

Yermak Plateau

ARK XX/3

Recovery: 3.13 m

81° 24.49' N, 13° 48.79' E

Water depth: 2178 m

	Lithology	Texture Color	Description	Age	
0		10YR4/3	<p>Note: overpenetration of gravity corer; based on GKG PS66/306, 40 cm of brown silty clay are probably missing</p> <p>0 - 5 cm: brown and very dark brown silty clay, mud clasts at 3 cm 5 - 11 cm: olive brown silty clay, brownish layer at 10 cm 11 - 24 cm: dark gray silty clay 24 - 28 cm: gray silty clay 28 - 34 cm: light gray silty clay 34 - 46 cm: grayish brown sandy silty clay 46 - 58 cm: grayish brown sandy silty clay, mud clasts ("cottage cheese") 58 - 68 cm: gray (sandy) silty clay 68 - 84 cm: olive gray silty clay 84 - 90 cm: dark olive gray silty clay 90 - 92 cm: very dark gray silty clay 92 - 103 cm: olive gray silty clay 103 - 127 cm: grayish brown silty clay 127 - 200 cm: light olive brown and olive gray silty clay, bioturbated; middle part disturbed 200 - 240 cm: olive gray, dark olive gray and dark grayish brown silty clay, black lenses, layers, and spots 240 - 267 cm: dark gray sandy silty clay to clayey silty sand, fining upwards 267 - 283 cm: olive gray silty clay 283 - 296 cm: dark gray to very dark gray silty clay 296 - 313 cm: very dark gray silty clay (300-313 cm core catcher) below 290 cm laminated</p> <p>(270 - 300 cm tilted)</p>		
		2.5Y 4/4			
		2.5Y 4/0			
		2.5Y 5/0			
		2.5Y 6/0			
		2.5Y 5/2			
		2.5Y 5/0			
		5Y 5/2			
		5Y 4/2			
		5Y 5/2			
1		2.5Y 5/2			
		2.5Y 5/4 and 5Y 5/2			
		5Y 4/2 and 5Y 3/2 and 2.5Y 4/2			
2		5Y 4/1			
		5Y 4/2			
		2.5Y 4/0 to 2.5Y 3/0			
3		5Y 3/2			
4					
5					

PS66/321-4 KAL

Yermak Plateau

ARK XX/3

Recovery: 7.11 m

82° 10.27' N, 18° 13.47' E

Water depth: 2360 m

Lithology	Texture	Color	Description	Age
		10YR 4/3	0 - 37 cm: brown silty clay, homogeneous, some bioturbation; dark brown laminae at 26 and 36 cm	
		10YR 3/3/2	37-45 cm: (dark) brown and very dark grayish brown laminated silty clay; mud clasts at 42 cm	
		2.5Y 4/0	45-48 cm: grayish brown (2.5Y 5/2) and dark brown laminae	
		2.5Y 5/0	48-73 cm: dark gray silty clay; brownish near top (48-51 cm)	
		2.5Y 3/0	73-80 cm: gray silty clay	
		2.5Y 6/2	80-82 cm: dark gray silty clay	
		10YR 5/2	82-87 cm: very dark gray silty clay, sharp contact at bottom	
		10YR 4/3	87-113 cm: light brownish silty clay, brownish horizons at 95-100 cm	
		10YR 5/2	113-127 cm: grayish brown silty clay, lower part (123-127 cm) laminated	
		10YR 5/2	127-128 cm: very dark brown silty clay	
		10YR 5/2	128-135 cm: brown silty clay; very dark brown laminae at 129, 132 and 133 cm	
		10YR 4/3	135-146 cm: grayish brown silty clay, laminated	
		10YR 5/2	146-149 cm: very dark brown silty clay, mud clasts at base	
		10YR 5/2	149-159 cm: grayish brown silty clay	
		10YR 5/2	159-168 cm: gray silty clay	
		2.5Y 5/0	168-234 cm: grayish brown silty clay; brown laminae at 198 and 202 cm	
		2.5Y 5/2	234-247 cm: grayish brown and brown silty clay, laminated	
		2.5Y 5/2 to 10YR 4/3	247-302 cm: dark olive gray silty clay	
		5Y 3/2	302-308 cm: gray silty clay	
		5Y 5/1	308-457 cm: grayish brown and dark grayish brown silty clay; some bioturbation between 370 and 400 cm; dark gray interval at 309-310 cm, dark brown laminae at 384-386 cm and 390-391 cm	
2.5Y 5/2 to 2.5Y 4/2	457-459 cm: olive gray (5Y 4/2) clayey sandy silt			
2.5Y 5/0	459-461 cm: grayish brown silty clay			
2.5Y 5/2	461-468 cm: gray silty clay			
2.5Y 5/0	468-495 cm: grayish brown silty clay; olive gray sandy intervals at 475, 476, and 486-489 cm; 2 dropstones (1 cm in diameter) at 487-489 cm			
2.5Y 5/0	495-505 cm: gray silty clay; brownish horizons at 500-501 and 504-505 cm			
2.5Y 5/0	505-511 cm: grayish brown silty clay			
2.5Y 5/0	511-516 cm: dark grayish brown silty clay (515-516 cm dark gray)			
2.5Y 5/0	516-582 cm: dark olive gray to very dark grayish brown silty clay; dropstone at 557-558 cm			
2.5Y 5/0	582-595 cm: very dark gray (sandy) silty clay to silty sandy clay; fining upwards			
2.5Y 5/0	595-611 cm: very dark grayish brown to dark gray silty clay			
2.5Y 5/0	611-711 cm: dark olive gray to very dark gray silty clay; brownish laminae at 624 cm, black lenses at 627-628 cm and 698-699 cm			

		Lithology	Texture	Color	Description	Age
5				2.5Y 5/0		
				2.5Y 4/2		
				5Y 3/2 to 2.5Y 3/2		
				2.5Y 3/0		
				2.5Y 3/2		
6				5Y 3/1 to 5Y 3/2		
7						
8						
9						
10						

PS66/322-3 SL

Yermak Plateau

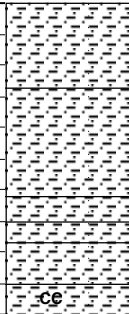

ARK XX/3

Recovery: 6.00 m

82° 05.40' N, 18° 05.25' E

Water depth: 3028 m

Depth in core (m)	Lithology	Texture	Color	Description	Age
0			10YR 4/3	0-14 cm: brown silty clay, some sand	
			10YR 3/2	14-27 cm: very dark grayish brown sandy silty clay to clayey sandy silty, fining upwards	
1			10YR 4/2	27-42 cm: brown silty clay	
			5Y 3/2	42-60 cm: dark olive gray silty clay	
			5Y 3/2	60-66 cm: dark olive gray silty sandy clay	
			5Y 3/2	66-80 cm: dark olive gray silty clay	
			5Y 3/2	80-86 cm: dark gray silty clay	
			5Y 3/2	86-101 cm: gray silty clay	
			2.5Y 4/0	101-107 cm: olive gray silty clay, some sand	
			2.5Y 5/0	107-138 cm: dark olive gray (sandy) silty clay to silty sandy clay, fining upwards	
			5Y 4/2	138-145 cm: dark olive clay silty clay; sharp base and top	
			5Y 3/2	145-147 cm: olive gray silty clay	
2			5Y 3/2	147-149 cm: olive gray silty sandy clay	
			5Y 3/2	149-154 cm: olive gray silty clay	
			5Y 3/2	154-161 cm: olive gray silty sandy clay	
			5Y 4/2	161-172 cm: olive gray silty clay; brownish interval at 170-172 cm	
			5Y 4/2	172-179 cm: dark gray silty clay	
			5Y 4/2	179-184 cm: dark olive gray silty clay to clayey sandy silt, fining upwards	
			2.5Y 4/0	184-186 cm: dark olive gray sandy clayey silt	
			5Y 3/2	186-188 cm: dark olive gray silty clay	
			5Y 3/2	188-200 cm: olive gray sand	
			5Y 4/2	200-207 cm: olive gray silty sand	
3			5Y 4/2	207-222 cm: olive gray silty clay; brownish laminae at 219 and 220 cm	
			5Y 4/2	222-226 cm: dark gray silty clay	
			2.5Y 4/0	226-232 cm: (dark) gray silty clay	
			5Y 4/2	232-269 cm: olive gray silty clay; more sandy layer at 249 cm	
			5Y 4/2	269-273 cm: dark olive gray silty sand	
			5Y 4/2	273-280 cm: dark olive gray silty clay	
			5Y 4/2	280-300 cm: dark gray silty clay	
			5Y 3/2	300-309 cm: olive gray silty sandy clay	
			5Y 3/2	309-319 cm: olive gray silty clay	
			5Y 4/1	319-322 cm: very dark gray silty clay	
4			5Y 4/1	322-329 cm: very dark gray clayey sandy silt	
			5Y 4/2	329-338 cm: olive gray silty clay	
			5Y 4/2	338-340 cm: dark gray silty clay	
			5Y 4/2	340-350 cm: dark gray clayey silty sand	
			5Y 3/1	350-365 cm: olive gray silty clay, sharp (erosional?) base	
			5Y 4/2	365-400 cm: dark olive gray sandy silty clay	
			5Y 4/1	400-405 cm: dark olive gray sandy silty clay	
			5Y 4/1	405-438 cm: very dark gray silty clay	
			5Y 4/2	438-453 cm: dark gray silty clay; brownish laminae at 444 and 449 cm	
			5Y 3/2	453-480 cm: dark olive gray silty clay	
5			5Y 3/2	480-496 cm: olive gray silty clay	
			5Y 3/2	496-500 cm: dark gray silty clay	
			5Y 3/2	500-527 cm: dark olive gray silty clay	
			5Y 3/2	527-563 cm: olive gray silty clay	
			5Y 3/2	563-569 cm: dark olive gray silty clay	
			5Y 3/2	569-600 cm: olive gray silty clay; dark gray layer at 577 cm	

	Lithology	Texture	Color	Description	Age
5			5Y 3/2		
			5Y 4/2		
			5Y 3/2		
			5Y 4/2		
6					
7					
8					
9					
10					

PS66/323-3

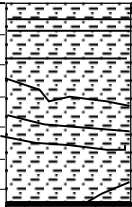
Yermak Plateau

ARK XX/3

Recovery: 0.66 m

82° 18.44'N, 22° 59.67' W

Water depth: 3913 m

Depth in core (m)	Lithology	Texture	Color	Description	Age
	0			10YR 5/3 2.5Y 4/0 2.5Y 6/0 2.5Y 4/0	<p>0 - 4 cm: brown (10YR 5/3) silty clay, soft</p> <p>4 - 7 cm: brown (10YR 4/3) silty clay, soft</p> <p>7 - 16 cm: brown (10YR 5/3) silty clay, soft</p> <p>16 - 19 cm: dark brown (10YR 3/3) silty clay, firm thin pale brown laminae at bottom, sharp contact</p> <p>19 - 30 cm: dark gray silty clay, firm</p> <p>30 - 38 cm: light gray silty clay, very firm: light gray/dark gray laminae, tilted, sharp contact at bottom</p> <p>38 - 66 cm: dark gray silty clay, firm; light gray interval at 40-44 cm</p> <p>Coring disturbance below 60 cm</p>
1					
2					
3					
4					
5					

PS66/325-3 SL

Svalbard Continental Margin


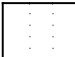
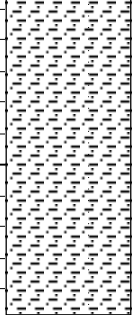
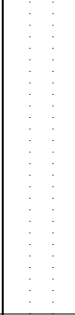
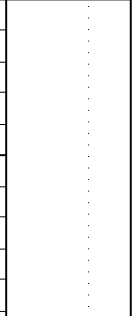

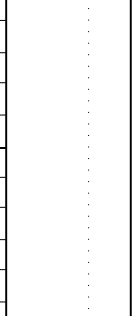

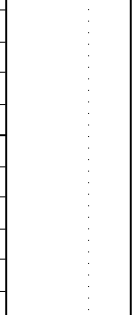

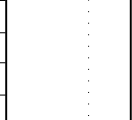

ARK XX/3

Recovery: 6.48 m

81° 26.18' N, 25° 59.86' E

Water depth: 896 m

	Lithology	Texture	Color	Description	Age
0				0 - 2 cm: very dark brown silty clay	
				2 - 4 cm: olive brown silty clay	
			5Y 4/1	4 - 5 cm: very dark brown silty clay	
			5Y 4/1	5 - 10 cm: olive brown silty clay, mud clasts at 5 and 8-9 cm	
			5Y 4/1	10 - 58 cm: dark gray silty clay, homogeneous	
			5Y 4/1	58 - 230 cm: very dark gray to dark olive gray silty clay, black spots between 85 and 108 cm and 159 and 230 cm; dropstone (1 cm in diameter) at 99-100 cm	
			5Y 4/1	230 - 252 cm: very dark gray to olive gray (sandy) silty clay, black spots; mud clast interval at 235-237 cm, dropstone (2 cm in diameter) at 248-250 cm	
			5Y 4/1	252 - 263 cm: gray silty clay	
			5Y 3/1 to 5Y 3/2	263 - 268 cm: light gray silty clay, some amount of sand	
			5Y 3/1 to 5Y 3/2	268 - 274 cm: grayish brown sandy silty clay; dropstone (1 cm in diameter) at 273-274 cm	
			5Y 3/1 to 5Y 3/2	274 - 318 cm: grayish brown silty clay (more gray between 279 and 283 cm); thin brownish layers at 273, 277, 287-288, 296, 303-304, 308-310 (mud clasts; "cottage cheese"), 314, 316, and 318 cm	
			5Y 3/1 to 5Y 3/2	318 - 347 cm: dark gray silty clay	
			5Y 3/1 to 5Y 3/2	347 - 516 cm: very dark gray to dark olive gray silty clay, black spots; dark brown laminae/intervals at 348-349, 350, 353, 358, 386-387, and 396-399 cm	
			5Y 3/1 to 5Y 3/2	516 - 524 cm: gray sandy silty clay with several dropstones (diameter of 3 and 1 cm, and smaller ones), diamicton	
			5Y 3/1 to 5Y 3/2	524 - 531 cm: olive gray sandy silty clay	
			5Y 3/1 to 5Y 3/2	531 - 533 cm: very gray sandy silty clay	
			5Y 3/1 to 5Y 3/2	533 - 545 cm: olive gray sandy silty clay	
			5Y 3/1 to 5Y 3/2	545 - 648 cm: very dark gray to dark olive gray silty clay, abundant black spots between 560 and 596 cm and 604 and 648 cm	
			5Y 3/1 to 5Y 3/2	545 - 648 cm: very dark gray to dark olive gray silty clay, abundant black spots between 560 and 596 cm and 604 and 648 cm	
			5Y 3/1 to 5Y 3/2	545 - 648 cm: very dark gray to dark olive gray silty clay, abundant black spots between 560 and 596 cm and 604 and 648 cm	
			5Y 3/1 to 5Y 3/2	545 - 648 cm: very dark gray to dark olive gray silty clay, abundant black spots between 560 and 596 cm and 604 and 648 cm	
			5Y 3/1 to 5Y 3/2	545 - 648 cm: very dark gray to dark olive gray silty clay, abundant black spots between 560 and 596 cm and 604 and 648 cm	
			5Y 3/1 to 5Y 3/2	545 - 648 cm: very dark gray to dark olive gray silty clay, abundant black spots between 560 and 596 cm and 604 and 648 cm	
			5Y 3/1 to 5Y 3/2	545 - 648 cm: very dark gray to dark olive gray silty clay, abundant black spots between 560 and 596 cm and 604 and 648 cm	
			5Y 3/1 to 5Y 3/2	545 - 648 cm: very dark gray to dark olive gray silty clay, abundant black spots between 560 and 596 cm and 604 and 648 cm	
			5Y 3/1 to 5Y 3/2	545 - 648 cm: very dark gray to dark olive gray silty clay, abundant black spots between 560 and 596 cm and 604 and 648 cm	
			5Y 3/1 to 5Y 3/2	545 - 648 cm: very dark gray to dark olive gray silty clay, abundant black spots between 560 and 596 cm and 604 and 648 cm	
			5Y 3/1 to 5Y 3/2	545 - 648 cm: very dark gray to dark olive gray silty clay, abundant black spots between 560 and 596 cm and 604 and 648 cm	
			5Y 3/1 to 5Y 3/2	545 - 648 cm: very dark gray to dark olive gray silty clay, abundant black spots between 560 and 596 cm and 604 and 648 cm	
			5Y 3/1 to 5Y 3/2	545 - 648 cm: very dark gray to dark olive gray silty clay, abundant black spots between 560 and 596 cm and 604 and 648 cm	
			5Y 3/1 to 5Y 3/2	545 - 648 cm: very dark gray to dark olive gray silty clay, abundant black spots between 560 and 596 cm and 604 and 648 cm	
			5Y 3/1 to 5Y 3/2	545 - 648 cm: very dark gray to dark olive gray silty clay, abundant black spots between 560 and 596 cm and 604 and 648 cm	
			5Y 3/1 to 5Y 3/2	545 - 648 cm: very dark gray to dark olive gray silty clay, abundant black spots between 560 and 596 cm and 604 and 648 cm	
			5Y 3/1 to 5Y 3/2	545 - 648 cm: very dark gray to dark olive gray silty clay, abundant black spots between 560 and 596 cm and 604 and 648 cm	
			5Y 3/1 to 5Y 3/2	545 - 648 cm: very dark gray to dark olive gray silty clay, abundant black spots between 560 and 596 cm and 604 and 648 cm	
			5Y 3/1 to 5Y 3/2	545 - 648 cm: very dark gray to dark olive gray silty clay, abundant black spots between 560 and 596 cm and 604 and 648 cm	
			5Y 3/1 to 5Y 3/2	545 - 648 cm: very dark gray to dark olive gray silty clay, abundant black spots between 560 and 596 cm and 604 and 648 cm	
			5Y 3/1 to 5Y 3/2	545 - 648 cm: very dark gray to dark olive gray silty clay, abundant black spots between 560 and 596 cm and 604 and 648 cm	
			5Y 3/1 to 5Y 3/2	545 - 648 cm: very dark gray to dark olive gray silty clay, abundant black spots between 560 and 596 cm and 604 and 648 cm	

Depth in core (m)	Lithology	Texture	Color	Description	Age
5			5Y 3/1, 5Y 3/2		
			5Y 4/1		
			5Y 4/2		
			5Y 3/1 to 5Y 3/2		
6					
7					
8					
9					
10					

PS66/327-3 KAL

Svalbard Continental Margin

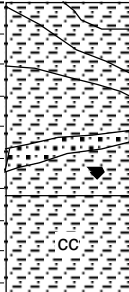
ARK XX/3

Recovery: 5.92 m

81° 00.92' N, 17° 09.39' E

Water depth: 701 m

	Lithology	Texture Color	Description	Age
0		5Y 5/2	0 - 22 cm: dark olive gray sandy silty clay, upper part disturbed	
			22 - 56 cm: dark olive gray silty clay, brownish horizons at 38-53 cm	
			56 - 200 cm: olive gray silty clay, brownish intervals of few cm in thickness, faulted	
			200 - 300 cm: dominantly silty clay with sandy silty clay intervals, colour changes from olive gray, dark gray, very dark gray, brown, to brownish gray;	
			interval between 265 and 285 cm folded?;	
			small dropstones at 210-240, 272-278, and 291-297 cm	
		5Y 4/2	300 - 400 cm: dark olive gray silty clay, brownish intervals (tilted/faulted)	
			400 - 500 cm: olive gray, brown, dark gray, dark grayish brown (sandy) silty clay, faulted/tilted;	
			large dropstones at 407-418 (2x6x10 in diameter), 474-478 (3 cm in diameter), 478-480 (1x3x5), and 480-482 cm (8x2x3)	
			500 - 562 cm: dark olive gray silty clay, brown horizons, faulted; clayey sandy silt at 543-552 cm; dropstone (3 cm in diameter) at 555-557 cm	
			562 - 592 cm: core catcher (dark olive gray silty clay)	
		5Y 4/2, 10YR 4/3 2.5Y 4/0 2.5Y 3/0		
		5Y 3/2		
		5Y 3/2, 10YR 4/2 2.5Y 4/2		
5				

	Lithology	Texture	Color	Description	Age
5			5Y 3/2		
6					
7					
8					
9					
10					

PS66/329-3 (SL)

Yermak Plateau

ARK-XX/3

Recovery: 4.82 m

81° 36.31' N, 13° 06.13' E

Water depth: 2211 m

	Lithology	Texture	Color	Description	Age
0			10YR4/3	0-43 cm: brown silty clay 43-50 cm: very dark brown and brown silty clay, coarser at 46-47 and 49 cm (mud clasts, "cottage cheese") 50-55 cm: olive gray silty clay 55-70 cm: gray silty clay	
			10YR3/2-4/3 5Y4/2	70-111 cm: (light) brownish gray silty clay	
			2.5Y5/0	111-114 cm: dark olive gray silty clay	
			2.5Y5/2	114-117 cm: very dark brown (10YR 3/2) silty clay, mud clasts	
				117-118 cm: very dark gray silty clay, sharp base	
			5Y 3/2	118-131 cm: gray silty clay	
				131-158 cm: grayish brown silty clay; bioturbation between 135 and 145 cm; brownish lamina at 149 cm	
1			5Y 3/2	158-167 cm: dark grayish brown silty clay, bioturbated	
				167-179 cm: olive gray and dark olive gray silty clay	
			5Y5/1	179-213 cm: grayish brown silty clay; dark brown laminae at 212 and 213 cm	
			2.5Y5/2	213-226 cm: olive gray silty clay	
				226-256 cm: grayish brown silty clay; dark brown lamina at 256 cm	
			2.5Y4/2	256-282 cm: dark grayish brown silty clay	
			5Y 4/1/2	282-295 cm: grayish brown silty clay; sandy layer at 289 cm	
				295-298 cm: brown and dark brown silty clay; coarser layers (mud clasts) at 297 and 298 cm	
			2.5Y5/2	298-300 cm: dark gray silty clay	
				300-305 cm: gray silty clay	
2			5Y4/2	305-307 cm: light gray silty clay	
				307-313 cm: grayish brown silty clay	
			2.5Y5/2	313-326 cm: grayish brown silty clay	
				326-336 cm: dark grayish brown silty clay	
			2.5Y4/2	336-341 cm: gray silty clay	
				341-356 cm: olive brown silty clay	
			10YR 5/2 -2.5Y5/2	356-360 cm: gray silty clay	
				360-374 cm: olive gray silty clay	
			2.5Y5/0	374-382 cm: dark olive gray silty clay; some bioturbation	
				382-393 cm: olive gray silty clay	
			2.5Y5/2	393-456 cm: alternation of gray (2.5Y 4/0), grayish brown (2.5Y 5/2), olive gray (5Y 5/2) and dark olive gray (5Y 4/2) silty clay	
	456-482 cm: dark olive gray silty clay; some bioturbation				
3	2.5Y5/0				
		10YR 5/2			
	2.5Y4/2				
		2.5Y5/0			
	2.5Y4/4				
		2.5Y5/0			
	5Y4/2				
		5Y3/2			
	5Y4/2				
		5Y4/2			
4	2.5Y 4/0 and 2.5Y 5/2 and 5Y 5/2 and 5Y3/2				
		5Y3/2			
5	End of core				

PS66/330-2

Yermak Plateau

ARK XX/3

Recovery: 4.54 m

81° 32.88' N, 13° 21.71' W

Water depth: 2305 m

	Lithology	Texture Color	Description	Age
0		10YR4/3	0 - 41 cm: brown silty clay, dark brown laminae at 37-38, 39, and 40-41 cm	
			41 - 48 cm: brown and dark brown silty clay, laminated; mud clasts ("cottage cheese") at 41-42 and 47-48 cm	
		10YR 3/2	48 - 53 cm: olive gray silty clay, brownish at 52-53 cm	
		5Y 4/2	53 - 62 cm: dark gray silty clay	
			62 - 67 cm: gray silty clay	
			67 - 71 cm: light gray silty clay	
			71 - 107 cm: grayish brown silty clay, brownish at 105-107 cm	
			107 - 111 cm: dark olive gray silty clay	
		2.5Y 5/2	111 - 114 cm: very dark gray silty clay	
1			114 - 126 cm: gray silty clay, brownish laminae at 116 and 119 cm	
			126 - 153 cm: dark grayish brown silty clay, brownish laminae at 137-138 and 146-147 cm	
		5Y 5/1	153 - 342 cm: olive gray silty clay with common dark gray lenses/layers throughout; very dark gray interval between 232 and 242 cm, light gray laminae at 140, 142, and 144 cm; dropstone (1 cm in diameter) at 72 cm	
		2.5Y 4/2	342 - 346 cm: olive gray silty clay	
			346 - 355 cm: dark grayish brown silty clay; brownish layer at top, very dark brown layer at bottom	
			355 - 358 cm: dark gray silty clay	
			358 - 371 cm: gray silty clay	
			371 - 372 cm: dark olive gray silty clay	
2			372 - 376 cm: olive gray silty clay	
			376 - 380 cm: dark olive gray silty clay	
			380 - 385 cm: olive gray silty clay	
			385 - 390 cm: dark olive gray silty clay	
			390 - 394 cm: very dark gray silty clay	
		5Y 5/2	394 - 432 cm: olive gray silty clay	
			432 - 437 cm: dark gray silty clay	
			437 - 452 cm: olive gray silty clay	
			452 - 457 cm: brown silty clay	
			457 - 459 cm: olive gray silty clay	
			disturbance between 180 and 280 cm ??	
3				
		5Y 5/0		
		5Y 5/1		
4		5Y 4/2		
		5Y 5/2		
5				

PS66/333-4

Yermak Plateau

ARK XX/3

Recovery: 3.02 m

81° 56.42 N, 08° 30.17' W

Water depth: 726 m

	Lithology	Texture Color	Description	Age
0		10YR4/3	0 - 15 cm: brown silty clay, single dark brown and gray layers at 7-8, 13, and 15 cm	
		2.5Y 5/4	15 - 19 cm: olive gray silty clay	
		5Y 5/1	19 - 52 cm: light olive gray (sandy) silty clay, common dropstones (0.5-2 cm in diameter) at 20-35 cm; mud clasts at 44-45 cm	
		2.5Y 5/4	52 - 59 cm: gray sandy silty clay	
		5Y 5/1	59 - 85 cm: light olive gray (sandy) silty clay, thin mud clasts layers at 68, 69, and 72 cm	
		5Y 5/1	85 - 92 cm: gray sandy silty clay	
		10YR5/6	92 - 119 cm: yellowish brown (sandy) silty clay, mud clasts at 99-102 and 108-109 cm	
		10YR5/6	119 - 131 cm: dark olive gray, dark gray, and very dark gray sandy silty clay, disturbed	
		5Y 5/1 to 5Y 4/2	131 - 171 cm: gray to olive gray sandy silty clay; sandy lenses/layers at 146-147 and 152-153 cm; dark gray between 162 and 167 cm	
		5Y 5/1 to 5Y 4/2	171 - 182 cm: olive gray silty clay, mottled/bioturbated	
		5Y 5/3	182 - 205 cm: light olive brown sandy silty clay, mottled(olive), sandy layer at 200 cm	
		5Y 5/3	205 - 221 cm: light olive brown, brown and dark olive gray silty clay, laminated	
		2.5Y 5/6	221 - 232 cm: very dark gray sandy silty clay	
		10YR3/2	232 - 244 cm: dark gray sandy silty clay	
		5Y 3/2	244 - 247 cm: gray sandy silty clay; dropstone at 245 cm	
		2.5Y 3/0	247 - 251 cm: light gray sandy silty clay	
		2.5Y 4/0	251 - 255 cm: olive gray sandy silty clay	
		5Y 3/2	255 - 258 cm: gray sandy silty clay; dropstone (0.5 cm in diameter) at 256 cm	
		5Y 3/2	258 - 267 cm: dark olive gray sandy silty clay	
		5Y 3/2	267 - 270 cm: dark gray sandy silty clay	
		5Y 3/2	270 - 272 cm: light gray sandy silty clay	
		5Y 3/2	272 - 276 cm: light olive gray sandy silty clay	
		5Y 3/2	276 - 280 cm: olive gray sandy silty clay; mud clasts	
		5Y 5/2	280 - 285 cm: gray silty clay	
		5Y 5/2	285 - 295 cm: olive gray sandy silty clay; brown layers at 290-295 cm	
		2.5Y 4/2	295 - 302 cm: dark gray sandy silty clay	
		2.5Y 4/2		
		2.5Y 4/2		
		2.5Y 4/2		
		2.5Y 4/2		
		2.5Y 4/2		
		2.5Y 4/2		
		2.5Y 4/2		
		2.5Y 4/2		
		2.5Y 4/2		
		2.5Y 4/2		
		2.5Y 4/2		
		2.5Y 4/2		
		2.5Y 4/2		
		2.5Y 4/2		
		2.5Y 4/2		
		2.5Y 4/2		
		2.5Y 4/2		
		2.5Y 4/2		
		2.5Y 4/2		
		2.5Y 4/2		
		2.5Y 4/2		

PS66/333-5

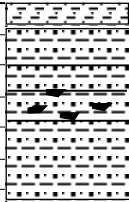
Yermak Plateau

ARK XX/3

Recovery: 0.63 m

81° 56.10'N, 08° 31.50' W

Water depth: 719 m

Depth in core (m)	Lithology	Texture	Color	Description	Age
	0			2.5Y 4/2 10YR5/2 10YR5/6 2.5Y 4/2	<p>0 - 4 cm: dark grayish brown sandy silty clay, partly laminated</p> <p>4 - 9 cm: grayish brown sandy silty clay</p> <p>9 - 18 cm: grayish brown silty sandy clay</p> <p>18 - 25 cm: grayish brown sandy silty clay</p> <p>25 - 28 cm: light brown silty clay</p> <p>28 - 38 cm: yellowish brown diamicton (common dropstones (1-2 cm in diameter))</p> <p>38 - 55 cm: dark grayish brown sandy silty clay, firm</p> <p>55 - 60 cm: weak red (10R 4/3) sandy silty clay ; white crystalls</p> <p>60 - 63 cm: dark gray sandy silty clay, mottled(olive), sandy layer at 200 cm</p> <p>50 - 63 cm coring disturbance</p>
1					
2					
3					
4					
5					

PS66/335-2 (SL)

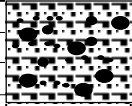
Yermak Plateau

ARK-XX/3

Recovery: 0.32 m

81° 36.05' N, 06° 34.06' E

Water depth: 658 m

Depth in core (m)	Lithology	Texture	Color	Description	Age
	0	 End of core		10YR4/3 10R4/3 10YR4/3	0 - 12 cm: brown silty sandy clay with abundant pebbles (up to 4 cm in diameter) 12 - 19 cm: weak red sandy silty clay with pebbles (up to 3 cm in diameter) 19 - 32 cm: brown silty sandy clay with abundant pebbles (up to 4 cm in diameter)
1					
2					
4					
5					

PS66/341-1 SL

Fram Strait

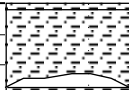
ARK XX/3

Recovery: 5.28 m

79° 44.07' N, 00° 44.97' E

Water depth: 2822 m

	Lithology	Texture	Color	Description	Age
0			10YR 4/3	0 - 30 cm: brown silty clay, homogeneous	
				30 - 35 cm: very dark brown silty clay; mud clasts at 34-35 cm	
			10YR 3/2	35 - 37 cm: yellowish brown silty clay	
			10YR 5/4	37 - 41 cm: grayish brown (2.5Y 5/2) and dark brown (10YR 3/3) silty clay	
			2.5Y 4/2	41 - 48 cm: dark grayish brown silty clay; dark brown lenses	
			2.5Y 4/1	48 - 61 cm: dark gray silty clay	
			2.5Y 5/1	61 - 66 cm: gray silty clay	
			2.5Y 5/2	66 - 86 cm: grayish brown silty clay	
				86 - 92 cm: dark gray silty clay, olive mottling (bioturbation)	
			2.5Y 4/1	92 - 109 cm: grayish brown silty clay	
1			2.5Y 5/2	109 - 111 cm: clayey silty sand, fining upwards; common foraminifer Pyrgo	
				111 - 128 cm: grayish brown silty clay, olive mottling (bioturbation)	
				128 - 132 cm: brown and dark brown silty clay, laminated	
			10YR 5/3	132 - 136 cm: dark grayish brown silty clay	
				136 - 142 cm: brown and dark brown silty clay	
			2.5Y 4/2	142 - 159 cm: dark grayish brown silty clay; dark brown sandy lenses	
			10YR 3/2	at 146-149 cm	
			2.5Y 4/2	159 - 242 cm: grayish brown silty clay, mottled/bioturbated	
				242 - 252 cm: dark gray silty clay	
			252 - 271 cm: dark gray silty clay		
			271 - 284 cm: olive gray silty clay		
			284 - 292 cm: light olive brown silty clay		
			292 - 307 cm: dark olive gray silty clay		
2		10YR 5/2	307 - 313 cm: dark gray silty clay		
			313 - 328 cm: light brownish gray silty clay		
			328 - 343 cm: dark olive gray silty clay; very dark gray intervals at 333-335 and 342-343 cm		
			343 - 364 cm: olive gray silty clay		
			364 - 397 cm: dark gray silty clay		
		10YR 4/1	397 - 410 cm: dark grayish brown silty clay		
			410 - 431 cm: dark gray silty clay		
		5Y 4/1	431 - 449 cm: olive gray silty clay		
			449 - 457 cm: dark brown and grayish silty clay		
		5Y 4/2	457 - 464 cm: dark gray silty clay		
		2.5Y 5/4	464 - 468 cm: dark olive gray silty clay, very dark gray horizons at 464 and 467 cm		
3		5Y 3/2	468 - 471 cm: gray silty clay		
		2.5Y 4/0	471 - 477 cm: grayish brown silty clay		
		2.5Y 6/2	477 - 481 cm: dark gray silty clay		
		5Y 3/2	481 - 483 cm: gray silty clay		
			483 - 490 cm: olive gray silty clay		
			490 - 495 cm: dark gray silty clay		
		5Y 4/2	495 - 502 cm: gray silty clay, dropstone (1cm in diameter) at 498 cm		
			502 - 522 cm: brown silty clay		
			(516 - 528 cm: core catcher; 522-528 cm empty)		
4		5Y 4/1			
		10YR 4/2			
		2.5Y 4/0			
		5Y 5/2			
		10YR 4/2			
		5Y 4/1			
		10YR 5/2			
		5Y 5/2			
		2.5Y 4/0			
5		2.5Y 5/0			

Depth in core (m)	Lithology	Texture	Color	Description	Age
5			10YR 5/3		
6					
7					
8					
9					
10					

PS66/345-2

East Greenland Continental Shelf

ARK XX/3

Recovery: 1.51 m

79° 03.58' N, 11° 16.03' W

Water depth: 313 m

Depth in core (m)	Lithology	Texture Color		Description	Age
0		10YR4/2		0 - 7 cm: dark grayish brown sandy silty clay 7 - 60 cm: very dark grayish brown sandy silty clay 60 - 83 cm: very dark grayish brown silty clay, more sandy layer with dropstone (diameter of 2 cm) at 73-74 cm 83 - 127 cm: very dark gray sandy silty clay, firm, common dropstones of 1 - 7 cm in diameter (--> tillite) 127 - 151 cm (core catcher): very dark gray sandy silty clay, firm, common "crystals" of gypsum (one large "crystal" of 4 cm in diameter in the lower part)	
		2.5Y 3/2			
		2.5Y 4/4			
1		2.5Y 3/1			
2					
3					
4					
5					

12.4 Geological data tables (Smear-slide data)

N. Kukina

Table 12.4.1a: Bulk mineralogy of sediments from Core PS66/304-3, based on smear-slide estimates

Depth	Quartz	Feldspar	Mica	Terr.	Volcanic	Clay	Org.	Fe-	Other	Sediment type
				carbonate	glass	minerals	remains	hydroxide	Heavy	
0 cm	28,7	16,7	8,3	4,6	2,8	3,7	4,6	7,4	23,2	dark gray sand
10 cm	31	13,3	5,3	10,6	0,1	4,4	8,8	3,5	23	dark gray sandy silt
19 cm	30,2	14,3	6,1	9,5	1,9	10,5	5,2	2,3	20	gray sandy silt
45 cm	25,1	11,1	4,3	5,1	1	30,2	8,2	1,1	13,9	dark olive gray sandy silt
80 cm	20,3	8,9	8,3	0,2	0	36	15	2,3	9	dark olive gray sandy silty clay
100 cm	25,6	11,6	7,2	0	0	29	11,1	5,3	10,2	dark olive gray sandy silty clay
119 cm	33,1	18,2	5,2	6,3	2,9	2,1	4,9	2,3	25	dark gray w ith black silty clay
186 cm	33,9	11,6	4,9	5,9	2,1	7,6	4,4	3,1	26,5	dark gray silty clay
196 cm	34,2	12,6	5,1	5,3	2,2	9,8	6,3	3,3	21,2	dark grayish brow n silty clay
219 cm	41	13,2	4,6	11,5	4,6	2,3	2,1	3,5	17,2	dark grayish brow n silty clay
281 cm	33,5	13,5	3,2	12,3	4,3	9,3	3,9	6,8	13,2	very dark gray sandy silt
295 cm	39,9	10,5	7,2	10,6	3,3	2,1	2,1	1,1	23,2	dark grayish brow n sand
306 cm	38,9	10,2	6,8	11,3	3,5	2,9	2,6	2,1	21,7	dark grayish brow n sand
319 cm	34,6	11,9	3,1	12,1	5	12,1	2,1	7,6	11,5	dark gray silty clay
360 cm	26,1	10,2	2,1	5,9	0	26	9,1	2,1	18,5	dark gray sand
397 cm	36,8	16,2	2,9	2,3	0	2,9	3,9	9,9	25,1	gray sand
410 cm	40,2	18,6	3,1	5,3	0	1,9	2,3	2,9	25,7	gray sand

Table 12.4.1b: Heavy minerals in sediments from Core PS66/304-3, based on smear-slide estimates

Depth	Pyroxene	Amphibole	Epidote	Garnet	Black ores	Opaque
0 cm	24.6	33.3	11.1	5.3	19.4	6.3
10 cm	31.3	25	6.3	6.3	18.8	12.3
19 cm	33.2	24.1	11.2	5.9	16.9	8.7
45 cm	29.6	29.8	6.2	11.3	18.5	4.6
80 cm	33.2	27.2	3.2	12.5	15.6	8.3
100 cm	33.9	25.1	3.1	13.6	16.3	8
119 cm	32	22	5.4	11.2	11.9	17.5
186 cm	35.2	33.5	6.9	13.9	5.3	5.2
196 cm	34.2	33.9	6.2	11.3	6.9	7.5
219 cm	30.3	37.1	5.4	10.2	7.2	9.8
281 cm	20.1	38.5	1.1	13.5	7.2	19.6
295 cm	20.1	39.8	2	13.8	6.5	17.8
306 cm	21.1	41.2	3.2	12.6	8.2	13.7
319 cm	20.9	37.9	3.9	11.9	9.7	15.7
360 cm	29.9	44.8	3.6	8.2	8.2	5.3
397 cm	26.9	48.2	4.1	8.2	8.4	4.2
410 cm	30.5	32.5	8.9	8.5	14.2	5.4
419 cm	31.5	32.6	9.8	7.9	5.2	13

Table 12.4.2a: Bulk mineralogy of sediments from Core PS66/308-3, based on smear-slide estimates

Depth	Quartz	Feldspar	Mica	Terr.	Biog.	Volcanic	Clay	Org.	Fe-	Other Heavy
				carbonate	carbonate	glass	minerals	remains	hydroxide	
0cm	25,3	10	7	1,2		0	36,2	8,2	2,6	9,5
42cm	20	8,2	5,6	0	0	0	2,1	2,3	54,8	7
48cm	20,5	10	10	2,1	4,2	0	40	5,3	1	6,9
54cm	20	11,3	8,6	1,6	2,2	0	34	12	2	8,3
154cm	30	11	7,6	0	0	0	32,1	10	4,1	5,2
173cm	40	15	6,1	2,3	3	6,5	0	0,5	1,2	25,4
180cm	40	12,5	5,8	3,6	1,6	2,2	11,1	3	6,8	13,4
225cm	30,5	8,9	5,2	0	0,2	2,6	40,6	2,2	2,6	7,2
254cm	30	11,3	2,1	6	3,2	2,6	30	4	2,2	8,6
295cm	33,2	11,2	2,6	8,2	4,1	2,3	25	2,1	1,2	10,1
354cm	30	12	5,6	6,8	4,1	0	24	2,2	2,3	13
454cm	31,6	11,2	5,9	7,5	3,9	0	23,9	2,2	3	10,8

Table 12.4.2b: Heavy minerals in sediments from Core PS66/308-3, based on smear-slide estimates

Depth	Pyroxene	Amphibole	Epidote	Chlorite	Garnet	Black ore	Opaque	Sulphides
0cm	44,9	26,3	8,2	0	6,6	10	4	0
42cm	26,9	45,6	0	2,1	8,9	8,3	8,2	0
48cm	25,5	44,6	0	0	8,9	12,9	8,1	0
54cm	30,3	45,9	0	0	6,9	10	6,9	0
154cm	35,2	36,1	6,9	1,6	3,2	8,9	8,1	0
173cm	39	18,2	11	6,9	2,1	12,3	8,4	2,1
180cm	10,9	18	2,6	0	3,6	51	10	3,9
225cm	22,6	39,8	1	0	6,5	17,9	8,9	3,3
254cm	20,1	40,2	2,6	0,2	5,6	18,2	9	4,1
254cm	12,9	40,5	3,1	0	7	20	15	1,5
295cm	12,6	41,2	4,1	0,5	6,5	22,6	12,5	0
354cm	22,3	39,5	2,6	0	8,4	10,3	16,9	0
454cm	43,6	22,6	11,2	4,2	2	10	5	1,4
513cm	45,6	20,3	15,5	6,9	2,3	4,2	3,1	2,1

Table 12.4.3a: Bulk mineralogy of sediments from Core PS66/309-1, based on smear-slide estimates

Depth	Quartz	Feldspar	Mica	Terr.	Volcanic	Clay	Org.	Fe-	Other	Sediment type
				carbonate	glass	minerals	remains	hydroxide	Heavy	
5 cm	29,3	10,2	1,8	8,5	1,7	18,6	13,6	0,5	15,8	dark brown silty clay
34cm	25,4	9,6	2,7	9,6	0,9	21,1	9,6	0,8	20,3	dark brown silty clay
59cm	30,1	9,9	2,1	6,3	1,1	3,2	7,2	29,1	11	very dark brown sandy silty clay
70cm	31,7	13,2	1,1	5,5	3,3	11	9,9	1,2	23,1	dark gray silty clay
88cm	36,5	7,7	2,9	9,6	1,9	1,9	9,6	2,9	27	dark grayish brown silty clay
96cm	24,1	7,9	2,5	7,5	1,1	15,1	12,3	13,6	15,9	dark grayish brown silty clay
128cm	28,2	8,1	4,2	7,9	1,3	15	5,6	18,2	11,5	dark grayish brown silty clay
151cm	20	7,2	2,1	6,7	0,2	2,1	2,1	47,4	12,2	very dark brown sandy silty clay
154cm	29,5	12,4	2,9	6,7	0	1,1	5,9	20,9	20,6	gray sandy silt
162cm	30,2	15,2	2,6	4,5	3,3	15,2	10,3	2,5	16,2	very dark gray sandy silt
198cm	40,9	21,3	3,1	6,9	1,1	2,1	2,9	2,1	19,6	dark grayish brown silty clay
214cm	37,4	22,5	4,6	2,1	3,4	1,5	5,8	2,1	20,6	dark gray sand
235cm	35,8	20,5	3,8	2,6	2,5	2,1	6,2	8,2	18,3	dark gray sand
268cm	26,9	14,6	3,9	2,3	1,2	2,2	4,1	18,9	25,9	dark gray sand
328cm	39,1	18,9	5,1	2,3	2,1	1,1	3,4	4,8	23,2	olive brown silty clay
336cm	29,1	15,2	7,9	0,9	2,1	12,9	7,2	6,9	17,8	dark brown silty clay
348cm	38,4	21,1	5,1	1,6	0	2,6	5,1	6,9	19,2	dark gray silty clay
369cm	21,9	13,4	5,6	3,2	0	23,9	6,9	8,6	16,5	dark gray silty clay
377cm	21,1	19,3	6,2	9,2	0	21,2	3,6	4,6	14,8	olive brown silty clay
416cm	22,6	19,6	4,2	10,3	0	22,9	3,3	5,1	12	olive brown silty clay
498cm	32,1	24,1	5,6	2,1	0	3,3	1,1	12,1	19,6	dark gray sandy silt
522cm	36,5	12,5	2,3	0,2	1,6	6,9	0,9	24,3	14,8	dark gray sandy silt
526cm	44,6	22,1	2,9	0,5	3,5	3,8	1,9	3,6	17,1	dark grayish brown silty clay
530cm	40,9	21,3	3,1	6,7	0,9	2,2	2,8	2,1	19,6	dark grayish brown silty clay
582cm	40	25	4,6	5,9	0	2,8	1,1	2,6	18	brown silty clay
587cm	34,6	28	4,2	1,2	0	3,3	5,9	6,9	15,9	dark brown silty clay
597cm	35,9	22,1	8,9	5,1	0	6,6	2,1	1,2	18,1	dark grayish brown silty clay
623cm	26	15	6,6	9,4	2,1	25,8	3,3	1,1	10,7	dark grayish brown silty clay
646cm	15,9	8,3	1,2	3,3	0	33,9	4,1	3,1	30,2	gray silty clay
670cm	27,9	8,9	5,9	2,1	0	11	4,1	5,1	35	dark gray silty clay
683cm	40	20	8	0	0	2,3	1,1	1	27,6	dark grayish brown silty clay
686cm	34,3	15	5,6	0	0	1,1	0,2	4,9	38,9	dark brown silty clay (kakao)
693cm	33,5	20	7,9	0	0	29	0,5	2,1	7	dark grayish brown silty clay

Table 12.4.3b: Heavy minerals in sediments from Core PS66/309-1, based on smear-slide estimates

Depth	Pyroxene	Amphibole	Epidote	Garnet	Black ores	Opaque	Sediment type
5 cm	29,4	35,3	8,8	11,8	8,9	5,8	dark brown silty clay
34cm	20,6	36,1	5,3	12	13,2	12,8	dark brown silty clay
59cm	32,2	28,1	6,5	8,8	12,5	11,9	very dark brown sandy silty clay
70cm	25,8	35,5	12,9	6,5	16,1	3,2	dark gray silty clay
88cm	25	35,7	14,3	3,6	12	9,4	dark grayish brown silty clay
96cm	26,9	33,1	11,2	2,1	11,2	25,5	dark grayish brown silty clay
128cm	31,2	34,8	9,5	8,2	12,1	4,2	dark grayish brown silty clay
151cm	30,2	38,2	8,4	12,1	8,9	2,2	very dark brown sandy silty clay
154cm	31,7	31,8	9,2	8,2	15,6	3,5	gray sandy silt
162cm	34	36,2	9,2	6,9	10,2	3,5	very dark gray sandy silt
198cm	30,1	36,2	12,1	6,1	9,2	6,3	dark grayish brown silty clay
214cm	37,1	27,8	14,2	9,1	3,6	8,2	dark gray sand
235cm	36	27,1	10,2	8,6	12,2	5,9	dark gray sand
268cm	31,5	28,6	11,3	7,9	12,5	8,2	dark gray sand
328cm	38,1	25,1	21,8	6,2	6,2	2,6	olive brown silty clay
336cm	35,1	28,1	15,2	11,7	9,9	0	dark brown silty clay
348cm	36,5	26,9	14,2	12,1	9,2	1,1	dark gray silty clay
369cm	36,6	26,1	9,5	13,6	12,3	1,9	dark gray silty clay
377cm	33,1	33,5	4,9	5	12,3	11,2	olive brown silty clay
416cm	33,2	33,2	5,2	6,2	11,1	11,1	olive brown silty clay
498cm	32,6	33,6	6,8	7,5	12,9	6,6	dark gray sandy silt
522cm	25,6	33,2	7,9	8,2	13,6	11,5	dark gray sandy silt
526cm	30,1	29,9	6,2	8,2	18,2	7,4	dark grayish brown silty clay
530cm	33,5	21,9	5,2	12,9	17,2	9,3	dark grayish brown silty clay
582cm	35,8	22,1	8,6	8,2	18,6	6,7	brown silty clay
587cm	22,6	38,5	8,7	7,9	11,2	11,1	dark brown silty clay
597cm	36,5	31,2	12,8	6,2	8,2	5,1	dark grayish brown silty clay
623cm	35,9	28,2	15,9	2,3	11,6	6,1	dark grayish brown silty clay
646cm	36,1	22,3	11,3	8,9	7,2	14,2	gray silty clay
670cm	33,6	26,9	9,2	6,3	6,9	17,1	dark gray silty clay
683cm	33,6	22,1	13,6	11,2	12,1	7,4	dark grayish brown silty clay
686cm	28,9	19,6	11,3	7,2	1,8	31,2	dark brown silty clay (kakao)
693cm	26,9	18,9	9,8	6,3	12,3	25,8	dark grayish brown silty clay
715cm	24,5	23,9	9,1	12,4	8,2	21,9	gray silty clay

Table 12.4.4a: Bulk mineralogy of sediments from Core PS66/312-2, based on smear-slide estimates

PS66/312-2SL	Quartz	Feldspar	Mica	Terr. carbonate	Biog. carbon	Volcanic glass	Clay minerals	Org. remains	Fe- hydroxite	Other Heavy
0 cm	25,3	10,2	7,3	4,3	1,3	2,1	25,3	8,6	5,6	10
32 cm	20,1	10,3	7,2	3,2	6	4,1	24,3	7,2	8	9,6
132 cm	30,2	18,9	5,2	12,3	6	3,9	8,3	5,2	2	8
228 cm	22,7	15	4	11,9	5	3,5	11,2	5,2	5	16,5
329 cm	23	14,7	4	12	3	4,1	10	3,6	5,6	20
432 cm	30	12	7,9	8	6	1	15	2,1	3	15
533 cm	30,5	15,2	3,6	0	0	4	7,5	3,2	15,9	20,1

Table 12.4.4b: Heavy minerals in sediments from Core PS66/312-2, based on smear-slide estimates

Depth	Pyroxene	Amphibole	Epidote	Chlorite	Garnet	Black ore	Opaque	Sulphides
0 cm	47,5	19	15,6	5,2	3,5	5,2	4	0
32 cm	44,2	18	14	5,2	3	8,8	6,8	0
132 cm	40	33	7,9	1,2	5,6	8,6	3,7	0
228 cm	44	29	8,2	2,6	4,1	8,1	4	
329 cm	35,9	20,6	11,3	2,6	4,8	9,9	8,8	6,1
432 cm	44,2	32,5	8,9	0	2,1	6,2	2,3	3,8
533 cm	30,5	15,2	6,1	8,1	4,2	10,1	15,2	10,6
633 cm	40,3	20	5	0	3,5	18	10,3	2,9

Table 12.4.5a: Bulk mineralogy of sediments from Core PS66/318-4, based on smear-slide estimates

Depth	Quartz	Field spar	Mica	Clay minerals	Org. remains	Fe-hydroxide	Other Heavy
4 cm	20	12	6,2	33,8	8,5	4,2	15,3
13 cm	26,3	13,2	7,5	11,4	10,8	9,6	21,2
58 cm	20,6	8,5	7,9	27	8,5	15,9	11,6
69 cm	21,3	9,6	7,6	25,3	6,3	16,2	13,7
101 cm	21,3	10,2	6,9	15,9	6,5	20,6	18,6
112 cm	29,3	16,2	7,9	5,6	4,9	14,9	21,2
124 cm	31,5	18,2	10,9	12,3	3,9	8,2	15
134 cm	35,9	21,3	11,2	6,9	3,3	6,5	14,9
139 cm	26,7	15,9	9,2	7,2	6,9	12,9	21,2
160 cm	40,2	22,5	7,2	15,9	3,6	2,1	8,5
172 cm	34,2	22,6	5,2	19	6,2	5,6	7,2
180 cm	28,6	18,2	13,9	6,9	7,1	4,2	21,1
189 cm	38,3	22,1	14,3	6,2	2,3	2,3	14,5
199 cm	42,1	15,9	9,2	8,2	2,6	3,5	18,5
206 cm	29	16,2	13,9	3,9	4,5	6,9	25,6
214 cm	18,9	7,4	4,4	35,1	8,2	12,5	13,5
222 cm	20,2	10,2	8,3	6,3	3,6	12,2	39,2
229 cm	33,2	18,2	7,9	22,9	5,4	2,3	10,1
238cm	32,9	18,5	7,7	21,5	5,2	3,8	10,4
246 cm	10,2	5,9	1,2	1,2	1,2	75,6	4,7
250 cm	29,2	18,5	6,9	20,1	2,3	2,5	20,5
255 cm	35,6	20,1	7,9	5,9	2,6	8,5	19,4
266 cm	36,6	20,1	8,9	5,9	1,8	8,8	17,9
278 cm	24,4	18,6	5,6	18,2	2,3	8,8	22,1

Table 12.4.5b: Heavy minerals in sediments from Core PS66/318-4, based on smear-slide estimates

Depth	Pyroxene	Amphibole	Epidote	Garnet	Black ores	Opaque
4 cm	26,9	40,2	5,9	3,8	13,7	9,5
13 cm	28,6	30,2	8,3	6,2	16,5	10,2
58 cm	25,3	36,8	6,8	6,9	16,3	7,9
69 cm	24,6	38,2	5,3	8,9	18,3	4,7
101 cm	26,3	40,5	6,2	9,1	11,3	6,6
112 cm	20,3	40,6	5,2	8,5	15,2	10,2
124 cm	24	40,2	3,2	11,9	16,2	4,5
134 cm	24,8	45,6	4,2	11,3	9,9	4,2
139 cm	22,1	36,6	3,2	11,2	15,3	11,6
160 cm	24,3	46,3	5,2	8,2	7,9	8,1
172 cm	20,3	48,2	4,3	5,6	14,2	7,4
180 cm	20,1	50,2	3,6	12,6	9,2	4,3
189 cm	18,9	46,3	4,2	11,3	10,2	9,1
199 cm	27,3	31,2	6,9	13,6	11,2	9,8
206 cm	28,6	29,3	8,9	12,5	12,5	8,2
214 cm	23,1	33,8	4,2	7,1	8,9	22,9
222 cm	5,5	13	0,5	3,6	6,9	70,5
229 cm	28,9	44,5	6,3	9,5	4,3	6,5
238cm	27,9	45,3	6,2	9,5	5,1	6
246 cm	22,1	44,6	5,2	8,2	6,3	13,6
250 cm	32,5	33,2	9,6	12,9	4,9	6,9
255 cm	33,6	34,2	12,5	11,5	5,2	3
266 cm	33,6	35,2	12,4	10,2	6,3	2,3
278 cm	34,8	38,2	13,5	9,2	2,6	1,7

Table 12.4.6a: Bulk mineralogy of sediments from Core PS66/319-1, based on smear-slide estimates

Depth	Quartz	Feldspar	Mica	Terr.	Biog.	Volcanic	Clay	Org.	Fe-	Other
				carbonate	carbonate	glass	minerals	remains	hydroxide	Heavy
0cm	20	6	2,3	0	0	0	2,1	5,6	56	8
5cm	30,2	10,6	6,3	0	0	0	32,1	3,1	10,2	7,5
20cm	40,2	19,5	6	2,6	1,3	0	8,3	2,1	2	18
50cm	40	15,6	8,3	18,2	8,1	0	4,3	1,2	0	4,3
60cm	35	15	5,3	12,3	6,2	0	11,5	4,2	0	10,5
80cm	36,2	14,2	6,1	11,2	7,2	0	9,6	3,1	0	12,4
90cm	36,4	10	3,4	0,5	0,6	2,6	8,9	4,3	19,6	13,7
100cm	32,1	9,9	7,3	1,2	1,3	2,1	35,1	2,1	2,1	6,8
114cm	35,1	11,5	6,6	4,6	1,6	3,2	20,3	2,5	4	10,6
200cm	40,5	18	8	0	0	0,2	15	1,3	9,6	7,4
260cm	35	15	6,6	8,9	4,3	1,3	18	0,5	0	10,4
280cm	35	11	3,2	10	6	1,5	10,1	1,2	2	20

Table 12.4.6b: Heavy minerals in sediments from Core PS66/319-1, based on smear-slide estimates

Depth	Pyroxene	Amphibole	Epidote	Chlorite	Garnet	Black ore	Opaque	Sulphides
0cm	40,3	20,3	8,4	4	3,9	8,2	10,3	4,6
5cm	44,6	14,3	12,3	8	3,2	4,3	11,3	2
20cm	35,6	18,9	13,5	3,2	4,9	12,8	4	7,1
50cm	22,6	36,9	3,4	0	8	8,2	5,6	15,3
60cm	44	20	11,3	4,9	4,1	5	5,2	5,5
80cm	44,2	26	12,3	5,3	3,1	4,9	3,1	1,1
90cm	33,6	20,1	4,9	2,1	5,6	16,9	10	6,8
100cm	41,2	32	8	0	4,2	6,1	4	4,5
114cm	32,9	25,6	4,6	5,6	2,1	15,9	10,3	3
200cm	41,1	15,2	18	8,2	6,2	7,3	4	0
260cm	33,8	21,1	12	2,1	3,9	18	2,3	6,8
280cm	40	18,6	10,1	4,6	1,9	10	3	11,8
300cm	45,2	35	5	2,2	5,6	2,3	0,5	4,2

Table 12.4.7a: Bulk mineralogy of sediments from Core PS66/325-3, based on smear-slide estimates

Depth	Quartz	Feldspar	Mica	Terr.	Biog.	volc.	Clay	Org.	Fe-	Other
				carbonate	carbonate	glass	minerals	remains	hydroxyde	Heavy
0 cm	26,3	11,2	5,6	2,1	0	0,1	30,2	11,1	8,1	5,3
4 cm	29,1	10,4	8,2	5,6	1,2	0	5,2	10,4	20,1	9,8
58 cm	36,5	14,2	7,4	12,2	4,9	2,3	4,6	4,9	3,9	9,1
159 cm	25	8	8,2	13,9	4,4	2,2	19	3	2,4	13,9
247 cm	35,8	15,3	4,2	11,1	3,5	4,6	12,2	2,6	2,1	8,6
347 cm	29,6	8,2	6,3	6,2	2,1	2,2	25	7,6	2,1	10,7
448 cm	30	10	6,8	7,9	2	2	24,2	8,1	2,1	6,9
548 cm	37	15,9	5,1	12,6	0,5	4,6	5,2	4,1	8,9	6,1

Table 12.4.7b: Heavy minerals in sediments from Core PS66/325-3, based on smear-slide estimates

Depth	Pyroxene	Amphibole	Epidote	Chlorite	Garnet	Black ore	Opaque
0 cm	38,1	15,6	8,1	0	8,9	17,2	12,1
4 cm	37,1	22,1	2,1	0	12,5	15	11,2
58 cm	50,2	19,6	10,2	4,2	5,1	6,2	4,5
159 cm	47,6	21,6	12,6	5,3	4,1	4,6	4,2
247 cm	40,1	20,3	11,3	5,2	7,1	6,6	9,4
347 cm	39,5	19,5	12,1	2,9	6,6	8,2	11,2
448 cm	40,2	27,7	8,8	4,2	7,6	4,9	6,6
548 cm	40,3	23,1	10,2	4,2	6,2	6,2	9,8

Table 12.4.8a: Bulk mineralogy of sediments from Core PS66/333-4, based on smear-slide estimates

Depth	Quartz	Feldspar	Mica	Terr.	Biog.	Clay	Org.	Fe-	Other	Sediment type
				carbonate	carbonate	minerals	remains	hydroxide	Heavy	
21 cm	30,2	10,5	7,1	5,1	0	20,3	7,2	7,1	12,5	olive brown sandy silty clay
89 cm	33,1	12,6	7,4	0	5,1	20	12	0	9,8	gray sandy silty clay
95 cm	25,1	11,1	12,4	0	0	4,6	8,1	30,9	7,8	yellowish brown sand silty clay
122 cm	37,9	20,1	10	0	0	5,1	5,6	3,1	18,2	black spots sandy silty clay
165 cm	40	20	8	3,1	2,2	10,8	5,6	3,9	6,4	dark olive gray sandy silty clay
194 cm	30,2	10,2	8,5	0,8	4,4	8,1	8,6	15,9	13,3	olive sandy silty clay
214 cm	35,9	19,1	4,2	0	1,1	5,1	10,5	3,1	21	olive gray sandy silty clay
231 cm	38,1	20,1	8,1	0	0	10,6	6,1	9,5	7,5	very dark gray sandy silty clay
284 cm	37,2	19,2	10,7.1	8	5,9	4	10	2,1	13,6	gray sandy silty clay

Table 12.4.8b: Heavy minerals in sediments from Core PS66/333-4, based on smear-slide estimates

Depth	Pyroxene	Amphibole	Epidote	Chlorite	Garnet	Turmaline	Black ore	Opaque	Sediment type
21 cm	40,2	28,1	9,6	2,1	2,3	1	11,6	5,1	olive brown sandy silty clay
89 cm	29	36,6	4,1	0	9,1	0	9,1	12,1	gray sandy silty clay
95 cm	33,9	34,6	11,3	2,1	2,2	1,1	12,3	2,5	yellowish brown sand silty clay
122 cm	20,5	20,4	10,1	0,9	4,8	1,6	30,2	11,5	black spots sandy silty clay
165 cm	40,2	22,3	8,9	2,2	3,6	1,1	11,2	10,5	dark olive gray sandy silty clay
194 cm	45,1	28,8	9,6	4,8	2,1	0	5,4	4,2	olive sandy silty clay
214 cm	38	30,5	9,5	5,2	7,1	1	6	2,7	olive gray sandy silty clay
231 cm	28	22,6	6,8	2,5	8,8	0,1	21	10,2	very dark gray sandy silty clay
284 cm	43,6	28,3	6,3	2,1	8,4	1,1	5,8	4,4	gray sandy silty clay

12.5

Summary plots of logging data for selected sediment cores

C. Gebhardt, F. Niessen, D. Penshorn, J. Rogenhagen, J. Schneider

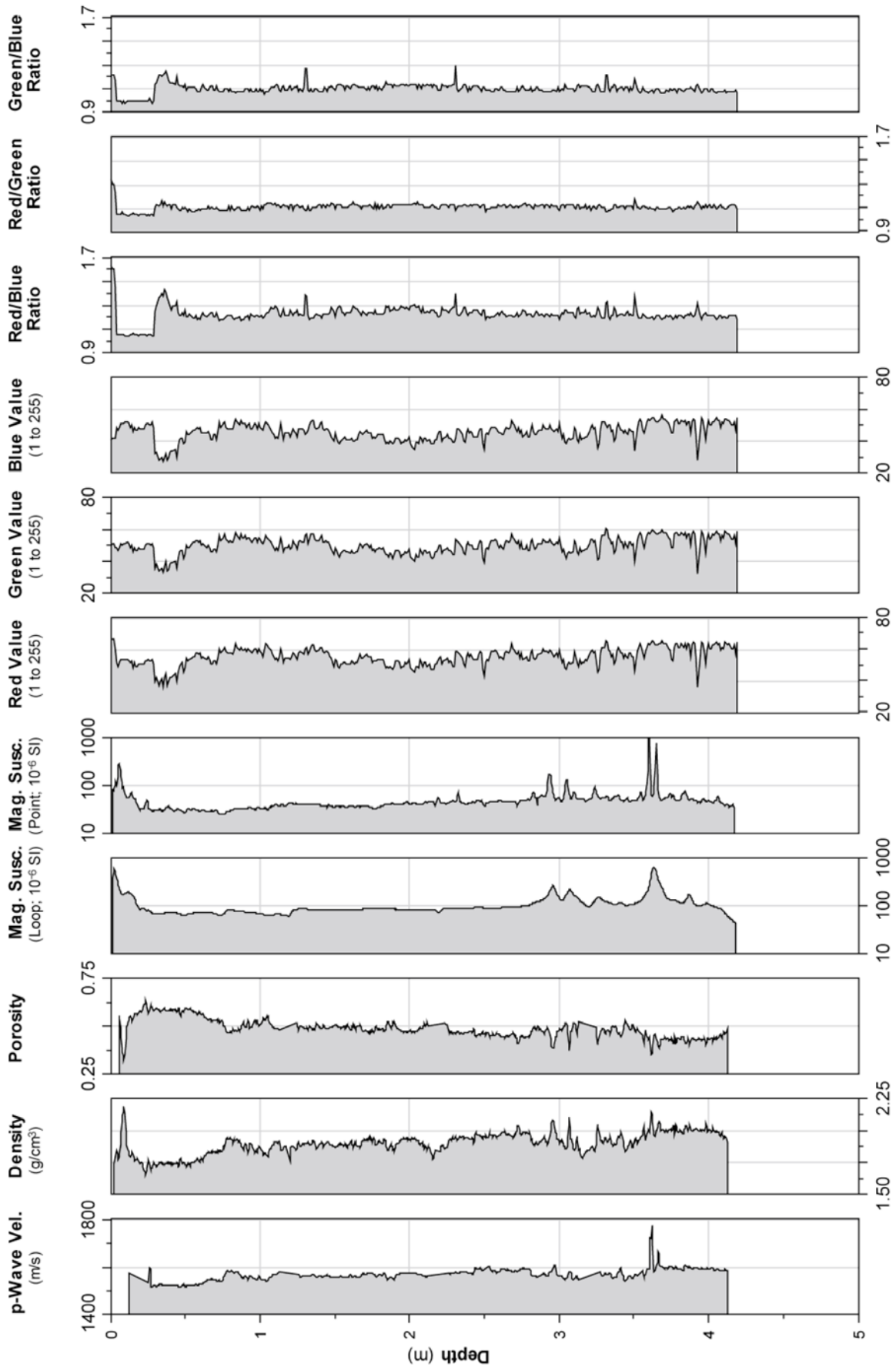


Fig. 12.5.1: Summary plot of logging data from core PS66/304-2

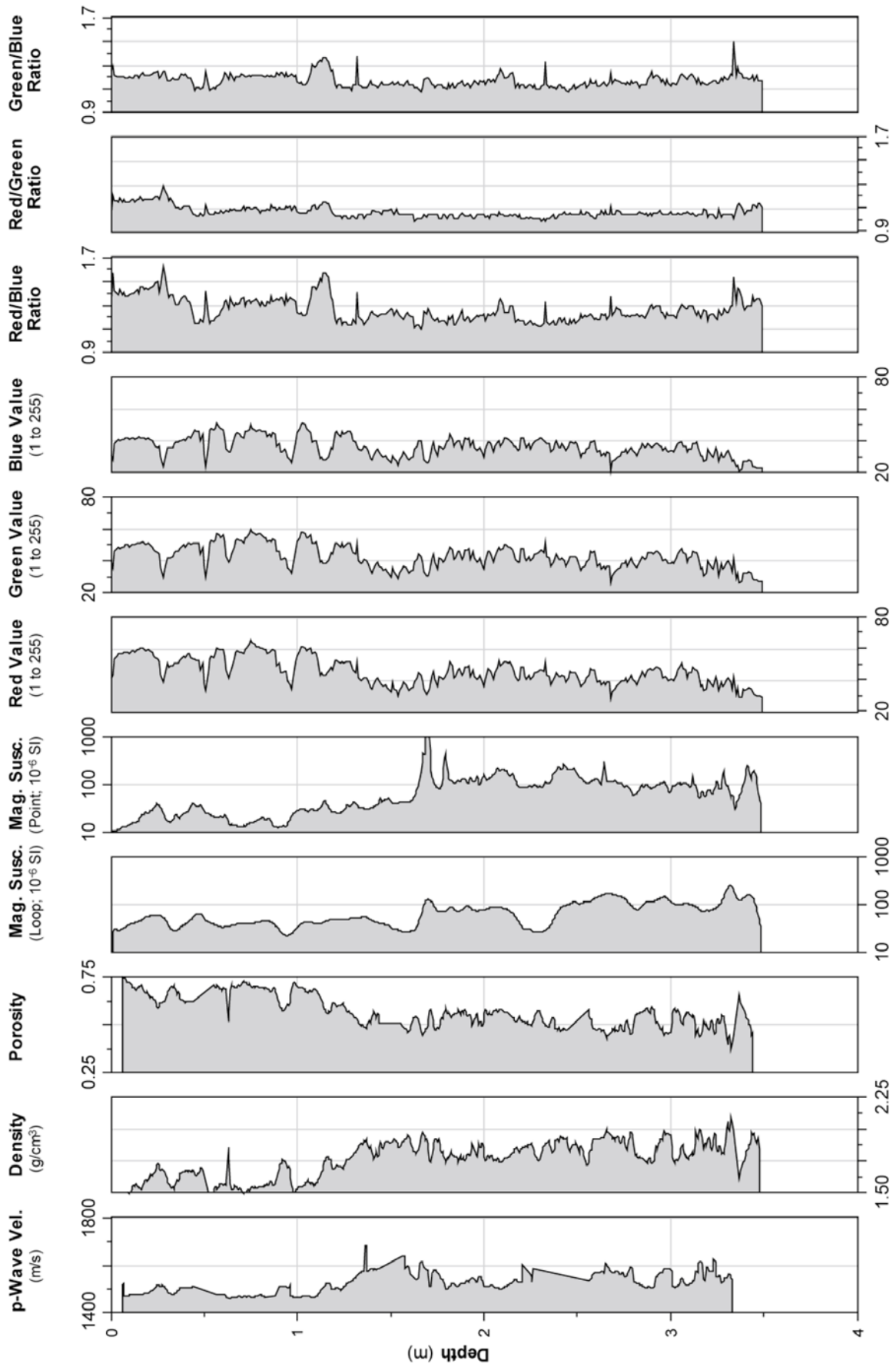


Fig. 12.5.2: Summary plot of logging data from core PS66/306-2

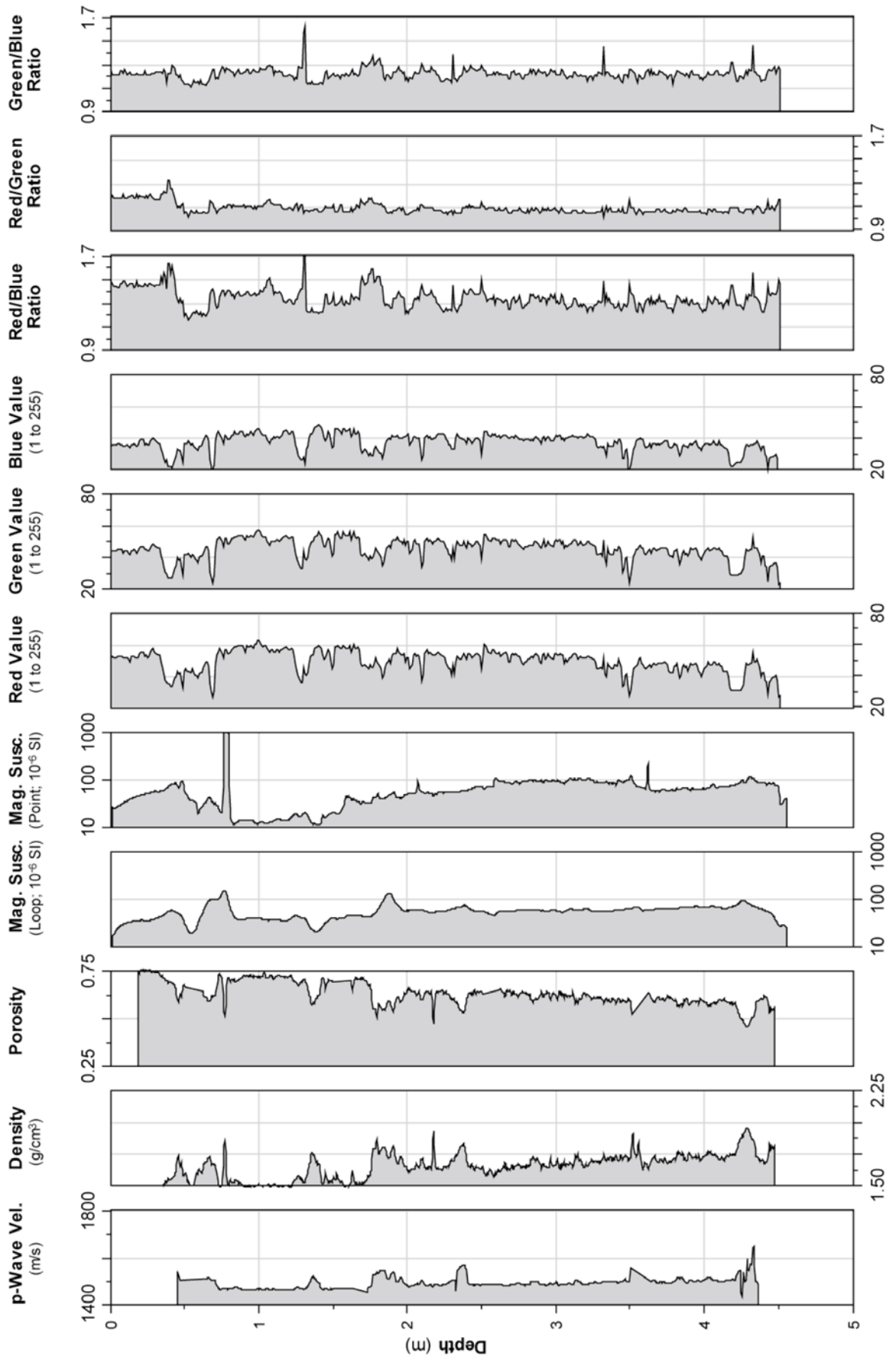


Fig. 12.5.3: Summary plot of logging data from core PS66/307-2

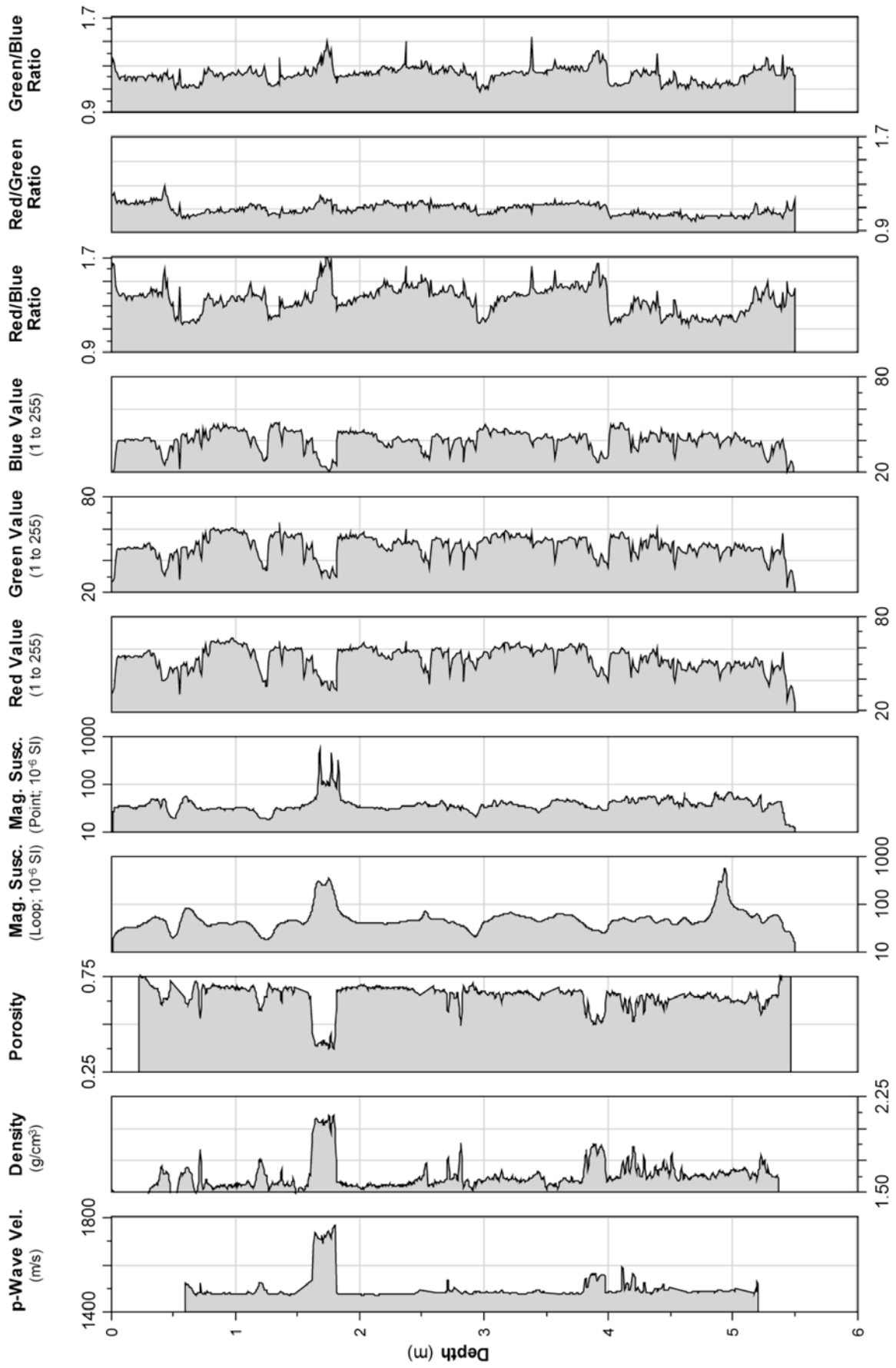


Fig. 12.5.4: Summary plot of logging data from core PS66/308-3

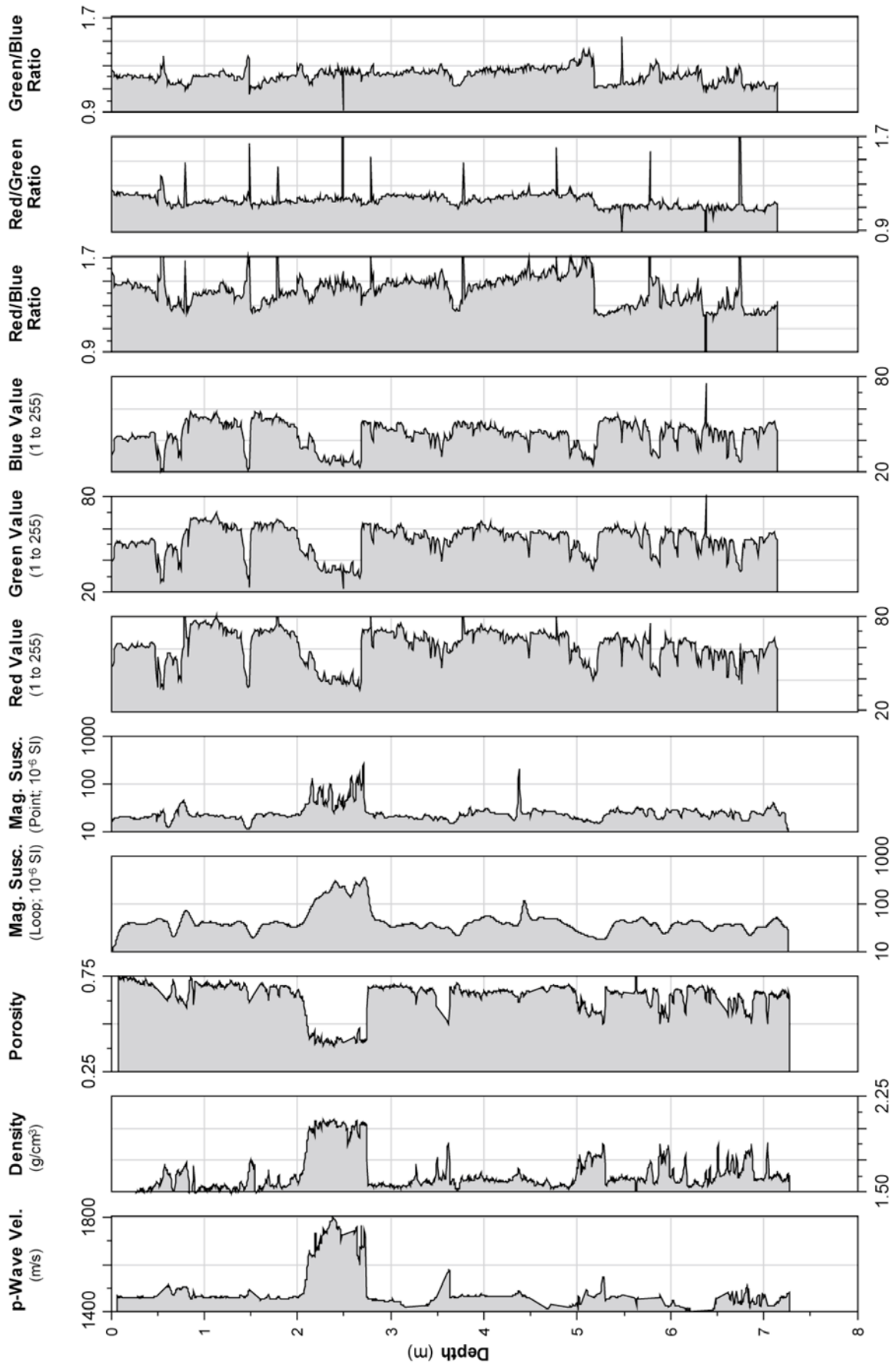


Fig. 12.5.5: Summary plot of logging data from core PS66/309-1

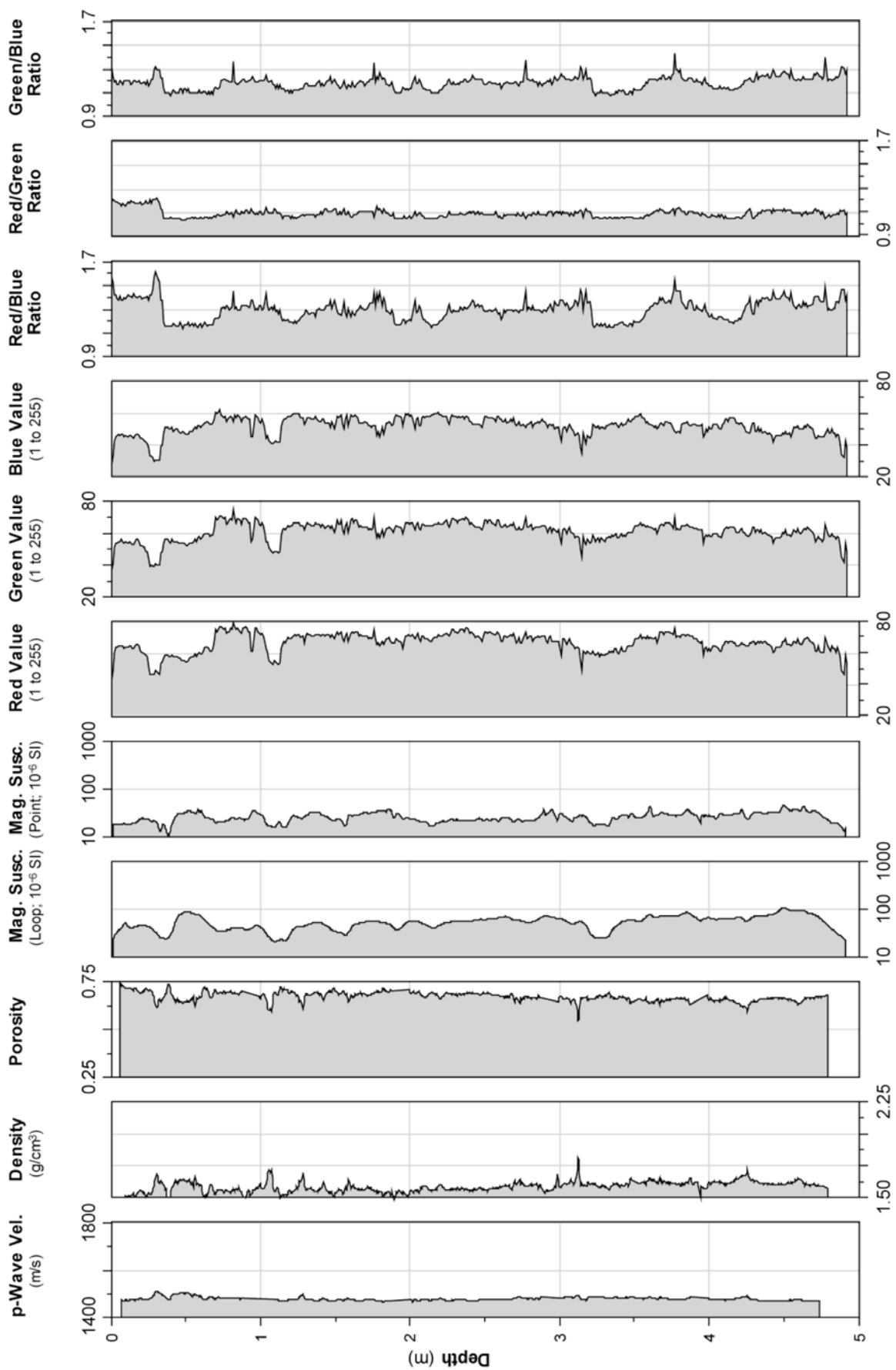


Fig. 12.5.6: Summary plot of logging data from core PS66/311-3

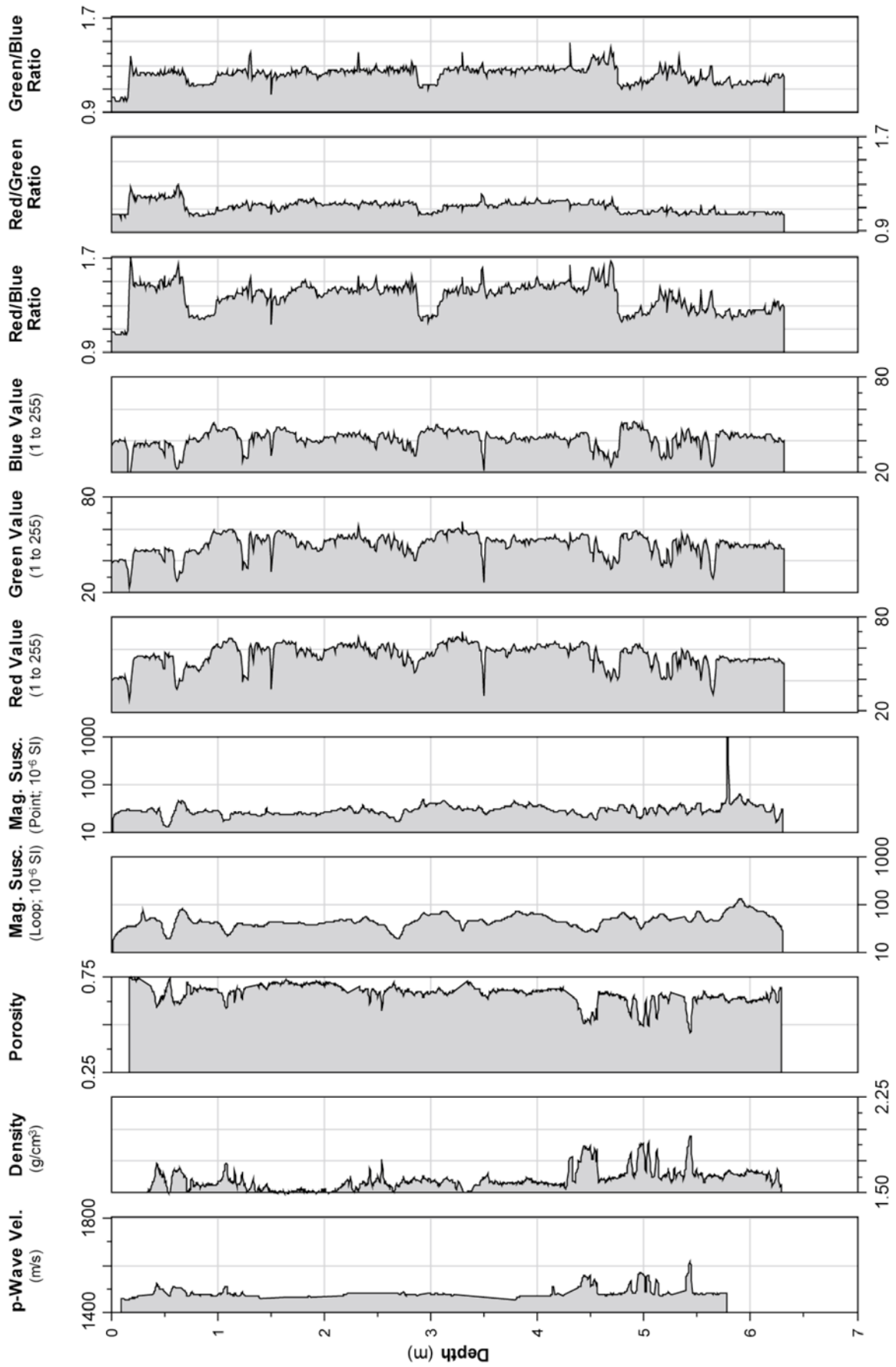


Fig. 12.5.7: Summary plot of logging data from core PS66/312-2

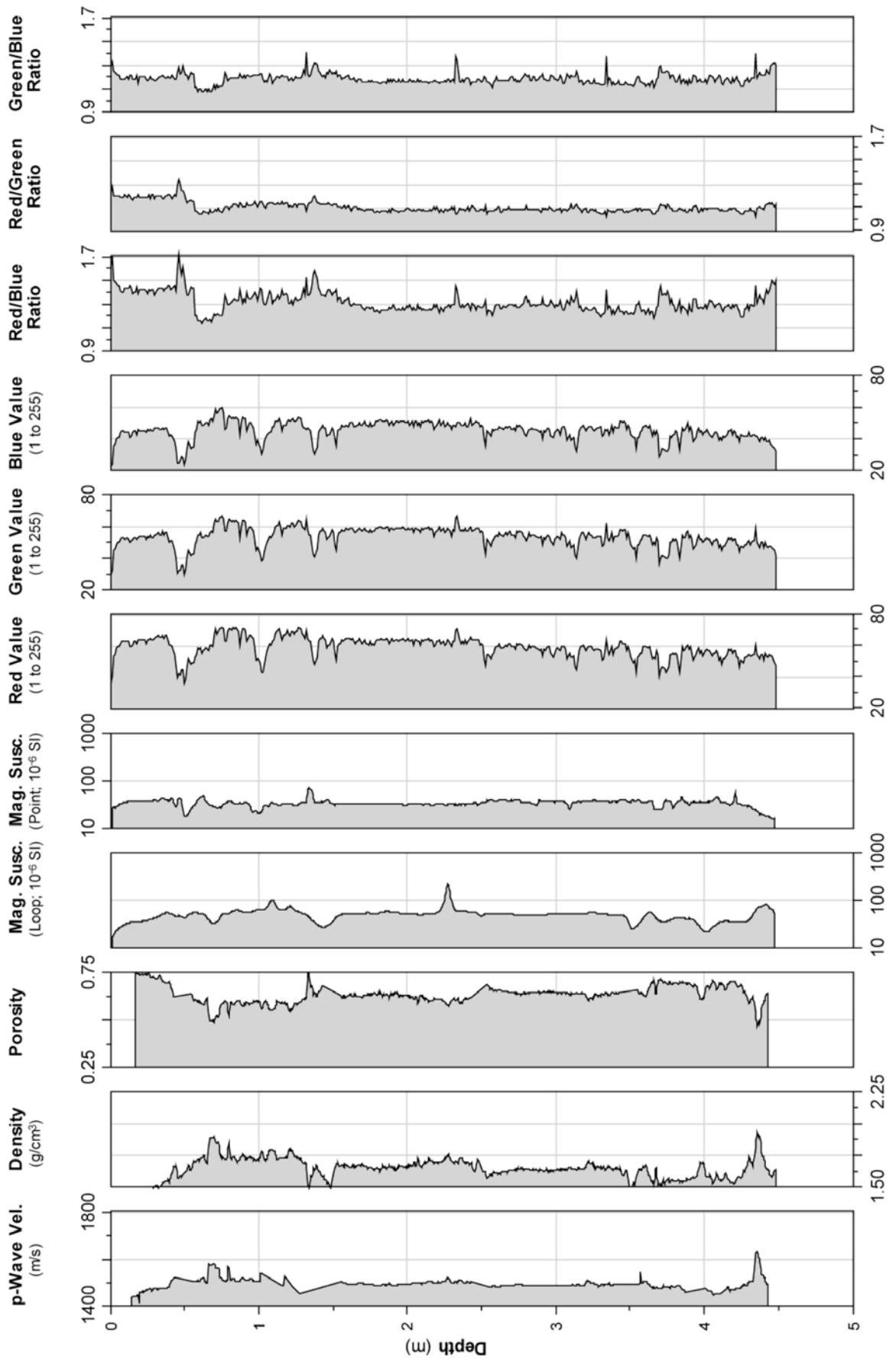


Fig. 12.5.8: Summary plot of logging data from core PS66/313-3

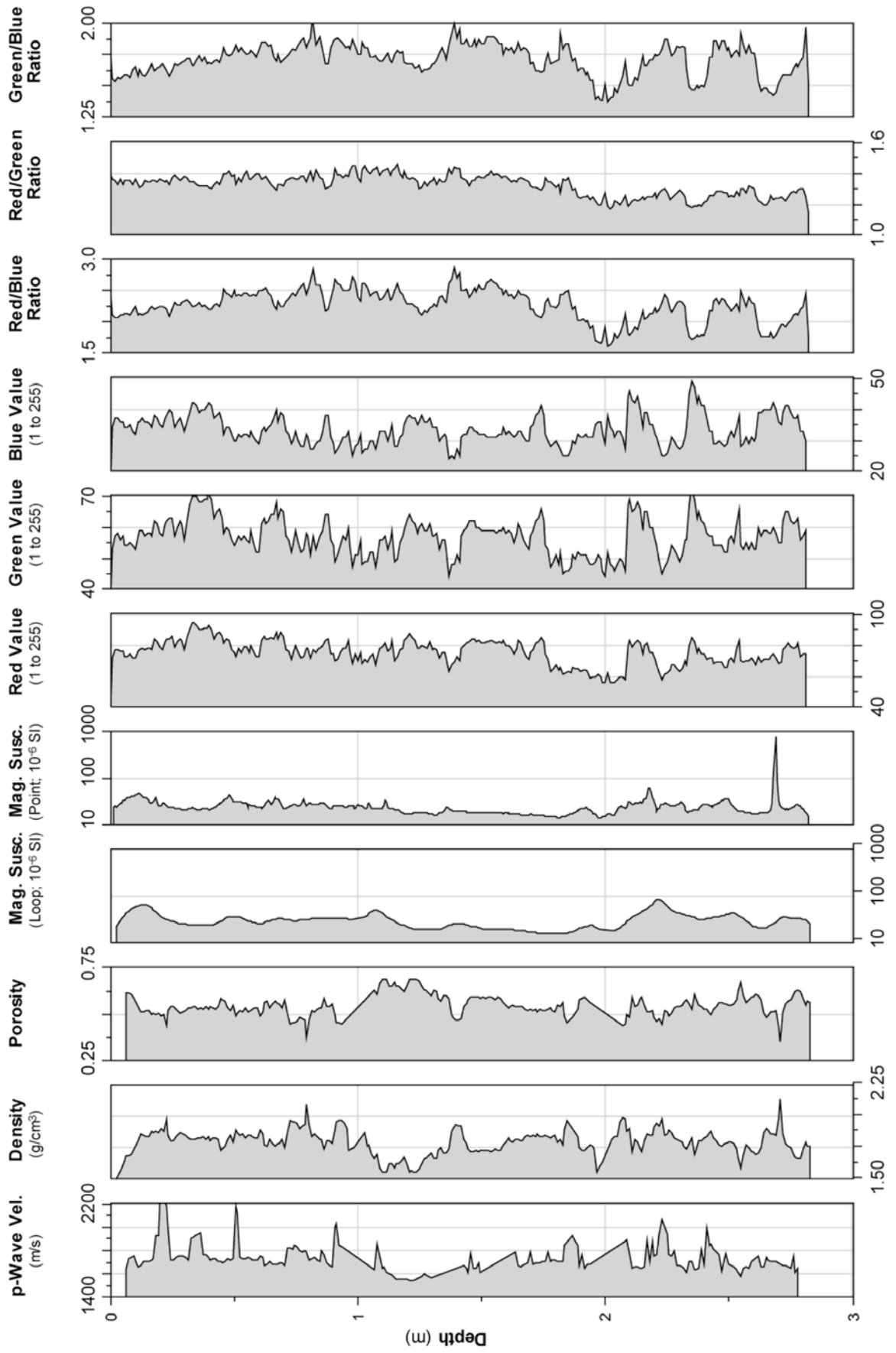


Fig. 12.5.9: Summary plot of logging data from core PS66/318-4

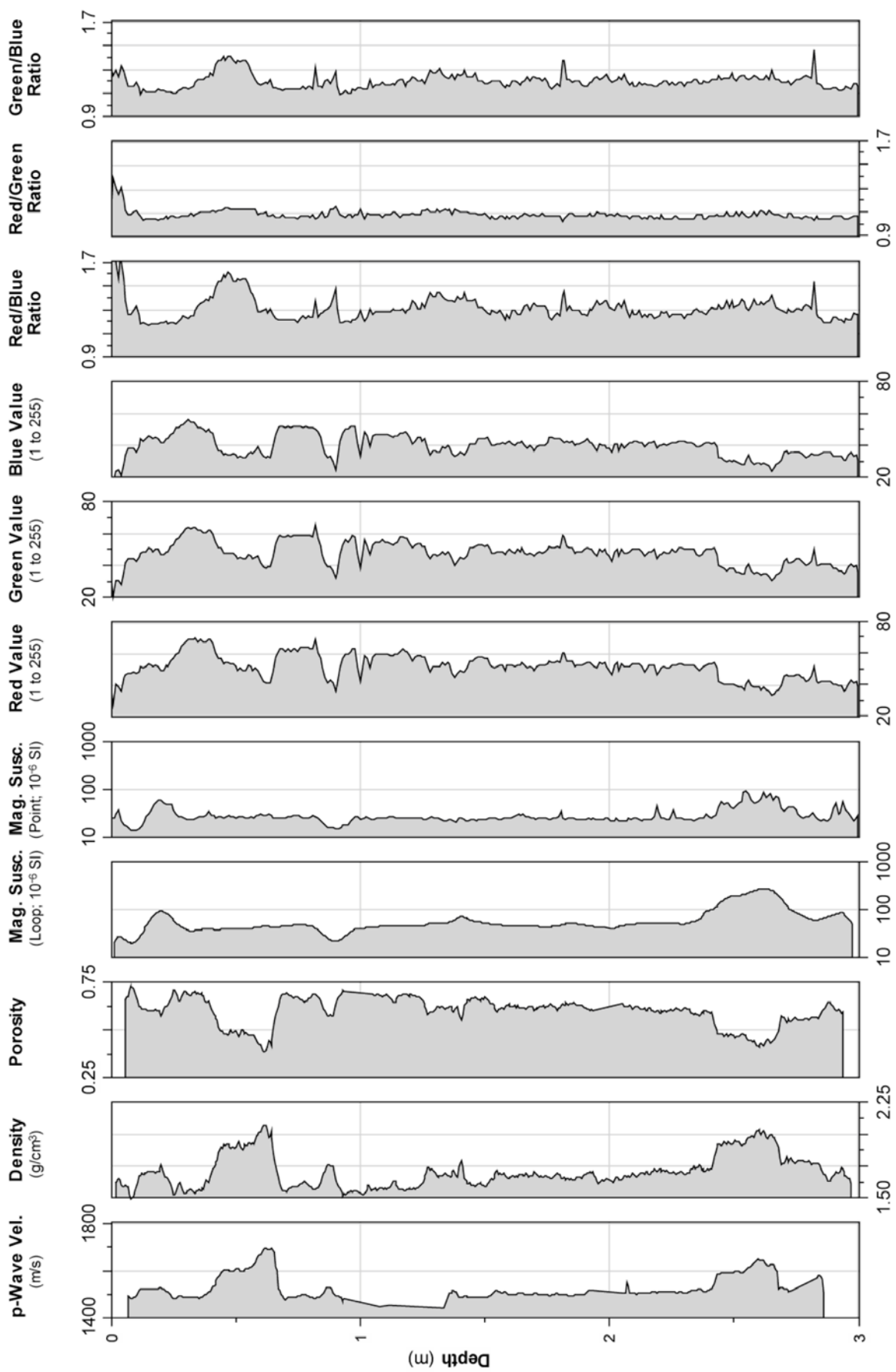


Fig. 12.5.10: Summary plot of logging data from core PS66/319-1

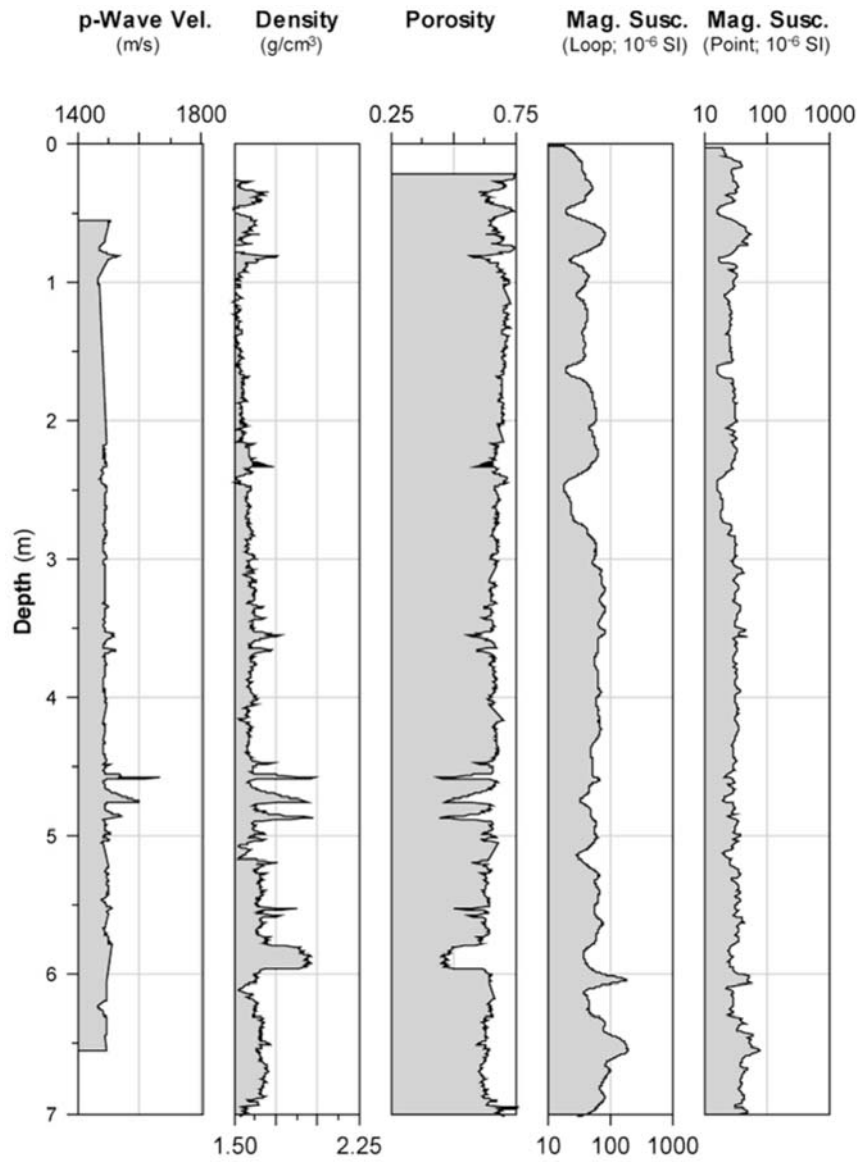


Fig. 12.5.11: Summary plot of logging data from core PS66/321-4

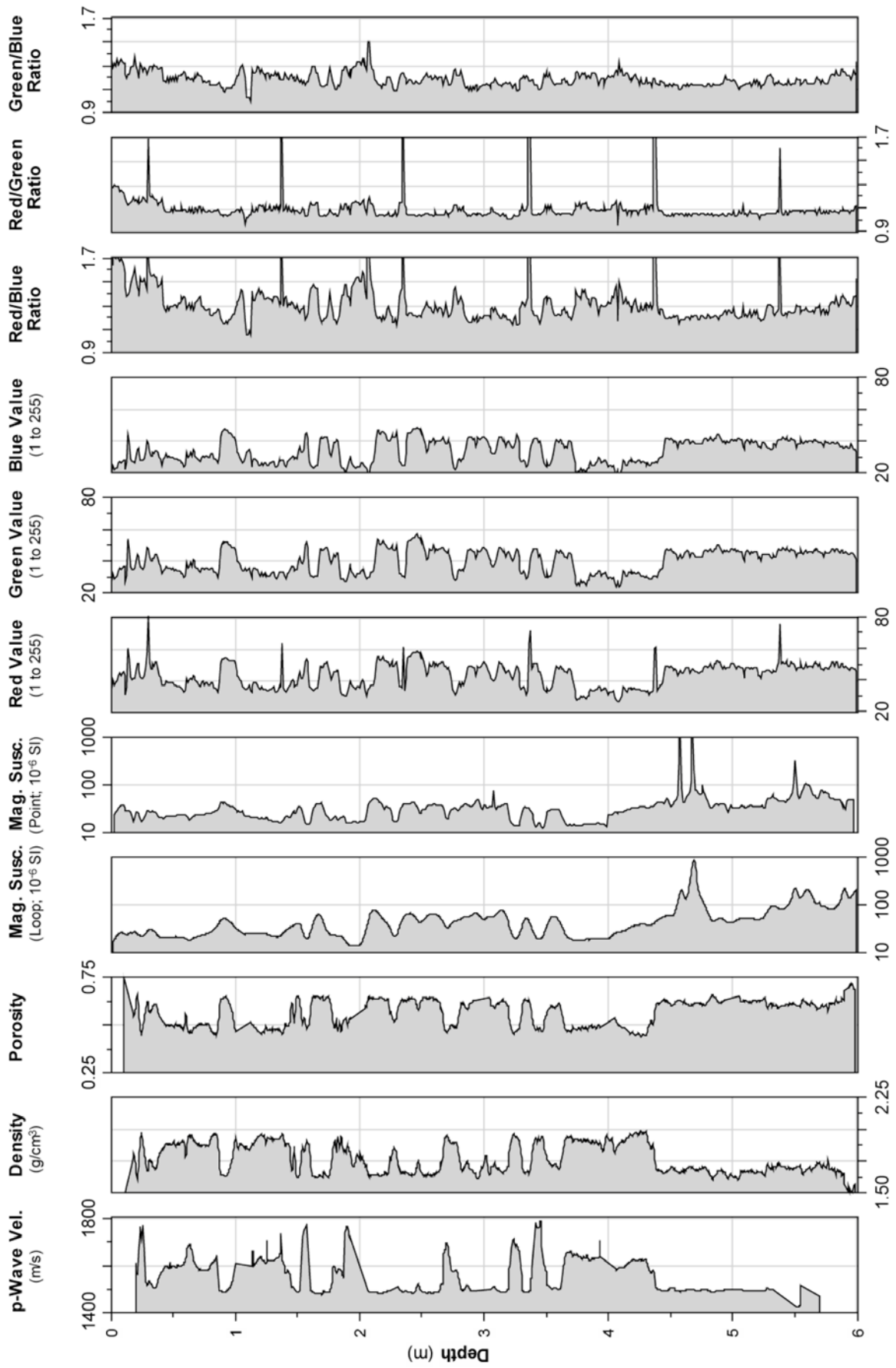


Fig. 12.5.12: Summary plot of logging data from core PS66/322-3

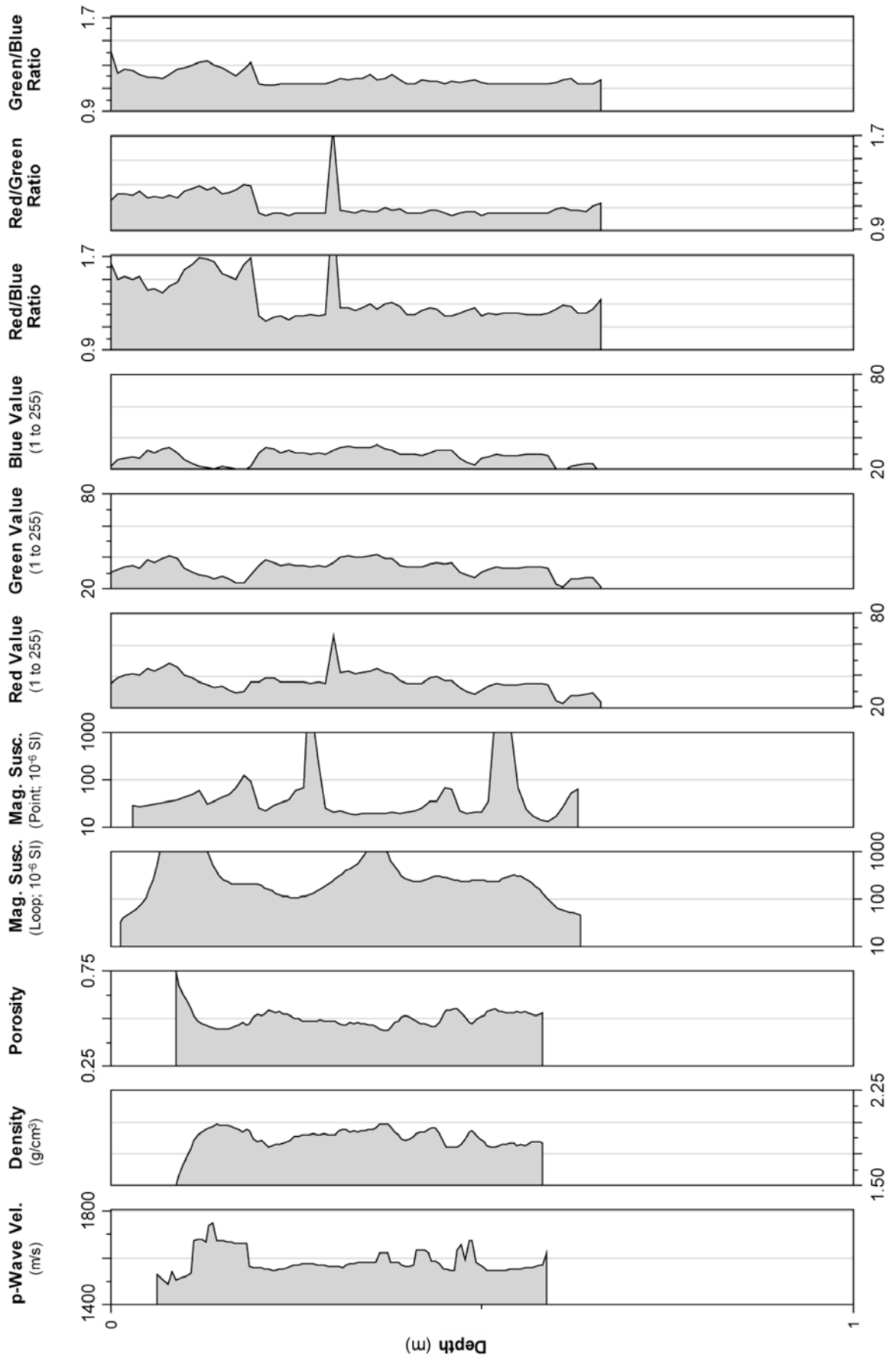


Fig. 12.5.13: Summary plot of logging data from core PS66/323-3

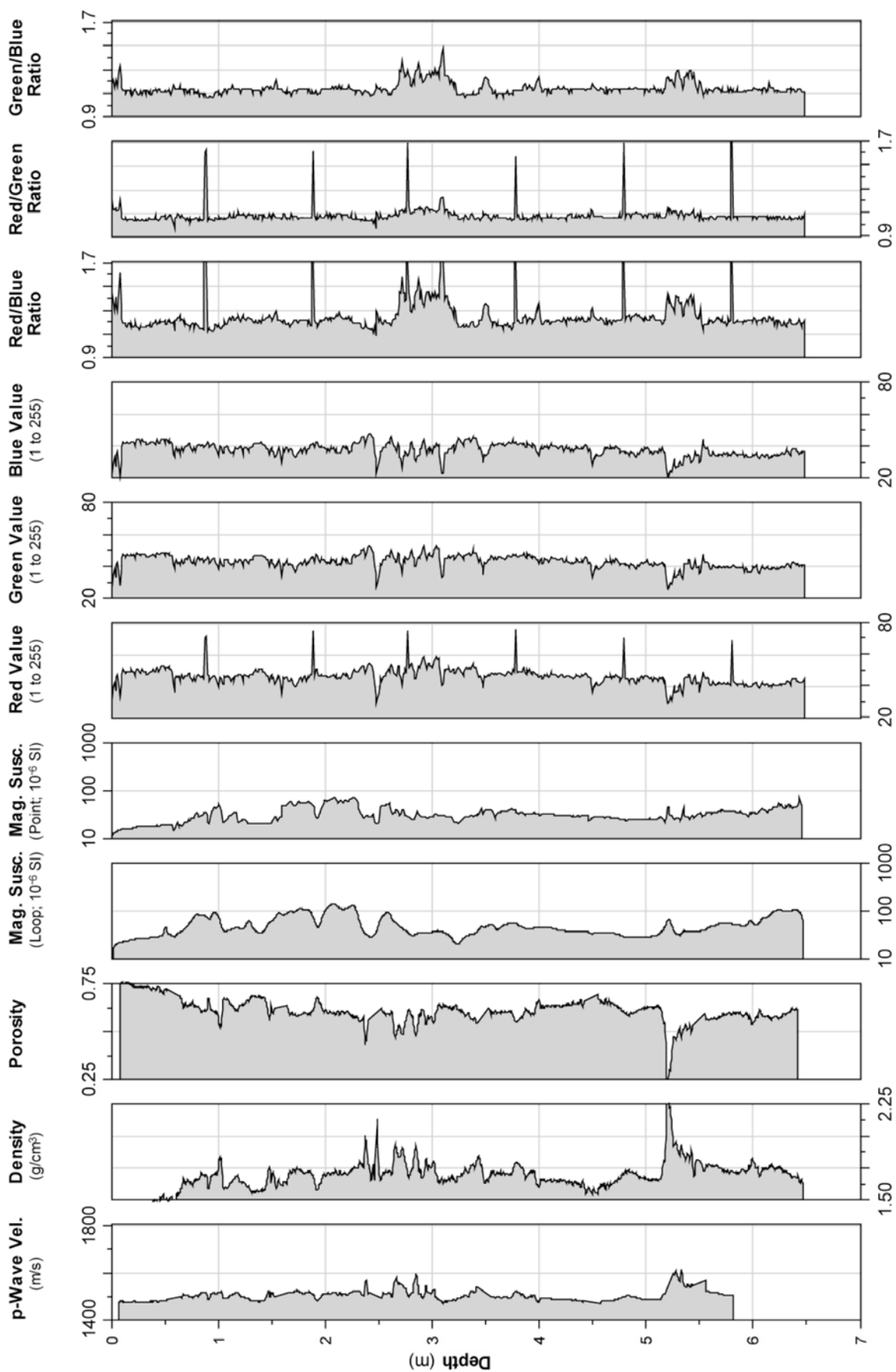


Fig. 12.5.14: Summary plot of logging data from core PS66/325-3

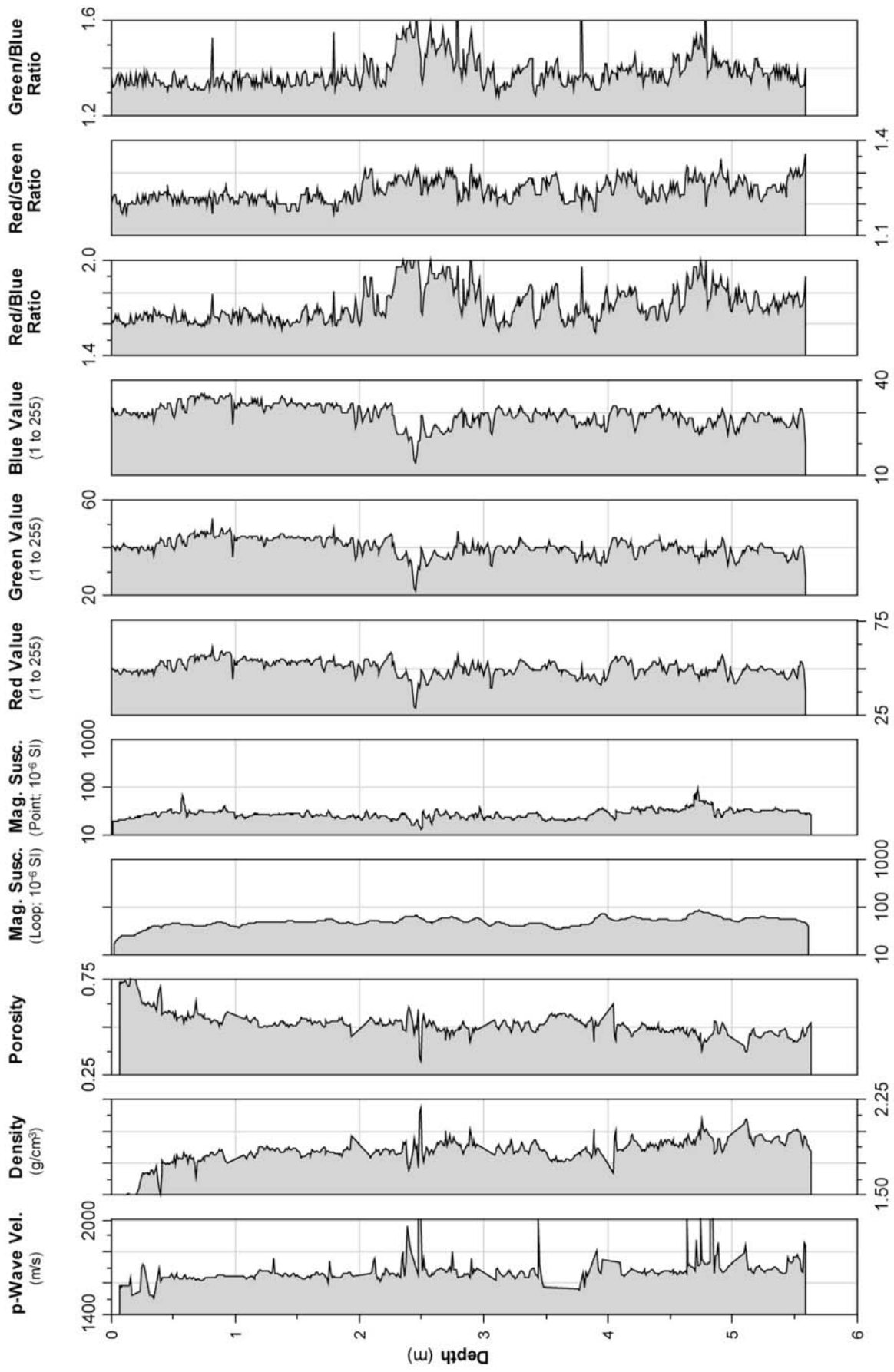


Fig. 12.5.15: Summary plot of logging data from core PS66/327-3

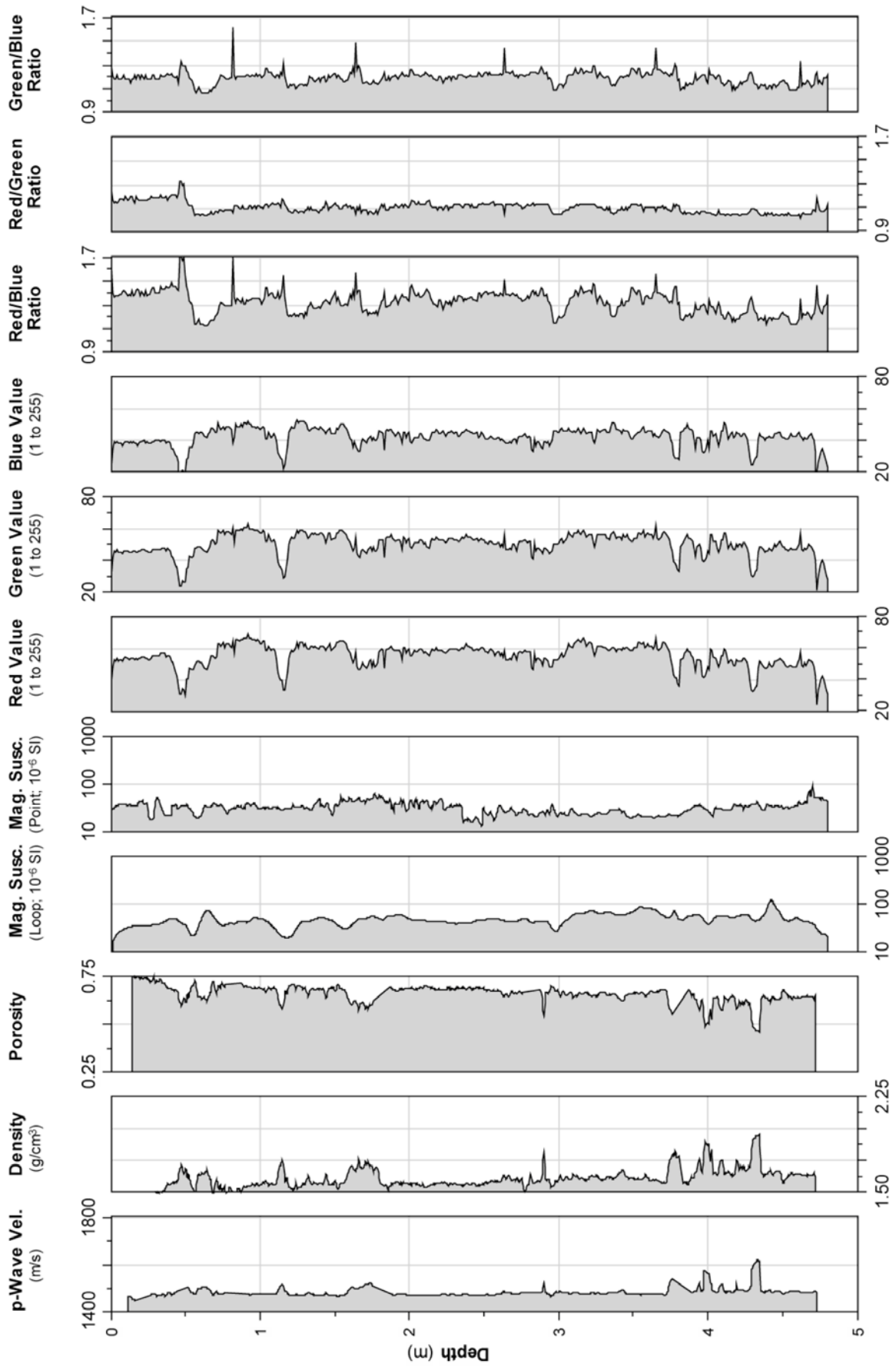


Fig. 12.5.16: Summary plot of logging data from core PS66/329-3

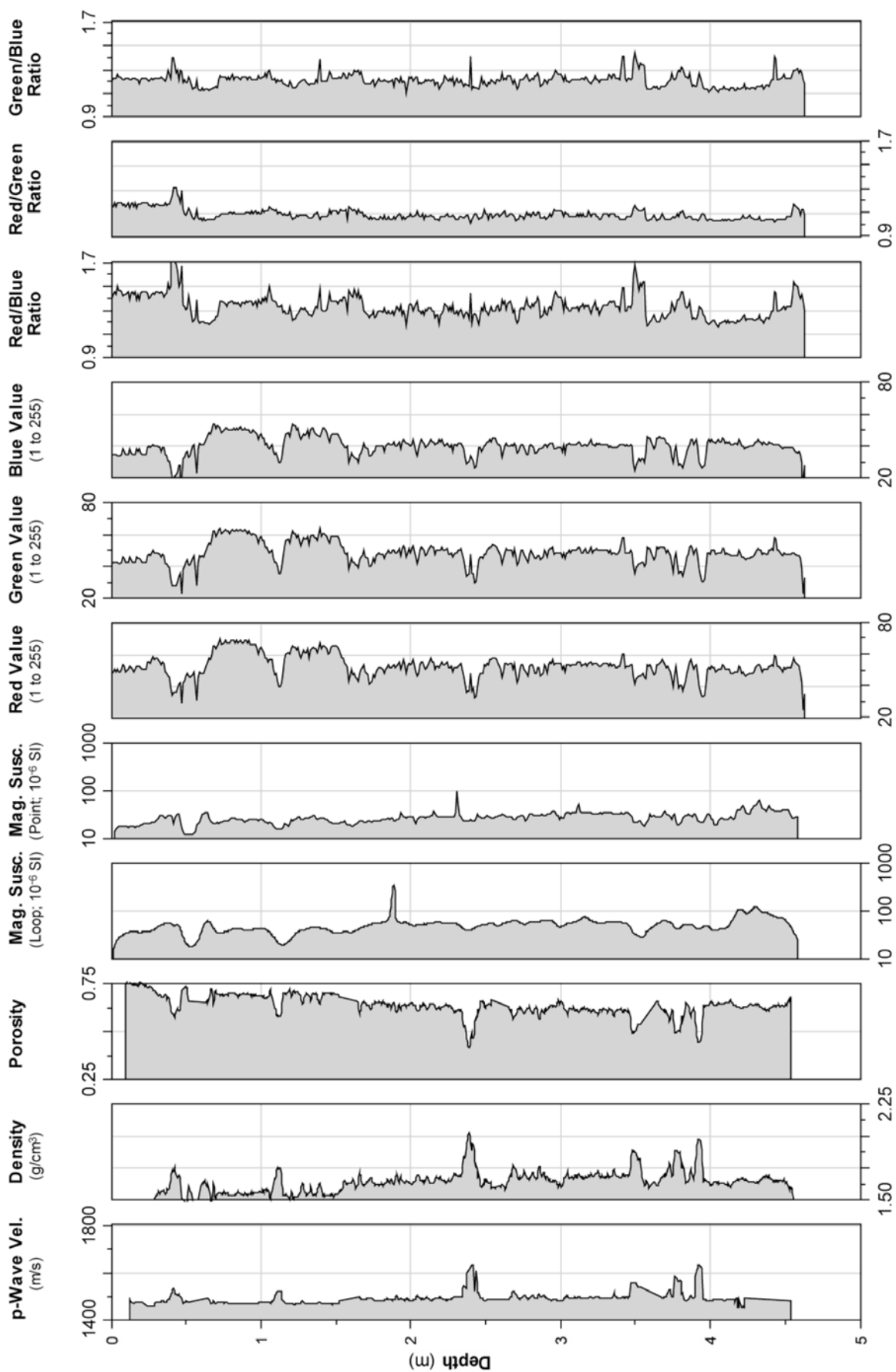


Fig. 12.5.17: Summary plot of logging data from core PS66/330-2

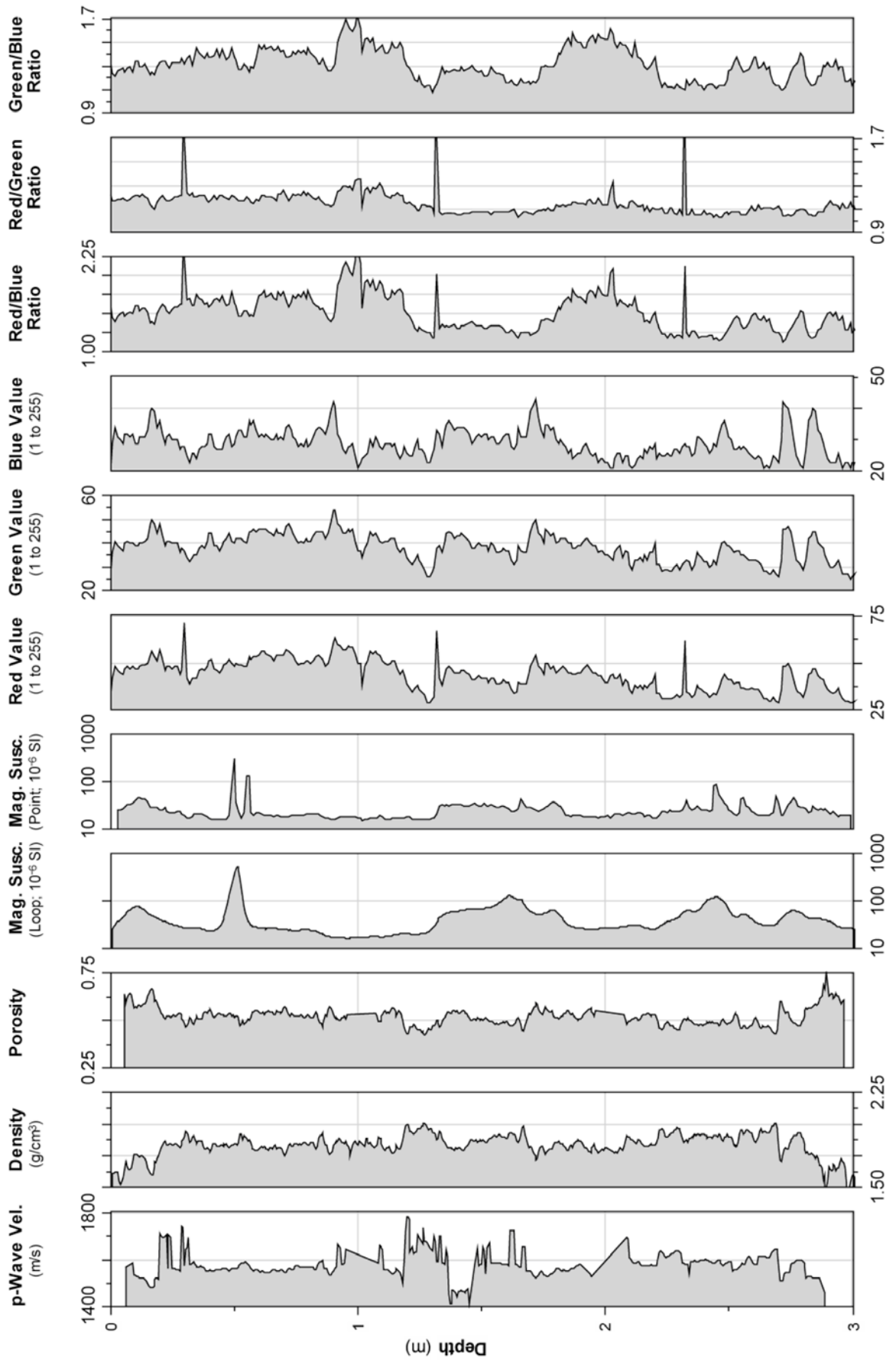


Fig. 12.5.18: Summary plot of logging data from core PS66/333-4

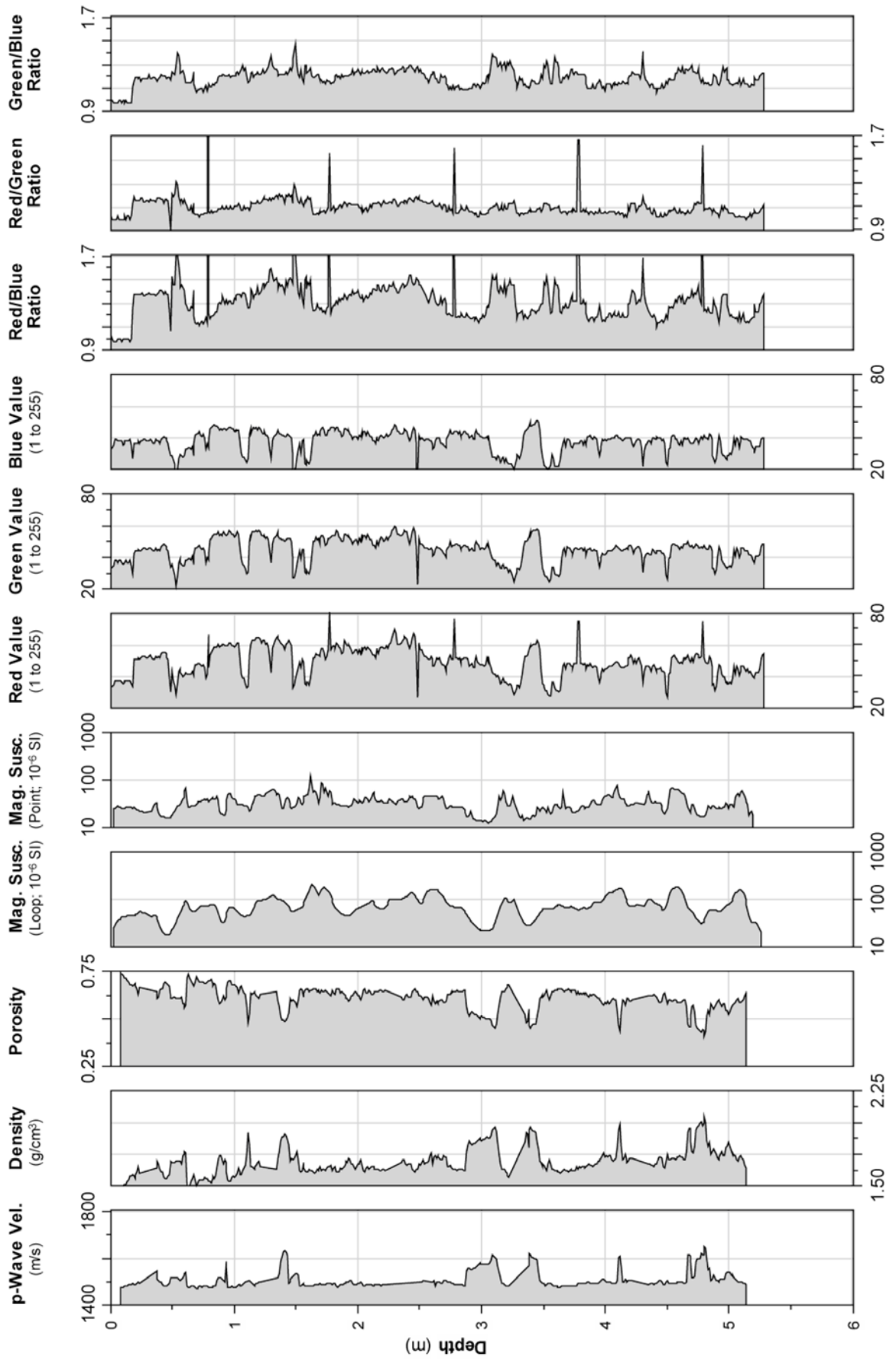


Fig. 12.5.19: Summary plot of logging data from core PS66/341-1

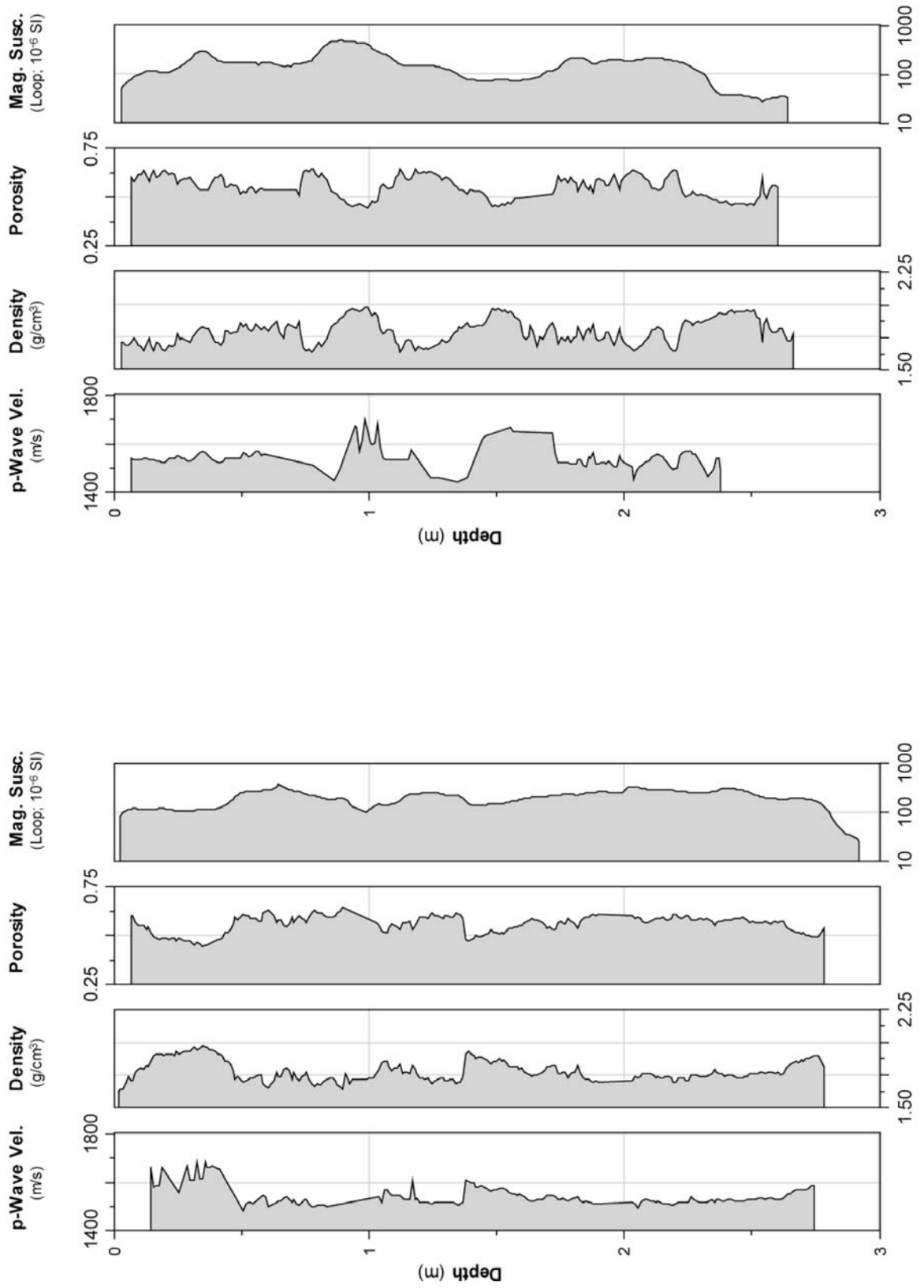


Fig. 12.5.20: Summary plots of logging data from cores PS66/343-1 (left) and PS66/343-2 (right)

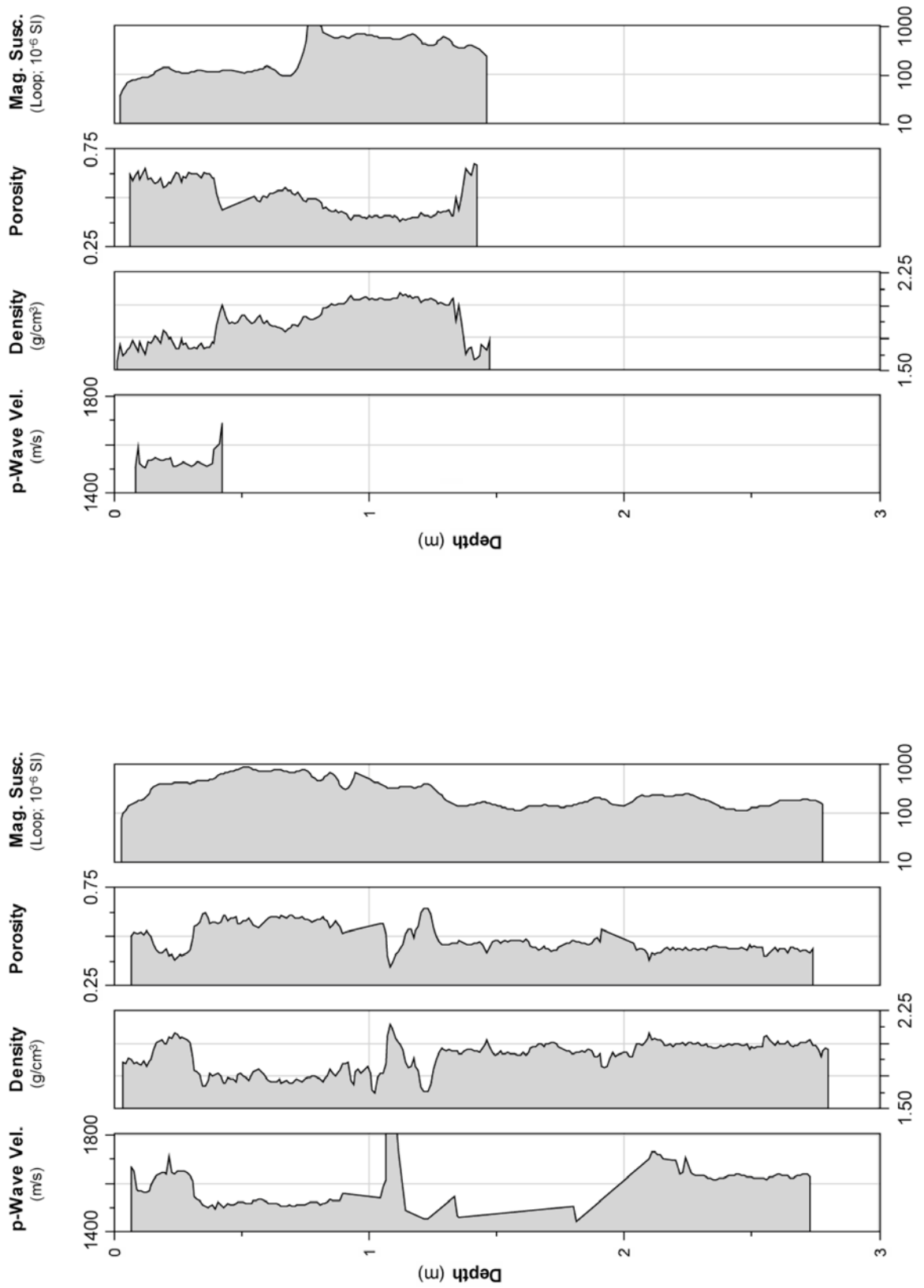


Fig. 12.5.21: Summary plots of logging data from cores PS66/343-3 (left) and PS66/343-4 (right)

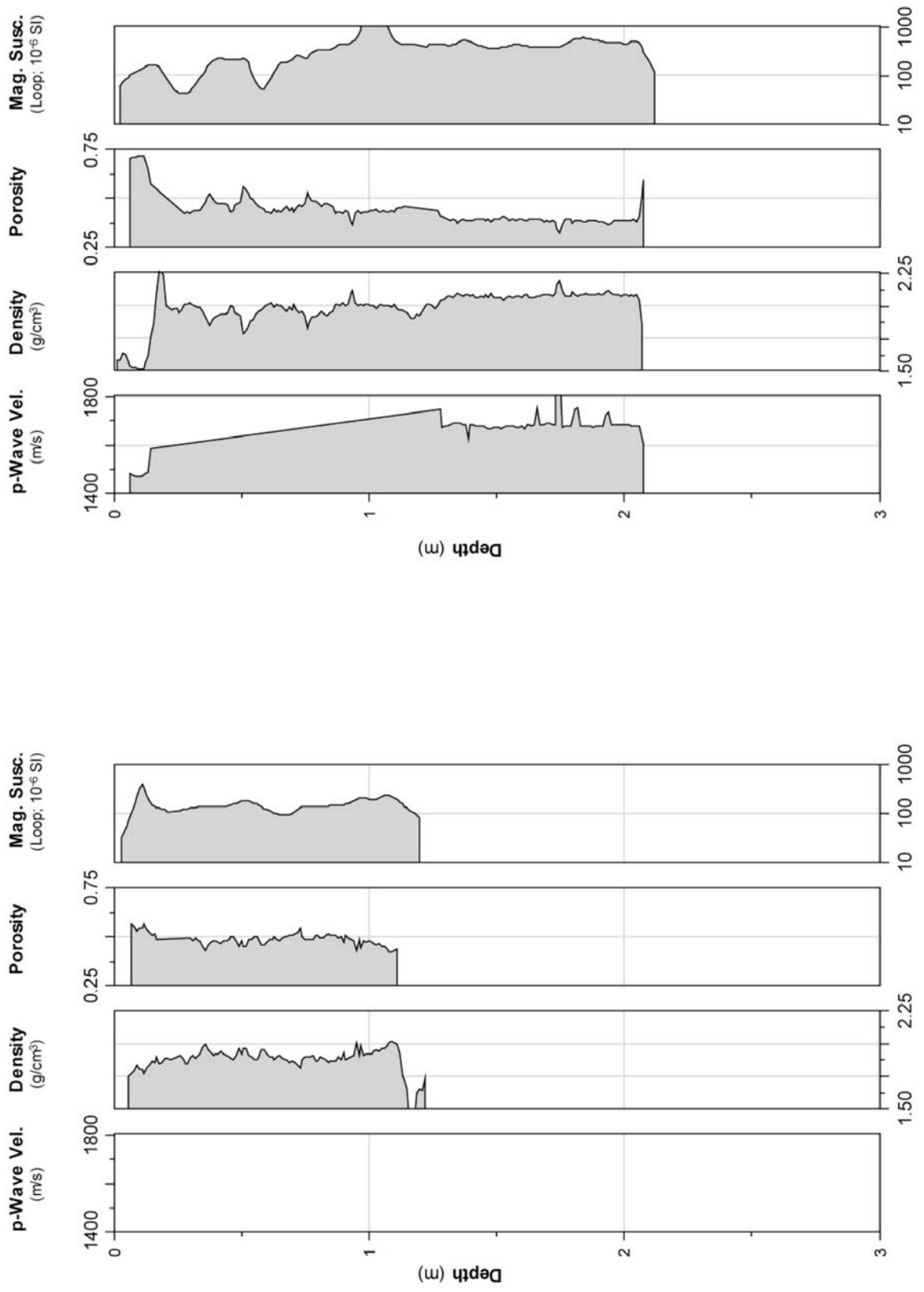


Fig. 12.5.22: Summary plots of logging data from cores PS66/343-5 (left) and PS66/343-6 (right)

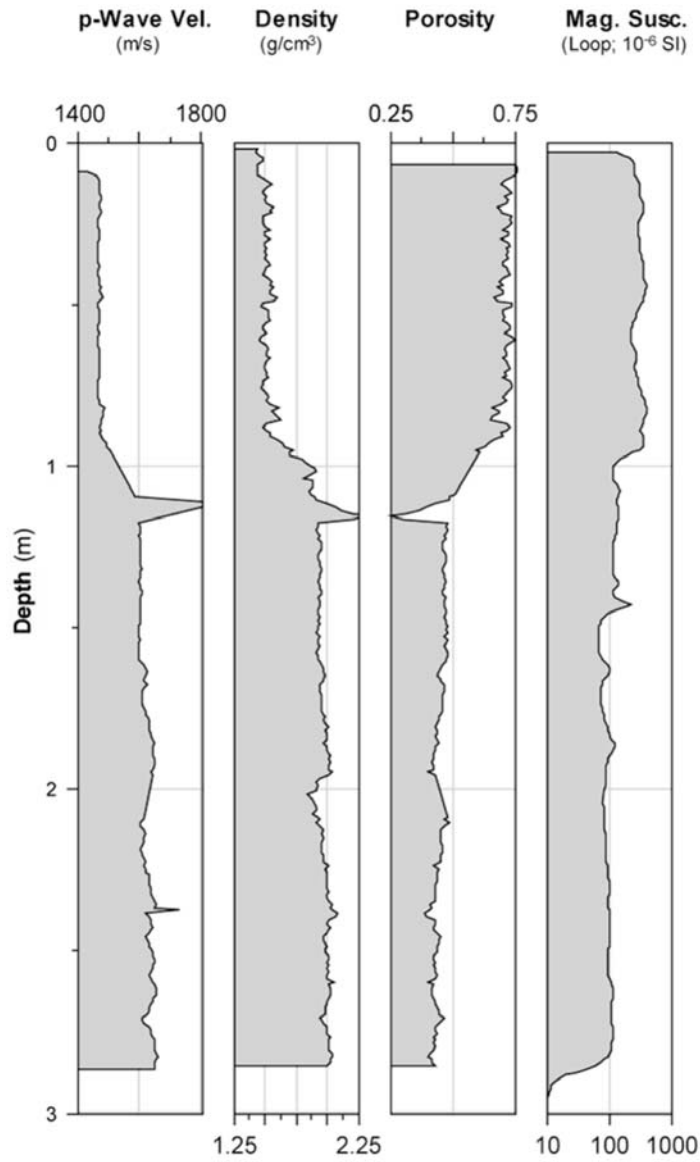


Fig. 12.5.23: Summary plot of logging data from core PS66/344-1

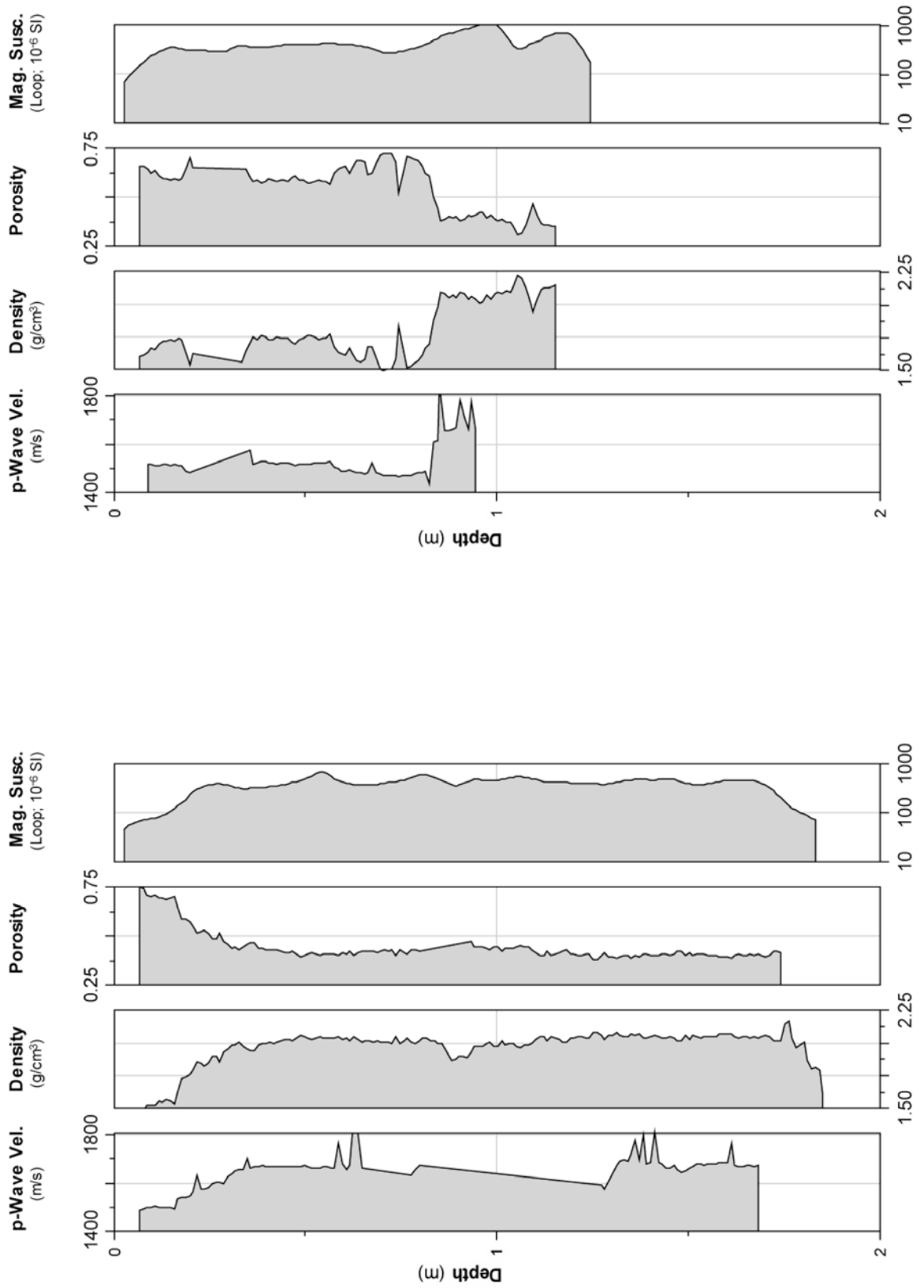


Fig. 12.5.24: Summary plots of logging data from cores PS66/345-1 (left) and PS66/345-2 (right)

12.6

Parasound profiles at coring stations

F. Niessen, J. Rogenhagen

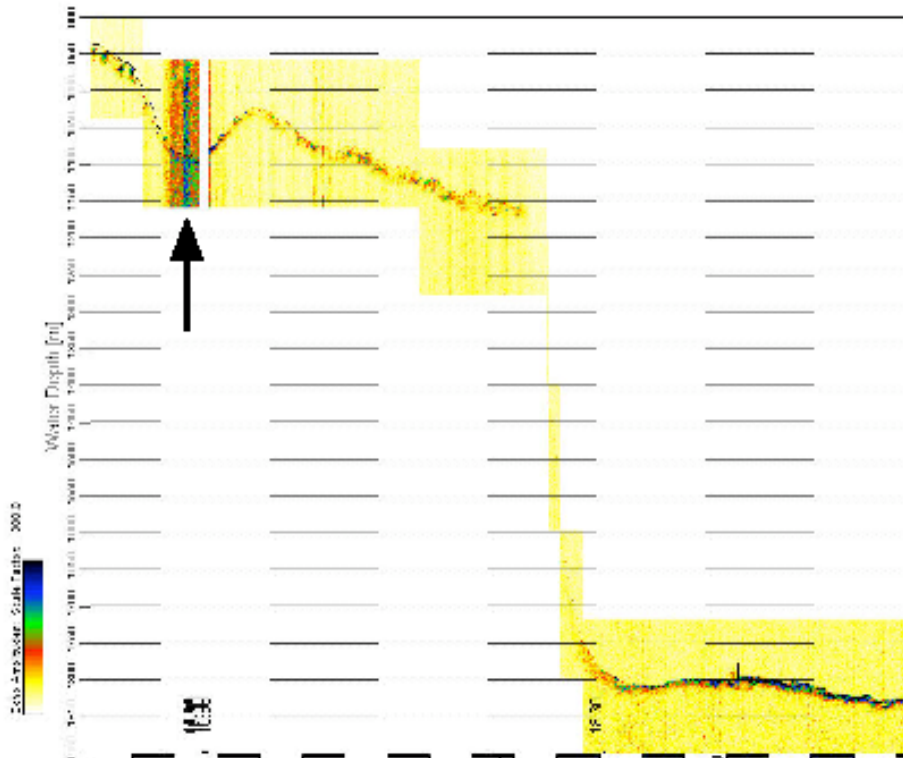


Fig. 12.6.1: Geological Situation at Station PS66/304 as recorded by PARASOUND. For details see Station List. Horizontal distance bar (black or white) is 1 km. Numbers are time UTC.

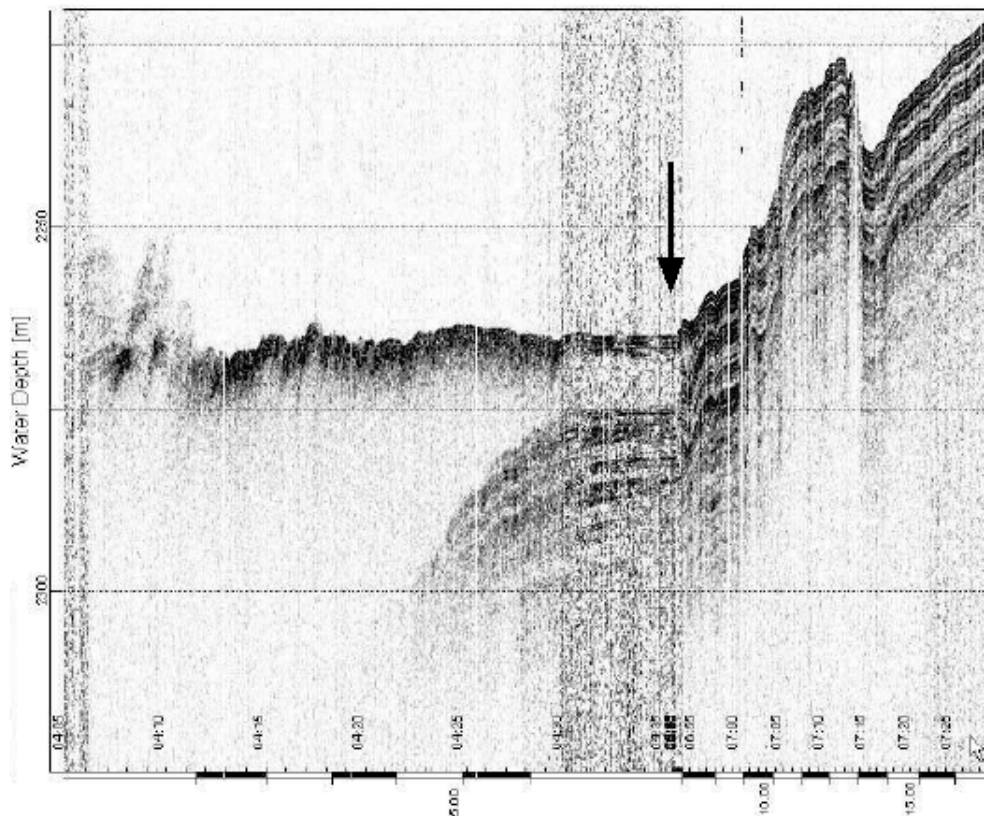


Fig. 12.6.2: Geological Situation at Station PS6/307 as recorded by PARASOUND. For details see Station List. Horizontal distance bar (black or white) is 1 km. Numbers are time UTC.

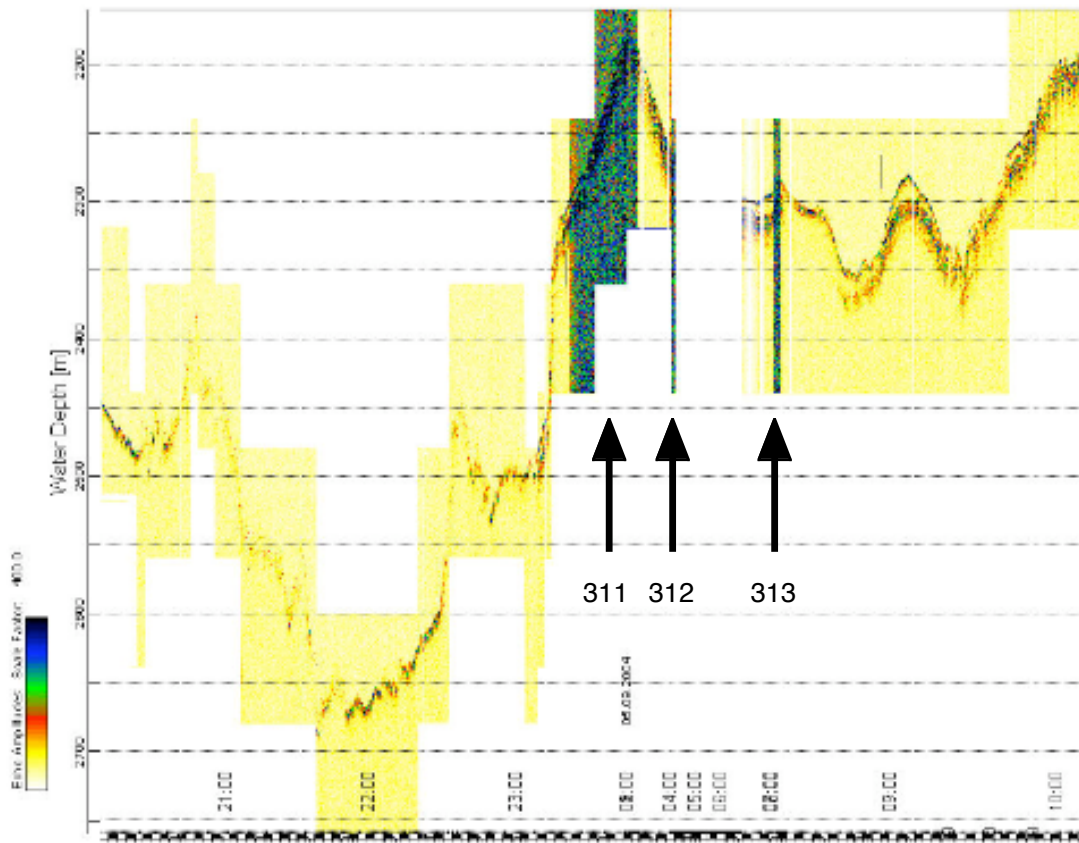


Fig. 12.6.3: Geological Situation at Stations PS66/311, /312, /313 as recorded by PARASOUND. For details see Station List. Horizontal distance bar (black or white) is 1 km. Numbers are date and time UTC.

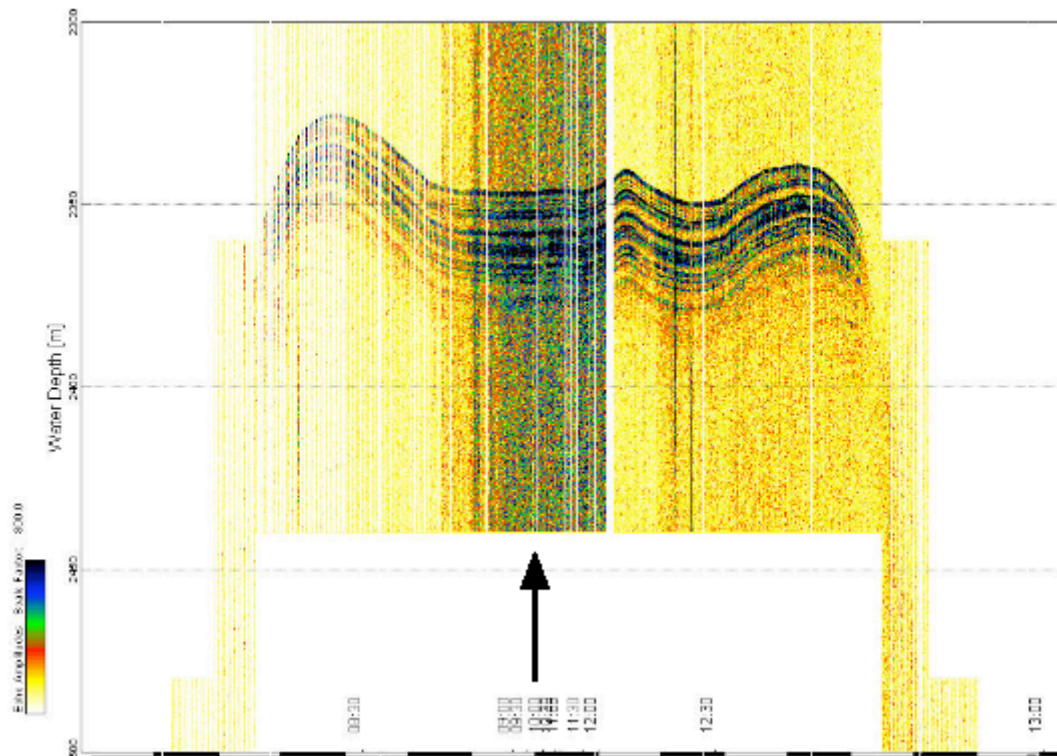


Fig. 12.6.4: Geological Situation at Station PS66/321 as recorded by PARASOUND. For details see Station List. Horizontal distance bar (black or white) is 1 km. Numbers are time UTC.

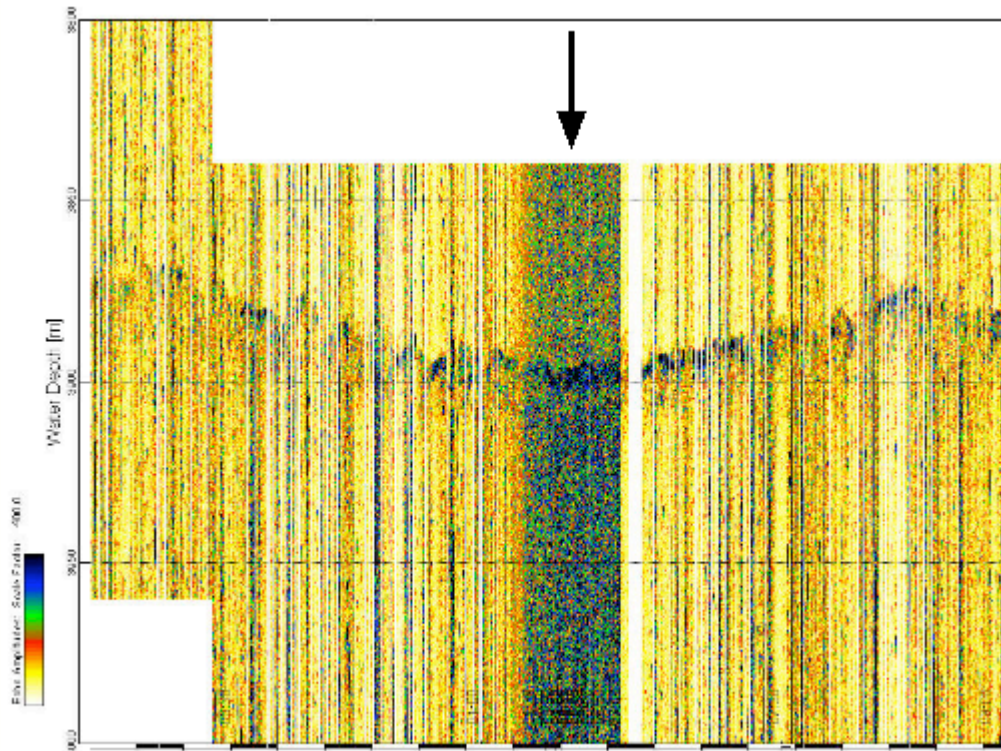


Fig. 12.6.5: Geological Situation at Station PS66/323 as recorded by PARASOUND. For details see Station List. Horizontal distance bar (black or white) is 1 km. Numbers are time UTC.

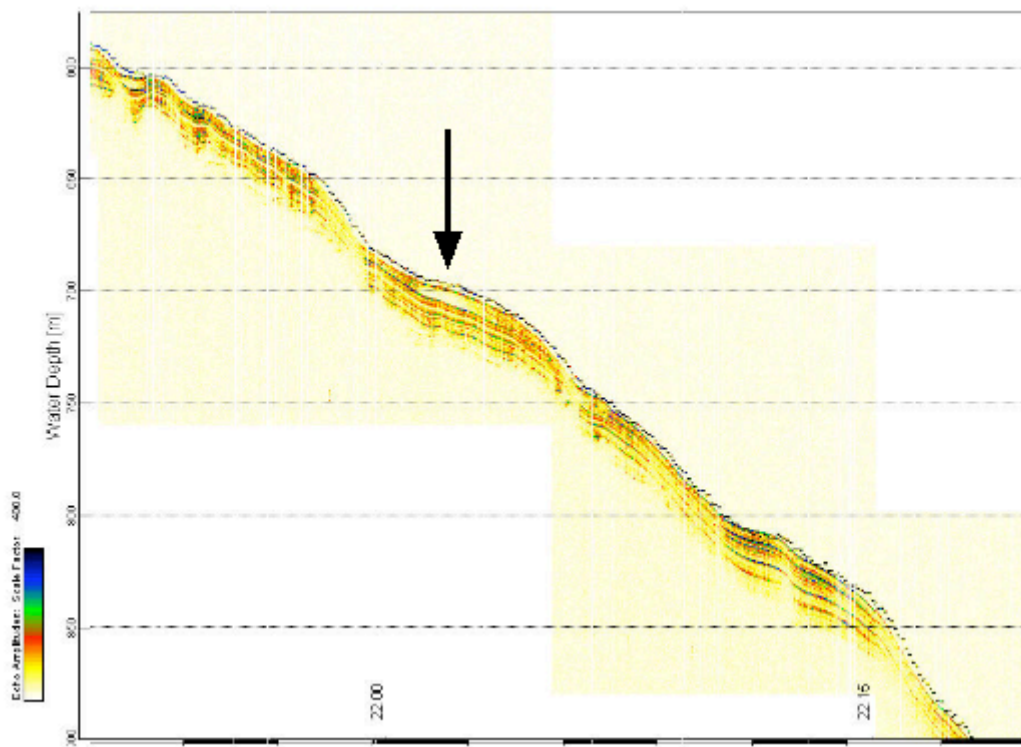


Fig. 12.6.6: Geological Situation at Station PS66/327 as recorded by PARASOUND. For details see Station List. Horizontal distance bar (black or white) is 1 km. Numbers are time UTC.

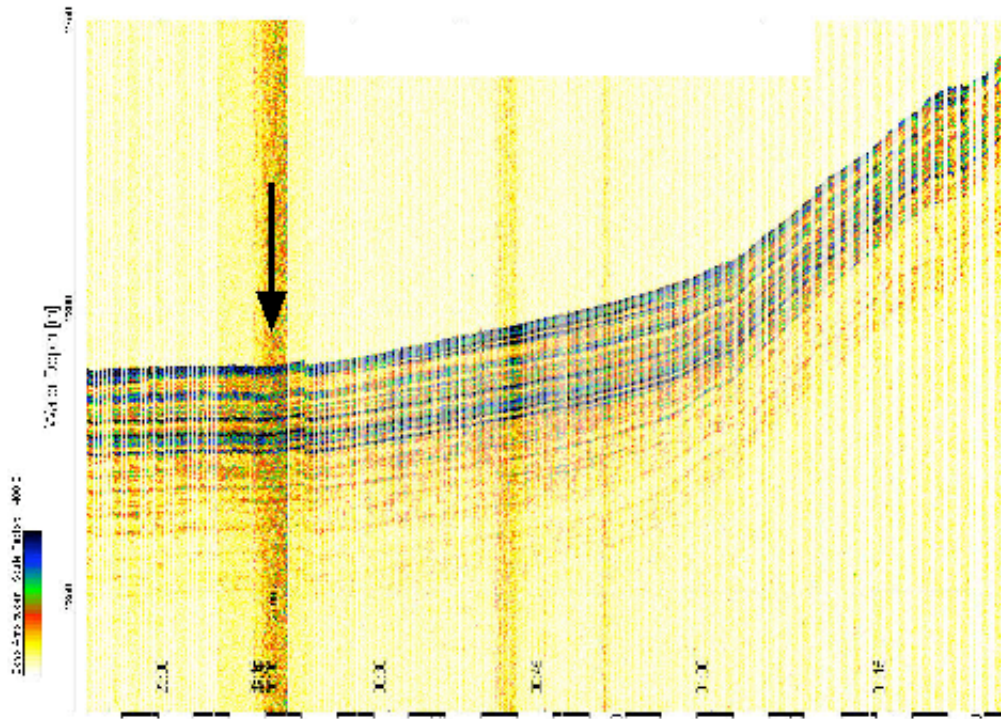


Fig. 12.6.7: Geological Situation at Station PS66/341 as recorded by PARASOUND. For details see Station List. Horizontal distance bar (black or white) is 1 km. Numbers are time UTC.

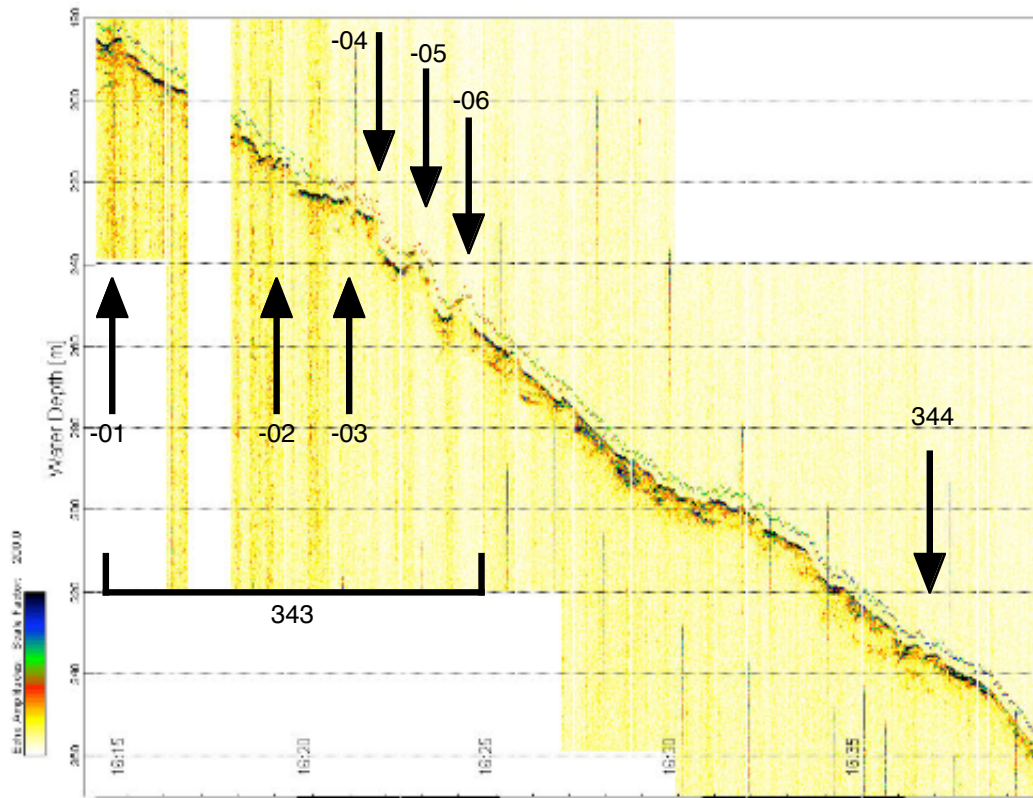


Fig. 12.6.8: Geological Situation at Stations PS66/343 and /344 as recorded by PARASOUND. For details see Station List. Horizontal distance bar (black or white) is 1 km. Numbers are time UTC.

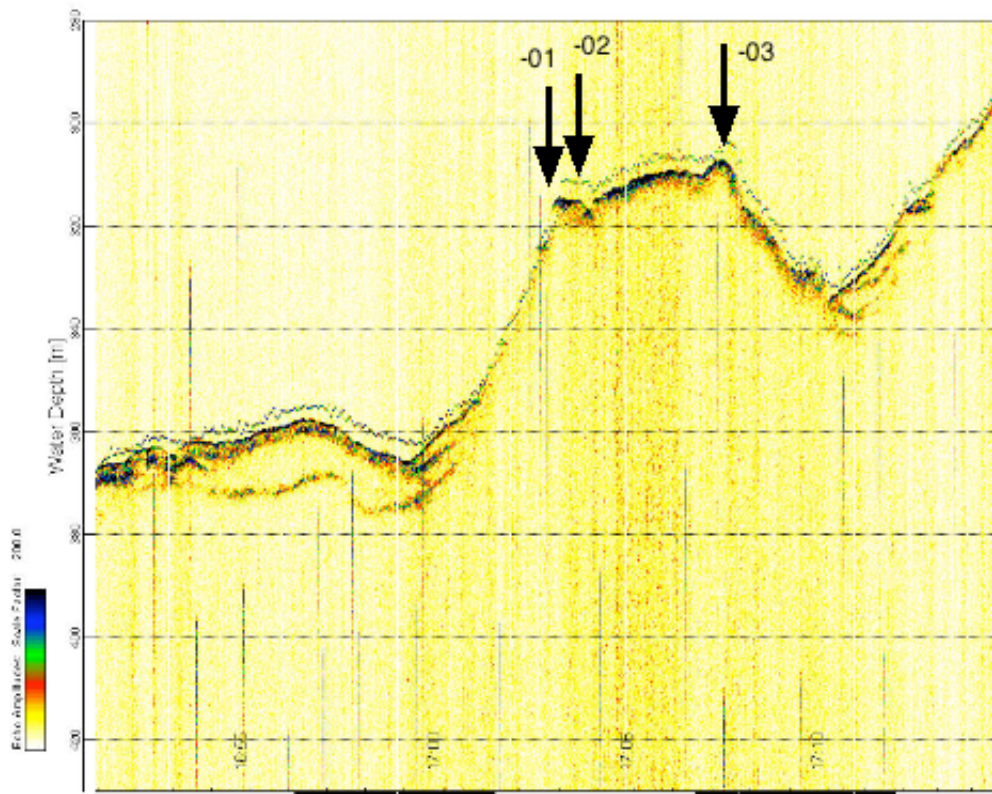


Fig. 12.6.9: Geological Situation at Station PS66/345 (-01-03) as recorded by PARASOUND. For details see Station List. Horizontal distance bar (black or white) is 1 km. Numbers are time UTC.

12.7 List of Participants

Scientific Crew

Bahr	Barbara	AWI
Behr	Yannik	AWI
Birnstiel	Hendrik	AWI
Büchner	Jürgen	HeliTransair
Buldt	Klaus	DWD
Feldt	Oliver	HeliTransair
Fricke	Nikolas	MPI
Gebauer	André	AWI
Gebauer	Manfred	DWD
Gebhardt	Catalina	AWI
Gößling	Karsten	AWI
Günther	Daniel	AWI
Jokat	Wilfried	AWI
Kukina	Natalia	MMBI
Lensch	Norbert	AWI
Martens	Hartmut	AWI
Mende	Ingo	MPI
Nam	Seung-il	KIGAM
Niessen	Frank	AWI
Noffke	Hannah	AWI
Penshorn	Dietmar	AWI
Platten	Bettina	AWI
Puhr	Andreas	AWI
Raabe	Wolfgang	AWI
Rathlau	Rike	AWI
Ropenhagen	Johannes	FIELAX
Saraswat	Rajeev	AWI
Schäfer	Christoph	AWI
Schmidt-Aursch	Michita	AWI
Schneider	Julia	AWI
Schoster	Frank	AWI
Schroeder	Max	AWI
Shevchenko	Vladimir	IORAS
Spengler	Thomas	AWI
Stein	Ruediger (Chief scientist)	AWI
Thiele	Julia	AWI
Winkelmann	Daniel	AWI
Winkler	Andreas	AWI
Winter	Stefan	HeliTransair
Yaroslava	Yanina	MMBI
Yousif	Khalaf	HeliTransair

Participating Institutions

- AWI: Alfred-Wegener-Institut for Polar and Marine Research
Columbusstrasse
27568 Bremerhaven
Germany
- IORAS P.P. Shirshov Institute of Oceanology
The Russian Academy of Sciences
36, Nakhimovsky Prospekt
Moscow 117997
Russia
- KIGAM Korean Institute of Geoscience and Mineral Resources
30 Gajeong-dong, Yuseong-gu
305-350 Daejeon
Korea
- MMBI Murmansk Marine Biological Institute
Vladimirskaia 17
Murmansk 183010
Russia
- MPI Max Planck Institute Seewiesen
82319 Seewiesen
Germany

Ship's Crew

01.	Domke, Udo	Master
02.	Grundmann, Uwe	1.Offc.
03.	Farysch, Bernd	Ch. Eng.
04.	Hartung, René	2.Offc.
05.	Peine, Lutz	2.Offc.
06.	Fallei, Holger	2.Offc.
07.	Grigoleit, Urte	Doctor
08.	Riess	R.Offc.
09.	Delff, Wolfgang	1.Eng.
10.	Ziemann, Olaf	2.Eng.
11.	Kotnik, Herbert	2.Eng.
12.	Muhle, Heiko	Electr.
13.	Nasis, Ilias	FielaxElo
14.	Verhoeven, Roger	FielaxElo
15.	Muhle, Helmut	FielaxElo
16.	Kahrs, Thomas	FielaxElo
17.	Loidl, Reiner	Boatsw.
18.	Reise, Lutz	Carpenter
19.	NN	A.B.
20.	NN	A.B.
21.	Winkler, Michael	A.B.
22.	Guse, Hartmut	A.B.
23.	Hagemann, Manfred	A.B.
24.	Schmidt, Uwe	A.B.
25.	Vehlow, Ringo	A.B.
26.	Bäcker, Andreas	A.B.
27.	Preußner, Jörg	Storek.
28.	Ipsen, Michael	Mot-man
29.	Voy, Bernd	Mot-man
30.	Elsner, Klaus	Mot-man
31.	Hartmann,Ernst-Uwe	Mot-man
32.	Grafe, Jens	Mot-man
33.	Müller-Homburg, Ralf-Dieter	Cook
34.	Völske, Thomas	Cooksmate
35.	Silinski, Frank	Cooksmate
36.	Jürgens, Monika	1.Stwdess
37.	Wöckener, Martina	Stwdss/KS
38.	Czyborra, Bärbel	2.Stwdess
39.	Silinski, Carmen	2.Stwdess
40.	Gaude, Hans-Jürgen	2.Steward
41.	Möller, Wolfgang	2.Steward
42.	Huang, Wu-Mei	2.Steward
43.	Yu, Chung Leung	Laundrym.